Universitat Autònoma de Barcelona

The role of α9β1 integrin in tumour progression: development of inhibitory strategies to prevent metastasis

Natalia Navarro Barea

Universitat Autònoma de Barcelona

Vall d'Hebron Institut de Recerca VHIR

DOCTORAL THESIS

The role of $\alpha 9\beta 1$ integrin in tumour progression: development of inhibitory strategies to prevent metastasis

PhD thesis presented by

Natalia Navarro Barea

To obtain the degree of

PhD in Biochemistry, Molecular Biology and Biomedicine

Tutor: José Ramón Bayascas, PhD

Thesis directors:

Josep Roma, PhD Soledad Gallego, MD Miguel F. Segura, PhD

Student: Natalia Navarro Barea

Department of Biochemistry and Molecular Biology
Universitat Autònoma de Barcelona, 2021

ABSTRACT

Cancer is a major burden of disease worldwide since each year millions of people are diagnosed with this disease around the world and it is the second cause of premature death in developed countries. Despite substantial progress has been made in the early detection and treatment of adult and paediatric cancer, disease progression and metastasis still occur in a subset of patients. Patients with metastatic cancer have a very poor prognosis and are likely to be refractory to conventional treatments. Thus, the onset of metastasis very often involves crossing a boundary beyond which the probability of cure becomes clearly lower. As a matter of fact, metastasis is considered the main cause of cancer-associated deaths. This emphasizes the necessity of developing new therapeutic strategies directed to prevent the formation of distant metastases and thus, reduce cancer mortality. Nonetheless, the biology underlying the complex process of metastasis remain not fully understood and studies addressing this pending issue are still essential to develop new therapeutic approaches against it.

The family of integrins have been extensively related to metastasis and altered integrin expression or downstream signalling proteins have been related to almost all the different phases of the metastatic cascade. This postulate them as good therapeutic targets to prevent metastasis onset. Integrin α9β1 has been previously described as playing an essential role in cell invasion and metastasis; however, little is known about the mechanism that links this protein to this process, being one of the less studied integrins. This project aims to further characterize the role of integrin α9β1, in three different tumour types: [1] rhabdomyosarcoma, the most prevalent soft tissue sarcoma in children, [2] neuroblastoma, the most common

extracranial solid tumour in children, and [3] breast cancer, the most frequent cancer in women and worldwide. These three cancers have a different cell of origin and affect different tissues and populations. Nevertheless, they have one trait in common: although they have a good general overall survival (around 70% for rhabdomyosarcoma and neuroblastoma, and around 80% for breast cancer), a subset of patients develop metastasis and this drastically worsens their survival rates (approximately 30% for rhabdomyosarcoma, 50% for neuroblastoma and below 40% for breast cancer patients).

In this project different strategies to inhibit α9β1 integrin expression or to block its interaction with other proteins have been addressed. And evidence demonstrating that α9β1 integrin is essential for metastatic dissemination of rhabdomyosarcoma, neuroblastoma and breast cancer cells is provided. However, the most translational advance of this study is to validate *in vivo* the effects of a specific blocking peptide, named RA08. It is a synthetic peptide that simulates a key interaction domain between ADAM12 and α9β1 integrin and acts as a pharmacologic inhibitor of α9β1 integrin. Treatment with RA08 turned out to reduce metastatic spreading in murine models of metastasis and is postulated as a possible new therapeutic approach to prevent metastasis. Altogether, results here presented revealed an important role of α9β1 integrin in the establishment of metastasis and present its inhibition as a possible therapeutic strategy to prevent metastasis in a wide range of tumour types. Further investigation on this issue is still necessary, but we consider that data generated in this thesis gives new insights to metastasis biology and opens the door to the development of new compounds aimed at preventing metastasis and, thus, reducing cancer mortality.

INDEX

TABLE OF CONTENTS: FIGURES

TABLE OF CONTENTS: TABLES

ABBREVIATIONS

ACAP1	ArfGAP with coiled-coil, ankyrin repeat and PH domains 1
ADAM	A disintegrin and metalloprotease
ADMIDAS	Adjacent to metal-ion-dependent adhesion site
ALK	Anaplastic lymphoma kinase
AP2M1	Adaptor related protein complex 2 subunit Mu 1
ARID1A	AT rich interactive domain 1A
ARID1B	AT rich interactive domain 1B
ARMS	Alveolar rhabdomyosarcoma
ATCC	American Type Culture Collection
ATM	Ataxia telangiectasia mutated
AUP1	Ancient ubiquitous protein 1
BC	Breast cancer
BCOR	BLC6 corepressor
BIN1	Bridging interactor 1
BLBC	Basal-like breast cancer
BRCA1/2	Breast cancer type 1/2 susceptibility protein
BRD1	Bromodomain-containing protein 4
BSA	Bovine serum albumin
BSP	Bone sialic protein
CAF	Cancer-associated fibroblast
CCDN1	Cyclin D1
CDK4	Cyclin dependent kinase 4
cDNA	Complementary DNA
cFN	Cellular fibronectin
CHD4	Chromodomain helicase DNA binding protein 4
CHD5	Chromodomain helicase DNA binding domain 5
CHIP	Chromatin immunoprecipitation
CIB1	Calcium and integrin binding 1
CNS	Central nervous system
COMP	Cartilage oligomeric matrix protein
COSMIC	Catalogue of Somatic Mutations in Cancer
CSF	Cerebrospinal fluid
Ct	Threshold cycle
CT	Computerized tomography

CTC	Circulating tumour cell
CXCR4	CXC motif chemokine receptor 4
Cyr61	Cysteine-rich protein 61
DEPC	Diethyl pyrocarbonate
DISC	Death-inducing signalling complex
DMEM	Dulbecco's Modified Eagle Medium
DMF	Dimethylformamide
DMSO	Dimethyl sulfoxide
DNA	Deoxyribonucleic acid
dNTP	Deoxynucleoside triphosphate
DOX	Doxycycline
DTC	Disseminated tumour cell
DTT	Dithiothreitol
EC	Endothelial cell
ECM	Extracellular matrix
EDA	Extra domain A of fibronectin
EDTA	Ethylenediaminetetraacetic acid
EDB	Extra domain B of fibronectin
EED	Embryonic ectoderm development
EGF	Epidermal growth factor
EMILIN1	Elastic microfibril interface-located protein 1
EMT	Epithelial-to-mesenchymal transition
EPS8	Epidermal growth factor receptor pathway substrate 8
EpSSG	European paediatric Soft tissue sarcoma Study Group
ER	Oestrogen receptor
ERMS	Embryonal rhabdomyosarcoma
ERK	Extracellular Signal-Regulated Kinase
FABP3	Fatty acid binding protein
FAK	Focal adhesion kinase
FBXW7	F-box and WD repeat domain containing 7
FDG-PET	Fluorodeoxyglucose positron emission tomography
FGF	Fibroblast growth factor
FGFR	Fibroblast growth factor receptor
FHL	Four and a half LIM domain
FISH	Fluorescent *in-situ* hybridization
FN	Fibronectin
FN-ARMS	Fusion-negative alveolar rhabdomyosarcoma

FOXO1	Forkhead box O1
FOXO4	Forkhead box O4
FP-ARMS	Fusion-positive alveolar rhabdomyosarcoma
FRMD5	FERM domain containing protein 5
FSC	Forward scatter
FXIII	Blood coagulation factor XIII
GAB1	GRB2 associated binding protein 1
GATA3	GATA Binding Protein 3
GFP	Green fluorescent protein
GIPC1	GIPC PDZ domain containing family member 1
GWAS	Genome-wide association studies
HAX1	HCLS1 associated protein X 1
HER2	Human epidermal growth factor receptor 2
HIF	Hypoxia inducible factor
IAP	Inhibitor of apoptosis protein 1
iC3b	Inactivated complement component
ICAM	Intercellular cell adhesion molecule
ICAP1	Integrin cytoplasmic domain-associated protein 1
ICCC	International Classification of Childhood Cancer
ICD	International Classification of Diseases
ICR	International Classification of Rhabdomyosarcoma
IDC-NST	Invasive ductal carcinoma no special type
IGF2	Insulin growth factor 2
IHC	Immunohistochemistry
ILK	Integrin linked kinase
IMDM	Iscove's Modified Dulbecco's Medium
INRG	International Neuroblastoma Risk Group
INSS	International Neuroblastoma Staging System
IRS	Intergroup Rhabdomyosarcoma Study
ITGA9	Integrin α9 subunit
IVA	Ifosfamide-Vincristine-ActinomycinD
JAB1	Jun activation domain-binding protein 1
KAT2B	Lysine acetyltransferase 2B
L1-CAM	L1-cell adhesion molecule
LAP-TGF-β	TGF-β latency-associated peptide
LDV	Leucine-aspartate-valine
LOH	Loss of heterozygosity

LTBP4	Latent Transforming Growth Factor Beta Binding Protein 4
LTR	Long terminal repeat
mA	Milliamps
MAPK	Mitogen-activated protein kinase
MaSC	Mammary epithelium stem cell
MEM	Minimum essential media
MET	Mesenchymal-to-epithelial transition
MIBG	Metaiodobenzylguanidine
MIBP	Muscle-specific beta 1 integrin binding protein
MIDAS	Metal-ion-dependent adhesion site
MKI	Mitotic-karyorrhectic index
M-MLV	Maloney-murine leukemia virus
MMP	Matrix metalloproteinase
MRI	Magnetic resonance imaging
mRNA	Messenger ribonucleic acid
MSC	Mesenchymal stem cell
MYCN	Neuroblastoma-derived V-Myc avian myelocytomatosis viral
MYF6	Myogenic factor 6
MYOD1	Myogenic differentiation 1
MYOG	Myogenin
NB	Neuroblastoma
NCOA1	Nuclear receptor co-activator 1
NCOA2	Nuclear receptor co-activator 2
NF1	Neurofibromin 1
NGF	Nerve growth factor
NICD	Notch intracellular domain
NRK2	Nicotinamide riboside kinase 2
OMM	Outer mitochondrial membrane
OPN	Osteopontin
PAKA4	p21 activated kinase 4
PAM50	Prediction Analysis of Microarray 50 genes
PARP	Poly-ADP ribose polymerase
PAX3	Paired box gene 3
PAX7	Paired box gene 7
PBS	Phosphate buffered saline
PCR	Polymerase chain reaction
PDX	Patient derived xenograft

PDGF	Platelet derived growth factor
PECAM	Platelet and endothelial cell adhesion molecule
PFA	Paraformaldehyde
pFN	Plasma fibronectin
PHOX2B	Paired like homeobox 2B
PI3K	Phosphoinositide-3-kinase
PI3KCa	Phosphoinositide-3-kinase catalytic subunit α
PKC	Protein kinase C
PKD1	Polycystic kidney disease-associated protein
PLK1	Polo like kinase 1
PP1C	Protein phosphatase 1 catalytic subunit
PP2A	Protein phosphatase 2 activator
pp-vWF	Propolypeptide of von Willebrand factor
PR	Progesterone receptor
PRMS	Pleomorphic rhabdomyosarcoma
PS	Posphatidylserine
PSI	Plexin-semaphorin-integrin
PTB	Phosphotyrosine-binding
PTEN	Phosphatase and tensin homolog
PTPN1	Protein tyrosine phosphatase non-receptor type 1
PVDF	Polyvinylidene difluoride
qPCR	Quantitative polymerase chain reaction
RACK1	Receptor for activated C kinase 1
RFP	Red fluorescent protein
RGD	Arginine-glycine-aspartate
RIPA	Radioimmunoprecipitation assay
RISC	RNA-induced silencing complex
RMS	Rhabdomyosarcoma
RNA	Ribonucleic acid
RNF181	Ring finger protein 181
ROBO1	Roundabout guidance receptor 1
RT	Reverse transcription
RT-PCR	Reverse transcription polymerase chain reaction
SCID	Severe combined immunodeficiency
SD	Standard deviation
SDS	Sodium dodecyl sulphate
SDS-PAGE	Sodium dodecyl sulphate-polyacrylamide gel electrophoresis

SFK	Src family kinases
SHARPIN	SHANK associated RH domain interactor
SHC1	SHC adaptor protein
SmoM2	Constitutively active Smoothened
SNX	Sorting nexin
SPECT	Single-photon emission computerized tomography
SRMS	Spindle/sclerosing rhabdomyosarcoma
SSC	Side scatter
STS	Soft tissue sarcomas
SYK	Spleen associated tyrosine kinase
TAM	Tumour-associated macrophage
TBP	TATA-binding protein
TBS	Tris-buffered saline
TBS-T	Tris-buffered saline with Tween20
TEM	Transendothelial migration
TFA	Trifluoroacetic acid
TFF3	Trefoil Factor 3
TGF-β	Transforming growth factor β
TNBC	Triple negative breast cancer
TNF	Tumour necrosis factor
TRAIL	TNF-related apoptosis-inducing ligand
TRFR1	TNF receptor 1
TNM	Tumour, Node, Metastasis
tTG	Tissue transglutaminase
uPA	Urokinase
uPAR	Urokinase receptor
VAC	Vincristine-ActinomycinD-Cyclophosphamide
VCAM	Vascular cell adhesion molecule
VEGF	Vascular endothelial growth factor
vWF	Von Willebrand Factor
WHO	World Health Organization

I. INTRODUCTION

"One never notices what has been done; one can only see what remains to be done."
Marie Curie

1. Cancer

"Cancer is a large group of diseases that can start in almost any organ or tissue of the body when abnormal cells grow uncontrollably, go beyond their usual boundaries to invade adjoining parts of the body and/or spread to other organs. The latter process is called metastasizing and is a major cause of death from cancer", definition of cancer according to the World Health Organization (WHO).

Cancer is the second cause of premature death worldwide and it is expected to achieve the first position in the 21st century due to the rapid population growth and aging. Global cancer incidence was around 18 million new cases worldwide and 9.6 million deaths in 2018, and the distribution of cancer cases was not homogeneous in the different world regions, highlighting differences due to risk factors associated to social and economic development (1).

Adult cancer is usually classified according to the International Classification of Diseases (ICD), updated last time in 2019 (2). In this classification, cancers other than leukaemia, lymphomas, Kaposi sarcoma, cutaneous melanoma, and mesothelioma, which are mainly carcinomas (tumours derived from epithelial cells), are classified only by primary site.

Breast cancer (11.7% of the total cases) is the most commonly diagnosed cancer, followed by lung cancer (11.4%). However, when cases are separated by sex, lung (14.5%) and prostate (13.5%) cancer represent the most frequent cancer in males, while breast cancer (24.2%) is the most common neoplasia in women (1,3) (Figure 1).

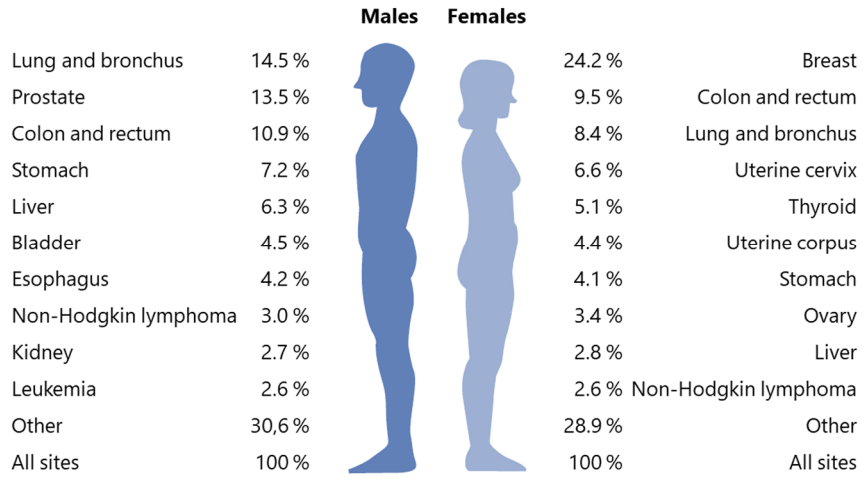

Figure 1. Cancer incidence by sex. Estimates from GLOBOCAN 2018 study (1).

Improvements in cancer detection and treatment have increased considerable patient's survival rates. However, cancer-associated mortality is still a challenge. Lung cancer (22% of all cancer deaths) in men and breast cancer (15% of all cancer deaths) in women are the tumour types that produce more cancer-associated deaths worldwide (Figure 2).

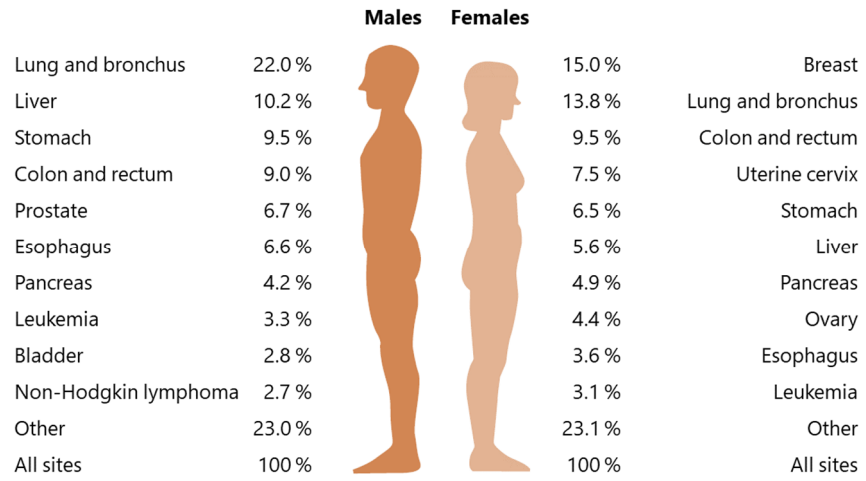

Figure 2. Cancer-associated deaths by sex. Estimates from GLOBOCAN 2018 study (1).

2. Childhood cancer

Childhood cancer includes cancer in children under 15 years, but also in adolescents (between 15 and 19 years). Childhood cancer is a rare disease which accounts for approximately 1% of all cancers diagnosed worldwide each year (4) and has an incidence of approximately 150 newly diagnosed cases per million children and 200 new cases per million adolescents (5), which is translated into approximately 1000 new cases per year in Spain (6). Nevertheless, the real global magnitude of childhood and adolescent cancer remains unrevealed due to the lack of global estimates of incidence, survival and mortality for children in most underdeveloped countries (4).

Childhood cancers are more diverse than adult cancers and include some distinctive types that arise from embryonal precursor cells and are very infrequent in adults. This is the reason why childhood cancers are classified according to the International Classification of Childhood Cancer (ICCC), which is based on morphology instead of primary site. This classification has 12 main diagnostic groups (Table 1), that can be classified into further divisions (7).

The most frequent cancers in children and adolescents are leukaemia, lymphomas and central nervous system (CNS) tumours (6). These differences in cancer subtype incidence between adults and children are thought to be related to risk factor exposure. Whereas in adults the most frequent tumours are carcinomas related to environmental risk factor (smoking, unhealthy diet, alcohol, etc.), childhood cancer is not associated with them and only weak association has been found with radiation and chemotherapy exposure, maternal pesticide exposure or maternal age. Instead of this, intrinsic and genetic risk factors (birth weight, structural birth

defects, genetic alterations, inherited syndromes, etc.) have been more consistently associated with childhood cancer incidence. However, studies in bigger populations are still needed to determine new risk factors (8).

Fortunately, substantial progress has been made in the detection and treatment of childhood cancer over the past decades, and survival rate has achieved almost 80% (4,9). Despite this, cancer is still the first cause of death during childhood due to health problems (5), and some subtypes still have a reduced survival. This is the case of bone tumours, soft tissue sarcomas, CNS tumours and neuroblastoma (Table 1).

Table 1. Diagnostic groups according to the International Classification of Childhood Cancer (7) and estimates from the Spanish registry 1980-2016 (6).

	Diagnostic groups	**% in children**	**% in adolescents**	**5-year survival**
I	Leukaemia, myeloproliferative diseases, and myelodysplastic diseases	26.5 %	12.8 %	80 %
II	Lymphomas and reticuloendothelial neoplasms	13.1 %	21.5 %	87 - 97 %
III	Central nervous system and miscellaneous intracranial and intraspinal neoplasms	21.2 %	15.9 %	68 %
IV	Neuroblastoma and other peripheral nervous cell tumours	9.8 %	1.2 %	76 %
V	Retinoblastoma	3.1 %	0.0 %	96 %
VI	Renal tumours	5.9 %	1.5 %	92 %
VII	Hepatic tumours	1.3 %	0.3 %	85 %
VIII	Malignant bone sarcomas	6.8 %	24.8 %	66 - 68 %
IX	Soft tissue and other extraosseous sarcomas	6.9 %	11.0 %	66 - 68 %
X	Germ cell tumours, trophoblastic tumours, and neoplasms of gonads	3.2 %	5.8 %	92 - 98 %
XI	Other malignant epithelial neoplasms and malignant melanomas	1.9 %	5.0 %	85 %
XII	Other and unspecified malignant neoplasms	0.2 %	0.3 %	-
	All malignancies	100 %	100 %	78 %

Despite substantial progress has been made in the early detection and treatment of adult and paediatric cancer, disease progression and development of metastasis still occur in certain subsets of patients. Patients with metastatic cancer have a very poor prognosis and are likely to be refractory to the conventional treatments. This emphasizes the necessity of developing new therapeutic strategies to prevent the formation of distant metastases and thus, reduce cancer mortality. Nonetheless, cellular components that control motility, invasiveness and metastasis formation, as well as the molecules responsible for these processes, remain partially unknown. Besides, specific treatments aimed at reducing metastatic dissemination have not reached the clinics yet. Therefore, this doctoral thesis is focused on the study of underlying mechanisms of metastasis, with the objective of developing strategies to prevent its onset.

3. Metastasis

Metastasis is one of the final events of tumour progression and consists on the development of secondary tumours in parts of the body which are far from the original primary cancer site. As previously mentioned, this process is the main responsible for cancer-associated mortality, as well as one of the most valuable prognostic factors for cancer patients (10,11). Probably, the lack of therapeutic success against cancer metastasis is partially due to the limited understanding of the metastatic process. This highlights the necessity to better understand the biology of this process, and to develop new therapeutic approaches against it to reduce cancer mortality.

The activation of invasion and metastasis is one of the hallmarks of cancer (12) and is followed by a large cascade of events that culminate in the onset

of macroscopic metastatic lesions. Metastasis requires that tumour cells successfully overcome a series of obstacles to leave the primary tumour, intravasate into the blood vessels, travel and survive along the bloodstream, extravasate into the tissue parenchyma, survive in the new microenvironment, escape from the immune system and, eventually, form a secondary tumour in the "soil" tissue (Figure 3). This complex cascade of events is thought to be a poorly efficient process, since only a minority of all tumour cells that escape from the primary tumour are able to finally form macrometastases (11,13).

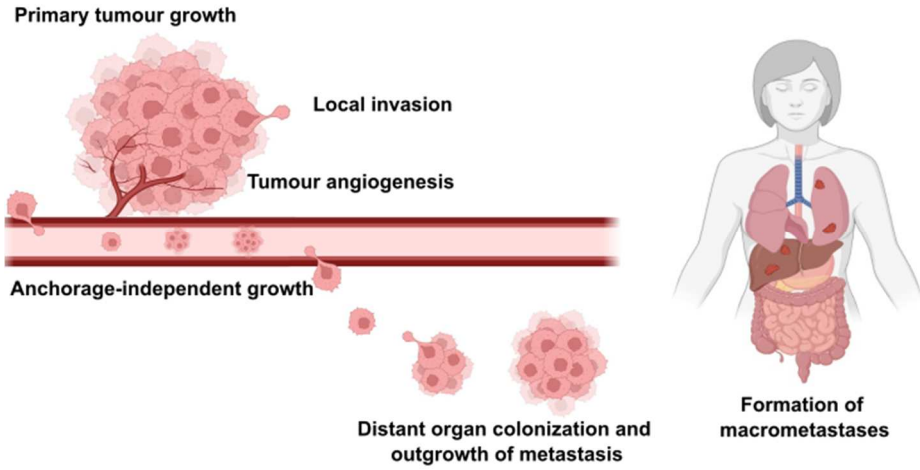

Figure 3. Cascade of events that lead to formation of metastasis.

3.1 Local invasion

The first step of the metastatic cascade is the invasion of tumour-associated stroma and adjacent normal tissues. For this purpose, cancer cells need to acquire a more plastic phenotype that allows them to increase migration and invasion capabilities and reorganize their cytoskeleton in order to change shape and interactions with other cells and the extracellular matrix (ECM) (14-16).

Usually, this step has been linked to epithelial-to-mesenchymal transition (EMT), a partially or fully reversible process characterized by the transition of cells from epithelial state to a more mesenchymal phenotype. This facilitates the loss of cell adhesion and polarity, reorganization of the actin cytoskeleton to acquire spindle-shaped mesenchymal morphology, formation of protrusions to gain motility and degradation and invasion of the ECM. EMT also allows tumour cells to acquire enhanced stemness and increased resistance to chemotherapeutic agents and immune clearance (14-17). All these changes in cell phenotype are mediated by several changes in gene expression (i.e., downregulation of E-cadherin and cytokeratins, and upregulation of vimentin, fibronectin, N-cadherin, β1 and β3 integrins) and are orchestrated by transcription factors (i.e., Snail, Twist and Zeb) and epigenetic, post-transcriptional and post-translational modifications (18,19).

EMT is a complex and diverse program that can be activated by multiple intrinsic and extrinsic factors and is extremely dependent on the extracellular environment. EMT is also a highly dynamic and plastic process, meaning that it can generate tumour cells in a wide spectrum of intermediate states that can be different in each tumour type or even, heterogeneous within a tumour population. As a matter of fact, there is evidence to support different EMT states in migrating cell clusters: while cells localized at the invasive front turn to a more mesenchymal phenotype to drive migration, cells inside the clusters retain a more epithelial phenotype and intact junctions that allow their migration by the pulling force generated by cells in the front (17,18).

Whereas the implication of EMT in modulating the behaviour of carcinoma (i.e., in breast cancer (20-22)) invading cells has been broadly described, the involvement of this process in other non-epithelial tumours remains to be better characterized. Sarcoma cells, for example, already have some features typically induced by EMT. However, the existence of intermediate or incomplete EMT states in these cells is now accepted and there is evidence that sarcoma cells undergo changes similar to EMT that give them highly aggressive phenotypes (23-25). This phenomenon has been recently described in a genetic mouse model of RMS (26) and has been related to the invasive and metastatic capabilities of these cancer cells (27-29). As a matter of fact, our group has previously described an upregulation of N-cadherin and integrin α9β1 in RMS cell lines, associated to increased invasiveness (30). In addition, these changes have been described also in tumours derived from the neural lineage, such as melanomas (23) and neuroblastoma (31,32).

Besides direct changes affecting tumour cells, interactions with other components of tumour-adjacent tissues can influence the invasion of cancer cells, such as the interactions with cancer-associated fibroblasts (CAFs) and tumour-associated macrophages (TAMs). Examples of this pro-invasive interactions are the release of TGF-β by CAFs that contribute to cancer cell EMT and the release of matrix proteases by CAFs and TAMs that helps the degradation of the stroma (16).

3.2 Intravasation

After local invasion, tumour cells that escape from the primary tumour can intravasate into the blood or lymphatic circulation and travel to distant sites to form new metastatic foci. This is also a complex process that can be

influenced by a plethora of factors, including changes in tumour cell behaviour and morphology, but also composition of the stroma and vasculature.

To get to the circulation, tumour cells need to disrupt and move through the endothelial basement membrane in a process called transendothelial migration (TEM). For this purpose, cancer cells need to modify their cytoskeleton to form protrusions and degrade the adjacent ECM by releasing proteases, such as metalloproteinases (MMP). This reshapes the composition of the environment, increasing ECM stiffness and inducing changes in protein expression such as higher integrin expression and focal adhesion kinase (FAK) signalling, which on its behalf enhances cell invasiveness and ECM remodelling. The process of EMT and the interaction with stromal cells have been also related to intravasation, therefore defining which proteins are specifically involved in intravasation rather than local invasion has not been possible yet (16,33).

Studies using leukocytes have revealed that the TEM of cells has mainly two ways: the paracellular and the transcellular. The paracellular TEM is used by most cancer cells *in vitro* and in this case, cells insert protrusions between the endothelial cells (EC) and induce the opening of their cell junctions. Several proteins have been related to this kind of TEM, including β1 (34) and β3 integrins and the secretion of factors, such as ADAM12, VEGF and TGFβ1, by cancer cells o tumour-associated cells. The expression of these factors, for example, cause the disruption of the endothelial junctions formed by VE-cadherin (main transmembrane component of EC adherent junctions) (35,36). On the other hand, although transcellular TEM has been less described and more studies are still needed to determine possible

pathways involved, it has been described in migrating colorectal (37) and breast cancer cells (33,38). In this case, TEM consists on the formation of cell protrusion that passes directly through a pore on an individual EC (39).

Another important point that eases the intravasation of cancer cells are the changes related to the vasculature. Abnormal leaky vasculature and activation of angiogenesis and lymphangiogenesis have been described to facilitate the intravasation and consequently, the metastatization of tumour cells. During local invasion, degradation of the ECM occurs and this liberates growth factors and pro-angiogenic factors (VEGF and other chemokines). This, together with hypoxia-inducible factors (HIF, TNF, PDGF) release by the primary tumour, induces a rapid growth of new vessels that exhibit structural abnormalities, such as dilatation, hyper-branched pattern, faint VE-cadherin junctions, and weak association between EC and surrounding pericytes. This facilitates the opening of cells junctions and the intravasation of tumour cells to the blood steam (16,40).

3.3 Survival along bloodstream

Once the metastasizing tumour cells have reached the blood circulation, they are called circulating tumour cells (CTCs) and can travel as individual cells or forming multicellular clumps that persist in the circulation until they get stuck into a small vessel and proceed to the extravasation. During this period CTCs need to adapt to survive in this new environment and overcome the lack of cell attachment.

In the absence of attachment to the ECM or other surrounding cells, cells undergo a particular type of apoptosis, termed anoikis. The resistance of

anoikis has emerged as a hallmark of cancer as is necessary for the formation of metastasis in distant organs. The initiation and the execution of anoikis is mediated by different pathways that converge into the activation of caspases and eventually, in the activation of endonucleases, DNA fragmentation and cell death. Generally, the involved molecular pathways are similar to the well-established apoptotic pathways (41).

Anoikis is initiated after loss of cell attachment and can be triggered by two different pathways: the intrinsic and the extrinsic. The intrinsic pathway is activated in response to intracellular signals. When cells loss their attachment and consequently integrin engagement, Bim is protected from the proteasomal degradation and released from the cytoskeletal complexes. After Bim accumulation, Bim and Bad activation occurs and Bax-Bak oligomerization at the outer mitochondrial membrane (OMM) is promoted. This creates a channel at the OMM, causing the mitochondrial permeabilization and the release of the cytochrome c that leads to the formation of the "apoptosome" that triggers the activation of the caspase-3 and the execution of the apoptotic process. On the other hand, the extrinsic pathway is initiated by ligand binding of the superfamily of death receptors, such as Fas receptor, TNFR1 (Tumour necrosis factor receptor-1) and TRAIL (TNF-related apoptosis inducing ligand). This results in the formation of the death-inducing signalling complex (DISC) and the activation of caspase-8. This eventually activates caspase-3 and the apoptotic cascade. Both intrinsic and extrinsic pathways converge in the activation of caspase-3, which apart from activating the apoptosis cascade, also cleaves signalling molecules such as FAK. The caspase-mediated cleavage of FAK disrupts focal adhesion architecture and inhibits integrin-mediated survival signals (41).

Although the study of CTCs is relatively recent, different mechanisms to achieve anoikis resistance have been described in tumour cells: for instance, integrin switch and EMT, activation of pro-survival signals and adaptation of cell metabolism.

There is evidence demonstrating that CTCs change their integrin expression profile to survive along the bloodstream downregulating certain integrins, while upregulating others, a phenomenon that is also observed during EMT. For example, expression of β1 and β3 integrins has been reported to support anchorage-independent survival of carcinoma cells, due to the activation of FAK and the subsequent pro-survival signalling (42-45). On the other hand, constitutive activation of pro-survival and anti-apoptotic signals have been also reported in CTCs. Results from gene expression analysis of CTCs compared to primary tumour cells revealed genetic alterations in CTCs involving survival-related genes (AKT2, PTEN, KRAS…) and apoptosis-resistance genes (LTBP4, NUMBL, TFF3…) (41,46-48). Eventually, there is growing evidence for a metabolic switch in CTCs. Along the circulation, cancer cells need to adapt their metabolism to this new environment with less glucose availability, so they can potentiate their glucose uptake systems and the use of other sources of energy, such as fatty acids (16).

Finally, CTCs need to avoid the recognition by components of the immune system to survive in circulation. CTCs interact with other cells present in the blood (neutrophils, platelets, CAFs…) to prevent their recognition. In addition, the metastasizing cells travelling in clusters are less easily recognized by immune cells. As a matter of fact, it has been suggested that

the presence of CTCs clusters is a bad prognosis factor and increases the probability of metastasis (16,49).

3.4 Extravasation and colonization

The mechanisms by which cancer cells intravasate and extravasate from the blood circulation are likely to be similar. However, the signals that trigger and mediate their TEM might be different. For example, proteases and released factors from the primary tumour are important for the intravasation but are not present during extravasation (33).

The first step for extravasation is the arrest of CTCs at small vessel capillaries. In this step, physical and molecular parameters are involved since cancer cells tend to slow down and get physically restricted at capillaries of similar diameter of the cell clump and then, they establish stronger molecular interactions with the endothelium. Several ligands and receptors contribute to these interactions, including selectins, integrins, cadherins, cytokines and immunoglobulin superfamily receptors. EC express E-selectin and L-selectin, while CTCs express some of their ligands (CD44, MUC1, CD24…), facilitating the interaction between these two types of cells. Interestingly, the expression of selectins in EC can be induced by inflammatory cytokines that, at the same time, can be released by cancer cells or cancer-associated leukocytes (50-52), suggesting that the cancer cells are able to prepare the niche for extravasation. Integrins are also important proteins for this step and the expression of β1, β3 and β4 integrins in cancer cells has been broadly implicated in their attachment to the endothelium (since EC express integrin ligands such as L1CAM, VCAM and other integrins), transmigration across it, and their subsequent attachment to surrounding matrix (16,33,34,53,54).

Once cancer cells have cross through the endothelium are called disseminated tumour cells (DTC) and need to invade the surrounding tissues and adapt to the new environment. During this phase, DTCs use similar mechanisms to the local invasion phase and exploit the expression of cell adhesion proteins and the secretion of proteases. After that, the survived cells need to switch their phenotype from a dormant[1] to a proliferative state to form macrometastases. The mechanisms that control this switch remain poorly characterized, although evidence indicates that many intrinsic and extrinsic factors are involved: tumour-specific characteristics, intracellular signals, communication with cells in the surrounding microenvironment and characteristics of the niche (16,33). Integrins and ECM remodelling have been described during dormant cells reactivation. Indeed, activation of β1 signalling and their downstream effector FAK have been associated to the proliferation of tumour cells in the seeded organs after extravasation (42,55). Another described mechanism that triggers the reactivation of dormant cells is the activation of angiogenesis. Tumour cells located in stable perivascular niches are associated to a dormant state, while sprouting of new blood vessels increases the supplies of nutrients and oxygen and promotes the reactivation of tumour cell proliferation (56-58). Other biological processes that have been related to this phase are hypoxia, EMT/MET fluctuations, inflammation, and autophagy. However, the role of this last one is still controversial (16,59).

Whereas some DTCs switch to a proliferative phenotype, there is evidence supporting a reminiscent of cells that remain in a dormant state and

[1] Cellular dormancy: reversible nondividing state of single tumour cells trying to adapt and survive in changing environments (57).

generate a minimal residual disease responsible for patients' relapse. These cells are arrested in G_0 cell cycle phase and can survive for long periods. The epigenetic and signalling pathways that maintain these cells are not completely understood yet, although studies have identified certain features associated with dormant cells. For example, factors such as TGFβ2, p21, p27, AXL, VCAM-1, HIF-1α or Oct4 have been detected in metastatic permissive niches (lung parenchyma, perivascular areas, or bone marrow). Another example is the ratio of p38/ERK signalling. Studies have shown that the interaction between DTCs and cells in the surrounding environment can result in higher p38 signalling that allows the maintenance of dormant cells, or high ERK signalling, which results in the switch to cell proliferation (58-60).

As this section may reflect, the metastatic process is a very complex cascade of events and, although fortunately it is a very inefficient process, it still is the main cause of cancer-associated mortality. Many proteins are involved in the complex regulation of this process, of particular note those belonging to the family of integrins, since altered integrin expression or downstream signalling proteins have been related to almost all the different phases of the metastatic cascade. Considering this, it seems important to focus the study of metastasis on integrin family, since a better knowledge of integrin contribution to the process of metastatic spreading would give insight into how prevent metastasis onset and improve cancer patient survival.

4. Integrins

4.1 Main traits and classification

Integrins were first characterized at the molecular level in the 1980s (61). Since then, they have emerged as fundamental cell adhesion receptors due to their ability to recognize ECM ligands, cell-surface receptors, and soluble ligands. In fact, the name "integrin" was given to highlight the importance of these receptors in maintaining the integrity of the interactions between the cytoskeleton and the ECM (62,63). Members of this family have been found in mammals (including humans, mouse and chicken), zebrafish, *Xenopus laevis*, *Drosophila melanogaster* and lower eukaryotes such as sponges and *Caenorhabditis elegans* (64).

Integrins are heterodimeric receptors of non-covalently associated α and β subunits. In vertebrates, 18 α and 8 β subunits have been described to date, generating 24 different heterodimers with different binding specificities and tissue distribution (62-65). Integrins can be classified into subgroups according to their subunit composition or based on their ligand-binding properties (Figure 4). Whereas some subunits appear in only a single heterodimer, other subunits are more promiscuous. Examples of this phenomena are the β1, β2, and αv-containing integrins which are the three largest groups in the composition-based classification (62,63). Regarding their ligand-binding affinities, integrins can be grouped into collagen, arginine-glycine-aspartate (RGD)-recognizing, leukocyte-specific and laminin receptors, being the RGD and the leukocyte-specific receptors the largest groups (63).

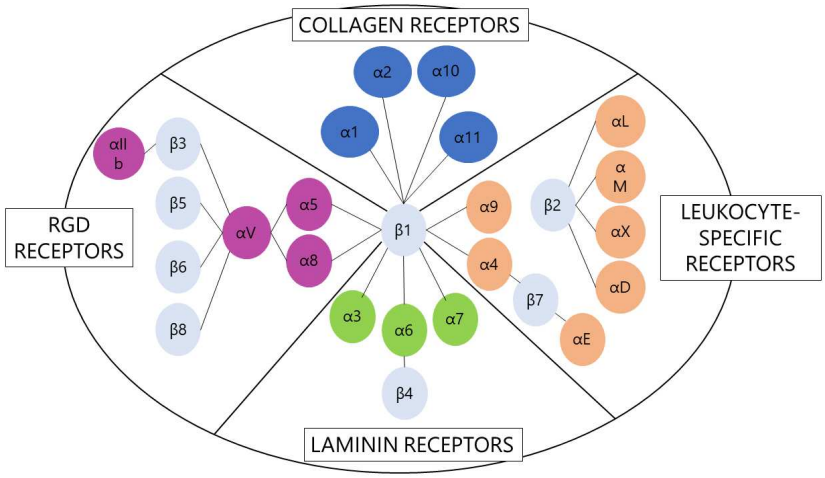

Figure 4. Classification of integrins based on ligand-binding properties. Adapted from (63).

4.2 Structure

The integrin α and β subunits are type I transmembrane proteins since they cross the cellular membrane through a single α-helix with the N-terminus on the extracellular side of the membrane. In addition, they have a large extracellular and a short cytoplasmic fragment (with the exception of the β4 subunit which has a large intracellular fragment) (63).

The integrin α and β subunits have no homology between them, although there are conserved regions between both subunits (63,64). Nevertheless, sequence identity among all α and all β subunits is about 30% and 45%, respectively, and studies on integrin genes indicate that α and β subunits were derived by gene duplications from a common ancestral gene. In humans, genes for both subunits are located on various chromosomes. However, genes corresponding to integrins expressed in leukocytes are clustered at 16p11, and those expressed in platelets and endothelial cells are clustered at 17q21.32 and 2q31 (64), although they are expressed in a variety of tissues.

4.2.1 α subunit

The α subunit consists of four extracellular domains: a seven-bladed β-propeller, a thigh and two calf domains, calf-1 and calf-2 (Figure 5).

The β-propeller, which is considered part of the integrin "head", contains Ca^{2+} binding sites at the three or four last blades, which have been shown to influence ligand binding. Moreover, this domain can also contain an α-I domain, or also called the A domain. This domain has been described only in 9 of the 18 integrin α chains (in some collagen-binding integrins and leukocyte-specific integrins (66)) and is located between blades two and three of the β-propeller. It has approximately 200 amino acids, is composed by five β-sheets surrounded by seven α-helixes and contains a metal-ion-dependent adhesion site (MIDAS) motif able to bind Mg^{2+} ions. This domain can directly interact with collagen (63,65).

The thigh and calf domains are immunoglobulin-like domains with β-sandwich folds. Calf-1 and calf-2 domains form the "leg" structure that supports the integrin "head". Finally, two regions of interdomain flexibility have been described: one between the β-propeller and the thigh, and another between the thigh and calf-1. In addition, the α-I domain also shows conformational changes that are important for regulating binding affinity. Conversely, the other domains have relatively rigid structures (65).

4.2.2 β subunit

The β-subunit consists of seven domains with complex interconnections (Figure 5). The integrin "head" contains the plexin-semaphorin-integrin (PSI) domain, a hybrid domain and a β-I domain. These domains are followed by

four cysteine-rich epidermal growth factor (EGF) modules and a β-tail domain, which are part of the "leg" structure (65). The β-I domain is homologous to the α-I domain in the α-leg. It contains a MIDAS site able to bind Mg^{2+} ions and has a site adjacent to MIDAS (ADMIDAS) able to bind Ca^{2+} ions. Ion union in this domain can lead to conformational changes resulting in an active form of the integrin (63).

In general, the β-leg is more flexible than the α-leg and there is evidence for important conformational changes occurring not only in the β-I, but also in the hybrid domain (65).

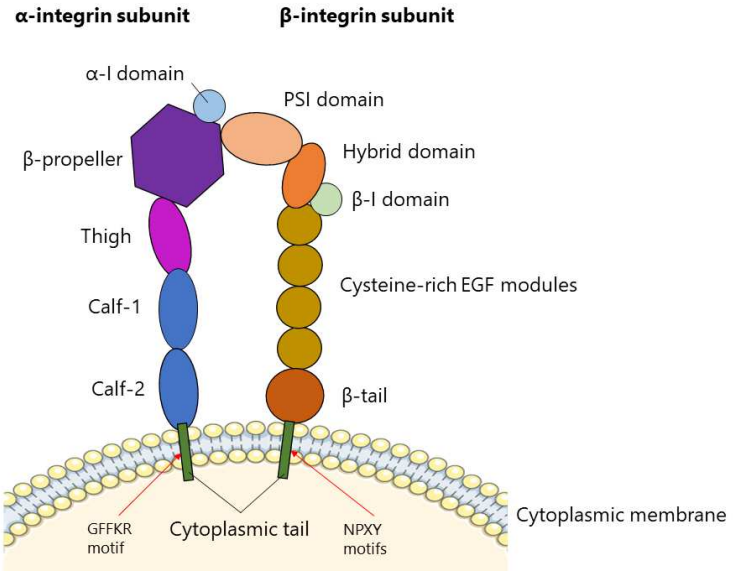

Figure 5. Structure of α and β-integrin subunits. Abbreviations: EGF, epidermal growth factor; PSI, plexin-semaphorin-integrin.

4.2.3 Cytoplasmic tail

Both subunits have a short cytoplasmic tail, which usually has less than 75 amino acids (except for β4 tail with an approximate length of 1000 amino acids). While β subunits exhibit a huge homology, α subunits tend to be

more divergent. However, all α subunits have a conserved GFFKR motif next to the transmembrane region, which is important for the association between α and β chains (64). Several cytoskeletal and signalling proteins have been reported to interact with the β cytoplasmic tail, although only a few have been found to bind to the α one. In fact, two conserved NPXY motifs have been described in the β cytoplasmic tail which are recognized by phosphotyrosine-binding (PTB) domains present in intracellular proteins, such as talin and kindlin, both known integrin-signalling mediators (64,65). Besides, β-subunit intracellular interactions have been related to integrin activity regulation and actin linkage (66) (Figure 5).

4.3 Trafficking and signalling

Newly synthesized α and β subunits heterodimerize in the endoplasmic reticulum and are transported to the cell membrane where they are obligate heterodimers (62,66). Normally, there is an excess of β subunits and the quantity of α chains determines the total amount of integrin heterodimers that arrive to the cell surface (63). Heterodimerization occurs by interactions between the α-propeller and the β-I domain, both in the extracellular "head" of integrin subunits (66).

Once at the cell membrane, integrins provide communication between the cell and their microenvironment since they interact with extracellular and intracellular molecules to generate bidirectional signals. Mechanical and chemical changes from outside the cell generate intracellular signals that can exert effects on cytoskeletal structure, gene expression, cell survival, cell proliferation, and cell motility (outside-in signalling). On the other hand, intracellular changes leading to receptor activation modify their affinity for

extracellular ligands and regulate cell adhesion, cell migration and ECM remodelling and assembly (inside-out signalling). These two ways of signalling are often closely linked, since integrin activation by intracellular proteins increases ligand affinity (inside-out signalling), and ligand recognition generates intracellular cascades (outside-in signalling) (42,67,68). Since integrins lack enzymatic activity, these two kinds of cellular signalling are mediated by conformational changes in the tri-dimensional protein structure and the assembly of signalling complexes at the intracellular face of the membrane (64-66).

In summary, integrins can regulate cell behaviour in response to changes in the environment and are important for a wide range of cellular events, such as cell survival or migration. These events are necessary for physiological processes such as morphogenesis, wound healing, or regeneration. However, they are also fundamental for some pathological conditions such as cancer (62,64).

4.3.1 Outside-in signalling

Integrin receptors can recognize many extracellular and soluble ligands, and similarly, many ECM molecules and cell surface receptors can bind to multiple integrins (Table 2). The interaction between integrins and their extracellular ligands occurs through the "head" of the heterodimer, which comprises parts of the β-propeller in the α chain and the β-I domain in the β leg. Integrins with α-I domain recognize ligands only with this domain which is coupled to the β-I domain, while in integrins without α-I domain, recognition happens thorough a pocked formed by the α-propeller and the MIDAS motif in the β-I domain (66).

Table 2. Extracellular integrin ligands and traits that influence ligand binding (63-65,69,70).

Integrins	I-domain	Motif	Extracellular ligands
α1β1	Yes	GFOGER	Laminin, collagen, semaphorin 7A
α2β1	Yes	GFOGER	Laminin, collagen, thrombospondin, E-cadherin, tenascin, fibronectin, endorepellin
α3β1	-	-	Laminin, thrombospondin, fibronectin, uPAR
α4β1	-	VLD	Thrombospondin, fibronectin, VCAM-1, ICAM-4, ADAM, osteopontin, endostatin
α5β1	-	RGD	Thrombospondin, fibronectin, ADAM, osteopontin, fibrillin, fibrinogen, COMP, CD171
α6β1	-	-	Laminin, thrombospondin, ADAM, Cyr61
α7β1	-	-	Laminin
α8β1	-	RGD	Tenascin, fibronectin, osteopontin, vitronectin, LAP-TGF-β, nephronectin
α9β1	-	VLD	Tenascin, fibronectin, uPAR, VCAM-1, ADAM, osteopontin, plasmin, angiostatin, VEGF-C, VEGF-D
α10β1	Yes	GFOGER	Laminin, collagen
α11β1	Yes	GFOGER	Collagen
αVβ1	-	RGD	Fibronectin, osteopontin, CD171, vitronectin, LAP-TGF-β
αLβ2	Yes	VLD	ICAM
αMβ2	Yes	VLD	ICAM, fibrinogen, iC3b, factor X, heparin
αXβ2	Yes	VLD	Collagen, ICAM, fibrinogen, iC3b, heparin
αDβ2	Yes	VLD	Fibronectin, VCAM-1, ICAM, fibrinogen, Cyr61, vitronectin, plasminogen
αIIbβ3	-	RGD	Thrombospondin, fibronectin, ICAM, fibrinogen, CD171, Cyr61, vitronectin, plasminogen, vWF, CD40 ligand
αVβ3	-	RGD	Laminin, thrombospondin, fibrillin, tenascin, fibronectin, uPA, uPAR, ICAM, ADAM, osteopontin, fibrinogen, COMP, CD171, Cyr61, vitronectin, LAP-TGF-β, plasmin, angiostatin, vWF, PECAM-1, BSP, MMP, FGF-2, tumstatin
α6β4	-	-	Laminin
αVβ5	-	RGD	Fibronectin, osteopontin, vitronectin, LAP-TGF-β, BSP
αVβ6	-	RGD	Fibronectin, osteopontin, tenascin, ADAM, LAP-TGF-β
α4β7	-	VLD	Fibronectin, osteopontin, VCAM-1
αEβ7	Yes	VLD	E-cadherin
αVβ8	-	RGD	Fibronectin, vitronectin, LAP-TGF-β

Some integrins (αV integrins, α5β1, α8β1 and αIIbβ3 integrins) recognize ligands which contain the RGD tripeptide active site (it binds at the interface between α and β subunits). Nevertheless, the presence of this short sequence is not necessary for ligand recognition in other integrins. For example, α4β1, α4β7, α9β1, the β2 subfamily and αEβ7 integrins bind to the leucine-aspartate-valine (LDV) motif, which is likely to interact at the same point than the RGD motif, and collagen-binding subfamily interacts with the GFOGER motif. Finally, a particular sequence or residue has not been found for the laminin-binding integrins (65). In addition to the extracellular ligands, integrins can also be activated by divalent cations that bind to the MIDAS motifs present in the I domain of both subunits (64).

As previously said, integrins lack enzymatic activity, therefore their activation after ligand-binding is mediated by conformational changes and integrin clustering at the cell membrane. Regions of interdomain flexibility, movements of the hybrid domain and dissociation of the α and β chains appear to be central for allowing the interaction of the cytoplasmic tail with intracellular proteins. These includes adaptor proteins, such as talin and kindlin that mediate the interaction with the actin cytoskeleton, and signalling molecules, such as focal adhesion kinase (FAK) and Src family kinases (SFK) (Table 3). After the recruitment and autophosphorylation of FAK (at Tyr397) and subsequent recruitment of SFK, multiple signalling pathways can be activated, for instance the RAS-MAPK and the PI3K-AKT signalling pathways. This way, integrins are able to modulate important cell functions such as gene expression, survival, proliferation, migration and invasion, after ligand recognition (64,65) (Figure 6).

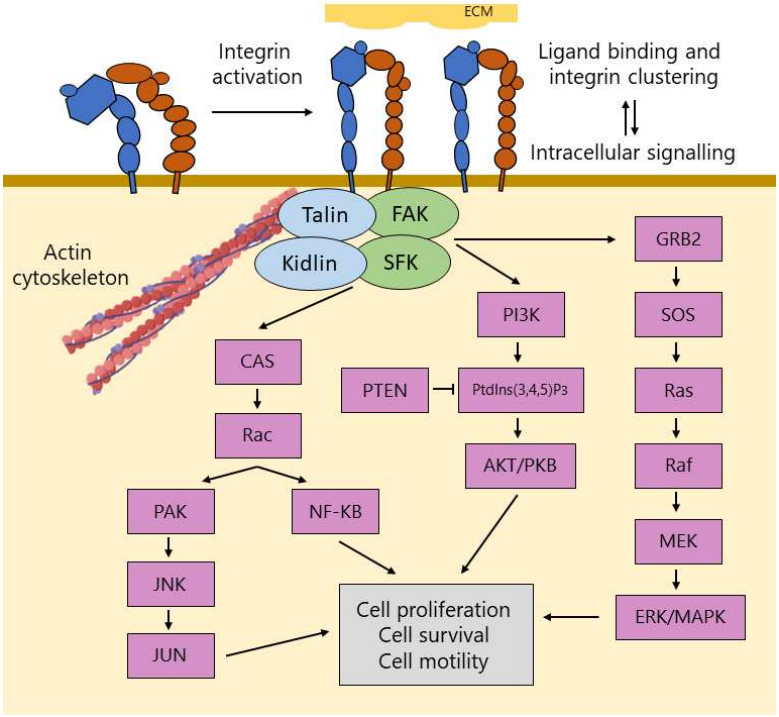

Figure 6. Integrin adaptor proteins and signalling pathways. Ligand binding or intracellular integrin activation induces conformational changes and integrin clustering. Afterward, intracellular downstream signalling can modulate several pathways, including PI3K and MAPK, that eventually regulate cell proliferation, survival and motility.

4.3.2 Inside-out signalling

Integrins can be activated by intracellular signals from G-protein-coupled receptors and other signalling proteins such as talin, kindlin and paxillin (Table 3). These signals induce the phosphorylation of the β cytoplasmic domain, and this leads to conformational changes in the protein structure that modify extracellular ligand affinity.

These conformational changes are not completely understood, although a switch from a bend to an extended integrin position have been described. In the inactive bend form, the α and the β intracellular domains are connected and the ligand-binding pocket is not exposed, thereby impeding

ligand recognition. However, in the extended integrin position, this interaction is dissociated and the binding-pocked is exposed, thereby increasing ligand affinity (Figure 6). Movement of the hybrid domain seems to be also important for the integrin unbending.

Table 3. Integrin cytoplasmic adaptors. Adapted from (66,71,72).

Integrin subunit	Adapter proteins
α1	FABP3, p120RasGAP, Rab21, SHARPIN
α2	FABP3, CIB1, p120RasGAP, Rab21, SHARPIN
α3	FHL3, GIPC1, BIN1, CIB1, FHL2
α4	AP2M1, CIB1, EED, RACK1, paxilin
α5	GIPC1, CIB1, neuropilin-1, nischarin, Rab21, SHARPIN
α6	GIPC1, Rab21
α7	FHL3, FHL2
α8	
α9	Paxilin
α10	FABP3
α11	FABP3, CIB1, Rab21
αV	FHL3, MAPK3, CIB1, RACK1, SHC1
αL	CIB1, SHARPIN
αM	CIB1, SHARPIN
αX	
αD	SHARPIN
αIIb	Filamin A, ICIn, AUP1, CIB1, PP1C, PP2A, RNF181, skelemin
αE	EED
β1	FHL3, filamin A, filamin B, filamin C, Hck, ICAP1, ILK, Kidlin1, Kidlin2, Kidlin3, Lyn, melusin, moesin, MYO1O, 14-3-3, 4.1G, 4.1R, Abl2, ACAP1, CD98, Dab1, Dok1, EPS8, FAK, FHL2, NRK2, paxillin, PKD1, plastin2, PP2A, Rab25, RACK1, RanBP9, SHC1, SNX17, SNX31, talin1, talin2, tensin-1, tensin-2, Yes, α-actinin, myosin, skelemin, MIBP, ICAP1α
β2	Filamin A, Hck, Kidlin2, Kidlin3, Lyn, 14-3-3, Cytohesin-1, Dab1, Dok1, FAK, FHL2, PKC, Plastin2, RACK1, radixin, RanBP9, SNX17, SNX31, SYK, talin1, Yes, α-actinin, JAB1
β3	Filamin A, filamin B, Fyn, Hck, ILK, Kidlin1, Kidlin2, Kidlin3, Lyn, MAPK1, MAPK3, MYO1O, AKT1, CD98 hc, CENP-R, Csk, 14-3-3, CD98, Dab1, Dab2, Dok1, EPS8, FAK1, FAK2, FHL2, numb, paxillin, PDK1, plectin, PTPN1, Rab34, RACK1, SHC1, skelemin, SNX17, SNX31, SRC, talin1, talin2, tensin-1, tensin-2, Yes, α-actinin, myosin, Grb2, IAP
β4	12-LOX, 14-3-3, EIF6, erbin, erzin, RACK1, SHC1, Shp2, BP180, plectin
β5	FRMD5, Kidlin2, MYO7A, MYO1O, Annexin A5, Dab1, Dab2, Dok1, EPS8, FAK1, numb, RACK1, PAK4, SNX17, SNX31, syntrophin1, tensin-2, myosin, TAP20
β6	Filamin A, filamin B, HAX1, Kidlin1, MAPK1, FHL2, SNX17, SNX31
β7	Filamin A, Dab1, Dok1, EED, talin1, tensin-2
β8	4.1B

Besides integrin activation, integrin inactivation is also important to regulate physiological processes in which cell adhesion is involved, for instance cell detachment and migration during embryogenesis. Integrin endocytosis or proteolytic degradation of adaptor proteins are examples of mechanisms of inactivation. Integrin phosphorylation by kinases, such as FAK and Src, also increases the turnover of integrins and integrin-mediated adhesions (66).

4.4 Integrins in cancer

Integrins connect the ECM and the cell cytoskeleton, meaning they are responsible for the interactions between the extracellular and the intracellular microenvironment. They are considered the main cell adhesion receptors and are involved in multiple cell and tissue functions in health, but also in disease.

In physiological conditions, integrins are necessary to maintain, remodel and repair the ECM that is to maintain tissue structural integrity and functionality. Besides tissue homeostasis, integrins also participate in embryo morphogenesis, wound healing, regeneration or immunity. In fact, some integrin knockout mice have perinatal or embryonic lethality, demonstrating integrins have important biological functions during development (64). On the contrary, a dysregulated integrin-mediated adhesion and signalling has been related to many human diseases, such as bleeding disorders, cardiovascular disease, viral and bacterial infection, skin disease and cancer (42,62,66).

Integrin-mediated signalling can modulate gene expression, cell survival, cell proliferation and cell motility, processes which are employed by tumour

cells to promote tumour growth and metastatic spread. In fact, changes in integrin expression have been related to many types of cancer and correlated with some clinical features (Table 4).

Table 4. Alterations in integrin expression and associated features in cancer. Adapted from (42).

Tumour	Integrin	Associated features
Myeloma multiple	β1	Correlation with tumour cell invasion, tumour progression and metastatic disease. Contradictory information about prognostic value.
	β3	Correlation with tumour progression, metastatic disease, and decreased survival.
	α6β4	Inverse correlation with tumour progression.
	αvβ8	Increased expression in brain metastasis, compared with primary tumours.
Breast cancer	β1	Correlation with tumour cell invasion, metastatic disease, decreased survival and therapy resistance.
	α9β1	Correlation with reduced survival and metastasis-free survival. Reported as marker of basal-like subtype and aggressive tumours.
	β3	Increased expression in bone metastasis.
	α6β4	Increased expression in high grade tumours.
	αvβ5	Decreased expression in tumour cells, compared to benign lesions.
	αvβ8	Increased expression in brain metastasis, compared with primary tumours.
Colorectal cancer	αvβ6	Correlation with decreased survival. Expression at the invasion front of tumours.
Lung cancer	α2β1	Associated with therapy resistance, tumour cell angiogenesis and tumour growth.
	α9β1	Correlation with decreased survival in SCLC.
	α11	Overexpression reported as biomarker for NSCLC.
	αvβ5	Increased expression in tumour and stroma-associated cells, but not with survival.
	αvβ8	Increased expression in brain metastasis, compared with primary tumours.
Ovarian cancer	α5β1	Correlation with clinical stage.
	αvβ6	Correlation with disease grade.
Prostate cancer	α2β1	Increased expression in lymphatic metastasis.
	α6β4	Correlation with lymphatic metastasis.
	α7	Downregulated in tumours and associated with recurrence.
	α9β1	Associated with bone metastasis.
Rhabdomyosarcoma	α9β1	Confers increased cell invasiveness.

In addition, and as I have previously mention in Metastasis section, integrins or downstream signalling proteins have been related to almost all the different phases of the metastatic cascade, including local invasion, intravasation and extravasation from vasculature, survival of CTCs and growth in distant organs to form macrometastases (28,42,54,73,74). This points integrins as a potential therapeutic target for cancer treatment and metastasis prevention.

5. Integrin α9β1

5.1 Main traits

Integrin α9β1 is composed by the α9 and the β1 subunits and is included in the leukocyte-specific receptor family of integrins (63). The α9 subunit is codified by the *ITGA9* gene (gene ID: 3680), located at chromosome 3 (locus 3p22.2), while the β1 subunit is codified by the *ITGB1* gene (gene ID: 3688), located at chromosome 10 (locus 10p11.22).

The α9 subunit was first described in 1993 as a novel partner of the β1 subunit in humans (75) and it is expressed in multiple tissues, including epithelial cells, skeletal and smooth muscle, keratinocytes, hepatocytes, neutrophils and osteoclasts (75-77). This subunit has the same protein structure as the other α subunits, including the GFFKR conserved sequence in the cytoplasmic domain. The only particularity of this subunit is that it does not contain the I-domain and consequently, it does not interact with collagen (75). Besides, a short form of the α9 subunit (SFα9) without the transmembrane and the intracellular domains has been also reported. This alternative splice variant constitutes a 632-aa protein with the β propeller,

and the thigh domain followed by a 19-aa sequence at the C-terminus (78) (Figure 7).

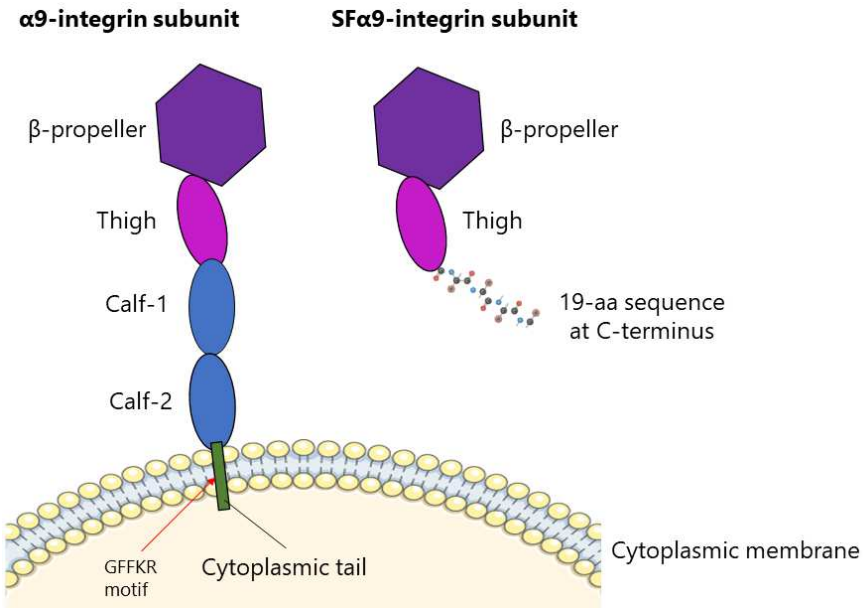

Figure 7. Schematic representation of α9-integrin subunit and its short form. Abbreviations: aa, amino acid; SFα9, short for of the α9 subunit.

The α9 subunit shares about 40% of amino acid identity with the α4 subunit. The percentage of identity between the α9 and the α4 subunits is significantly higher comparing to the identity of the α9 with the other α subunits (18-22%), suggesting that these two α subunits constitute another integrin subfamily (75). In addition, α9 and α4-containing integrins have several common ligands (Table 5), fact that reinforces this idea. Nevertheless, results from *in vivo* studies described different phenotypes for α9 and α4 knockouts, thereby concluding these two integrin subunits have different biological functions. Whereas α4 knockout mice have embryonic lethality due to placental and heart defects (79), α9 knockout

mice have perinatal lethality due to respiratory failure and defects in lymphatic drainage (80-83).

Little is known about the transcriptional regulation of α9 subunit and only a few transcription factors have been reported to directly bind the *ITGA9* promoter gene sequence (NFI, Sp1 and c-Myb) (84). Regulation by Notch pathway (30), Prox1 (85), miR-148a (86) and miR-296-3p (87) have also been described in different tissues.

5.2 Integrin α9β1 extracellular ligands

Integrin α9β1 is located at the cellular membrane, where it interacts with different extracellular ligands, some of them common to other integrins (Table 5). It does not depend on the RGD sequence for ligand recognition and instead of this, it mainly uses the LDV motif (65). The most important α9β1 extracellular ligands are: ADAMs, EMILIN1, FN, OPN, tenascin-C and VEGFs (81,82).

Table 5. ITGA9 extracellular ligands and their function. Adapted from (81,82,88,89).

Extracellular ligand	Functions	Interaction with α4β1
ADAM1	Cell adhesion	
ADAM2	Cell adhesion	√
ADAM3	Cell adhesion	√
ADAM7	Cell adhesion	√
ADAM8	Cell adhesion	
ADAM9	Cell adhesion	
ADAM12	Cell adhesion and myoblast fusion	
ADAM15	Cell adhesion	
ADAM28	Cell adhesion	√
ADAM33	Cell adhesion	√
EMILIN1	Fibroblast and keratinocyte proliferation	√
FN (EDA domain)	Cell adhesion, filipodia formation, matrix assembly and valve morphogenesis	√
FXIII	Cell adhesion	√
L1-CAM	Cell adhesion	
NGF	Cell proliferation	

OPN	Cell migration	√
Plasmin	Cell migration	
pp-vWF	Cell adhesion	√
Tenascin-C	Cell adhesion	
Thrombospondin-1	Cell migration, cell proliferation and angiogenesis	√
tTG	Cell adhesion	√
VCAM-1	Cell adhesion	√
VEGF-A	Cell adhesion and angiogenesis	
VEGF-C	Cell adhesion and cell migration	
VEGF-D	Cell adhesion and cell migration	

5.2.1 A disintegrin and metalloproteinases (ADAMs)

The ADAMs are a family of proteins that participate in the communication between cells and their microenvironment. They interact and participate in the cleavage of cytokines, growth factors and other adhesion molecules, modulating biological processes such as cell signalling, protein processing, ECM remodelling and cell adhesion (88-90).

They are primarily multidomain transmembrane proteins, although soluble forms of ADAM12 and ADAM33 have been described (90-92). The general structure of ADAMs has seven different domains: amino-terminal prodomain, metalloproteinase, disintegrin, cysteine-rich, EGF-like, transmembrane and cytoplasmic domain. Half of this protein family conserves the proteolytic activity of the metalloproteinase domain (93).

The interaction between ADAMs and integrins has been described for several members of this family and as with most of the integrin ligands, a single integrin can interact with several ADAMs and vice versa, a single ADAM can interact with several integrins. The binding of ADAMs to integrins occur through the disintegrin domain. In the case of α9β1, this binding is thought to be mediated by the RX(6)DLPEF motif, present in the

disintegrin loop of ADAM structure. This sequence is conserved in the majority of ADAMs, except for ADAM10 and ADAM17. In fact, there is experimental evidence that prove the binding of ITGA9 to several ADAMs, but not to ADAM10 and ADAM17 (Table 6). The interaction between ADAMs and integrins can modulate their function, both inhibiting and promoting it. This has been reported to have consequences in cell behaviour, for example in cell migration or cell-cell adhesion, and has been related to a variety of biological conditions, such as myogenic differentiation and cancer (81,88).

The upregulation of ADAMs has been described in several tumour tissues (Table 6), as well as the correlation with more aggressive tumours. For example, ADAM expression has been detected in the invasive front of tumours and the surrounding stroma, suggesting that this family of proteins may be involved in tumour invasion (89).

Table 6. ADAMs able to interact with ITGA9 and reported overexpression in cancer cells. Adapted from (88,89).

	Interaction motif	Proteolytic activity	Overexpression in cancer cells	Reference
ADAM1	RX(6)DLPEF			(94)
ADAM2	RX(6)DLPEF			(94)
ADAM3	RX(6)DLPEF			(94)
ADAM7	Unknown			(95)
ADAM8	Unknown	√	Lung, brain, pancreas, and kidney	(77)
ADAM9	RX(6)DLPEF	√	Breast, pancreas, liver, lung, prostate and stomach	(94)
ADAM12	RX(6)DLPEF	√	Breast, liver, brain, stomach, bladder, and colon	(96)
ADAM15	RX(6)DLPEF	√	Lung, breast, prostate, and stomach	(94),(96)
ADAM28	Unknown	√	Lung, breast, and kidney	(95)
ADAM33	Unknown	√		(95)

α9β1 is considered the main receptor for ADAM12. Although few studies have focused on the direct interaction between ADAM12 and α9β1, a co-expression and co-immunoprecipitation of these two proteins was proven during *in vitro* differentiation of human myogenic cells (97). The interaction between these two proteins is highly dependent on the cellular context since it has been demonstrated that ADAM12 preferentially binds to α9β1, but when this integrin is not expressed or when the interaction motif of the α9β1 is mutated, ADAM12 can also interact with other β1 or β3-containing integrins, such as α7β1 (98-100).

ADAM12 was first identified in 1998 as being involved in muscle cell fusion (91). It is one of the proteolytic members of the family and two different forms of this protein have been described: the membrane-bound form (ADAM12-L), which contains all the domains mentioned above, and the secreted form (ADAM12-S), which lacks the transmembrane and cytoplasmic domains. ADAM12 is expressed in healthy tissues that are characterized by cell fusion, growth, or frequent repair such as cartilage, bone, muscle, adipose tissue, liver, uterine and brain tissues. In these tissues, ADAM12 has been involved in cell adhesion and fusion, ECM remodelling and cell signalling.

ADAM12 expression has also been well characterized in cancer. Overexpression of ADAM12 has been detected in several tumours and it correlated with clinical stage, presence of metastasis or poor patient prognosis in a wide range of tumours, including breast cancer, bladder cancer and lung adenocarcinoma. On the contrary, an inverse correlation between ADAM12 and tumour grade has been also described for brain tumours.

Studies have shown that ADAM12 support α9β1-dependent cell adhesion and migration in cancer cells (101,102), and can directly interact with integrin downstream mediator FAK, promoting also cell migration and invasion (103). In addition, the cleavage of ECM components by ADAM12, including gelatin, type IV collagen and fibronectin, has been reported, suggesting that ADAM12 could contribute to cancer spreading by digestion of ECM surrounding tumour cells (90,104).

5.2.2 Other extracellular ligands

Elastic microfibril interface-located protein 1 (EMILIN1)

EMILIN1 is a glycoprotein able to interact with α9β1 and α4β1 integrins. EMILIN1 and α9β1 are expressed in lymphatic endothelial cells and knockout mice for both proteins exhibit defects in lymphatic structures, suggesting that their interaction is important for lymphatic morphogenesis during embryonic development (81).

Fibronectins (FNs)

FNs are a family of essential glycoproteins that are present in the ECM, connective tissues, basal membranes, and some body fluids. They have been related to cell adhesion and cell migration during embryonic development, wound healing and tumour progression, due to their ability to interact with collagen, fibrin and integrins, among other cellular ligands (105).

FNs exist in two different forms: the cellular FN (cFN) and the plasma FN (pFN). In turn, the cFN can have different variant segments: the extra domain A (EDA) and the extra domain B (EDB). The EDA domain (through

the EDGIHEL sequence) allows the interaction of cFN with α9β1 and α4β1 integrins (81,105). This interaction has been related to filipodia formation (105) and EMT transition in lung cancer (106).

Tenascin-C

Tenascin-C is an ECM protein able to interact with many integrins, including α9β1 (through the AEIDGIEL sequence in Tenascin-C). This protein seems to be upregulated during wound healing, in tumour stroma and has been reported to be upregulated in metastatic melanoma (81).

Osteopontin (OPN)

OPN is a cytokine able to interact with many integrins, including α9β1 and α4-containing integrins. The interaction between OPN and α9β1 has been related to chemotaxis and immune responsiveness (81).

Vascular endothelial growth factors (VEGFs)

Different members of the VEGF family bind to α9β1 with different effects on cell migration and proliferation, this seems to be especially important in endothelial cells where it controls lymphangiogenesis and angiogenesis. Enhanced cell migration has been reported after the interaction between VEGF-A and α9β1 in endothelial and cancer cells. On the contrary, interactions with VEGF-C and VEGF-D contribute to proliferation of endothelial cells and consequently to angiogenesis and lymphangiogenesis (81,107).

5.3 Integrin α9β1 activation and intracellular signalling

Like other integrins, studies suggest that α9β1 can be found in different activation states and this can be modulated by extracellular ligand recognition (Table 2) and intracellular adaptor proteins (Table 3). At least, two different activation states have been suggested for α9β1 and they are associated with different cellular behaviour in terms of cell adhesion and motility (81).

After α9β1 activation, conformational changes occur and this allows the binding of intracellular adaptor proteins, such as Tallin, that connect this protein with the cytoskeleton architecture. This causes the clustering of integrins and the activation of intracellular signalling. Integrin α9β1 activation of FAK and Src tyrosine kinases is one of the first signalling associated events. Then, FAK undergoes auto-phosphorylation at Tyr397, which promotes binding to Src, and forms the FAK-Src tyrosine kinase complex which is responsible for the activation of multiple proteins including the small GTPases Rac-1 and Cdc42, both related to enhanced proliferation, survival and motility (108). Activation of MAPK-related proteins and other well-known pathways such as PI3K-Akt have been proposed, although more studies addressing their activation and the corresponding effects on cell behaviour are still needed. On the contrary, activation of α9β1 has been associated with other particular pathways such as iNOS (inducible nitric oxide synthase) (109) and the catabolism of spermidine and spermine that regulates potassium channels (110,111). Activation of these signalling pathways seems to enhance cell motility, although the underlying mechanisms are still not clear (107).

5.4 Integrin α9β1 in cancer

Like other integrins, α9β1 interacts with elements of the microenvironment to generate bidirectional signals that control cell proliferation and motility, among other processes. The tumour microenvironment provides a huge number of these elements and cancer cells exploit integrins and their signalling to enhance tumour growth and metastatic dissemination.

Unfortunately, there is no abundant data on α9β1 cancer cell expression, but dysregulation of α9β1 expression has been described in some cancers. α9β1 is upregulated in small-cell lung cancers (112), medulloblastoma (113), high-grade glioblastoma (114) and colon adenocarcinomas (115). On the contrary, *in silico* analysis showed that α9β1 is downregulated in bladder cancer, CNS tumours, leukaemia and liver cancer (116,117). On the other side, heterogeneous expression of α9β1 has been observed in breast tumour samples: while increased expression of α9β1 has been associated with basal-like subset of patients (118,119), absent or decreased expression due to gene promoter hypermethylation has also been reported (120,121).

Gene expression inactivation by promoter hypermethylation has not only been detected in breast tumours (44% of analysed samples) (120), but in several cancers including renal, ovarian, lung and prostate cancer (>40% of analysed samples) (81), and head and neck squamous cell carcinoma (>20%) (122). In addition, deletions of α9β1 gene have been detected in renal, breast, lung (123) and cervical cancer (>40%) (124). Although multiple mutations in α9β1 integrin have been annotated in the Catalogue of Somatic Mutations in Cancer (COSMIC), they are much less frequent than deletions or alterations in the methylation profile, suggesting that

mutations of this protein are less important for tumour progression. Other epigenetic regulators of α9β1 integrin, such as miRNAs, have been also reported. Inhibition of α9β1 by expression of miR-125b, miR-296-3p and miR-148a and subsequent modulation of cell proliferation, apoptosis and invasion has been described in melanoma (82,87) and glioblastoma (125).

Integrin α9β1 has been related to reduced overall survival and metastasis-free survival of breast cancer patients, especially of those of the basal-like subtype (118,119). High expression of α9β1 has also been associated with worse overall survival in small-cell lung (126), colorectal and oesophagus cancer, and acute myeloid leukaemia, while it has been associated with increased survival in lung cancer and multiple myeloma (116). Altogether, this suggest that in certain types of cancer α9β1 could act as a tumour suppressor or pro-oncogenic gene (81,82). Nevertheless, most of the available bibliography and studies addressing the role of α9β1 in controlling cancer cell behaviour point to a preponderant role of this protein in promoting tumorigenic and invasive behaviour. As a matter of fact, α9β1 expression has been related to increased cell proliferation, migration, invasion and EMT and consequently, to enhanced tumour growth and metastasis, in a variety of tumour types, including breast cancer, melanoma, glioblastoma and rhabdomyosarcoma among others. These effects are mediated by activation of intracellular kinases FAK and Src that modulate other intracellular pathways such as iNOS, β-catenin or PI3K-Akt (30,106,109,118,119,125-127).

Our group has reported that α9β1 expression, under the regulation of Notch pathway, confers a higher invasive phenotype to RMS cells (30). Similarly, enhanced cell migration has been described after α9β1

overexpression in colon cancer cells, as consequence of iNOS and Rac-1 activation by Src kinase (109). Studies have shown that expression of α9β1 also induces changes consistent with EMT (downregulation of E-cadherin, upregulation of N-cadherin and vimentin, etc.) in breast, lung, and colon cancer cells due to stabilization of β-catenin. According to these studies, α9β1 activation prevents the proteasomal degradation of β-catenin by direct interaction and stabilization of the complex between β-catenin and E-cadherin (126), or by inhibition of GSK3 kinase activity, which mediates the phosphorylation of β-catenin that precedes its ubiquitination and proteasomal degradation (119). In addition, activation of α9β1 by binding of EDA fibronectin domain has been reported to promote EMT via activation of FAK, PI3K pathway and Rac-1 (106,128). These expression changes enhance cell migration and invasion and promote tumour growth and metastasis *in vivo*.

Finally, besides the described effects on tumour cells, studies have confirmed that α9β1 can also influence endothelial cells and induce angiogenesis and lymphangiogenesis due to the interaction with VEGFs and EDA fibronectin domain and subsequent activation of FAK and Src kinases (129-132). This facilitates nutrient and oxygen supplies for tumour growth and metastatic dissemination of invading cells.

To sum up, there is increasing evidence that supports an essential role of α9β1 at different stages of tumour progression and metastatic spreading. Thus, the main focus of this thesis is to study the role of α9β1 in metastasis and the effects of its downregulation or blockade. For this purpose, three different tumour models will be studied: rhabdomyosarcoma, the most prevalent soft tissue sarcoma in children, neuroblastoma, the most common

extracranial solid tumour in children, and breast cancer, the most frequent cancer in women and worldwide. These three cancers have a different cell of origin and affect different tissues and populations. Nevertheless, they have one trait in common: although they have a good general overall survival, a subset of patients develop metastasis and this drastically worsens their survival rates.

Previous studies of the group have addressed the role of α9β1 integrin in rhabdomyosarcoma and neuroblastoma, pointing to a preponderant role of this protein in the biology of metastasis. In addition, there are studies that suggest a crucial role of this integrin also in breast cancer. Therefore, developing strategies to inhibit the expression of α9β1 integrin in these neoplasia seems to be a good therapeutical option to prevent or reduce their metastatic dissemination.

Next sections will summarize the main clinical and molecular features of these three cancers in order to get a detailed picture of the current situation of these diseases and their pending clinical needs.

6. Rhabdomyosarcoma

6.1 Epidemiology

Rhabdomyosarcoma (RMS) is the most frequent soft tissue sarcoma[2] in children and adolescents, although it is still a rare disease. It is a high-grade malignancy that accounts for approximately 3% of all childhood cancers

[2] Soft tissue sarcomas (STS): group of tumours derived from cells of the mesoderm that undergo pathological transformation. These cells can give rise to multiple tissues, including bones and muscles, so STS can be found in multiples body locations (350).

and is extremely rare in adults, being less than 1% of all cancers (133,134). This is translated into approximately 30 new cases per year in Spain (6).

Data from several groups showed that RMS incidence is influenced by sex, ethnicity, tumour histology and age. Male children have a higher incidence of RMS than female children and children with Hispanic parents have a lower incidence of RMS compared to other ethnicities (134). Histology and age effects will be described on the following section.

Some genetic disorders have also been associated to RMS, this includes Li-Fraumeni syndrome (mutations in *TP53*), neurofibromatosis type I (deletions in *NF1*), Costello syndrome (mutations in *HRAS*), Noonan syndrome (mutations in *RAS-MAPK* pathway), Beckwith-Wiedemann syndrome and DICER1 syndrome (mutations in *DICER1*). However, only a small percentage of patients with RMS have one of these genetic disorders. In addition, other environmental risk factors have been reported such as prenatal X-ray exposure, maternal or paternal drug use, vaginal bleeding during pregnancy, premature birth, birth defects or relatives with RMS (134).

Improvements in early detection and treatment have increased RMS survival in the last 30 years. Currently, 5-year survival is around 70% (6,134), although the development of metastasis continues being a key factor that drastically worsen this prognosis. Survival of metastatic RMS is under 40%, making metastatic RMS one of the solid tumours with worse prognosis in children (135).

6.2 Clinical presentation and diagnosis

The clinical presentation of RMS can be very variable since it can arise anywhere in the body. The most frequent locations are the head and neck region (which includes orbital, parameningeal and non-parameningeal areas), the genitourinary tract and the extremities (Figure 8). In addition, between 15% and 25% of patients present distant metastases in the initial diagnosis. The most common sites of metastasis are bone, bone marrow, lung and lymph nodes. The signs and symptoms of RMS are also very variable, they depend basically on the tumour location and size, and usually are the result of the compression or invasion of tumour-surrounding areas (134,136).

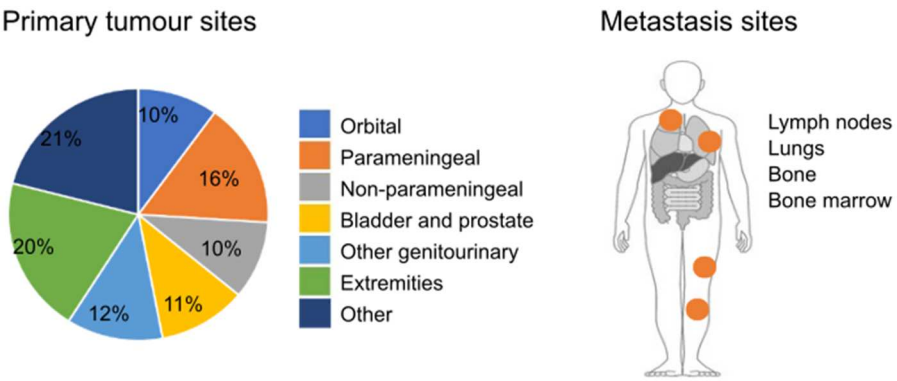

Figure 8. Most frequent RMS locations and sites of metastasis. Adapted from (136).

The diagnosis of RMS patients needs to accurately assess location, size, and disease extension. For this purpose, several diagnostic tests are applied, including imaging techniques, immunohistochemical staining and molecular assays (summarized in Table 7). Once clinical, histological, and molecular characteristics of the tumour are determined, patients can be

stratified into different risk groups and receive the most favourable treatment according to that (risk-adapted therapy).

Table 7. Procedures for RMS diagnosis (136,137).

1.	Detection of primary tumour location and size.
	• MRI scan • CT scan • Ultrasounds scan
2.	Histological and molecular studies after biopsy.
	• Morphology assessment: RMS cells normally resemble developing skeletal muscle. • IHC staining: RMS cells are typically positive for desmin, myogenin, MYOD1 and muscle-specific actin staining. • FISH: detection of chromosomal translocations. • RT-PCR: detection of specific fusion transcripts.
3.	Evaluation of the extent of the disease.
	• Cross-sectional MRI or CT scan to assess lymph node affection. • Whole body FDG-PET or MRI scan to detect distant metastases. • CT of chest to detect pulmonary metastases. • Bone marrow aspirates to detect bone marrow metastases. • Neuroimaging and cerebrospinal fluid cytology to assess CNS disease extension in patients with parameningeal tumours. • CT scan of the abdomen and pelvis for patients with lower extremity or genitourinary primary tumours.

*Abbreviations: MRI, magnetic resonance imaging; CT, computerized tomography; RMS, rhabdomyosarcoma; IHC, immunohistochemistry; FISH, fluorescence in situ hybridization; RT-PCR, real time PCR; FDG-PET, fluorodeoxyglucose positron emission tomography; CNS, central nervous system.

6.3 Classification and genetic alterations

The International Classification of Rhabdomyosarcomas (ICR) was established in 1995 and divided RMS in 4 different categories, according to the histology and the prognosis: botryoid and spindle cell RMS, with good prognosis, embryonal RMS with intermediate prognosis, and alveolar RMS with poor prognosis.

In 2013, the WHO published a revised Classification of Tumours of Soft Tissue and Bone that include some modifications in the RMS classification.

The botryoid subtype was eliminated and included into the embryonal RMS division, and spindle cell/sclerosing RMS subtype was introduced (138,139). This classification was also based on the histological tumour characteristics and each category was associated with certain clinical and molecular features (Table 8). The two main histopathological subtypes in children are embryonal (ERMS) and alveolar (ARMS) RMS, followed by the pleomorphic (PRMS) and spindle/sclerosing (SRMS) RMS, which are rare in children.

Table 8. Histopathological classification of RMS and molecular and clinical features (134,140).

RMS subtype	**Molecular features**	**Main location**	**Age**	**Prognosis**
Alveolar (ARMS) 20%	Balanced chromosomal translocations involving PAX3/PAX7 and FOXO1 locus (80% of ARMS)	Extremities, head and neck regions and torso	Children and young adults (between 10 and 25 years)	Unfavourable
Embryonal (ERMS) 60%	LOH in chromosome 11 and gains in chromosomes 2, 7, 8, 11, 12, 13 and 17	Genitourinary tract, head and neck regions	Children under 10 years	Favourable
Pleomorphic (PRMS) 10%	Complex karyotypes	Extremities, chest and abdomen	Adults over 60	Unfavourable
Spindle/ Sclerosing (SRMS) 10%	*NCOA2* gene rearrangements and mutations in *MYOD1*	Paratesticular in children and head and neck in adults	Children under 10 years and adults over 40	Favourable in children

The ERMS subtype is the most frequent and represents around 60% of all RMS cases. It normally appears in children under 10 years and has a good general prognosis. The most common locations for this subtype are the genitourinary tract and the head and neck regions. Histologically, it is recognized for the presence of small, round tumour cells with hyperchromatic nuclei and loose myxoid stroma (140). From a molecular point of view, ERMS are characterized by a wide range of genetic alterations including loss of heterozygosity (LOH) on the short arm of chromosome 11 (141) and gains in chromosomes 2, 7, 8, 11, 12, 13 and 17 (142). LOH of the

chromosome 11, usually affects the locus 11p15.5, where is located the Insulin Growth Factor II (*IGF2*) gene. ERMS have a higher mutation burden compared to the ARMS subtype and several non-synonymous mutations have been detected. The most recurrent ones are mutations in the *RAS* family (*NRAS, KRAS* and *HRAS*) but also in genes related to the RAS-PI3K pathway, such as *NF1* (Neurofibromin 1) and *PI3KCa* (Phosphoinositide-3-Kinase Catalytic subunit α). Other tyrosine kinases and cell cycle related genes are also frequently mutated, including *FGFR4* (Fibroblast Growth Factor Receptor 4) and *FBXW7* (F-Box and WD repeat domain containing 7). Finally, mutations in *TP53*, mutations in the chromatin modifier *BCOR* (BLC6 corepressor) and focal amplifications affecting the *MDM2* gene have also been detected in high frequency. What is more remarkably is that the one-third of patients with ERMS have activating mutations directly or indirectly related to the RAS pathway (134,143,144).

On the other hand, ARMS subtype represents around 20% of RMS cases and usually appears in children and young adults (between 10 and 25 years). The most frequent locations for this subtype are the extremities, although it can also arise in the head and neck regions and the torso. Histologically, is characterized by undifferentiated round tumour cells, separated by fibrous tissue. This subtype is associated with a poorer prognosis and in the 80% of cases to a balanced chromosomal translocation involving paired box gene 3 or 7 (*PAX3* or *PAX7*) and the forkhead box O1 (*FOXO1*). These chromosomal translocations generate the anomalous fusion genes *PAX3-FOXO1* (60% of ARMS) or *PAX7-FOXO1* (20% of ARMS) (145,146) and their presence is associated with unfavourable prognosis, especially *PAX3-FOXO1*. A small portion of ARMS patients have other variants of the fusion genes such as *PAX3-NCOA1* (Nuclear receptor Co-Activator 1) or *PAX3-*

INO80D, but their clinical relevance is still unclear. Finally, approximately 20% of ARMS patients do not show any recurrent chromosomal translocation and are considered fusion-negative ARMS (FN-ARMS). This subset of patient shows similar genetic alterations and expression profiles to the ERMS subtype (143) and a more favourable prognosis. In fact, in some recent studies and treatment protocols fusion status is gradually replacing histology criteria since it better classifies patients according to their risk and prognosis (134,140). ARMS subtype is characterized by a lower mutation burden and mutations in the RAS pathway are not detected. However, focal amplifications affecting *MYCN* and *CDK4* (Cyclin Dependent Kinase 4) genes have been detected in fusion positive ARMS (FP-ARMS) patients, as well as mutations in *ARID1A*, *ROBO1* and *GAB1* (143,144).

The fusion genes *PAX3-FOXO1* and *PAX7-FOXO1* combine the DNA-binding domain of the *PAX3* or *PAX7* genes (located in chromosomes 2 and 1, respectively) and the transcriptional activating domain of the *FOXO1* gene (located at chromosome 13). Therefore, the fusion protein that is generated is a transcription factor that binds to PAX3 or PAX7 DNA binding sequences but has an enhanced transcriptional activity due to the FOXO1 activating domain (9) (Figure 9). Some downstream targets of the fusions are *ALK*, *FGFR4, MYCN, MYOD1*, *MYOG*, *CXCR4* and *MET* genes. *PAX3* and *PAX7* are expressed in skeletal muscle progenitors and the presence of these fusion proteins has been related to ARMS pathogenicity. Indeed, they are related to dysregulation of multiple cellular pathways that result in oncogenic effects, including increased cell survival, proliferation, motility, differentiation, and anchorage independent growth. These fusion proteins have multiple phosphorylation sites and are post-transcriptionally regulated by other proteins such as AKT, PLK1 and KAT2B. In addition, they

interact with chromatin-related proteins such as BRD4 and CHD4, suggesting a complex regulation and network with many oncogenic pathways (134,147).

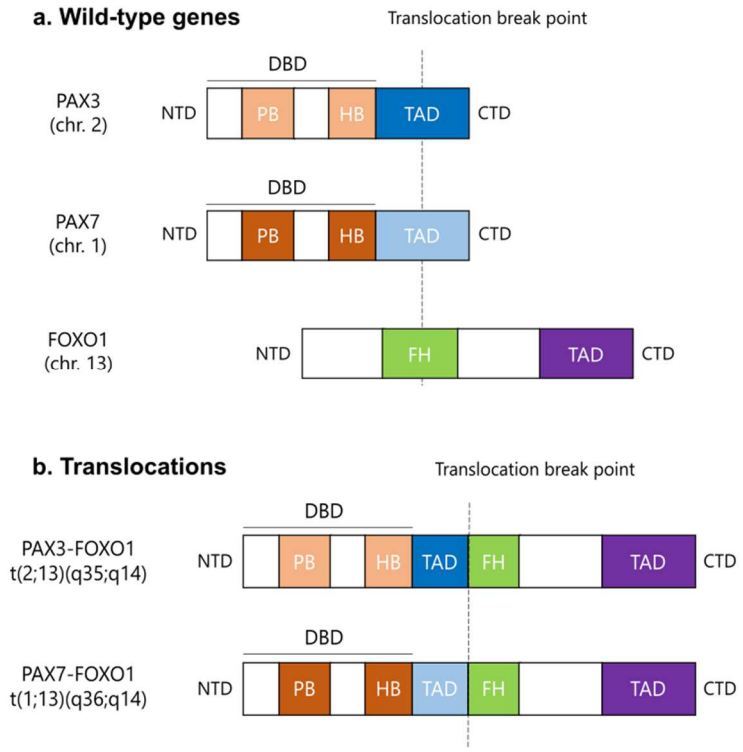

Figure 9. Recurrent chromosomal translocations in ARMS. Adapted from (134). **a.** Structure of wild-type genes. **b.** Structure of the fusion genes PAX3-FOXO1 and PAX7-FOXO1. Abbreviations: CTD, carboxy-terminal domain; DBD, DNA-binding domain; FH, forkhead-related domain; FOXO1, forkhead box O1; HB, homeobox domain; NTD, amino-terminal domain; PAX, paired box gene1; PB, paired box domain; TAD, transcriptional activation domain.

The PRMS subtype is exceedingly rare in children and normally appears in adults over 60 years. Morphologically, it is characterized by cells with skeletal muscle lineage commitment or differentiation, and from a molecular point of view has complex cytogenetic and chromosomal abnormalities (134).

Finally, the SRMS subtype represents about 10% of RMS cases in children and usually appears during the first decade of life and in the paratesticular region. Histologically, it is characterized by relatively differentiated spindle cells with features like smooth muscle tumours. Gene rearrangements involving *NCOA2* gene have been detected in this subtype and are associated with a good prognosis. In addition, mutations in *MYOD1* have also been detected and are associated with poorer prognosis in SRMS patients (134,140).

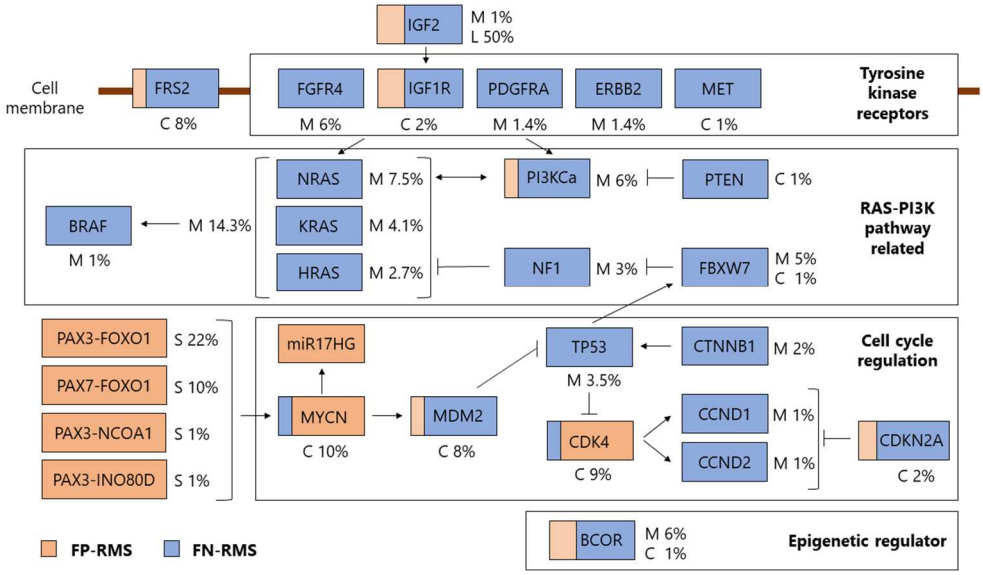

Figure 10. Most frequent alterations in RMS. Adapted from (143). Abbreviations: FP-RMS, fusion-positive rhabdomyosarcoma; FN-RMS, fusion-negative rhabdomyosarcoma; C, copy number variation; L, loss of heterogeneity; M, mutation; S, structural variation.

6.4 Origin

RMS cells partially resemble developing skeletal muscle to some extent and for example, they express proteins related to the myogenic lineage, such as MYOG or MYOD1. In addition, RMS typically arises in or near muscle beds, suggesting that RMS could be originated from aberrant skeletal muscle

differentiation. Nevertheless, RMS also appears in areas that lack skeletal muscle, such as the biliary and the genitourinary tract, and cases of atypical RMS with widespread tumour infiltration to the bone marrow, but absence of any detectable primary tumour have been reported (148-150). These cases suggest that other cellular sources, different from the progenitor muscle cells, may give rise to RMS. Besides, the fact that RMS has two main histopathological subtypes with markedly distinct clinical and molecular features, reinforces the possibility that RMS subtypes can be originated from different cells of origin and by different biological mechanisms. Several experimental groups have addressed this question and multiple works trying to decipher RMS origin have been published (151,152).

Since the most accepted theory of RMS origin is that it is originated by an incomplete skeletal muscle differentiation, studies on normal skeletal muscle development have been used for the identification of RMS-initiating cells. In the embryo, mesodermal cells generate myogenic precursor cells, the majority of whom differentiate into skeletal muscle cells. However, a subset of these precursor cells escapes from terminal differentiation and originates the satellite cells which act as myogenic precursors to allow muscle regeneration and growth after birth (153). *In vivo* studies revealed that KRAS-induced ERMS in zebrafish have a subset of cells that resemble to muscle stem cells and have an expression profile similar to satellite cells (154). In addition, an elevated PAX7 and MET expression have been described in ERMS primary tumours, but not ARMS tumours. Since PAX7 is necessary for the specification and maintenance of satellite cells, these results reinforce the possible role of myogenic satellite cells in the origin of ERMS subtype (155).

Other proposed RMS-initiating cells are the mesenchymal stem cells (MSCs), which are mesodermal cells which are not yet committed to the myogenic lineage and give rise to multiple cell types, including skeletal muscle, adipocytes, and osteoblasts. These cells are not limited to one organ and circulate between them, providing a possible explanation for RMS affecting regions where there are no muscles and the atypical RMS. Studies using mouse MSCs revealed that after induced expression of PAX3-FOXO1 or PAX7-FOXO1 fusion proteins and mutations in *TP53*, mice developed tumours that resemble ARMS. This suggests that ARMS subtype may be originated from the malignant transformation of MSCs after the accumulation of more than one genetic alteration (156). Nevertheless, ARMS tumours in mice have been developed also after induced expression of PAX3-FOXO1 in differentiating myoblasts expressing Myogenic Factor 6 (MYF6). This suggests that this subtype may also be originated after the dedifferentiation of mature muscle cells (157).

Finally, a model of FN-RMS affecting the head and neck region was recently published. In this case, FN-RMS was originated from endothelial progenitor cells and as a consequence of aberrant Hedgehog pathway activation mediated by SmoM2 (constitutively active Smoothened). Therefore, endothelial cells (that have a common multipotent progenitor with myogenic precursors) could be another possible cell of origin for RMS (158).

In summary, it seems that there is not a unique cell of origin for RMS. Instead, multiple biological mechanisms of malignant transformation have been described and this concurs with the different RMS subtypes, suggesting a relationship between their molecular characteristics and their origin (Figure 11).

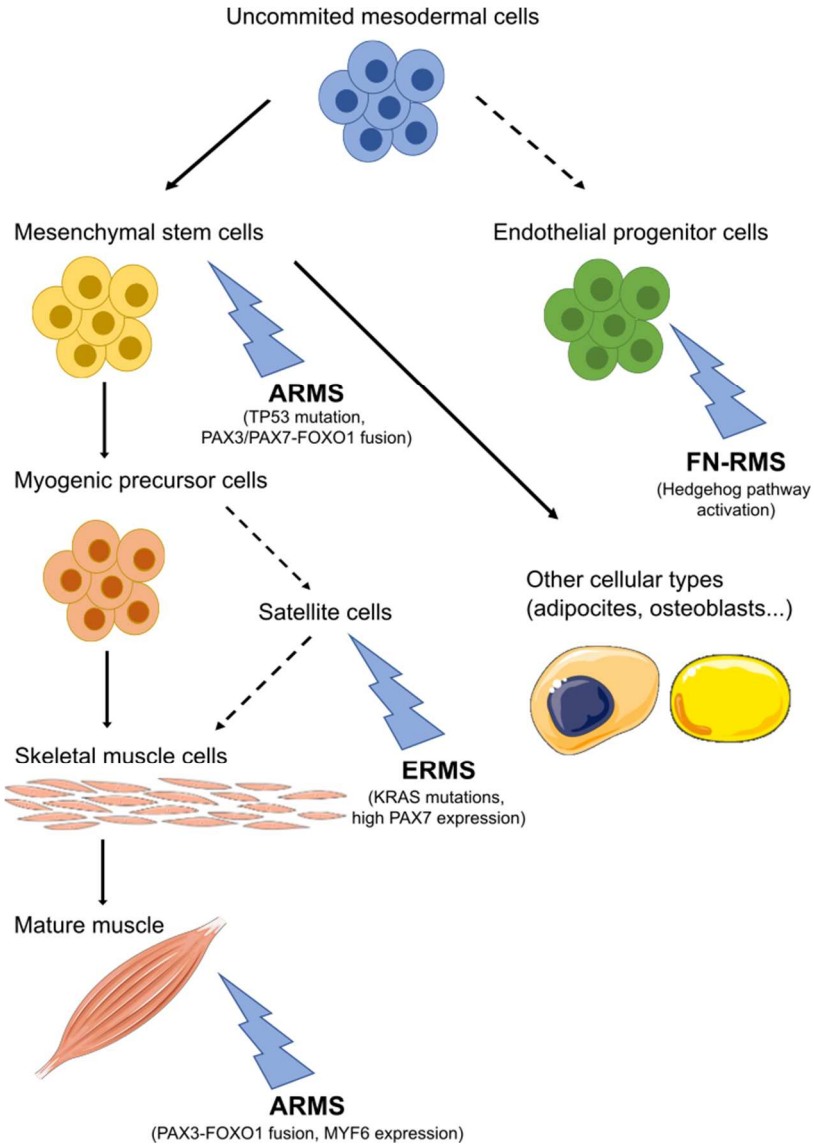

Figure 11. Possible RMS cells of origin and molecular alterations involved in tumorigenesis.

6.5 Prognostic factors and risk stratification

The most important prognostic factors for RMS patients are tumour location and size, age, histology or fusion status, lymph node dissemination and presence of metastases (Table 9). According to these clinical,

pathological, and molecular features, RMS patients can be divided into different risk groups that will determine their prognosis and the most appropriate treatments to achieve the best outcome and minimize late effects. Besides, this classification is also used to allocate patients into open clinical trials.

Table 9. Prognostic factors and clinical relevance (136).

Tumour location	Favourable: orbit and non-parameningeal head and neck region, and genitourinary sites.
	Unfavourable: extremities and parameningeal sites.
Tumour size	Favourable: <5 cm
	Unfavourable: >5 cm
Age	Favourable: <10 years
	Unfavourable: > 10 years
Histology (and fusion status)	Favourable: ERMS, FN-ARMS and SRMS.
	Unfavourable: FP-ARMS and PRMS.
Lymph node status	Favourable: no evidence of lymph node involvement.
	Unfavourable: evidence of lymph node involvement.
Metastasis	Favourable: no evidence of metastasis or non-regional lymph nodes involvement.
	Unfavourable: evidence of distant metastasis or involvement of non-regional lymph nodes.

Taking all these prognostic factors into account, different systems of risk stratification have been established. The most frequently used is the division in clinical groups described by the Intergroup Rhabdomyosarcoma Study (IRS) for the first time in 1988 (159). This classification is applied after primary surgery and considers the prognostic factors mentioned before and the degree of surgical resection (160) (Table 10).

Finally, another system for patient risk stratification is the TNM (Tumour, Node, Metastasis; Table 11), which is a pre-surgery classification that considers the extent of the disease, the involvement of local and regional lymph nodes and the presence or absence of distant metastases (136).

Table 10. Clinical group classification by the IRS (136,160).

Group 1	Localized disease, completely excised, no microscopic residual.
A	Confined to site of origin and completely resected.
B	Infiltrating beyond site of origin, but completely resected.
Group 2	Macroscopic complete resection with regional disease spread.
A	Localized disease with evidence of microscopic local residual.
B	Regional disease with involved lymph nodes, but completely resected with no microscopic residual
C	Regional disease with involved lymph nodes. Microscopic local and/or nodal residual.
Group 3	Incomplete resection or biopsy with macroscopic residual and/or lymph nodes affected and not removed.
A	Localized or regional disease after biopsy.
B	Localized or regional disease after surgery.
Group 4	Distant metastases present or non-regional lymph nodes involved.

Table 11. TNM classification of RMS. Adapted from (136,160).

Stage	Location	Tumour (T)	Lymph nodes (N)	Metastases (M)
I	Orbit, non-parameningeal region, non-bladder, and non-prostate genitourinary areas.	T1 or T2	N0, N1 or Nx	M0
II	Parameningeal area, bladder, prostate, extremities and other.	T1 or T2	N0 or Nx	M0
III	Parameningeal area, bladder, prostate, extremities and other.	T1 or T2	N0, N1 or Nx	M0
IV	All	T1 or T2	N0 or N1	M1

* Abbreviations: T1, tumour confined to organ or tissue of origin; T2, tumour not confined to organ or tissue of origin; N0, no evidence of lymph node involvement; N1, evidence of regional lymph node involvement; Nx, unknown regional lymph node involvement; M0, no evidence of metastases or non-regional lymph nodes; M1, evidence of distant metastasis or involvement of non-regional lymph nodes.

6.6 Treatment

Children with RMS receive multifaceted therapies that combine surgical tumour resection, radiotherapy and multi-agent chemotherapy. The therapeutic approach that each patient receive depends on the risk

stratification protocols and patient specific characteristics (tumour location and size, age, presence of other comorbidities, etc.).

Local disease control is normally the first part of the treatment and usually consists of surgical primary tumour resection and radiotherapy. Surgical resection is only applied when it will not result in functional compromise or organ dysfunction, for this reason it is not extensively used in patients with orbital or genitourinary tumours. When surgical procedures can be compromising, neoadjuvant chemotherapy is previously applied to reduce the primary tumour mass and facilitate the extirpation. Complete resection is achieved when all primary tumour and a surrounding normal area are removed. Regarding radiotherapy, dose is adjusted depending on the site of primary tumour, the residual disease after surgery and other risk factors to avoid late effects, such as skeletal muscle or soft tissue changes, skeletal growth problems or secondary malignancies. This is especially important in patients under 3 years (134,137,161).

After local disease control, all RMS patients should receive adjuvant chemotherapy, although intensity and duration vary according to the characteristics of the patient. Studies with sensitive molecular techniques have demonstrated that almost all patients have disseminated tumour cells in peripheral blood or bone marrow (162), and chemotherapy should be applied to avoid recurrence after local therapy.

The main chemotherapeutic regimen consists of vincristine, actinomycin D and either cyclophosphamide or ifosfamide (VAC or IVA regimens), although other chemotherapeutic agents, such as doxorubicin, irinotecan or etoposide can be included in regimens of high-risk patients (134,137).

Most of them are alkylating agents that produce DNA strand-breaks or impair cell division, affecting proliferative cells, such as tumour cells, but also normal ones (Table 12). Therefore, they can produce important side effects (neurotoxicity, nephrotoxicity, infertility or secondary malignancies), especially in growing children (136).

Table 12. Mechanism of action of the principal chemotherapeutic agents used in RMS treatment (163).

Agent	Mechanism of action
Vincristine	It is and alkaloid isolated from Vinca Rosea. It interacts with tubulin and inhibits microtubule formation in mitotic spindle, resulting in the arrest of dividing cells.
Actinomycin D	It binds to DNA and inhibits RNA synthesis and transcription. As a result, mRNA production and protein synthesis are impaired.
Cyclophosphamide	It is an alkylating agent that must be activated in the liver to form the active aldophosphamide. It attaches to the DNA bases, resulting in separation of double-helix strands and DNA fragmentation. Consequently, DNA synthesis, RNA transcription and protein synthesis are impaired.
Ifosfamide	Synthetic analogue of cyclophosphamide that must be activated in the liver. It attaches to DNA bases, resulting in DNA fragmentation. As a result, DNA synthesis, RNA transcription and protein synthesis are impaired.
Doxorubicin	It is a cytotoxic antibiotic that binds to DNA and inhibits RNA synthesis and transcription. As a result, mRNA production and protein synthesis are impaired. In addition, it inhibits the action of topoisomerase II and induces double-strand DNA breaks.
Irinotecan	It inhibits the action of topoisomerase I and prevents the religation of the DNA strand, causing double-strand DNA breaks. Accumulated breaks in DNA prevent the entry into the mitotic phase of cell division and lead to cell death.
Etoposide	It inhibits the action of topoisomerase II and induces double-strand DNA breaks. Accumulated breaks in DNA prevent the entry into the mitotic phase of cell division and lead to cell death.

Despite the use of intensive treatment regimens, overall survival for RMS remains below 70% and metastatic or recurrent RMS have extremely poor outcomes. In fact, metastatic RMS is one of the solid tumours with worse prognosis in children since metastatic ERMS has a survival rate around 40% and metastatic ARMS, around 20% (135). This highlights the necessity of developing new therapeutic approaches. Patients with recurrent or

metastatic RMS are considered for open clinical trials that evaluate new chemotherapeutic combinations or targeted therapies. However, research on new compounds is still necessary to improve RMS patient survival.

7. Neuroblastoma

7.1 Epidemiology

Neuroblastoma (NB) is a neuroendocrine tumour that arises in the developing sympathetic nervous system. It comprises around 10% of all childhood tumours, while it is very rare in adolescents and young adults, being 1.2% of cancers in this population (6). In fact, 90% of NB are diagnosed in children under 10 years and with a media age around 18 months (164,165). This is translated into approximately 80 new cases of NB per year in Spain (6).

As previously mentioned, NB incidence is clearly influenced by age since most of the cases appear during the perinatal period. Other factors that affect NB incidence are sex (it is more frequent in males) and ethnicity (it is less frequent in black individuals). Environmental risk factors or exposures have not been clearly associated with this malignancy (166).

Familiar cases of NB are extremely uncommon since only represents 1-2% of cases and are associated with gain-of-function germline mutations in the Anaplastic Lymphoma Kinase (*ALK*) gene and germline deletions at the 1p36 or 11q14-23 locus. Besides, syndromic NB cases that appear concomitant to central congenital hypoventilation syndrome or Hirschsprung disease have been described and are associated to loss-of-function germline mutations of the Paired Like Homeobox 2B (*PHOX2B*)

gene. Other syndromes associated with NB predisposition are Costello syndrome, Noonan syndrome and neurofibromatosis type 1. Finally, genome-wide association studies (GWAS) have defined several genetic alterations associated with NB susceptibility, this includes mutations in *ALK*, *PHOX2B*, *TP53*, *NRAS* and *BRCA2* (164,167).

Improvements in early detection and treatment have increased NB survival in the last decades and current 5-year survival is around 75% (6). However, NB has a broad spectrum of clinical behaviour and high risk NB or metastatic NB present a worse prognosis in children, with a survival rate below 50% (135,168).

7.2 Clinical presentation and diagnosis

NB originates from the sympaticoadrenal lineage of the neural crest and consequently, it can appear anywhere in the sympathetic nervous system. However, more than 50% of cases appear in the medulla of the adrenal gland. Other less frequent locations are the neck, the chest, and the pelvis (Figure 12). The signs and symptoms of NB are very variable and depend on the tumour location, size and the presence of metastasis (164,168).

Around 40% of NB patients have localized disease at diagnosis. These patients have symptoms related to the primary tumour site and usually caused by compression of tumour-surrounding tissues. Examples of this are the neurological signs (motor weakness, pain, or sensory loss) due to cord pressure by tumours arising in the paraspinal sympathetic ganglia or symptoms derived from large abdominal tumours such as hypertension, abdominal distension, and pain (165,169).

On the other hand, around half of NB patients present metastatic dissemination at diagnosis. The most frequent metastatic sites are regional lymph nodes, bone marrow, bone, liver, and skin, and rarely affect other parts of the body such as the CNS or the lungs (Figure 12). These patients present a general alteration of heath (pain, weight loss, loss of appetite, anaemia…) and may present other symptoms related to the site of metastasis, for instance, bone pain, limping or irritability when they have bone or bone marrow metastases (164-168).

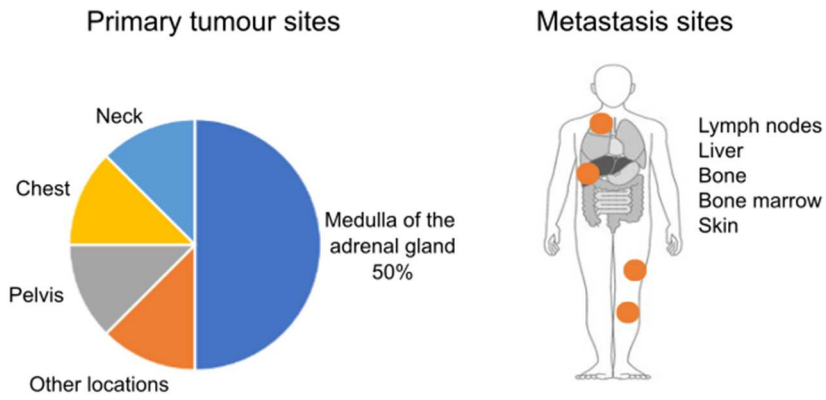

Figure 12. Most frequent NB locations and sites of metastasis.

Finally, 5% of NB patients are diagnosed with Stage 4S (or also called metastatic special). These patients have small localized primary tumours but already metastasized to liver, skin, or bone marrow, that generally spontaneously regress (164,168).

The diagnosis of NB needs a combination of imaging, histological and molecular analysis to assess the presence of tumour lesions and determine the tumour stage (summarized in Table 13). These characteristics are later used to classify NB patients into risk groups (164,167-170).

Table 13. Procedure for the diagnosis of NB.

1.	Detection of primary tumour location and size.
	• Ultrasonography • MRI scan • CT scan
2.	Histological and molecular studies after biopsy.
	• Morphology assessment: typically, immature small round tumour cells. • Immunohistochemistry • Molecular profiling: MYCN copy number, DNA index, evaluation of segmental chromosomal aberrations, genomic analysis for ALK mutations, etc.
3.	Evaluation of the extent of the disease.
	• MIBG scan to detect distant metastases. • Whole body FDG-PET scan to detect distant metastases. • Diphosphate bone scan to detect bone metastases. • Bilateral bone marrow aspirates to detect bone marrow metastases.

* Abbreviations: MRI, magnetic resonance imaging; CT, computerized tomography; FDG-PET, fluorodeoxyglucose positron emission tomography.

7.3 Genetic alterations

A remarkable histological and molecular heterogeneity has been observed in NB tumours. Genetic alterations in NB, as well as other prognostic factors (stage, age, and histology) are used for risk stratification of patients. Genetic aberrations present in NB consist of whole chromosome and segmental alterations. While whole chromosome gains (aneuploidy or triploidy) tend to occur in younger patients with more favourable prognosis, segmental changes are generally associated with poorer prognosis. The most common segmental changes are *MYCN* amplifications, deletions in 1p and 11q, and gains in 17q. Point mutations in *ALK*, *ATRX*, *ARID1A* and *ARID1B* are also frequently observed (164,168,171).

MYCN amplification

MYCN status is the most important molecular prognostic factor for patients with NB since it is associated with poor outcome regardless of other

prognostic factors. *MYCN* gene is located in chromosome 2p24 and amplifications (more than 10 copies) affecting this region occur in 15-30% of NB tumours. Mutations in *MYCN* are less frequent and have only been observed in around 2% of patients. *MYCN* amplifications are associated with poor clinical outcome, advanced-stage (40-50% of patients at stage 3 and 4), treatment failure and unfavourable histology (undifferentiated or poorly differentiated tumours with high mitotic-karyorrhectic index[3,4]) (171-173).

MYCN is expressed in developing neural tissues and acts as a transcription factor that regulates neural progenitor cell proliferation and differentiation. An increased number of copies of this gene in NB has been related to promotion of proliferation, drug resistance and angiogenesis, and inhibition of apoptosis and neural differentiation, all tumour promoting features. From a molecular point of view, these changes in cellular behaviour are mediated by the activation or repression of multiple genes (Figure 13), being MYCN considered as a master regulator of transcription (164,174).

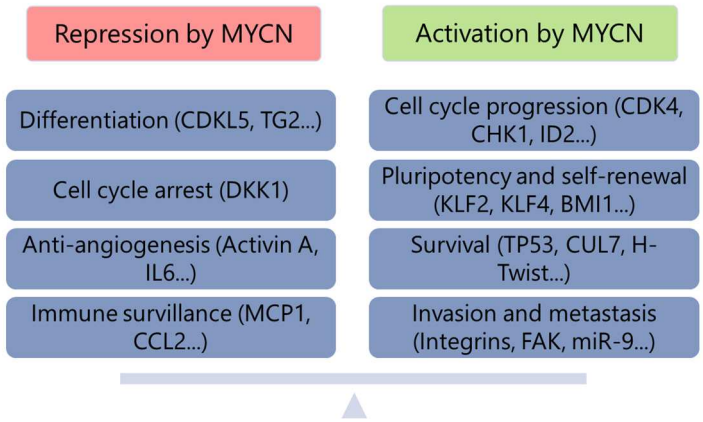

Figure 13. Regulation of gene expression by MYCN.

[3] Mitotic-karyorrhectic index (MKI): sum of mitotic and/or karyorrhectic cells per unit area (351).
[4] Karyorrhexis: fragmentation of the nuclei. It can occur as a result of either programmed cell death, cellular senescence or necrosis (352).

1p deletions (region 1p36.2 – 1p36.3)

Deletions affecting chromosome 1p have been observed in 25-35% of NB tumours and LOH of this region in more than 90% of advanced stage NB. These alterations are independently associated with poor prognosis, but also with *MYCN* amplification and 17q gain (171).

This region encodes for multiple genes, but the ones involved in the pathogenesis of NB have not been fully identified. *CDH5* (Chromatin helicase-binding domain 5) has stand out as a potential candidate of tumour suppressor gene located in this region. It is a chromatin remodeler that shows high expression in neural tissues but almost no expression in neuroblastoma, and whose expression levels correlate with favourable outcome and parameters (age, stage, histology, MYCN status, etc.) (175,176). However, other studies claim that unfavourable prognosis of 1p deletion is a result of the loss of a combination of genes, rather than only one pathogenic gene (177).

11q deletions (region 11q23)

Aberrations affecting chromosome 11q (deletions or LOH) have been reported in 20-45% of NB cases and is associated with poor outcome (estimated overall survival of 45%) (171,172). These alterations are associated with 17q gains but are negatively correlated with *MYCN* amplification, making them a powerful prognostic factor for MYCN non-amplified patients. This region is supposed to contain multiple tumour suppressor genes, although consistent association between prognostic

value and certain genes has not been concluded yet. *CADM1*, *ATM* and *H2AFX* genes have been suggested as candidates (178).

17q gains

Gains affecting chromosome 17q have been observed in more than 45% of NB tumours, being the most frequent segmental alteration in this neoplasia. They are associated with poor outcome (estimated overall survival of 31%), segmental deletions and *MYCN* amplifications. This region contains multiple genes, including *nm23-H1* and *nm23-H2*, both *MYCN* target genes, and *BiCR5* and *PMM1D*, genes that regulate cell proliferation and apoptosis (171,172).

***ALK* gene mutations**

Point mutations in *ALK* gene have been observed in 50% of familiar NB and 8-14% of sporadic cases (179,180). In addition, trisomy of chromosome 2p containing this gene (23%) and specific amplifications (2%) have been observed in NB sporadic cases. Nevertheless, the prognosis related to these mutations remains uncertain, and only a poor prognosis has been associated to F1174L specific mutation of this gene. Besides, coexisting F1174L mutation and *MYCN* amplification have been associated with extremely poor patient outcome (171).

Other genes

Mutations in chromatin remodelling genes such as *ATRX* (mutually exclusive with *MYCN* amplifications (181,182)), *ARID1A* and *ARID1B* have also been

reported in NB tumours (overall frequency of 9-11%) and are associated with poor patient outcome (183). Eventually, *TP53* gene is rarely mutated in NB and amplifications of *MDM2* gene have not been reported. However, since MDM2 is target of MYCN, high expression of this protein and consequently, inhibition of TP53 is commonly observed (171,184).

7.4 Origin

It is well accepted that NB originates from the neural crest cells, which come from the embryonic ectoderm layer and specifically from the neural tube (164,185,186). These cells are only found in vertebrates and give rise to multiple cell types including melanocytes, craniofacial cartilage and bone cells, smooth muscle cells, peripheral neurons, and glial cells. Neural crest cells differentiation occurs after a process of EMT and migration from the neural tube to different regions of the embryo. This process is controlled by complex epigenetic and transcriptional programs (187,188). Thus, neural crest cells act as transitional cells between multipotent progenitors and differentiated cells. It was thought that neural crest cells lose their multipotency after migration from the neural tube. However, a population of neural crest cells with stem cell properties remain in multiple tissues at postnatal stages and in the adult body, for instance in the skin, the adrenal medulla, and the bone marrow. These cells might contribute to the development of tumours such as neuroblastoma, melanoma, pheochromocytoma, paraganglioma or schwannoma (186,189).

During normal embryogenesis, neural crest cells migrate to the trunk region of the embryo and differentiate into sympathoadrenal progenitors that later give rise to sympathetic neurons or chromaffin cells that will form part of the adrenal glands. Migration of neural crest cells and their differentiation

are controlled by the expression of MYCN and bone morphogenic proteins (BMPs), among others excreted ligands. Studies based on the expression pattern of neuroblastoma cells and transgenic mice overexpressing MYCN suggest that the direct cell of origin of neuroblastoma may be the sympathoadrenal progenitors that get stuck into this undifferentiated state and do not proceed into neuronal or chromaffin cell differentiation due to a persistent MYCN high expression (190,191). This would explain why NB tumours most often appear in the sites of location of sympathoadrenal progenitor cells such as the adrenal cortex or the paraspinal ganglia (186,192). In addition, mutations in other genes related to sympathoadrenal development have been also reported to be involved in NB pathogenesis. This is the case of ALK (F1174L) and PHOX2B mutations. Collaboration between MYCN and these proteins has been described during the onset of tumours and they are considered as probable first hits of NB (191-194).

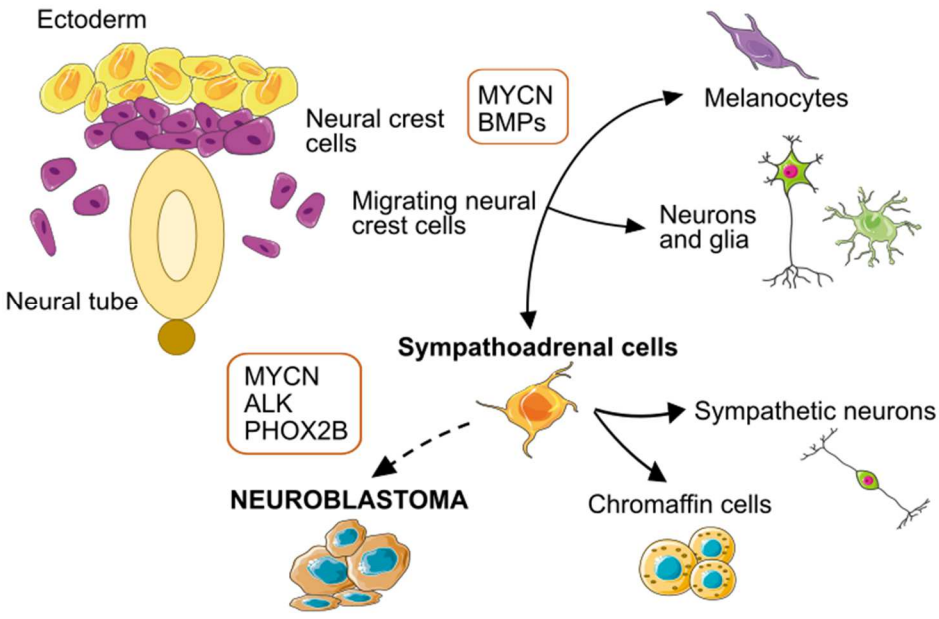

Figure 14. Possible NB cells of origin and molecular alterations involved in tumorigenesis.

7.5 Prognostic factors and risk stratification

Patients with NB have been classified using multiple staging systems along the past decades. Nevertheless, the most accepted systems are the International Neuroblastoma Staging System (INSS; Table 14) for reporting studies, and the International Neuroblastoma Risk Group (INRG; Table 16) Staging System for determining the treatment plan and comparison of international clinical trials (164,167).

Table 14. INSS classification used in reporting studies. Adapted from (164).

Stage 1	Localized tumour with complete surgical excision and without metastasis.
Stage 2	Localized tumour with incomplete surgical excision and without metastasis.
Stage 2B	Localized tumour with or without complete surgical excision, with metastasis to regional lymph nodes.
Stage 3	Unresectable infiltrating tumour, with or without metastasis to regional lymph nodes, or localized tumour with contralateral region lymph nodes metastasis or bilateral involvement.
Stage 4	Presence of metastasis to distant lymph nodes and/or other organs.
Stage 4S	Localized tumour in patients younger than 1 year of age, with metastasis limited to skin, liver or bone marrow.

Table 15. Specifications of NB prognostic factors (196,197).

Extent of the disease	L1: localized tumour restricted to one body compartment (neck, thorax, abdomen, or pelvis). Absence of any IDRF.
	L2: localized tumour restricted to one body compartment (neck, thorax, abdomen, or pelvis). Presence of IDRF.
	M: presence of distant metastasis.
	MS: presence of distant metastasis restricted to skin, liver, or bone marrow in patients <18 months.
Histology	Neuroblastoma (NB): small round blue cells, primary immature.
	Ganglioneuroma (GN): presence of cells that have matured and completed differentiation as ganglion cells.
	Ganglioneuroblastoma (GNB): presence of differentiated and undifferentiated cells.

The INRG allows the classification of NB patients into risk groups to adjust the treatment regimen to the prognosis of each patient. In this classification several factors are considered: age, extent of the disease, presence of metastasis, and histological and molecular characteristics of the tumour

(195-197). The presence of metastasis, as well as other factor such as age over 18-months, poor cellular differentiation, and certain molecular characteristics (specially MYCN amplification, but also 11q deletion) are considered as bad prognostic factors and increase the risk category (Table 16)

Table 16. Risk stratification of NB patients according to the INRG. Adapted from (195,198).

Risk group	Disease extent	Age (months)	Histology	MYCN status	11q deletion	Ploidy
Very-low	L1/L2	-	GN or GNB	-	-	-
	L1	-	-	Non-amp	-	-
	MS	<18	-	Non-amp	No	-
Low	L2	<18	-	Non-amp	No	-
	L2	>18	NB or GNB	Non-amp	No	-
	M	<18	-	Non-amp	-	Hyper.
Intermediate	L2	<18	-	Non-amp	Yes	-
	L2	>18	NB or GNB	Non-amp	-	-
	L2	>18	NB or GNB	Non-amp	-	-
	M	<12	-	Non-amp	-	Diploid
High	L1	-	-	Amp	-	-
	L2	>18	NB or GNB	Amp	-	-
	M	<18	-	Amp	-	-
	M	>18	-	-	-	-
	MS	-	-	Non-amp	Yes	-
	MS	-	-	Amp	-	-

7.6 Treatment

Therapeutic approaches for NB patients can consist of a combination of surgery, chemotherapy, radiation, and targeted therapies (including immunotherapy, differentiation therapy and autologous stem cell

transplant). The specific regiment of treatment for each patient depends on the risk group allocation (Figure 16).

Surgical resection is the recommended standard treatment for very-low and low-risk patients with localized disease. Together with surgery, limited chemotherapy can be applied to reduce tumour burden in patients older than 12 months. On the contrary, in patients younger than 6 months and/or patients at 4S stage without symptoms and with localized disease, only observation is recommended since spontaneous regression is frequently observed in this subset of patients. Patients at 4S stage with massive hepatomegaly or with unfavourable molecular alterations (MYCN amplification or 11q deletion) are an exemption and are treated with chemotherapy like high-risk patients.

Intermediate-risk patients are treated with more variable regimens depending on individual responses and specific tumour features. Generally, they are treated with induction chemotherapy to reduce tumour burden and eliminate metastatic deposits. After this, surgery is applied when resection is possible. Patients older than 18 months can be also treated with radiotherapy when tumour resection is not complete.

More intensive therapeutical approaches are applied to high-risk patients. In this case, multiple cycles of induction chemotherapy are used, followed by surgical resection when is possible. If complete resection is difficult or dangerous (due to important vessels are involved or neural tissues could be affected), patients can be treated again with high-dose chemotherapy and/or radiation. Later than, myeloablative therapy with autologous stem cell transplantation is used as consolidation therapy and finally,

maintenance therapy is based on differentiation treatment and immunotherapy (195).

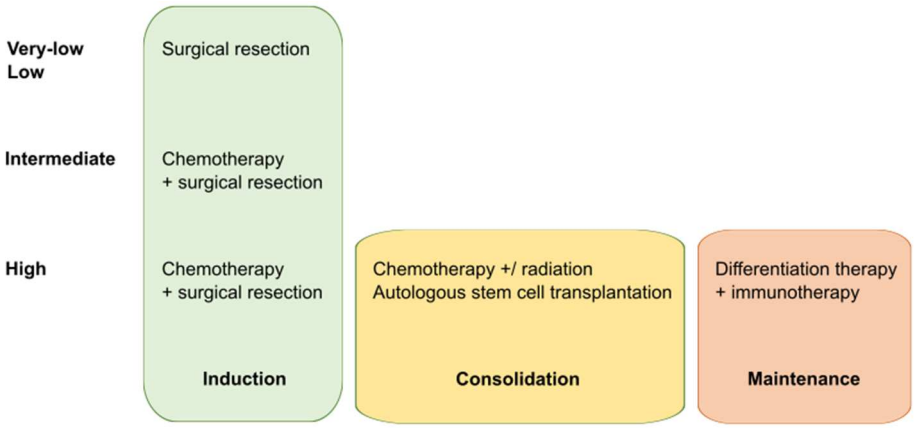

Figure 15. Treatment overview for NB patients, depending on the risk group stratification. Adapted from (195).

Table 17. Mechanism of action of the principal chemotherapeutic agents used in NB treatment (163).

Agent	Mechanism of action
Cisplatin	It is a platinum drug that establish cross-links with DNA and this inhibits transcription, resulting in cell apoptosis.
Vincristine	It is and alkaloid isolated from Vinca Rosea. It interacts with tubulin and inhibits microtubule formation in mitotic spindle, resulting in the arrest of dividing cells.
Carboplatin	It is a platinum drug that establish cross-links with DNA and this inhibits transcription, resulting in cell apoptosis.
Etoposide	It inhibits the action of topoisomerase II and induces double-strand DNA breaks. Accumulated breaks in DNA prevent the entry into the mitotic phase of cell division and lead to cell death.
Cyclophosphamide	It is an alkylating agent that must be activated in the liver to form the active aldophosphamide. It attaches to the DNA bases, resulting in separation of double-helix strands and DNA fragmentation. Consequently, DNA synthesis, RNA transcription and protein synthesis are impaired.
Topotecan	It inhibits the action of topoisomerase I and prevents the religation of the DNA strand, causing double-strand DNA breaks. Accumulated breaks in DNA prevent the entry into the mitotic phase of cell division and lead to cell death.
Doxorubicin	It is a cytotoxic antibiotic that binds to DNA and inhibits RNA synthesis and transcription. As a result, mRNA production and protein synthesis are impaired. In addition, it inhibits the action of topoisomerase II and induces double-strand DNA breaks.

Chemotherapeutic regimen used for NB patients consists of a combination of platinum drugs (cisplatin and carboplatin), alkylating agents (vincristine and cyclophosphamide) and topoisomerase inhibitors (etoposide). In European protocols, high-risk patients are treated with COJEC schedule: cisplatin (C), vincristine (O), carboplatin (J), etoposide (E) and cyclophosphamide (C) (199,200), although combination of topotecan, vincristine and doxorubicin agents can be added to try to achieve complete metastatic response (201) (Table 17).

The aim of consolidation therapy for high-risk patients is to eliminate any residual tumour cell that may have survive after induction chemotherapy and surgery. During this phase, autologous stem cell transplantation is applied. For this purpose, peripheral blood stem cells have to be collected and myeloablative therapy (based on single high-dose combined chemotherapy) is conducted previous to the transplant (195,202).

For maintenance therapy, patients are treated with differentiating agents and immunotherapy in order to eliminate minimal residual disease and prevent patient's relapse. Retinoid derivates, such as isotretinoin, are used as cell differentiating agents, while monoclonal antibodies targeting GD2 are used as immunotherapeutic agent. GD2 is an acidic glycolipid found on the outer cell membrane. During pre-natal development it is expressed in neural and mesenchymal stem cells, and NB tumour cells tend to have a high expression of this protein, as well as other several embryonal cancers (including RMS). GD2 expression in NB cell membranes is ubiquitous, regardless of the tumour stage and persist after treatment. Therefore, the use of antibodies against this protein and the consequent activation of cell-mediated cytotoxic response is part of the maintenance treatment. The

combination of differentiating agents and immunotherapy has proven effects on increasing event-free survival of high-risk NB patients (195,203).

Despite the intensification of treatment regimens NB patients, the overall survival for NB remains around 75% (6). In addition, there are big differences in terms of survival between the different risk groups, being greater than 90% in the low- and intermediate-risk groups but below 50% in the high-risk group of patients (135,168,195).

This again highlights the necessity of developing new therapeutic approaches, especially for patients with bad prognosis-associated characteristics that normally relapse from the disease and/or metastasize, and whose survival is clearly diminished. Patients with recurrent or metastatic NB are considered for open clinical trials that evaluate new chemotherapeutic combinations or targeted therapies. However, research on new compounds is still necessary to improve NB patient survival.

8. Breast cancer

8.1 Epidemiology

Breast cancer (BC) is the most frequent tumour in women, being around 24% of total malignancies. Indeed, in 2018 it was estimated that 2.1 million women were diagnosed with breast cancer worldwide and more than 600.000 died as consequence of the disease (1).

Incidence of BC is affected by several factors including ethnicity, lifestyle, environmental factors, and genetic predisposition. Asian women, for example, tend to develop breast tumours earlier in life (40-50 years-old)

than western women (60-70 years-old). Other factors that have been related to breast cancer onset are advanced maternal age, early menarche, lack of breast feeding, late menopause, obesity, or alcohol use (204).

Familiar cases of BC represent approximately 10% of cases and are frequently associated to bilateral presentation and early-onset of malignancies (<35 years-old). Mutations in *BRCA1* and *BRCA2* tumour suppressors genes are associated to familiar cases and show an autosomal-dominant inheritance pattern. Other syndromes associated with BC are Li Fraumeni (*TP53* mutations), ataxia telangiectasia (*ATM* mutations), Cowden (*PTEN* mutations) or neurofibromatosis (*NF1* mutations) (204,205).

Improvements in early detection and multimodal therapies have increased BC survival in the last decades and overall survival is around 80% (206,207). However, a subset of patients develop metastasis and this drastically worsens their survival rate, reducing it under 40% (207). Despite the good overall survival, BC is still the first cause of cancer deaths in women (1).

8.2 Clinical presentation and diagnosis

BC is a carcinoma that arises in the mammary epithelium (208), specifically in the terminal ducts of the collecting duct (204). Around 50-60% of patients are diagnosed with localized disease restricted to the mammary gland. Most common signs and symptoms in these patients are breast lump nipple abnormalities, breast pain and breast skin abnormalities (209). On the other side, around 30% of patients are diagnosed with regional dissemination and only 5-6% of patients have distant metastasis by this time. Preferential sites for metastatization are axillary lymph nodes, bones, liver, lungs and brain (204,207) (Figure 16).

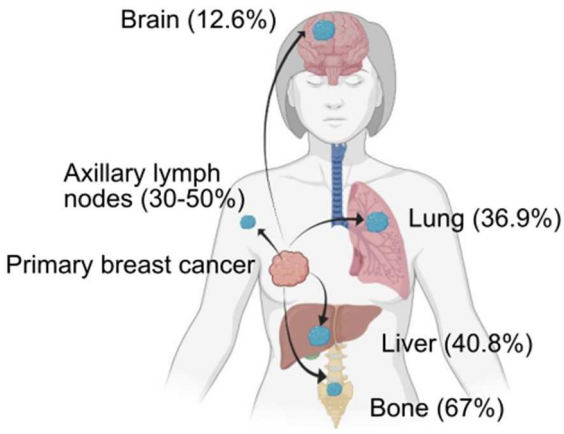

Figure 16. Most frequent sites of metastasis in BC patients. Percentages refer to metastatic BC cases. Adapted from (204).

BC patients are diagnosed due to routine screening or presence of symptoms. Patients that are diagnosed after screening are associated with smaller tumours and restricted to the mammary gland, these is translated into less intense treatments and better overall survival and highlights the importance of this screening in healthy women (210). Several diagnostic tests are applied, including imaging techniques, immunohistochemical staining and molecular assays for the diagnosis (summarized in Table 18).

Table 18. Diagnostic procedures for BC patients (210,211).

1. Detection of primary tumour location and size.
• Ultrasonography or mammography • Combination with MRI scan
2. Histological and molecular studies after biopsy.
• Histological characterization. • Immunohistochemistry: oestrogen receptor (ER), progesterone receptor (PR), HER2 and KI67 assessment. • Molecular profiling by DNA or RNA microarrays.
3. Evaluation of the extent of the disease.
• MRI or CT scan. • FDG-PET or SPECT scan to detect distant metastases. • Bone scan to detect bone metastases.

*Abbreviations: MRI, magnetic resonance imaging; CT, computerized tomography; FDG-PET, fluorodeoxyglucose positron emission tomography; SPECT, single-photon emission computerized tomography.

8.3 Classification and molecular alterations

From a histological point of view BC tumours can be classified according to multiple criteria, including tumour cell type, extracellular secretion, architecture features and immunohistochemical profile. However, this classification does not reflect the biological heterogeneity of BC since it categorises 70-80% of cases as invasive ductal carcinoma no special type (IDC-NST). Instead of this, molecular divisions better reflect the heterogeneity of BC tumours and are more useful for determining prognosis and patient's management (212,213).

The expression of oestrogen receptor (ER), progesterone receptor (PR) and HER2 (Human epidermal growth factor receptor 2) is routinely assessed in BC samples and are the base for the immunophenotyping classification. Around 75% of cases express both ER and PR which are steroid receptors that stimulate the growth of normal but also neoplastic breast epithelium. The expression of these markers is associated with low-grade tumours and less aggressive behaviour. A small percentage of BC tumours only express one of these receptors and are associated with a more aggressive behaviour. On the other side, HER2 is a membrane tyrosine kinase overexpressed or amplified (region 17q12) in about 15% of BC. It is associated to more aggressive clinical course and poor prognosis. The remaining 10-15% of tumours do not express any of these receptors and are called triple negative (TNBC). They are high-grade tumours and are associated with poor prognosis (212).

Nevertheless, gene expression profiling studies have allowed the molecular classification of tumours into the so-called intrinsic subtypes that consider

the expression of ER, PR and HER2, but also the differential expression of genes related to proliferation, HER2 amplicon and myoepithelial cells. Prediction Analysis of Microarray using 50 classifier genes (called PAM50) is a standardized method that divides BC tumours into intrinsic subtypes: luminal A, luminal B, HER2-enriched and basal-like subgroups (214,215).

Luminal A and B tumours resemble to normal luminal epithelial cells. Luminal A is the most frequent BC subtype, representing around 40-50% of all invasive tumours. It is characterized by expression of ER-related genes and normally are low-grade tumours. Luminal B is characterized by lower expression of ER-related genes and are higher-grade tumours. HER2-enriched subtype represents around 15% of tumours and is characterized by the expression of HER2 signalling-associated genes or genes located in the amplicon. They are high grade tumours with more aggressive behaviour. Finally, basal-like tumours are associated with the expression of genes in normal mammary basal or myoepithelial cells and proliferation-related genes, but not ER, PR or HER2. They are high grade tumours with very poor prognosis (Figure 17).

Despite this molecular classification defines the different molecular subgroups and their prognosis better, due to high associated costs they are not used in the clinical practise. Instead of this, the expression of ER, PR, HER2 and KI67 is used to classify patients into (212):

- Luminal A-like (ER↑, PR↓, HER2-, KI67↓)
- Lumina B-like (ER↑, PR↓ and/or HER2+ and/or Ki67↑)
- HER2-overexpressed (ER-, PR-, HER2+, Ki67↑)
- Basal-like (ER-, PR-, HER2-, Ki67↑)

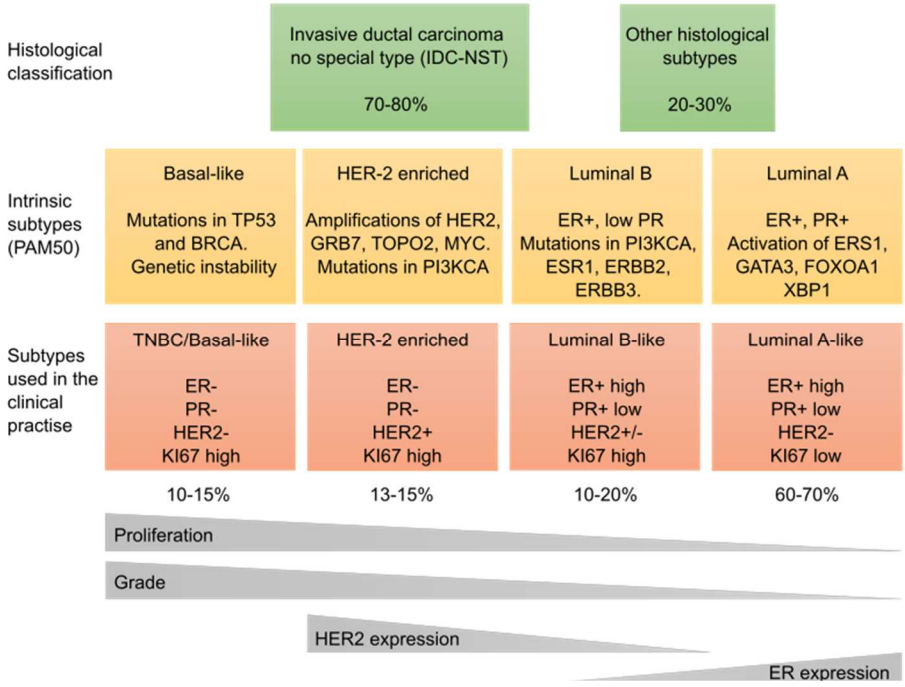

Figure 17. BC classification and associated characteristics. Adapted from (204).

Although major risk factors for sporadic BC are expression or absence of hormone receptors (ER and PR). Most frequent genetic aberrations in BC tumours are mutations or amplifications affecting *TP53* (41% of tumours), *PIK3CA* (30%), *MYC* (20%), *PTEN* (16%), *CCND1* (16%), *HER2* (13%), *FGFR1* (11%) and *GATA3* (10%) (216). These mutations are associated to enhanced cell cycle, proliferation, or apoptosis inhibition, and some of them to certain cancer subtypes: for example, luminal A has a high prevalence of *PI3KCA* mutations (49%), while most of basal-like tumours have mutations affecting *TP53* (84%) (204). In general terms, mutation burden in BC is higher than in paediatric cancers (including RMS and NB) (217), especially in basal-like tumours (218) (Figure 18). Other described aberrations are gain of 1q and loss of 16q, normally associated with low grade tumours, and loss of 13q and gain of 11q13 in high-grade tumours (204).

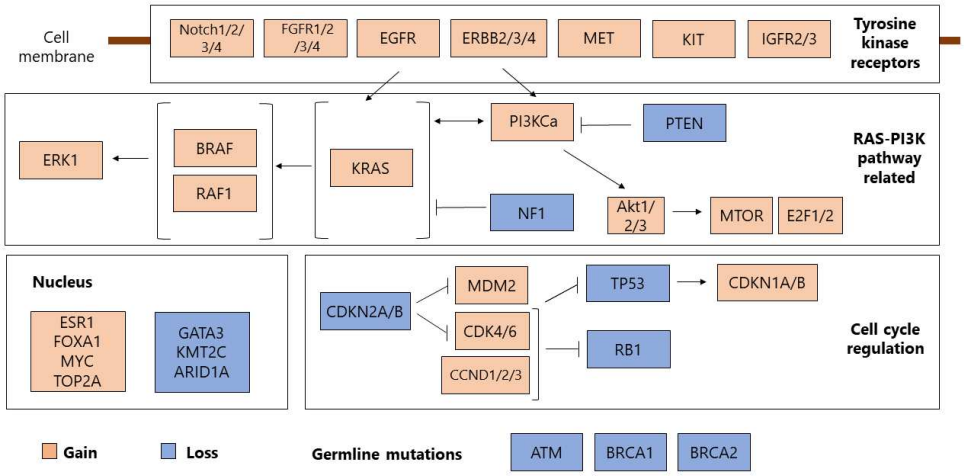

Figure 18. Genetic alterations in BC tumours (204).

8.4 Origin

The exact cell of origin and the mechanism by which breast cancer is initiated remain a subject of debate. Studies trying to determine the biological and molecular origin of BC have come with two different models. On one hand, the clonal evolution model determines that the accumulation of low-penetrance mutations and epigenetic changes along life can contribute to enhanced survival and proliferation of the fittest cells which will form the macroscopic tumour. On the other hand, the stem cell model determines that only precursor cells with stem cell characteristics can initiate and form the tumour mass. Currently, it is accepted that a combination of these two models can occur in BC onset and progression (204).

Human mammary epithelium originates during embryonic development from the epidermal placode and finishes its evolution during post-natal life. The breast undergoes many changes in size, shape and function during

puberty, pregnancy and lactation, and the mammary epithelium is especially responsive to local and systemic signals that induce morphologic changes during puberty and pregnancy. Interaction with the environment, steroid hormones and growth factor receptor signalling play a crucial role regulating epithelium growth and have been also related to BC tumorigenesis (219).

There is evidence to support the existence of stem cell and progenitor cells in the healthy mammary epithelium (MaSC). These cells form a small proportion of undifferentiated cells that maintain, repair, and regenerate the normal tissue along the course of reproductive life of women. There is still controversy about the role of MaSC and when mutations contributing to the carcinogenesis occur, early or along the process of differentiation to mammary epithelial cells. The most important signalling pathways implicated in the growth of mammary epithelium are ER-receptor, HER2 and Wnt/β-catenin pathway, although many other pathways can contribute to this process (219). For instance, aberrant Wnt signalling leads to altered mammary gland development and BC tumours in mice (220).

Regarding the origin of the different BC subtypes, it is believed that oncogenic events in progenitor cells at different stages may lead to different BC subtypes. According to this, it is thought that basal-like tumours arise from the most primitive stem cells, while more differentiated luminal tumours expressing ER receptors come from more committed luminal progenitor cells (221). Nevertheless, studies on animal models trying to reproduce the onset of BC have revealed that luminal progenitors are able to generate luminal and basal-like tumours, and basal progenitors can also give rise to luminal and basal-like subtypes, in both cases

depending on the oncogenic mutations that happen during transformation. For example, it has been reported that the expression of *PI3KCA* mutant in luminal progenitor cells induces luminal or basal-like breast tumours depending on other coexistent mutations (222,223). On the other hand, conditional mouse models have showed that loss of *BRCA1* and *TP53* in basal progenitors resulted in the development of basal-like tumours (224,225) (Figure 19).

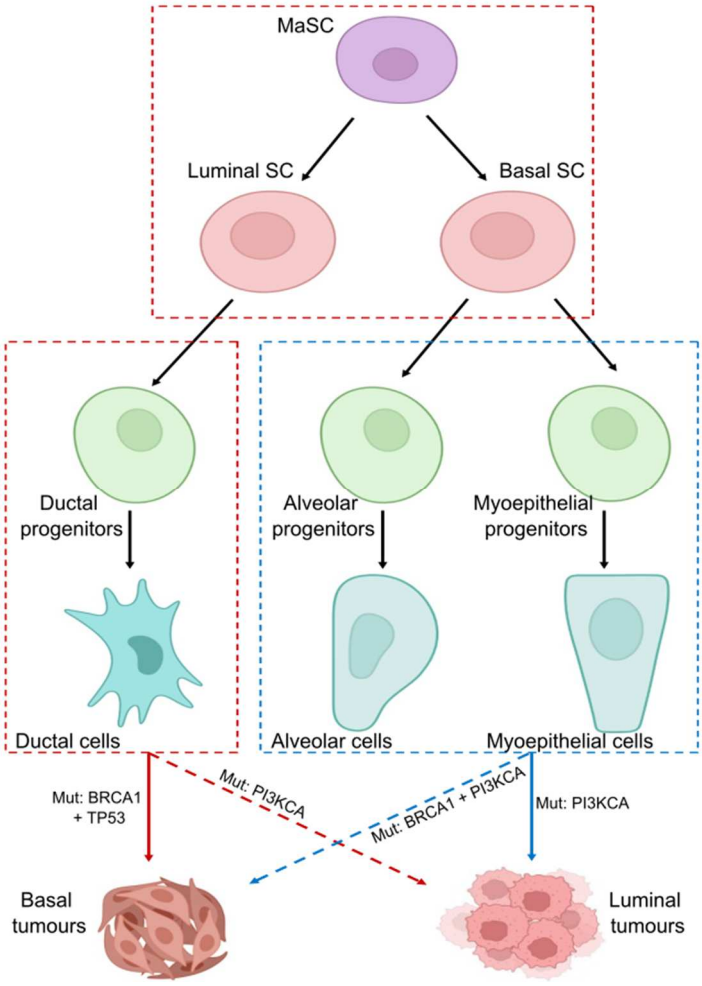

Figure 19. Possible BC cells of origin and molecular alterations involved in tumorigenesis. Adapted from (219,225).

8.5 Prognostic factors and risk stratification

The most important prognostic factor for BC patients are age, histology, grade, the extent of the disease (TNM status) and the intrinsic subtype of tumours (Table 19), being this last one the most important criteria for treatment decisions. Luminal A-like tumours are classified as low-risk and normally present low grade and low proliferation rates, while Luminal B-like are considered intermediate-risk since they currently display higher grade and higher proliferation rate. On the contrary, HER2-overexpressing and basal-like subtypes are considered high-risk tumours and show aggressive characteristics, such as high grade and high proliferation rate (204).

Table 19. BC risk factors and prognostic value (204,226,227). Abbreviations: IDC-NST, invasive ductal carcinoma no special type.

Risk factor	Prognosis
Age	<35 years-old: more aggressive and hereditary tumours. >75 years-old: higher risk of mortality.
Histology	The WHO recognizes 19 histologic subtypes. • IDC-NST (>70%): has not any special histological characteristics and is not associated to good or bad prognosis. • Favourable histology: tubular, cribriform and mucinous. • Unfavourable histology: pleomorphic lobular carcinoma, high-grade metaplastic and micropapillary carcinoma.
Grade (G1, G2 and G3)	Considers proportion of cancer cells, anisokaryosis (variation of nuclear size and shape between cells) and mitosis rate. Correlates with tumour aggressiveness.
TNM status	T: tumour size • T1: tumour ≤ 20 mm in greatest dimension • T2: tumour > 20 mm but ≤ 50 mm in greatest dimension • T3: tumour > 50 mm in greatest dimension • T4: tumour of any size with direct extension to chest wall or to skin
	N: regional lymph node affectation • N0: no regional lymph node affectation • Nx: affectation of ipsilateral lymph nodes. Subclassification depending on the number of affected nodes.
	M: distant metastasis • M0: no evidence of distant metastases. • M1: distant metastases detected.
Intrinsic subtype	Luminal A-like: favourable. Luminal B-like: intermediate. HER2-overexpressing: unfavourable. Basal-like: unfavourable.

In 2017, the American Joint Committee of Cancer revised the classification of BC patients that uses the Pathological Prognostic Stage Group (228) and allows the separation of patients according to their risk. This classification is used to determine patient management and in this revision the expression status of ER, PR and HER2 was introduced as one of the most important factors determining patient's risk (Table 20).

Table 20. Summary of the Pathological Prognostic Stage Group system (access to complete staging tables at (228)).

Stage group	TNM	Grade	ER status	PR status	HER2 status
IA	T1 N0 or N1 M0	Any	Any	Any	Any
IB		G2 or G3	Negative	Negative	Negative
IA/IB	T1 or t2 N0 or N1 M0	Any	Positive	Positive	Positive
IIA		Any	Negative	Negative	Negative
IA/IB	T2 or T3 N0 or N1 M0	Any	Positive	Positive	Positive
IIB		G1 or G2	Negative	Negative	Negative
IIIA		G3	Negative	Negative	Negative
IB	T1, T2 or T3 N1 or N2 M0	G1 or G2	Positive	Positive	Positive
IIA		G3	Positive	Positive	Positive
IIIA/IIIB		G1 or G2	Negative	Negative	Negative
IIIC		G3	Negative	Negative	Negative
IIIA/IIIB	T4 Any M0	Any	Positive	Positive	Positive
IIIB		G1	Negative	Negative	Negative
IIIC		G2 or G3	Negative	Negative	Negative
IV	T, N Any M1	Any	Any	Any	Any

8.6 Treatment

Treatment regimen for BC patients can combine surgery, chemotherapy, radiotherapy, and other targeted therapies, depending on the prognostic of each patient, the extent of the disease and the molecular characteristics of the tumour.

Surgery is the first line of treatment for early BC patients who have localized disease at diagnostic time, this includes the removal of primary tumour and affected lymph nodes. However, neoadjuvant therapy before surgery can be used to reduce the primary tumour in patients with larger or high-risk tumours (HER2 positive or basal-like tumours), facilitating primary tumour removal and normal breast conservation. Post-surgery adjuvant therapy, either radiotherapy or chemotherapy, can be also applied to these patients according to surgical results (it is recommended when margin infiltration is detected) or other parameters that confer bad prognosis (lymph node affection, molecular profile, age…). In addition, patients with hormone receptor expression (ER or PR positive) are candidates for sustained endocrine therapy, while HER2 positive patients receive HER2-blocking agents.

Endocrine therapy is used in all patients with luminal-like tumours as part of the adjuvant treatment. This therapy is based on the blockade of ER by competing agents, such as tamoxifen or aromatase inhibitors. Depending on tumour molecular features, tolerability, age (premenopausal or postmenopausal) and bone health, this can be combined with gonadotropin-releasing hormone (GhRH) analogues that inhibit oestradiol production to reduce relapse risk. Endocrine therapy is a sustained adjuvant therapy that lasts a minimum of 5 years, although in high-risk patients this can be extended up to 7-10 years.

HER2-blocking agents, normally a combination of trastuzumab and pertuzumab (both monoclonal antibodies against HER2 receptor) is used in patients with HER2-overexpressing tumours. This can be combined with chemotherapeutic agents depending on the extent of the disease.

Advanced BC patients, who have inoperable locally advanced primary tumours or have metastatic disease, are treated with more intense regimens that include radiotherapy and chemotherapy. Because metastatic disease is very often considered as incurable, the goal of therapy in the setting of metastatic disease is to extend life while minimizing symptoms and side effects.

Resection of primary tumour and metastasis remains controversial and although it is generally not recommended, certain patients with excellent therapy response undergo surgery. The use of single-agent or combined chemotherapy regimen depends on the extent of the disease, tumour intrinsic subtype, age (premenopausal or postmenopausal), tolerability and initial treatment response. Chemotherapeutic protocols normally include anthracyclines (such as doxorubicine) and taxanes (docetaxel, paclitaxel) as first line treatment, and other second line agents such as capecitabine, vinorelbine, eribulin, cyclophosphamide, bevazizumab and lapatinib, among others.

Luminal-like patients always combine chemotherapy with endocrine therapy and ovarian suppression or ablation as another way of reducing ER signalling is required in premenopausal patients. HER2-positive tumours combine chemotherapy with HER2-directed therapy. And finally, basal-like patients receive a combination of chemotherapeutic agents and are candidates for treatment with poly-ADP ribose polymerase (PARP) inhibitors when display mutations in *BRCA1/2* (204,210) (Table 21).

Patients with localized disease have a good general overall survival (around 80%). Nevertheless, despite intense treatment, patients with metastatic or

recurrent disease have a very dismal prognosis with an overall survival below 40% (207). Metastases are the main cause of cancer-associated mortality in BC patients, with a median overall survival around 2-3 years after dissemination of the disease. These patients continue in treatment to relieve symptoms and prolong quality-adjusted life expectancy (204).

Table 21. Agents used in BC treatment protocols and their mechanism of action.

Treatment	Agent	Mechanism of action
Chemotherapy	Taxanes (ie. docetaxel, paclitaxel)	Group of drugs that disrupt microtubule function, which are essential for cell division.
	Anthracyclines (i.e doxorubicine)	Group of drugs extracted from Streptomyces spp. They intercalate in DNA and inhibit topoisomerase II activity.
Endocrine therapy	Tamoxifen	It competes with 17β-oestradiol at the receptor site and blocks the signalling downstream ER receptor.
	GnRH analogue	Gonadotropin-releasing hormone analogue that inhibits oestradiol production.
Targeted therapies	PARP inhibitors	Inhibitors of poly-ADP ribose polymerase (PARP), involved in DNA repair. They are used when BRCA mutations are present.
	Anti-HER2 (trastuzumab, pertuzumab)	Humanized monoclonal antibodies against HER2. They are used when tumours overexpress HER2 receptor.

To sum up, these three cancers affect different populations and have different molecular and clinical features. Nevertheless, they have one common pending issue: although they have a good general overall survival and despite improvements in treatment options, a subset of patients develop metastasis and this drastically worsens their survival rates. This emphasizes the necessity of developing new therapeutic strategies specifically directed to prevent the formation of distant metastases and thus, reduce mortality of these neoplasia. As previously exposed, α9β1 integrin seems to be a potential therapeutic target for metastasis. However, its role in metastatic spreading of these neoplasia has not been fully addressed.

9. Integrin α9β1 in rhabdomyosarcoma

The role of α9β1 in RMS has been briefly addressed and only a few studies have been published regards this topic. As previously mentioned, our group described for the first time the regulation of α9-subunit expression by Notch pathway. In this study, a chromatin immunoprecipitation (CHIP) assay was performed to validate the binding of Notch intracellular domain (NICD) and Hes-1, both important elements of intracellular Notch signalling pathway, to α9 promoter. In addition, induction of Notch pathway and subsequent upregulation of α9-subunit were associated with an enhanced invasive phenotype of RMS cells (30). In concordance with these results, antibodies against α9-subunit reduced cell invasiveness or cell adhesion in RMS cells (30,229,230).

A previous doctoral thesis of the group has also addressed the role of α9β1 in RMS. In this study, silencing of α9β1 by shRNA reduced the invasiveness of RMS cells *in vitro* and the development of metastasis *in vivo*. Following these promising results, our group in collaboration with the pharmaceutical partner BCN Peptides, designed multiple short peptides inspired in the interaction sequence between α9β1 and ADAM12 (231). Their effects on cell invasiveness were assessed in RMS cell lines and the most effective peptide, named RA08, was selected for further study. Treatment with this inhibitor turned out to reduce cell invasiveness *in vitro* and metastasis growth *in vivo* (232). Altogether, this suggested that α9β1 is essential for metastatization of RMS cells and is a promising target for the treatment of RMS patients. However, the regulation by other elements, such as miRNAs, has not been addressed.

10. Integrin α9β1 in neuroblastoma

The role of other integrin heterodimers has been studied in NB, including α4β1 integrin, which shares high homology to α9β1 (233,234). The expression of α4β1 integrin in human NB cell lines turned out to enhance cell migration and metastasis in a syngeneic tumour model. In concordance with this, antagonism of α4β1 integrin reduced metastasis (233). Considering the high homology between α4β1 and α9β1 integrins and their redundancy in ligand interaction, this suggest that α9β1 could be also involved in the modulation of cell invasiveness and metastasis in NB. Nevertheless, the direct role of α9β1 in NB tumour growth or dissemination remained unexplored.

A previous doctoral thesis in our group studied the effects of α9β1 silencing by shRNA and blockade by RA08 on NB cell invasion *in vitro*. Results showed that both approaches reduced cell invasiveness *in vitro* (232), suggesting that α9β1 blockade could be a good therapeutic approach for NB treatment.

11. Integrin α9β1 in breast cancer

In the case of BC, the role of α9β1 has been more described. As previously mentioned, heterogeneous expression of α9β1 has been observed in breast tumour samples (118-121). However, high α9β1 expression has been associated with reduced overall survival and metastasis-free survival of BC patients, especially of those of the basal-like subtype. In addition, studies have revealed that the use of α9-blocking antibodies or α9 knockdown by genetic engineering reduced cell invasion, tumour growth and metastasis in BC animal models (119,119). Altogether, this suggests that α9β1 is

essential for tumour growth and metastatization of BC cells and it is a promising target for the treatment of BC patients.

12. Therapeutic opportunities

The importance of α9β1 in cancer as indicated by earlier studies suggest that developing strategies to block the expression and/or activity of this protein might be a good therapeutic approach for cancer patients. Unfortunately, no specific blocking agents for α9β1 have been developed so far. However, antibodies, synthetic peptides, and other specific strategies have been developed with the aim of blocking other integrins and impair tumour growth and disease progression (Table 22).

Table 22. Therapeutic strategies for integrin blockade. Adapted from (235).

Agent	Type of agent	Target	Clinical phase	Patients
Intetumumab	Humanized antibody	αvβ3 αvβ1	Phase II	Recurrent melanoma and prostate cancer.
Abciximab	Chimeric human-murine antibody	αIIbβ3		
LM609-derived (Vitaxin and Etaracizumab)	Humanized antibodies	αvβ3	Phase II	Recurrent melanoma and prostate cancer.
Volociximab	Chimeric human-murine antibody	α5β1	Phase II	Recurrent non-small cell lung cancer and metastatic melanoma.
Cilengitide	RGD containing peptide	αvβ3 αvβ5	Phase III	Recurrent glioblastoma, head and neck squamous cell carcinoma and non-small cell lung cancer.
ATN-161	Non-RGD-based peptide	β subunits	Phase I	Solid tumours
HM-3 and PEG-HM-3	RGD containing peptide	αvβ3	Pre-clinical studies	
AP25	RGD-modified peptide	αvβ3 α5β1	Pre-clinical studies	
αvβ3 CAR-T	Biological agent	αvβ3	Pre-clinical studies	

Although big efforts have been done in the development of new therapeutic approaches to inhibit integrins and improve survival of cancer patients, any of the above-mentioned agents have generated positive results in reducing primary tumour growth or metastasis and therefore, any of them have reached the clinics. This highlights the necessity to better understand the mechanisms that drive tumour progression and the role that integrins play in this process to find effective ways of blocking their function and hopefully, tumour growth and metastatic dissemination.

Our group in collaboration with the pharmaceutical partner BCN Peptides, has designed a short peptide inspired in the interaction sequence between α9β1 and ADAM12. This inhibitor, called RA08, has been tested in RMS in a previous doctoral thesis of the group with very promising preclinical evidence on preventing the establishment of metastasis. Considering that α9β1 is expressed in many tumour types and evidence presented before on modulation of cell invasion and metastasis, blocking of α9β1 may have potential applicability in a broad spectrum of tumour types. Thus, this doctoral thesis is focused on the study α9β1 and possible strategies to inhibit its function in different cancers with special interest on their potential anti-metastatic effects.

II. HYPOTHESIS AND OBJECTIVES

Most of the new developing therapies are aimed at reducing tumour growth, but there is a lack of viable pharmacological options to reduce the formation of metastasis. This is a paradox since most of cancer-associated deaths are attributable to metastatic progression. Integrin α9β1 has been previously described as playing an essential role in cell invasion and metastasis; however, little is known about the mechanism that links this protein to this process, being one of the less studied integrins.

This project aims to further characterize the role of α9 integrin subunit, herein after called ITGA9, in three different tumour types: [1] rhabdomyosarcoma, the most prevalent soft tissue sarcoma in children, [2] neuroblastoma, the most common extracranial solid tumour in children, and [3] breast cancer, the most frequent cancer in women and worldwide. These three cancers have a different cell of origin and affect different tissues and populations. Nevertheless, they have one trait in common: although they have a good general overall survival (around 70% for rhabdomyosarcoma and neuroblastoma, and around 80% for breast cancer), a subset of patients develop metastasis and this drastically worsens their survival rates (approximately 30% for rhabdomyosarcoma, 50% for neuroblastoma and below 40% for breast cancer patients).

We hypothesize that ITGA9 could be a key player in the metastatic spreading of these tumours. Therefore, the inhibition of this protein, either by miRNA, shRNA or by a specific blocking peptide (named RA08) inspired in the interaction domain between α9β1 and ADAM12, may have anti-oncogenic and anti-metastatic effects.

Main objective: To study the role of ITGA9 in RMS, NB and BC cells and the anti-oncogenic effects of its inhibition.

To accomplish the main objective, partial objectives have been established:

1. To identify miRNAs able to regulate ITGA9 expression and analyse the effects of this inhibition on tumour growth and metastatic dissemination of RMS cells.

2. To study the effects of ITGA9 blockade, either by shRNA or RA08, in metastatic dissemination of NB cells *in vivo*.

3. To study the effects of ITGA9 blockade, either by shRNA or RA08, in metastatic dissemination of BC cells *in vitro* and *in vivo*.

4. To study the role of ITGA9 in non-adherent cell survival of RMS, NB and BC cells.

5. To study the prognostic value of ITGA9 in RMS, NB and BC patients.

III. MATERIALS AND METHODS

1. Cell culture

All RMS cell lines were grown in Minimum Essential Medium with Earle's Balanced Salts (MEM, Biowest), NB cell lines were grown in Iscove's Modified Dulbecco's Medium (IMEM, Thermo Fisher Scientific) and BC and HEK293T (used for viral production) cell lines were grown in Dulbecco's Modified Eagle Medium (DMEM, Biowest). All media were supplemented with 10% foetal bovine serum (FBS, Sigma-Aldrich), 2 mM L-glutamine, 1 mM sodium pyruvate, 1x non-essential amino acids, 100 U/ml penicillin and 0.1 mg/ml streptomycin (all reagents from Biowest) and maintained at 37°C in a 5% CO2 atmosphere. The characteristics of each cell line and their origin are summarized in Table 23.

Table 13. Culture conditions and molecular features of the cell lines used.

Type of cancer	Cell line	Molecular alterations	Clinical subtype	Source	Subculture dilution
RMS	RD		ERMS	Dr. Beat Schäfer	1/3
	CW9019	PAX7/FOXO1 translocation	ARMS	Dr. Jaclyn Biegel	1/3
NB	BE(2)C	MYCN amplification		ATCC	1/6
BC	MDA-MB-468		Basal	ATCC	1/4
	MDA-MB-231		Basal	ATCC	1/4
Embryonic kidney	HEK293T			ATCC	1/6

For their subculture, cells at 80% of confluency were detached from the plates using trypsin-EDTA (Fisher Scientific) and centrifuged at 1500 rpm for 5 minutes. Then, pelleted cells were resuspended in the corresponding media and diluted before being seeded in a new culture dish.

The same procedure was used for counting the cells. In this case, pelleted cells were resuspended in the corresponding media and 10 µl of the

suspension were mixed with 10 µl of trypan blue (Fisher Scientific) and added to a counter slide (NanoEntek). Then, total and viable cells were counted using the Cell Counter (NanoEntek).

Finally, for cryopreservation, pelleted cells were resuspended in FBS containing 10% of dimethyl sulfoxide (DMSO, Sigma Aldrich) and stored at -80°C for some days or at the nitrogen tank at -196°C for longer periods. The cooldown was done using the Nalgene Mr. Frosty Freezing (Thermo Fisher Scientific) that reduced progressively the temperature (approximately 1°C every minute). This and the DMSO present in the freezing media prevented the formation of crystals that would result in dying of frozen cells and allowed cell cryopreservation for months or years.

2. miRNA screening and transfection of miRNA mimics

Screening of miRNA able to bind ITGA9 3'UTR was done using three different algorithms: PicTar, TargetScan and miRanda. miRNAs that were predicted to regulate ITGA9 by more than one algorithm were tested *in vitro* to assess ITGA9 downregulation (Table 24).

RD and CW9019 cells were transfected with miRNA mimics (GE Healthcare-Dharmacon, summarized in Table 27) and MiRIDIAN microRNA mimic negative controls (C-1 and C-2) to test the effects of predicted miRNAs. miRNA mimics were transfected at 50nM, whereas mimic controls were used at 25nM and were transfected using lipofectamine (Thermo Fisher Scientific) in OptiMEM media (Gibco). Then, 72 hours after transfection, cells were harvested for protein extraction and assessment of ITGA9 downregulation by Western blot.

Table 24. List of miRNAs predicted to bind ITGA9, their sequences and the used miRNA mimics (GE Healthcare-Dharmacon).

miRNA	Sequence	Reference
miR-296-3p	GAGGGUUGGGUGGAGGCUCUCC	C-301076-01-0005
miR-324-5p	CGCAUCCCCUAGGGCAUUGGUGU	C-300704-03-0005
miR-340-5p	UUAUAAAGCAAUGAGACUGAUU	C-301081-01-0005
miR-410	AAUAUAACACAGAUGGCCUGU	C-300740-03-0005
miR-431-5p	UGUCUUGCAGGCCGUCAUGCA	C-300729-03-0005
miR-7	UGGAAGACUAGUGAUUUUGUUGU	C-300546-07-0005

3. Plasmids, lentiviral production and infection

Along the project we have used two different lentiviral vectors: for the shRNA overexpression we used the pGIPZ (GE Healthcare Dharmacon) and for the miRNA overexpression, the pTRIPZ (GE Healthcare Dharmacon). Both are 2nd generation lentiviral vectors that allowed transgene integration into the host genome upon viral transduction. This implies that the components necessary for virus production are split across three different plasmids: [1] the plasmid encoding our insert of interest flanked by long terminal repeat (LTR) sequences that facilitate integration of insert sequence into the host genome, [2] the packaging plasmid and [3] the envelop plasmid.

The packaging plasmid used for the pTRIPZ or pGIPZ systems was the psPAX2, which contains Gag, Pol, Rev and Tat coding sequences, while the envelop plasmid was the pMD2G, which codifies for the VSV-G protein of the envelop. Both lentiviral vectors also contained a puromycin resistance element and a reporter element, which codifies for green fluorescent protein (GFP) in the case of pGIPZ and red fluorescent protein (RFP) in the case of pTRIPZ. In addition, pTRIPZ lentivirus vector contains a tetracycline-inducible promoter that activates the expression of the insert in presence of doxycycline (DOX; tetracycline derivate) (Figure 20 and Table 25).

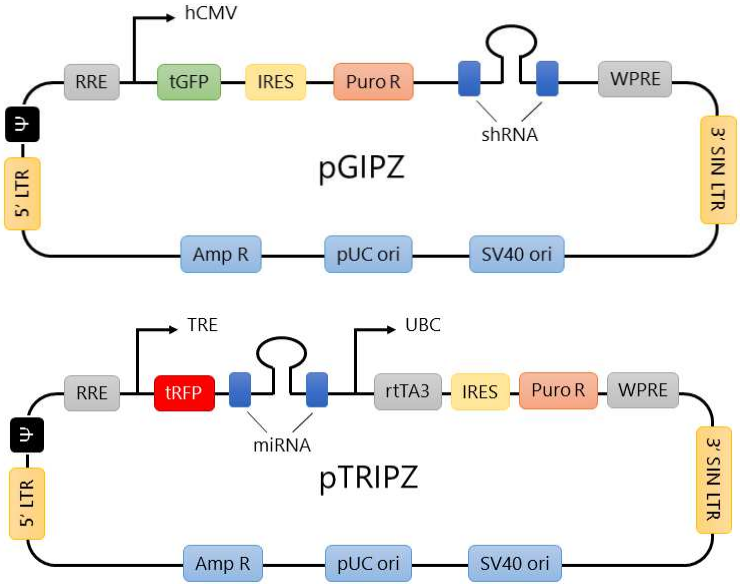

Figure 20. Schematic representation of the pGIPZ and pTRIZ plasmids (236,237).

Table 25. Elements present in the pGIPZ and pTRIPZ plasmids and their utility (236,237).

pGIPZ elements	**Utility**
hCMV	Human cytomegalovirus promoter that drives a strong transgene expression.
TGFP	TurboGFP reporter for selection of positively transduced cells.
shRNA	MiRNA-adapted shRNA (based on miR-30) for gene knockdown.
pTRIPZ elements	**Utility**
TRE	Tetracycline-inducible promoter.
tRFP	TurboRFP reporter for selection of positively transduced cells.
rtTA3	Reverse tetracycline-transactivator 3 for tetracycline-induction of the TRE promoter
UBC	Human ubiquitin C promoter for constitutive expression of rtTA3 and puromycin resistance genes.
miRNA	MiRNA-adapted shRNA (based on miR-30) for construct expression.
Common elements	**Utility**
Puro	Puromycin resistance that allows selection of positively transduced cells.
IRES	Internal ribosomal entry site that allows the expression of tGFP/rtTA3 and puromycin resistance genes in a single transcript.
5' LTR	5' long terminal repeat.
3' SIN LTR	3' self-inactivating long terminal repeat for increased lentivirus safety.
Ψ	Psi packaging sequences that allow viral genome packaging using lentiviral packaging systems.
RRE	Rev response element that enhances titer by increasing packaging efficiency of full-length viral genomes.
WPRE	Woodchuck hepatitis posttranscriptional regulatory element that enhances transgene expression in target cells.

The process of virus production and cell infection was the same in both cases. Briefly, viruses were produced in HEK293T cells by co-transfecting the three plasmids mentioned above (12 µg of insert vector, 8 µg of packaging and 4 µg of envelop plasmids) with lipofectamine (Thermo Fisher Scientific) in OptiMEM media (Gibco) supplemented with 5% of FBS. After 4h, the media was removed and replaced by supplemented media without antibiotics. HEK293T cells were grown for 36-48 hours and viruses were harvested and filtered through 0.45 µm pores. Then, confluent target cells were incubated with viruses diluted in supplemented media without antibiotics (standard dilution 1:2) for 24 hours. The excess of virus was stored at -80°C. Finally, 72 hours after infection, positive transduced target cells were selected with puromycin (1 µg/ml, Sigma-Aldrich) and reporter expression was assessed under the microscope.

4. miRNA induction by doxycycline

Overexpression of miR-7 and miR-324-5p in cells transduced with pTRIPZ lentiviral vector was induced by doxycycline treatment. Doxycycline was added to the culture media at 1 µg/ml and maintained for 72 hours.

miRNAs are short non-coding RNA sequences involved in the regulation of specific mRNA translation and the process of biogenesis of mature miRNA forms is complex. First pri-miRNAs (around a hundred base pairs long) are processed by Drosha, an enzyme that cleaves the stem of a hairpin structure formed by future miRNA mature sequence and produces the pre-miRNA (around 70-80 base pairs long). Pre-miRNA are exported from the nuclear region and once in the cytoplasm are processed by Dicer, which removes the loop region and produces a double strand form of the miRNA (miRNA

duplex). Then, the RNA-induced silencing complex (RISC) separates the two strands, and one of them generates the mature miRNA sequence (20-23 nucleotides) and the other is degraded (Figure 21) (238). In our case, two different sequences of miR-7 and miR-324-5p were tested, the form A corresponding to the pri-miRNA sequence, and the form B corresponding to the pre-miRNA sequence.

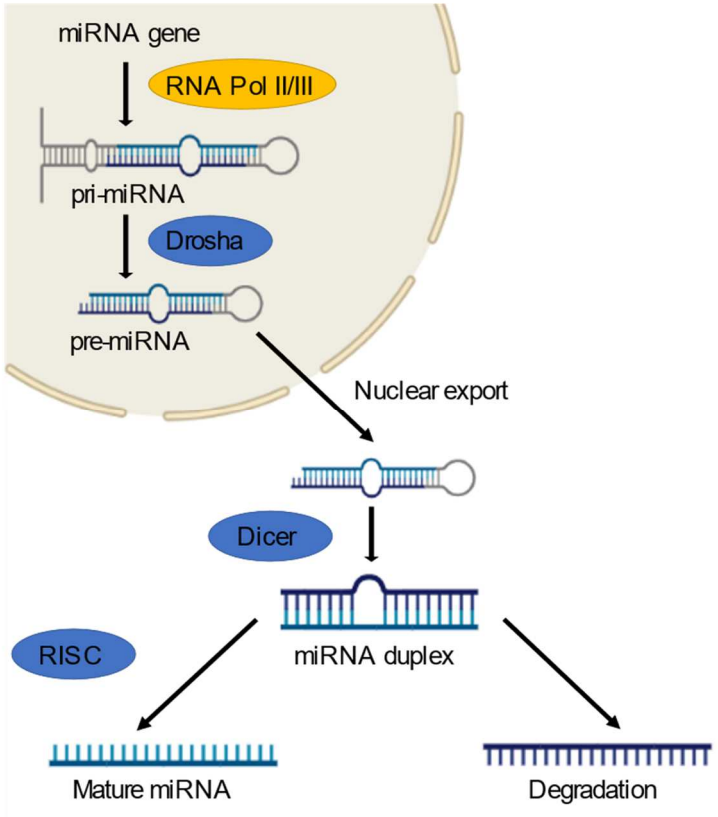

Figure 21. **Biogenesis of mature miRNA forms.** The first form that appears is the pri-miRNA which is processed by Drosha to generate the pre-miRNA. This form is exported from the nucleus to the cytoplasm, where it is processed by Dicer to generate the miRNA duplex. Finally, RISC complex separates the two miRNA strands and one of them is degraded, whereas the other becomes the mature miRNA form.

5. Protein detection by Western blot

Western blot was performed in order to determine the protein expression levels of certain genes. For this purpose, several steps were necessary, including protein extraction and quantification, gel electrophoresis, protein transfer intro membrane and antibody incubation.

5.1 Protein extraction, quantification and sample preparation

After being pelleted or using a cell scraper, cells were homogenized in RIPA lysis buffer (Thermo Fisher Scientific) supplemented with protease (Complete Tablets Mini EASYpack, Roche) and phosphatase inhibitors (Halt™ Protease and Phosphatase Inhibitor Single-Use Cocktail, Thermo Fisher Scientific).

Briefly, for the detection of cytoplasmic proteins, cultured cells were washed with PBS, detached from the plate using trypsin (Fisher Scientific) and centrifuged at 1500 rpm for 5 minutes. Afterwards, supernatant was discarded, the pellet was resuspended in 20-100 µl RIPA lysis buffer and incubated in ice for 20 minutes. Finally, it was centrifuged at maximum speed for 15-20 minutes at 4ºC to discard cell debris and supernatant was transferred to a new Eppendorf and frozen at -20ºC. On the other hand, for the detection of membrane proteins, cultured cells were washed with PBS and detached from the plate using a cell scraper and 75-100 µl of RIPA lysis buffer, whilst maintained in ice. Supernatant was transferred to an Eppendorf tube and centrifuged at maximum speed for 15-20 minutes at 4ºC to discard cell debris. Finally, supernatant was transferred to a new Eppendorf and frozen at -20ºC.

Total protein content was measured using the DC Protein Assay Kit (BioRad) following the manufacturer's instructions. This assay is a colorimetric assay for protein quantification following detergent solubilisation and is based on the Lowry assay method. Protein samples were diluted 1/5 in water and 5 µl of each sample were added into a 96-well plate (in triplicates). Immediately after, 25 µl of a mixture of solution A (alkaline copper tartrate solution) and solution S (surfactant solution) was added and eventually, 200 µl of solution B (Folin reagent) were added in each well. After an incubation of 15 minutes at room temperature, absorbance was measured at 750 nm using the Epoch Microplate Spectrophotometer (Biotek). Sample absorbance was compared to a bovine serum albumin (BSA) standard curve and protein concentrations were extrapolated.

5.2 Sample preparation, electrophoresis and protein transference

After protein quantification, 20-40 µg of protein were separated in a new Eppendorf tube and mixed with Laemmli loading buffer containing 10% of dithiothreitol 1M (DTT). Protein samples were heated at 70°C for 10 minutes to denature proteins and then, loaded into 8-15% SDS-polyacrylamide gels (SDS-PAGE) where electrical field (35 mA per gels) was applied to separate proteins. The presence of the strong reducing agents sodium dodecyl sulphate (SDS) and DTT in the Laemmli loading buffer, allowed a reduction in disulphide bonds and give proteins a negative charge. This way, proteins were directed to the anode during the gel electrophoresis and their separation was conducted exclusively due to their molecular weight. Small proteins move quickly through the gel matrix towards the positive electrode, while larger proteins move through more slowly, resulting in the separation of proteins according to their size.

After protein separation, they were transferred onto a polyvinylidene difluoride (PVDF) membrane with 0.45 µm pore (GE Healthcare Life Sciences), previously activated with methanol. In this case, an electrophoresis at 200 mA during 2 hours at 4°C was performed to assess the movement of the proteins from the gel to the membranes.

5.3 Antibody incubation and protein detection

After the transference, membranes were blocked for 1 hour at room temperature with TBS-T containing 5% of either bovine serum albumin (BSA) or milk (Fisher Scientific), to prevent non-specific binding of antibodies to the surface of the membrane. Then, membranes were incubated overnight at 4°C with the primary antibody diluted in the same blocking solution (Table 26).

The day after membranes were washed three times with TBS-T and incubated with the corresponding secondary antibody (specific to the host species of the primary antibody) also diluted in the same blocking solution for 1 hour at room temperature. Membranes were again washed three times with TBS-T and incubated in Amersham ECL Prime Western Blotting Detection (GE Healthcare Life Sciences). This kit is composed by two solutions, the peroxide and the luminol solution, which react to the horseradish peroxidase (HRP) enzyme in which the secondary antibodies are conjugated. Briefly, luminol is oxidated by HRP enzyme in presence of peroxide and this reaction generates light which can be detected using SuperRX Fuji Medical XRAY Films (Fujifilm), this way proteins can be detected. Finally, densitometric quantification of Western blot is done using the Image J software. Composition of the buffers used for Western blot is summarized in Table 27.

Table 26. List of antibodies used for protein detection.

1ry Ab	Origin	Blocking solution	1ry dilution	2ry Ab	Origin	2ry dilution	MW
Anti-ITGA9	Abnova, H00003680-M01	Milk 5% TBS-Tween	1:2000	Mouse	Dako	1:2000	150 KDa
Anti-FAK	Cell Signalling, 3285	BSA 5% TBS-Tween	1:1000	Rabbit	Sigma-Aldrich	1:10000	125 KDa
Anti-pFAK	Cell Signalling, 3283	BSA 5% TBS-Tween	1:500	Rabbit	Sigma-Aldrich	1:5000	125 KDa
Anti-pFAK	Santa Cruz Biotech., sc-81493	BSA 5% TBS-Tween	1:200	Mouse	Dako	1:2000	125 KDa
Anti-pRb	Cell Signalling, 9301	BSA 5% TBS-Tween	1:10000	Rabbit	Sigma-Aldrich	1:10000	110 KDa
Anti-p27	Cell Signalling, 3686	BSA 5% TBS-Tween	1:1000	Rabbit	Sigma-Aldrich	1:10000	27 KDa
Anti-p21	Cell Signalling, 2947	BSA 5% TBS-Tween	1:1000	Rabbit	Sigma-Aldrich	1:10000	21 KDa
Anti-PARP	Cell Signalling, 9542	BSA 5% TBS-Tween	1:2500	Rabbit	Sigma-Aldrich	1:10000	116, 89 KDa
Anti-BCL2	Dako, M0887	BSA 5% TBS-Tween	1:2000	Mouse	Dako	1:2000	26 KDa
Anti-BAX	Millipore, ABC11	BSA 5% TBS-Tween	1:2000	Rabbit	Sigma-Aldrich	1:10000	17 KDa
Anti-ACTIN	Santa Cruz Biotech., sc-47778	Milk 5% TBS-Tween	1:2000	Mouse	Dako	1:2000	40 KDa

Table 27. Composition of the buffers used for Western blot.

Buffer	Composition
Laemmli loading buffer	250mM Tris (pH 6.8), 10% SDS, 50% glycerol, 0.5% blue bromophenol and 10% DTT 1M
Running buffer	250nM Tris, 1.92M glycine (pH 8.3), 1% SDS and distil water
Transfer buffer	25mM Tris, 129mM glycine (pH 8.3), 20% methanol and distil water
TBS-T	200mM Tris-HCl, 150mM NaCl and 0.1% Tween20.

6. RNA detection and quantification by qPCR

Quantitative PCR (qPCR) is a PCR-based technique that couples amplification of a target DNA sequence with quantification of the concentration of that DNA in the reaction. This assay allows gene expression analysis by quantification messenger RNA (mRNA).

In order to determine the expression levels of certain genes, qPCR was performed using TaqMan assays. For this purpose, several steps were necessary, including RNA extraction, reverse transcription into complementary DNA (cDNA) and finally, detection using TaqMan probes.

6.1 RNA extraction

Total RNA, including the small RNA fraction, was extracted using the miRNeasy Mini Kit (Qiagen) using the manufacturer's instructions. This kit is based on phenol/guanidine lysis of the samples and silicamembrane-based purification of the RNA. Afterwards, extracted RNA was quantified using Nanodrop Spectrophotometer (Thermo Fisher Scientific) and stored at -80°C.

6.2 Reverse transcription

Reverse transcription was performed to obtain complementary DNA (cDNA), which is a DNA sequence synthesized form single-stranded RNA template by the enzyme reverse transcriptase.

For total RNA reverse transcription, 2 µg of RNA were isolated and incubated with 1 µg of random primers[5] (Invitrogen), at 70°C for 5 minutes. Then, 200U of M-MLV Reverse Transcriptase (Maloney Murine Leukemia Virus; Promega), 1.25 µl of deoxynucleoside triphosphate (dNTP; Thermo Fisher Scientific) and 5 µl of 5X M-MLV reaction buffer (Promega) were added. The reaction was maintained at 37°C for 1 hour and final cDNA was stored at -20°C.

On the other hand, for small RNA fraction detection, 12.5 ng of total RNA were isolated and reverse-transcribed using the TaqMan MicroRNA Reverse Transcription Kit (Thermo Fisher Scientific). Total RNA was mixed with 1.5 µl of 10X reaction buffer, 50U of the MultiScribe reverse transcription enzyme, 5U of RNase inhibitor, 0.15 µl of 100 mM dNTP and 3 µl of the specific RT primers included in the TaqMan assay (Table 32). These specific RT primers are custom made primers that target specific mRNA sequence, in this case the miRNA sequence, and that increases sensitivity and efficiency of the reverse transcription. The reaction was run in the thermal cycler (2720 Thermal Cycler, Applied Biosystems) with the program detailed in Table 28. Final cDNA was stored at -20°C.

Table 28. MicroRNA reverse transcription program.

Temperature (ºC)	Time (minutes)
16	30
42	30
85	5
4	Hold

[5] Six to nine bases sequences that anneal at multiple points along RNA transcript.

6.3 Quantitative PCR

Quantitative PCR (qPCR) was based on TaqMan Gene Expression Assays (Thermo Fisher Scientific) designed to efficiently detect the target genes (Table 29). TaqMan assays are based on fluorescent detection which correlates to the quantity of DNA amplified.

Table 29. TaqMan assays used for quantification of gene expression.

Gene	TaqMan assay
ITGA9	Hs00979865_m1
Mature form of miR-7	dme-miR-7, assay ID: 000268
Mature form of miR-324-5p	hsa-miR-324-5p, assay ID: 000539
RNU-44	RNU44, assay ID: 001094
TATA-binding protein	Hs00172424_m1

Each assay contains a pair of unlabelled primers (forward and reverse) and a label TaqMan probe which contains a fluorescent dye on the 5′ end and a non-fluorescent quencher on the 3′ end. The non-fluorescent quencher prevents the fluorescent emission while quencher and fluorescent dye are bonded to the probe. In each cycle of PCR, the unlabelled primers are used by the DNA polymerase to synthesize new strands and when the polymerase reaches a TaqMan probe, the fluorescent dye is released (Figure 22). With each cycle of PCR more dye molecules are released, resulting in an increased in fluorescence intensity proportional to the amount of amplified DNA. The cycle in which the fluorescent is first detected is the threshold cycle (Ct). It is inversely proportional to the initial DNA concentration and is used to quantify gene expression.

Briefly, 0.5 µl of cDNA were mixed with 5 µl TaqMan Universal Master Mix (Thermo Fisher Scientific) which contains the AmpliTaq Gold DNA Polymerase, 0.5 µl of the TaqMan Probe (Thermo Fisher Scientific; Table 30)

and 4 µl of DEPC-water (Thermo Fisher Scientific). The reaction was done in 384-well plates (Applied Biosystems) and 40 amplification cycles (Table 30) were performed using the ABI PRISM 7900HT thermo cycler (Life Technologies). TATA-binding protein (TBP) and RNU-44 were used as internal controls to normalize the gene expression. Relative levels of each gene were tested in triplicate and quantified by the 2−ΔΔCT method described by Livak and Schmittgen (239).

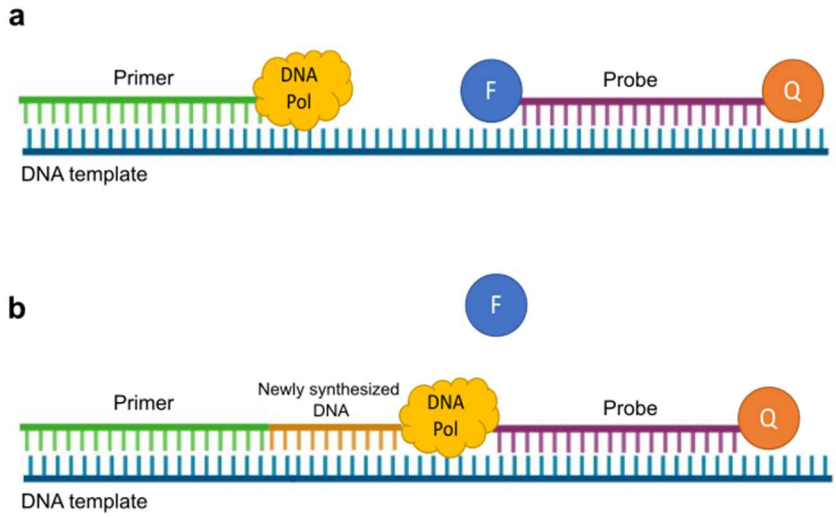

Figure 22. Representation of TaqMan assay working procedure. a. Binding of the primer, the DNA polymerase and the TaqMan probe to the DNA template. **b.** Polymerization and synthesis of new DNA strand. When the DNA polymerase reaches the probe, the fluorescent dye is released. This results in an increase of fluorescence intensity proportional to the amount of amplified DNA. Abbreviations: F, Fluorescent dye; Q, Non-fluorescent quencher.

Table 30. TaqMan gene expression program.

Temperature (°C)	Time	Cycles
50	3 minutes	1x
95	10 minutes	
95	15 seconds	40x
60	1 minute	
4	Hold	Hold

7. Proliferation assay

To assess the effects of ITGA9 inhibition (either by miRNA, shRNA or peptide agents) on cell proliferation, cells were seeded in 96-well plates at low density and were allowed to divide for 7 days. Media was changed every 48 hours and treatments (with doxycycline or RA08) were replaced at the same time. The number of cells was previously tested to ensure linear growth throughout the assay. Examples of this optimization are showed in Figure 23.

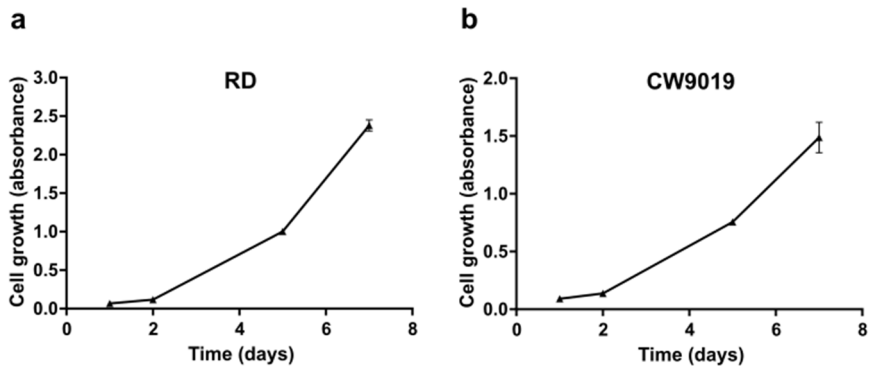

Figure 23. Cell growth of RD and CW9019 wild type cells. Seeding of 1 × 10^3 RD cells/well **(a)** and 2.5×10^3 CW9019 cells/well **(b)** was the optimal density to ensure linear growth throughout the assay.

At the end of the assay, cells were washed with PBS and stained with 0.5% crystal violet (Sigma-Aldrich) for 15 minutes. Plates were washed with PBS and dried overnight. Finally, crystals were dissolved with 15% acetic acid (Sigma-Aldrich) and absorbance was measured at 590 nm as a read out of the number of cells, using the Epoch Microplate Spectrophotometer (Biotek). Each assay contained 5 replicates per condition and was repeated at least three times.

8. Invasion assay

To assess the effects of ITGA9 inhibition (either by miRNA, shRNA or peptide agents) on cell invasion, transwell invasion assay was performed. This assay is based on the Boyden Chamber assay (240) in which a plastic chamber, sealed at one end with a porous membrane is placed in a 24-well plate and used to divide the well into two chambers. The upper chamber is where the cells are seeded, while the lower chamber is filled with medium and a chemoattractant. This way cells are directed from the upper to the lower chamber and allowed to migrate through the pores, to the other side of the membrane. Finally, migrated cells are stained and quantified. In the transwell invasion assay, apart from the migration capabilities, we can measure the invasion of these cells. For this purpose, the membrane is coated with a thin layer of ECM-like matrix.

In our experiments, cells were seeded with serum-free media in the upper chamber of an 8 μm pore size transwell (Corning), previously coated with Matrigel Growth Factor Reduced (Corning) diluted 1:3 also in serum-free media, and the lower chamber was filled with media supplemented with 10% FBS, used as chemoattractant. The number of cells seeded and the incubation time were previously tested to avoid oversaturation at the end of the assay. Finally, when peptide agents were tested, they were present in the upper and the lower chamber at the same final concentration.

After 18-24 hours of incubation, Matrigel and remaining cells were removed from the upper chamber and cells migrated to the lower surface of the membrane were washed with PBS, fixed with 4% paraformaldehyde (PFA; Fisher Scientific) and stained with Hoechst-33342 (Thermo Fisher Scientific)

at a final concentration of 5ng/ml. Then, 5 photos of each condition at 10X were recorded using fluorescence microscopy (Nikon) and the number of cells was counted using Image J Software. Each assay contained 3 replicates per condition and was repeated at least three times (Figure 24).

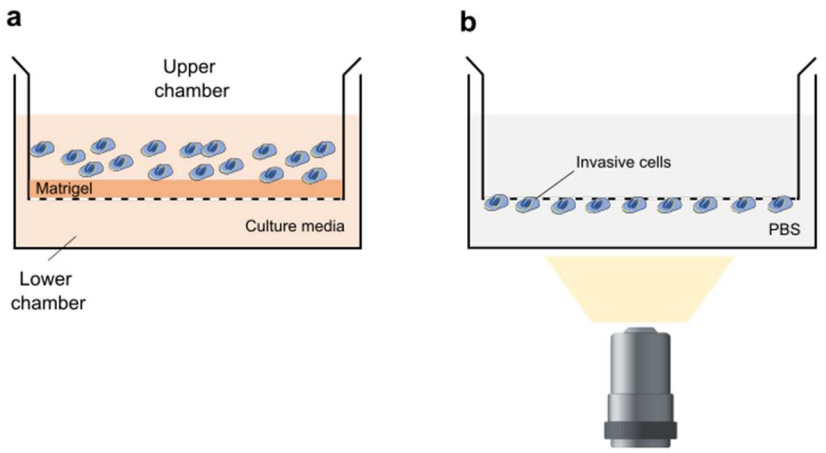

Figure 24. Representation of Transwell invasion assay. a. Cells are seeded in the upper chamber of a transwell insert previously coated with Matrigel in serum-free media. In the lower chamber, FBS is added to the media and used as cell chemoattractant. **b.** After 18-24 hours of incubation, the media and the Matrigel are removed and transwell inserts are washed with PBS. Cells migrated to the lower surface of the membrane are stained with Hoechst and quantified under the microscope.

9. RA08 development

A specific inhibitor for ITGA9, hereinafter referred as RA08, was designed in collaboration with BCN peptide. This inhibitor was based on the sequence of interaction of a known ITGA9 ligand, the ADAM12, and was designed to act as a blocking peptide agent able to bind the ITGA9 and prevent the interaction with other ligands. Nevertheless, the complete specificity of RA08 was not tested and we could not rule out the possibility that it can also interact with other molecules, such as other integrins and members of the ADAM family. RA08 is under patent protection PCT/EP2020/083987:

"Peptides for the treatment of cancer and/or metastasis" (231). Multiple peptides with small modifications were designed following this approach and their ability to reduce cell invasiveness in RMS cell lines was tested. RA08 was the candidate with best results in previous studies and was selected for further investigation (232).

RA08 was synthesized by solid-phase peptide synthesis following the Fmoc/tBu strategy with 4-Methylbenzhydrylamine (p-MBHA) resin at 30 mmol scale. Fmoc-AM-OH linker (2 eq.), HOBT (2 eq.) and DIPCDI (2 eq.) were used for attaching the linker to the resin. Then, synthesis proceeded with the removal of the Fmoc group by treatment with a solution of 20% piperidine in dimethylformamide (DMF, twice for 5 minutes and twice for 10 minutes). The peptide-resin was washed 5 times with DMF, filtered and the following amino acids were coupled. Couplings were done by using Fmoc-AA-OH:DIPCDI:HOBt (3 eq: 3 eq: 3 eq) in DMF (Fmoc-Msa-OH was coupled using 1.5 eq). All these coupling reactions were left to react for 40-60 minutes. The completion of each coupling reaction was controlled with a Ninhydrine test (or a Chloranyl test). After completion of the peptide sequence, the peptidyl-resin was washed with DMF, methanol and diethyl ether (Et_2O) and dried. Then, the peptidyl-resin was left to react for 2 hours in a trifluoroacetic acid (TFA) mixture at room temperature to cleave the peptide from the resin. The resin was washed with TFA and Et_2O. All the filtrates were plunged into cold ether. The suspension obtained was filtered through a filter plate and the filters discarded. The solid was freeze dried and the peptide crude product obtained.

The crude peptide was purified in a semipreparative system equipped with a NW50 Merck column filled with 10 µm of kromasil silica and the pure

fractions analysed in an analytical RP-HPLC were lyophilised. The ion-exchange step was carried out to get the peptide with the acetate counter ion. The final acetate compound was recovered via filtering and lyophilised. Finally, RA08 was characterised by Mass Spectrometry by ESI-MS spectrometry (MW =1806 a.m.u.).

RA08 was resuspended with PBS in sterile conditions and at a final concentration of 100 µM. This solution was stored at -20°C and was used as a stock solution for the experiments, since all the working concentrations were obtained after dilution of this in PBS. The working concentrations used were: 100nM, 200nM, 500nM and 1000nM. Treatment with PBS was used as a control condition (referred as vehicle).

10. Apoptosis assessment

Fluorescent conjugated Annexin V was used to assess apoptotic cell death in our cells by flow cytometry. Annexin V is a member of the annexin family of calcium-dependent phospholipid binding proteins that has high affinity for the phosphatidylserine (PS) residues. In healthy cells, PS is located on the cytoplasmic surface of the plasma membrane, whereas during apoptosis it translocates from the inner to the outer part of the plasma membrane. Thus, detection of PS by fluorescent conjugated Annexin V is used to quantify apoptotic cells (241,242).

In our experiments, APC-conjugated Annexin V (BD Biosciences) vas used to measure apoptotic cells and Sytox blue (Fisher Scientific) was used to quantify dead cells since it penetrates cells with compromised cellular membrane and stains nucleic acids. For this, cultured cells were detached, pelleted and counted. Ideally, 100.000 cells were isolated and resuspended

in 100 µl Annexin Binding buffer (BD Biosciences). Then, 5 µl of APC-Annexin V were added and samples were incubated for 15 minutes at room temperature. Afterwards, 400 µl of Annexin Binding buffer were added as well as 0.5 µl of Sytox blue.

To correctly adjust the apoptotic and dead cell populations, samples without any staining and samples with each single marker were needed. Besides, a positive control of apoptotic cells, such as cells treated with cisplatin for 24 hours, was also used. Samples were analysed using LSR Fortessa FACS cytometer (BD Biosciences). Forward scatter and side scatter were used to isolate single cells. Then, C-Red (excitation at 640nm) and F-Violet (excitation at 405nm) detectors were used to determine positive cells for Annexin V and Sytox blue, respectively. Segregation of alive, apoptotic and dead cells was done as follows (Figure 25):

(1) Negative cells for the two markers were considered alive cells.
(2) Only Annexin V positive cells were considered early apoptotic cells.
(3) Only Sytox blue positive cells were considered dead cells.
(4) Positive cells for the two markers were considered late apoptotic cells.

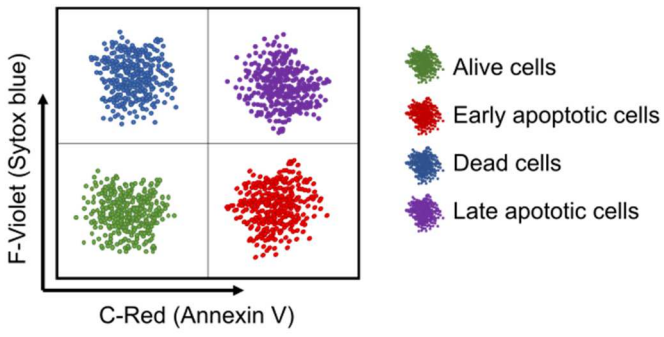

Figure 25. Segregation of alive, apoptotic and dead cells by Annexin V and Sytox blue staining.

BD FacsDiva and FCS Express software were used to record and analyse the data and each sample was processed in triplicates.

11. Cell cycle assay

Cell cycle analysis was performed by quantification of DNA content using a DNA-binding dye detected by flow cytometry. This assay is based on the fact that cells in G1 phase only have one copy of each chromosome and during the S phase all genetic material is duplicated, so at the G2/M phase the DNA content is the double compared to G1. This allows the quantification of cells staged at each cycle phase, since the amount of DNA-binding dye detected in G2/M phase is always the double of the amount detected in G1, and intermediate states correspond to cells in S phase (243).

In our experiments, cultured cells were detached, pelleted and counted. Ideally, at least 1 million cells were isolated and resuspended in PBS (300 µl per million cells). Then, cells were fixed with 100% pre-cold ethanol (700 µl per million cells) and samples were stored at 4ºC at least for 2 hours (alcohol-fixed cells are stable for several weeks at 4°C). Usually the day after, fixed cells were centrifuged at 5000 rpm for 5 minutes to remove the fixing solution and washed with PBS. Finally, cells were incubated overnight at 4ºC in the working solution containing sodium citrate (38 mM), propidium iodide (30 µl of 500 µg/ml solution, Sigma), RNAse A (30 µl of 10 mg/ml solution, Panreac) and PBS (up to 1 ml). Propidium iodide was the DNA-binding dye used in our experiments and since it also stains RNA, RNAse A was added to the solution to remove any possible RNA contamination. In addition, sodium citrate was also added to stabilize the propidium iodide staining for some days.

Cells and DNA content were detected using FACS Calibur cytometer (BD Biosciences). Forward scatter and side scatter were used to identify single cells and the amount of propidium iodide was used to segregate cells into the different cell cycle phases (Figure 26).

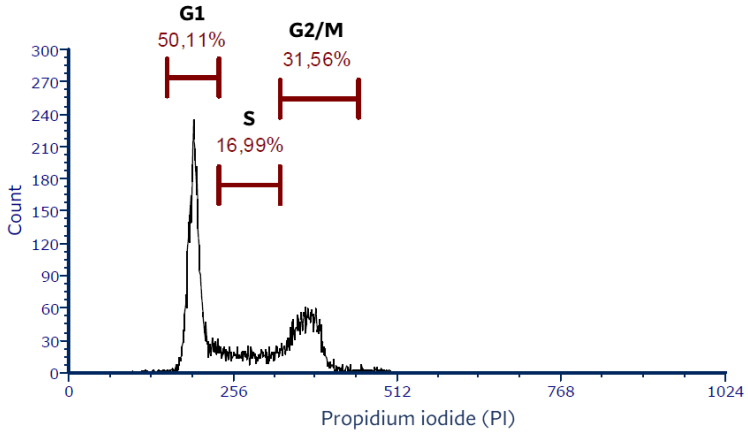

Figure 26. Example of cell cycle analysis of RD control cells. Plot showing the proportion of cells in each cell cycle phase. Cells in G2/M phase have the double amount of propidium iodide than the cells in the G1 phase. Cells with intermediate amount of propidium iodide correspond to cells in S phase.

12. WST-1 viability assay

Cell proliferation WST-1 reagent (Sigma-Aldrich) was used to quantify cell growth in non-adherent cell cultures. In this assay the measurement of cell growth was based on the cleavage of dyed tetrazolium salts to formazan by cellular enzymes. Generally, when cells accelerate their proliferation, they also increase the activity of mitochondrial dehydrogenases, which in turns increases the formation of formazan. Consequently, quantification of dyed formazan can be used as a measure of metabolically active cells.

In our experiments, cells were seeded at low density in 6-well polyHEMA-coated plates (Santa Cruz Biotechnology) that prevented cell attachment to

the plate and they were allowed to proliferate for 48 hours. At the end of the assay, cell spheres were disaggregated with accutase (Fisher Scientific) and replated in 96-well plates, where 10 µl of WST-1 reagent was added to each well. Three hours later, absorbance was measured at 440 and 690 nm using an Epoch Microplate Spectrophotometer (Biotek). The absorbance measured at 690 nm was used as a background control, while the one measured at 440 nm was the read out of the dyed formazan present in the sample. Time of WST-1 reagent incubation was previously tested to optimize the signal detection. Each assay contained 5 replicates per condition and was repeated at least three times.

13. *In vivo* studies

13.1 Primary orthotopic tumour model of RMS

To assess the effects of miRNA overexpression in tumour growth, 1 x 10^6 RD cells transduced with pTRIPZ-miRNA lentiviral vectors were injected into the right gastrocnemius muscle of severe combined immunodeficient mice (SCID[6], Charles River Laboratories) housed in specific pathogen-free conditions. Mice were split in three groups (n=7) depending on the injected cells, either transduced with the pTRIPZ empty, pTRIPZ-miR-7 or pTRIPZ-miR-324-5p plasmid. One week later, doxycycline (1 mg/ml, Sigma-Aldrich) was added to the water to induce miRNA overexpression and the treatment was maintained until the end of the experiment. Body weight and limb volume (with a calliper) were measured twice per week and the inferred tumour volume was calculated using the following formula, where L is length and A is amplitude:

[6] SCID mice: absence of mature T and B cells (353).

$$Tumour\ volume = \frac{4}{3} \cdot \pi \cdot \left(\frac{L + A}{4}\right)^3$$

All mice were euthanized 18 weeks after tail-vein injection. Tumours were dissected and half of each sample was freeze at -80ºC, whereas the other half was fixed in formalin and paraffin-embedded. Protein expression was assessed by Western blot in frozen samples, while immunohistochemical staining was performed in tissue sections from paraffin-embedded samples.

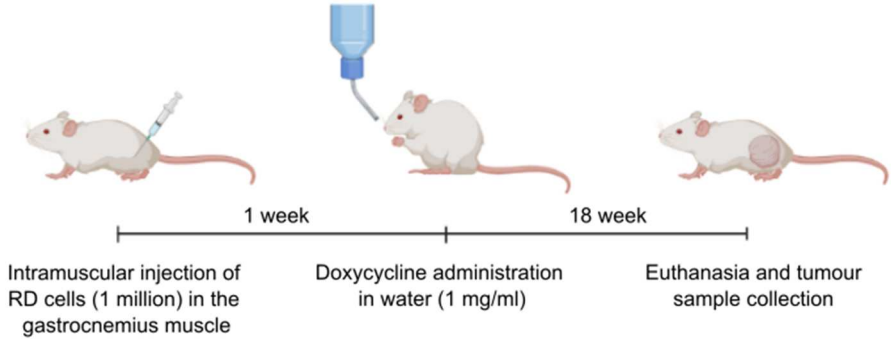

Figure 27. *In vivo* experimental design for primary orthotopic model.

13.2 Lung colonization model of RMS

To study lung colonization by tumour cells, 3 x 10^6 RD cells transduced with pTRIPZ-miRNA lentiviral vectors were intravenously injected through the tail vein of SCID-beige[7] mice (Charles River Laboratories) housed in specific pathogen-free conditions. Mice were split in two groups (n=4) depending on the injected cells, either transduced with the pTRIPZ empty or pTRIPZ-miR-7 plasmid. Cells were pre-treated with doxycycline (1 µg/ml) for 72 hours and mice were treated during the whole experiment with doxycycline

[7] SCID-beige mice: absence of mature T and B cells and defective dendritic, macrophages and NK cells (353).

in drinking water (1 mg/ml). One week after the injection, mice were euthanized and lungs were isolated and processed for FACS analysis (FacsAria, BD Bioscience).

Briefly, lungs were mechanically disaggregated and incubated with 2.5% collagenase type I (Fisher Scientific) diluted in culture media during 1 hour at 37ºC and subsequently, with trypsin-EDTA 0.05% (Fisher Scientific) for 5 minutes. Then samples were washed with PBS and incubated in erythrocytes lysis buffer (Qiagen) for 10 minutes at 4ºC. Finally, samples were washed again and resuspended in PBS containing a viability marker, in this case, Sytox blue (Life Technologies) at a final concentration of 1 µM. Analysis by FACS allowed the isolation and quantification of viable tumour cells (Sytox blue negative, RFP positive) present in the mice lungs. Samples from a mouse not injected were used as a negative control and samples in which pTRIPZ-miRNA transduced cells were added *in vitro* were used as a positive control for FACS analysis.

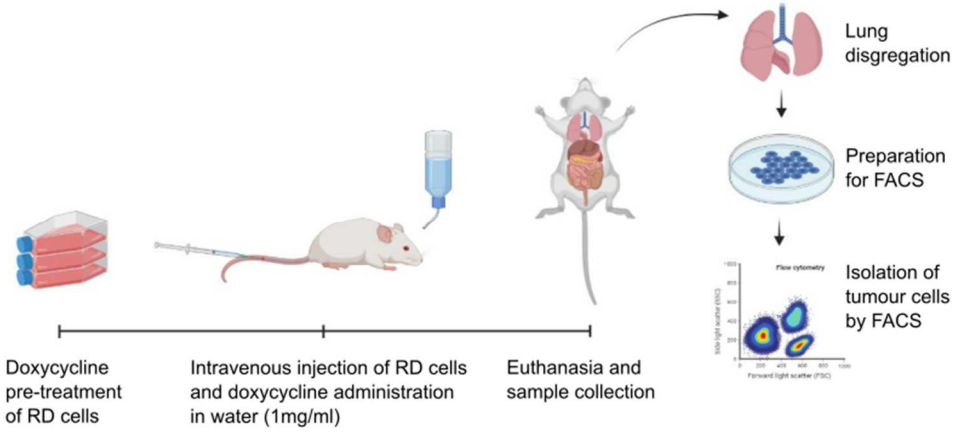

Figure 28. Experimental design of *in vivo* lung colonization model.

Gating procedure is summarized in Figure 29. Briefly, single cells were isolated form cell debris using forward (FSC) and side (SSC) scatter and Sytox blue was used to delimit alive cells. Finally, cell auto-fluorescence was corrected and tumour cells were detected due to the expression of RFP fluorescent protein.

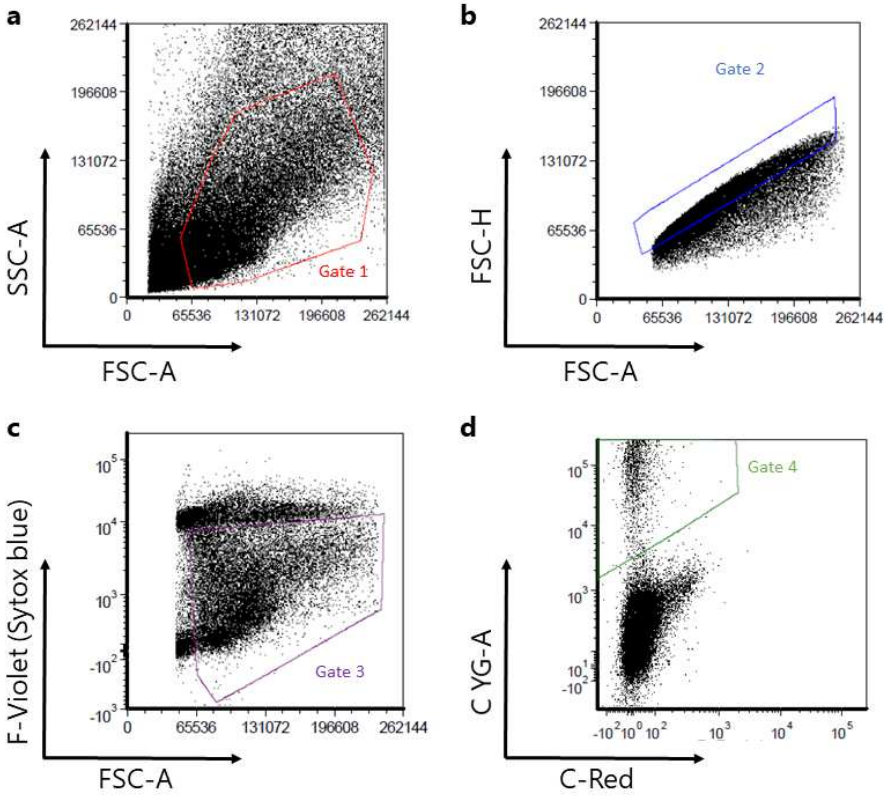

Figure 29. Gating procedure for detection of RFP positive cells by flow cytometry. a. Isolation of cells at Gate 1 and debris discard. Forward scatter (FSC) and side scatter (SSC) were used to delimit cells and discard cell debris. Forward and side scatter gave us a measure of size and complexity of cells, which is higher in cells than in debris. **b.** Isolation of single cells at Gate 2. Forward scatter (FSC) at height (FSC-H) and amplitude (FSC-A) allowed the delimitation of single cells and the discard of doublets. **c.** Delimitation of alive cells at Gate 3 using Sytox blue staining (F-Violet laser). Alive cells were not stained by Sytox blue. **d.** Delimitation of RFP positive cells at Gate 4. RFP fluorescent protein was detected by C-YG laser and cell auto-fluorescence was corrected using C-Red laser.

13.3 Metastasis model of NB and BC

A different concentration of tumour cells was intravenously injected through the tail vein of SCID-beige mice. *In vivo* experiments were performed to determine the optimal number of cells to inject in NB and BC metastasis models, considering each cell line ability to generate metastases. In the case of NB, 4 different amounts of BE(2)C cells were tested and eventually, 20.000 cells turned out to be the optimal number of cells for the metastasis model since it produced between 2 and 6 metastases per animal. On the other side, 125.000 MDA-MB-468 turned out to be the optimal number of cells for the BC model. In this case, lung colonization by tumour cells was quantified using GFP expression of tumour cells and the minimal amount of cells able to colonize the lungs was chosen for next experiments (Figure 30).

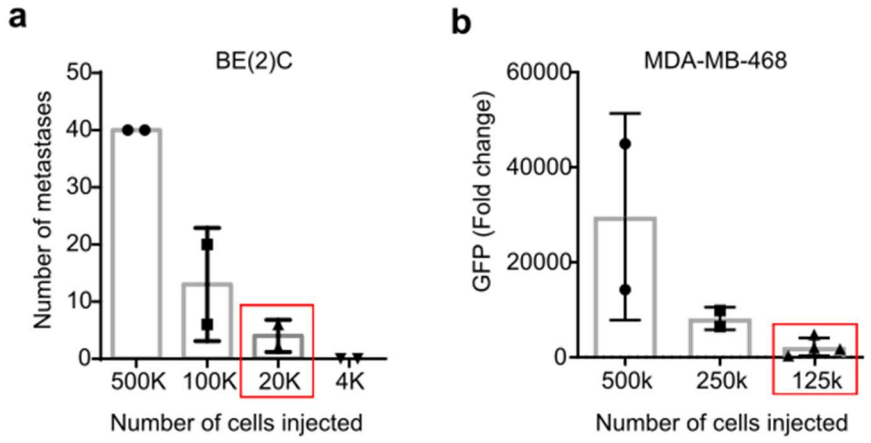

Figure 30. Optimization of number of injected tumour cells in metastasis models of NB and BC. a. The ability to form metastasis by BE(2)C using 4 different amounts of cells was tested and 20.000 cells (2-6 metastases/mice) was chosen for next experiments. **b.** The ability to colonize the lungs by 3 different amounts of MDA-MB-468 cells was tested and 125.000 was chosen for next experiments. Detection of GFP expressed by tumour cells was assessed by qPCR in lung tissue. Values are referred to those of the cell line in cell culture.

In NB shRNA model, mice were split into two groups (n=10) depending on the injected cells, either transduced with the pGIPZ empty or pGIPZ-shRNA#1 plasmid. On the other hand, when RA08 treatment was the main intervention, mice were split into three groups (n=10), according to the treatment they received, either the vehicle (saline solution) or two different RA08 doses (1 mg/kg and 2 mg/kg). The first RA08 administration was performed two hours before tail-vein injection and then three times per week throughout the experiment by subcutaneous injection. Mice were monitored and their body weight measured twice per week.

For the NB models, ethical endpoint criteria were based on acute weight loss (>10% of total body weight), clear detection of metastases (lumps or swelling) or poor general appearance of the animal. Metastasis foci were found in post-mortem analysis of mice fulfilling at least one of these end-point criteria and after euthanasia tissue samples were collected, fixed in formalin (Sigma-Aldrich) and paraffin-embedded. Whereas for the BC model, immunohistochemical staining of GATA3 was performed in tissue sections from paraffin-embedded lungs to quantify the presence of metastatic cells and foci. For this purpose, mice were euthanized at the same time point (9 weeks after cell injection) before they fulfil any of the above-mentioned end-point criteria. Quantification of metastatic cells was done using the Image J software and metastatic focus were considered when more than 4 GATA3+ cells were found in contact to each other.

13.4 Patient Derived Xenograft of BC

Tumour fragments from a patient-derived orthotopic xenograft model of BC were implanted in the breast of athymic Nude-Foxn1nu mice to generate

new orthotopic tumours (n=18/group). Seven days after implantation, mice were randomized and assigned to different groups in order to receive vehicle or RA08 (2 mg/kg). Treatment was conducted three times per week by subcutaneous injections.

Body weight and tumour volume were measured were monitored during the whole experiment. Ethical endpoint criteria were based on acute weight loss (>10% of total body weight), tumour mass of more than 2000 mm^3 or poor general appearance of the animal. All mice were euthanized 60 days after tumour implantation. Tumours were dissected and half of each sample was freeze at -80ºC, whereas the other half was fixed in formalin and paraffin-embedded. This part of the work was conducted by Alberto Villanueva's group and Xenopat, a company specialized in animal models.

13.5 Immunohistochemistry of tissue samples

Immunohistochemistry staining was used to determine the expression of certain proteins in tissue sections (either tumour samples or resected organs). For this, paraffin-embedded tissues were deparaffinised by incubating them at 65°C for 1 hour. Then, they were rehydrated by incubation in xylene and decreasing concentration of ethanol solutions. Finally, tissue sections were incubated with antibodies (Table 30) and dehydrated again by incubating them with increasing concentration of ethanol solutions and xylene.

This part of the work was done by the Pathology department of the Hospital Vall d'Hebron.

Table 31. Antibodies used for immunohistochemistry staining of tissue samples.

Antibody	Origin	Protein function	2ary antibody
KI67	Roche, 05278384001	Nuclear protein that is associated with cellular proliferation, in fact it is widely used in routine pathological investigation as a proliferation marker.	Rabbit
CD31	Abcam, 124432	It is found on endothelial cell intercellular junctions. It was used as a marker for tumour vessels.	Rabbit
GATA3	Sigma Aldrich, L50-823	Member of the GATA family of transcription factors. Nuclear marker with expression in many epithelial neoplasms, including breast cancer. It was used to quantify the presence of metastatic cells in mouse lungs.	Mouse

14. Analysis of patient datasets

Analysis of expression data from patients was performed on publicly available datasets. For the analysis of RMS and NB patients the R2: Genomics Analysis and Visualization Platform (244) was used. In particular, "Tumour Rhabdomyosarcoma-Davicioni-147-MAS5.0-u133a" (245) data set was used for RMS patients, while "Tumour Neuroblastoma-SEQC-498-RPM-seqcnb1" (246) and "Tumour Neuroblastoma non *MYCN* amplified-Seeger-102-MAS5.0-u133a" (247) were used for NB patients and metastatic non-*MYCN*-amplified subset of patients, respectively. For analysis of BC patients "Tumour Breast-1110-rma-hta2t" (248) dataset from the R2: Genomics Analysis and Visualization Platform (244) and Kaplan-Meier Plotter were used (249).

15. Statistics

At least three independent replicates were performed for each *in vitro* experiment and statistical significance was determined by Student's t-test

(when only two data sets were compared) or ANOVA (when more than two data sets were compared). For multiple comparisons, Bonferroni correction was used. On the other hand, *in vivo* models were only performed once and statistical significance was determined by Log-Rank test for survival analysis and two-way ANOVA for primary tumour models.

All the analysis was made using Graph Pad Prism Software and data was presented as mean ± standard deviation (SD). Statistical significance followed this criteria: *$p < 0.05$, **$p < 0.01$ and ***$p < 0.001$.

IV. RESULTS

"One of the basic rules of the universe is that nothing is perfect.
Perfection simply doesn't exist. Without imperfection, neither you nor I would exist"
Stephen Hawking

1. Regulation of ITGA9 by miRNA in RMS

1.1 miR-7 and miR-324 regulated ITGA9 in RMS cell lines

In order to describe the regulation of ITGA9 by miRNAs, three different algorithms (PicTar, TargetScan and miRANDA) were used to identify miRNAs that potentially were able to bind ITGA9 3' UTR. *In vitro* validation of candidates was done in RD and CW9019 cell lines, both expressing high levels of ITGA9. For this, cells were transfected with miRNA mimics and two miRNA mimic negative controls (C-1 and C-2) and ITGA9 protein expression was assessed by Western blot (Figure 31). Results showed that miR-7 and miR-324-5p significantly reduced ITGA9 levels in both cell lines and were selected for further study.

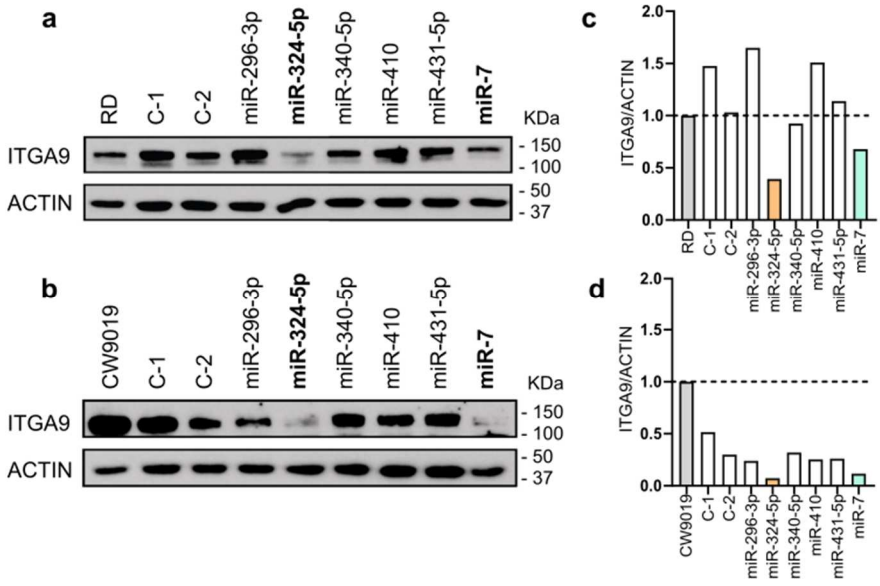

Figure 31. miR-7 and miR-324-5p target ITGA9 in RMS cell lines. a,b. Western blots showing ITGA9 expression after miRNA transfection in RD and CW9019 cell lines, respectively. **c,d.** Densitometric quantification of Western blot. This part of the work was done in collaboration with Molist C (250).

Once miR-7 and miR-324-5p were chosen as the best candidates for ITGA9 downregulation and with the aim of studying the effect of their overexpression in long-term experiments, miR-7 and miR-324-5p were cloned into the inducible pTRIPZ lentiviral vector.

Two different miRNA forms of miR-7 and miR-324-5p were used: the form A, as pri-miRNA, and the form B, as pre-miRNA. Both forms of miRNA needed to be further processed to become the mature form of the miRNAs (detailed at Materials and Methods section, Figure 21). RD cell line was infected with lentivirus containing all miRNA-pTRIPZ constructs and positively transduced cells were selected with puromycin. Then, ITGA9 expression was assessed by Western blot after miRNA induction by doxycycline (Figure 32 a,b). In addition, the overexpression of mature forms of each miRNA was assessed by qPCR (Figure 32c). Both forms of miR-7 were able to decrease ITGA9 expression at the protein level after induction by doxycycline, but only form B was detected by qPCR using a Taqman assay for mature miR-7. On the contrary, only form B of miR-324-5p was able to strongly decrease ITGA9 expression and was detected by qPCR using Taqman assay for mature miR-324-5p. Based on these results, further experiments were only performed with forms B of miR-7 and miR-324-5p. We hypothesized that the processing of pri-miRNA (forms A) was not completed and mature forms of miR-7 and miR-324-5p were not achieved, so that ITGA9 inhibition was not effective. However, the processing of pre-miRNA (forms B) and, consequently, the downregulation of ITGA9 was more efficient.

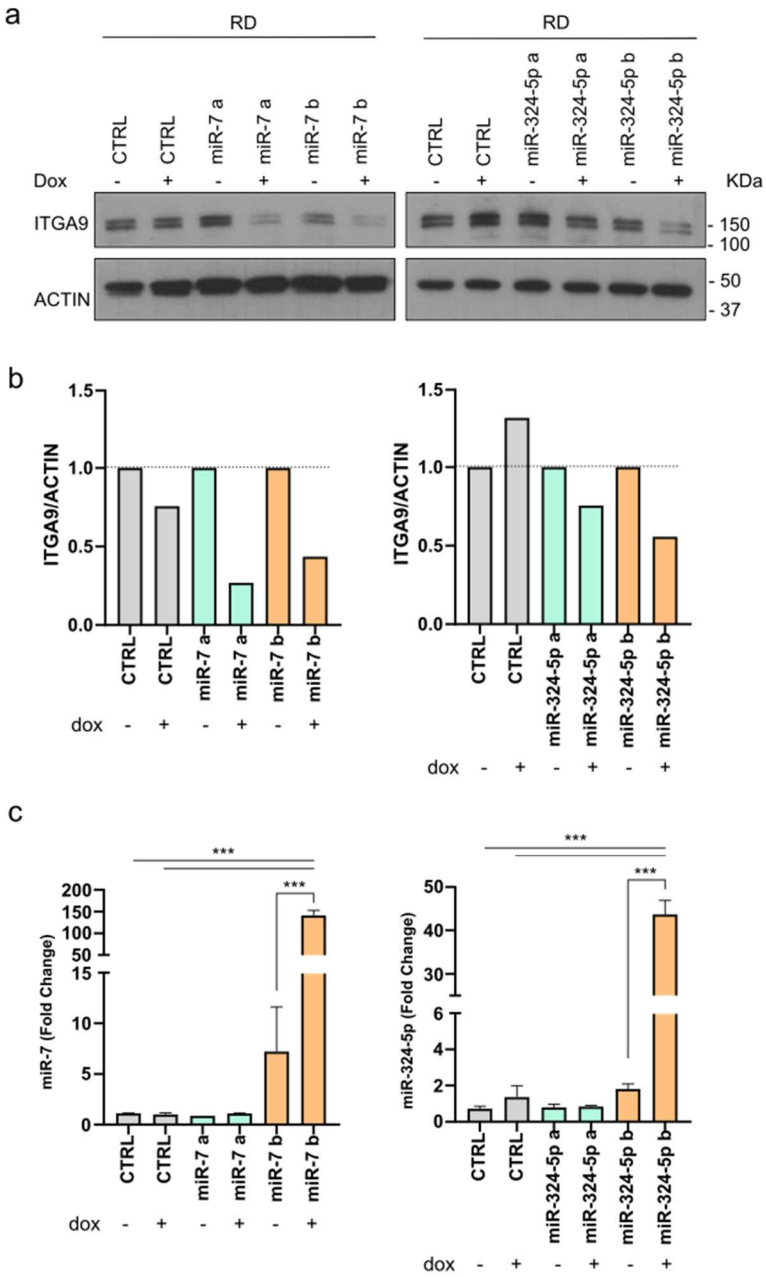

Figure 32. Induction of miR-7 and miR-324-5p, forms A and B, reduced ITGA9 expression. a. Western blots showing depletion of ITGA9 after miRNA induction with doxycycline in RD cell line. **b.** Densitometric quantification of Western blot. Each condition was referred to the corresponding basal condition (non-treated with doxycycline). **c.** miRNA relative expression by qPCR after induction with doxycycline in RD cell line. All conditions were normalized to the endogenous expression of RNU-44 and referred to the non-treated CTRL (empty vector). Statistical significance was determined by ANOVA, considering ***$p<0.001$.

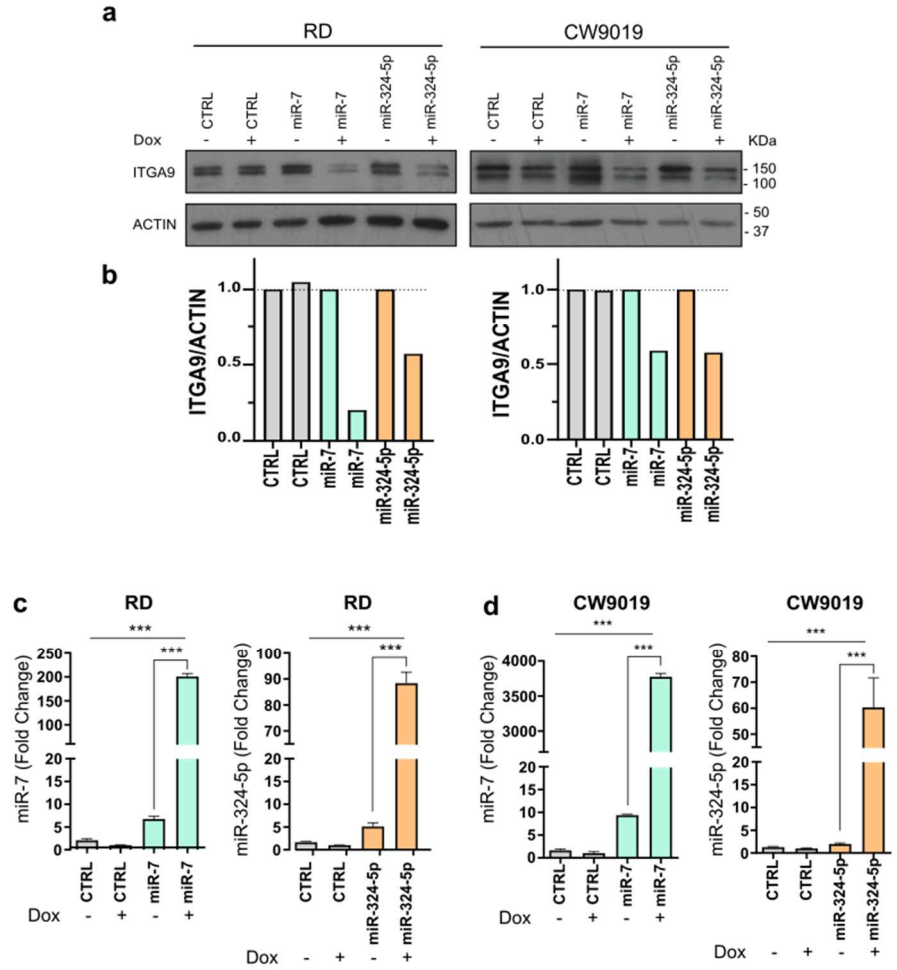

Figure 33. Induction of miR-7 and miR-324-5p reduced ITGA9 expression. a. Western blots showing depletion of ITGA9 after miRNA induction with doxycycline in RD and CW9019 cell lines. **b.** Densitometric quantification of Western blot. Each condition was referred to the corresponding basal condition (non-treated with doxycycline). **c,d.** miRNA relative expression by qPCR after induction with doxycycline in RD and CW9019 cell lines, respectively. All conditions were normalized to the endogenous expression of RNU-44 and referred to the non-treated CTRL (empty vector). Statistical significance was determined by one-way ANOVA, considering ***p<0.001.

Then, two cell lines representing both subtypes of RMS, RD as embryonal and CW9019 as alveolar subtype (251), were transduced with forms B of miR-7 and miR-324-5p. After miRNA induction with doxycycline, expression of ITGA9 was assessed by Western blot (Figure 33 a,b) and the expression

of miRNA by qPCR (Figure 33 c,d). Western blots showed a clear reduction of ITGA9, only when miRNAs were induced by doxycycline. Similarly, miRNA expression analysis revealed a clear induction of miR-7 and miR-324-5p after doxycycline treatment in both cell lines. Cells transfected with both miRNA vectors in absence of doxycycline had some residual miRNA expression; however, the levels found in these cells did not suffice to modify ITGA9 expression as shown by Western blot (Figure 33a).

1.2 Overexpression of miR-7 and miR-324-5p led to reduced proliferation and invasion in RMS cell lines *in vitro*

In order to assess the effects of miR-7 and miR-324-5p on cell behaviour, proliferation and invasion assays were performed after miRNA doxycycline-dependent induction in RD and CW9019 cell lines (Figure 34).

For assessing effects on cell proliferation, cell growth was quantified after 7 days with or without doxycycline treatment. Both miRNA turned out to promote a reduction, with a more pronounced decrease caused by miR-7 overexpression (more than 50% reduction in both cell lines) than by miR-324-5p, with a less important, albeit significant reduction (ranging from 25 to 35%) (Figure 34 a,b).

Cell invasiveness was assessed after Transwell invasion assays and in this case, only conditions treated with doxycycline were used. In terms of cell invasion, miR-7 overexpression promoted a very clear reduction (60-80%) in both cell lines. Nevertheless, no significant variation was observed after miR-324-5p induction (Figure 34 c,d), suggesting that only miR-7 play a potential role on cell invasion.

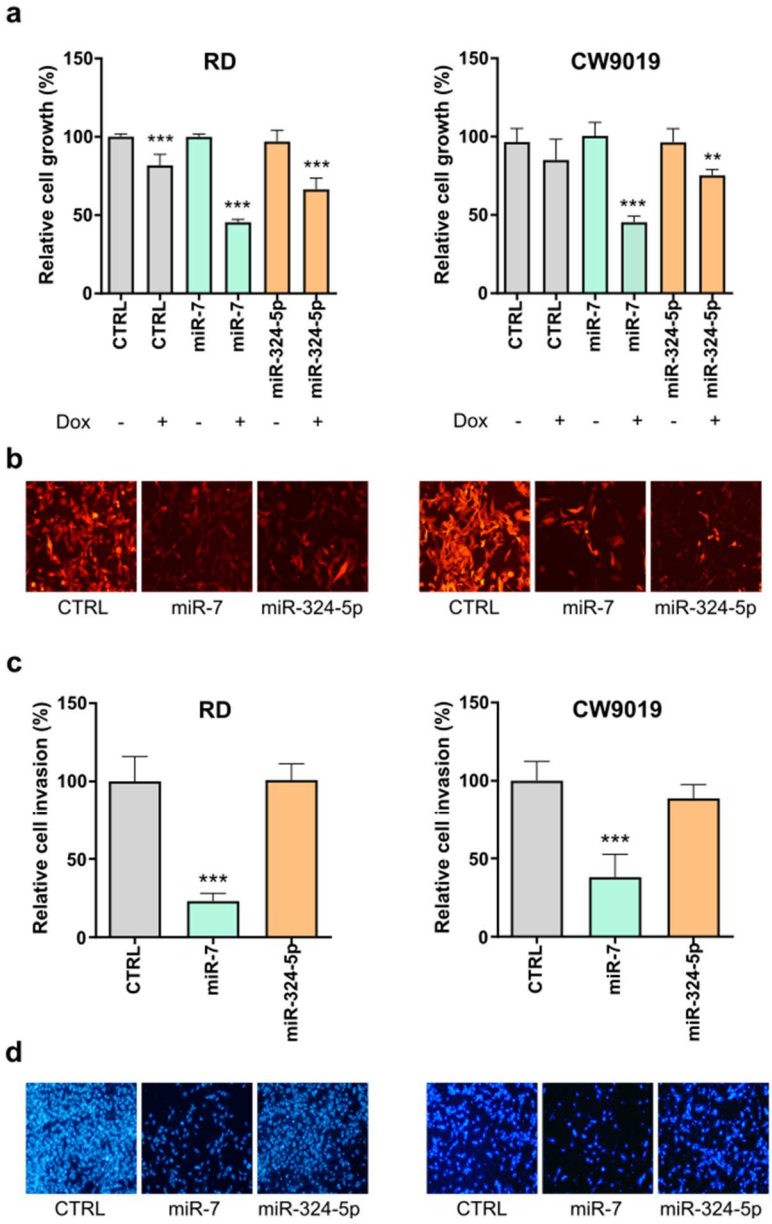

Figure 34. ITGA9 depletion by miR-7 and miR-324-5p rediced cell growth and invasiveness in RMS cell lines. a. Relative cell proliferation after miR-7 and miR-324-5p doxycycline-dependent induction in RD and CW9019 cells, respectively. Each condition was referred to the corresponding basal condition (non-treated with doxycycline). **b.** Representative images of miRNA-induced conditions at the end of the assay. **c.** Relative cell invasiveness after miR-7 and miR-324-5p induction in RD and CW9019 cells, respectively. Values of invasiveness were referred to the control vector treated with doxycycline. **d.** Representative images of miRNA-induced conditions at the end of the invasion assay. Statistical significance: **p < 0.01, ***p < 0.001.

1.3 ITGA9 knockdown recapitulated the effects of miR-7 and miR-324-5p overexpression

With the aim of demonstrating that the effects observed with miR-7 and miR-324-5p overexpression were mediated by ITGA9 downregulation, the effects of ITGA9 knockdown by shRNA were tested. RD and CW9019 cell lines were transduced with pGIPZ lentiviral vector containing shRNA sequences targeting ITGA9 and sh#2 was selected as the most efficient shRNA downregulating ITGA9 (Figure 35 a,b).

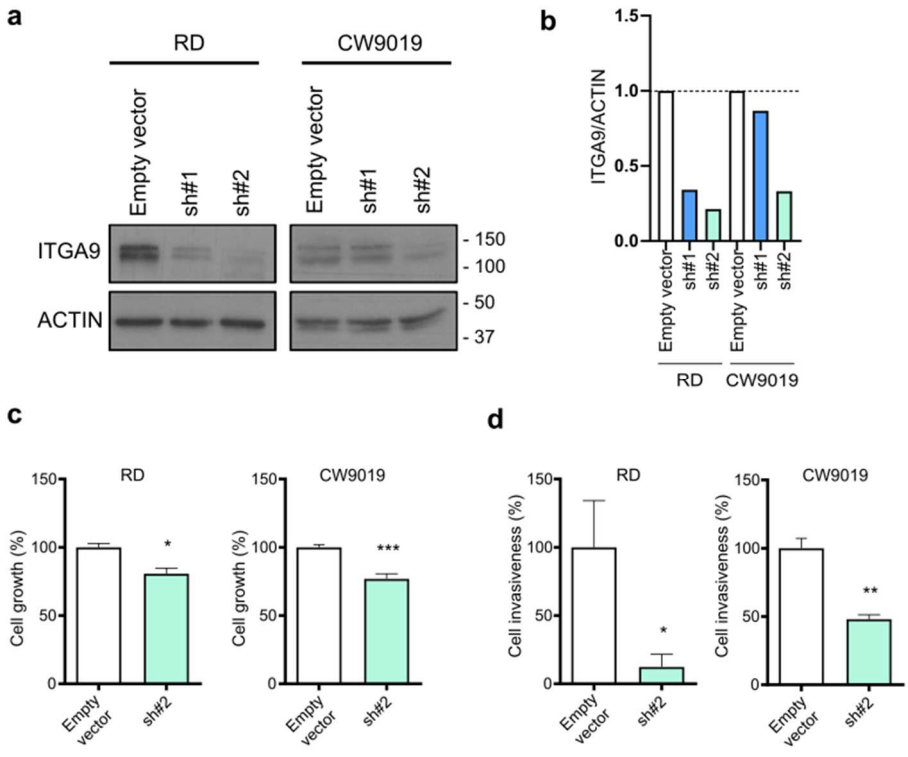

Figure 35. ITGA9 depletion by shRNA reduced cell growth and cell invasiveness in RMS cell lines. a. Western blots showing a reduction in ITGA9 protein expression by shRNA. **b.** Densitometric quantification of Western blots. **c.** Relative cell proliferation and **d.** cell invasiveness after ITGA9 knockdown in RD and CW9019 cell lines. Statistical significance was determined by t-test, considering *p<0.05, **p<0.01 and ***p<0.001.

Then, proliferation and invasion assays were performed to assess its effects on cell behaviour. Results revealed that ITGA9 knockdown reduced cell growth and cell invasiveness (Figure 35 c,d), recapitulating the observed effects after miR-7 and miR-324-5p overexpression.

1.4 miR-7 and miR-324-5p overexpression in RMS cells reduced tumour growth *in vivo*

To validate the effects on cell proliferation *in vivo*, a primary orthotopic model of RMS was used. For this experiment RD cells, slightly more sensitive to miRNA effects than CW9019, transduced with both miRNAs were used. One million of cells were injected in the gastrocnemius muscle of immunocompromised mice and one week after, treatment with doxycycline was initiated and maintained throughout the experiment (Figure 27, Material and methods section).

The first tumours that were detected by palpation appeared at week 11th, although differences in tumour volume between groups were not evident until week 14th. These differences were statistically significant from week 16th to the end of the experiment, showing a clearly faster growth in tumours of the control group (Figure 36a). In addition, a 2-3 week delay in tumour detection was also observed in mice injected with miRNA-overexpressing cells, compared to control mice (Figure 36b).

At the end of the study, mice were euthanized and tumours were isolated from healthy muscle to be measured and weighted *ex vivo*. Tumour weight and volume were clearly higher in the control group, compared to miRNA groups (Figure 36 c-e).

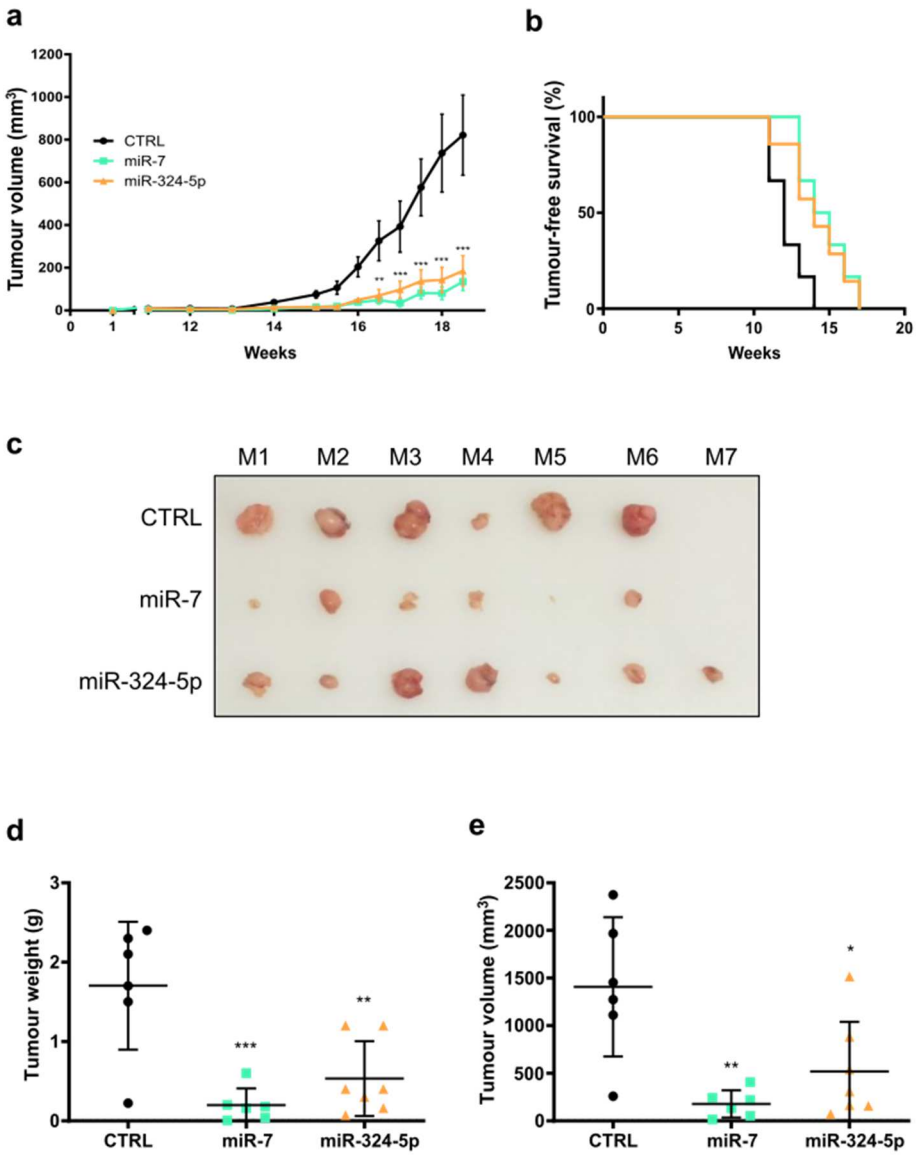

Figure 36. ITGA9 depletion caused by miR-7 and miR-324-5p reduced tumour growth in SCID mice. a. Kinetics of tumour growth expressed as mm^3 of tumour volume. Two-way ANOVA was used to determine statistical significance. **b.** Tumour-free survival curves, considering the first positive palpation of tumours as the detection point. **c.** Photograph of all dissected tumours showing a reduction in tumour size in miRNA-overexpressing groups. **d.** Average tumour weight at the end point of the study. **e.** Tumour volume measured *ex vivo* at the end point of the study. One-way ANOVA was used to determine statistical significance, considering: *p<0.05, **p<0.01 and ***p<0.001.

With the aim of ascertaining the inhibition of ITGA9 and the stability of miRNA expression throughout the experiment, Western blot of representative samples assessing ITGA9 expression and qPCR for miRNA detection were perfomed at the end point of the study (Figure 37 a-c). For Western blot analysis, in order to assure protein obtention, samples from the biggest tumours in each group were used (M5 and M6 from control group, M2 and M5 from miR-7 group and M3 and M4 from miR-324-5p group). Results showed that ITGA9 inhibition was maintained until the end of the study, since a redution of ITGA9 expression is observed in miRNA-overexpressing tumours, compared to control tumours (Figure 37 a,b). In addition, the expression of miR-7 and, particularly, miR-324-5p was maintained. Despite miR-7 relative expression was higher than miR-324-5p in the original injected cells, at the end of the study it was the opposite, being clearly higher the expression of miR-324-5p (Figure 37c). This suggests a possible negative selecction of miR-7 overexpressing cells during tumour growth.

To further characterize tumours, immunostochemical staining of KI67 was used to evaluate the proliferative capacities of tumour cells. KI67 is a nuclear protein that is expressed in cycling cells, but downregulated in G_0 resting cells. This protein is upregulated during G_1 cell cycle phase by G_1-regulators, such as E2F family of transcription factors and is involved in chromosomal condensation and correct nucleolar localization during mitosis. This is why it is used as a proliferation marker and for evaluating the proportion of proliferating cells in tumour samples (252,253). For this purpose, only three ramdomly selected samples of each group were used. A reduction in the percentage of KI67-positive cells for both miRNA was observed, suggesting

a reduction in the proliferative capacities of tumour cells when miR-7 or miR-324-5p were overexpressed (Figure 37 d,e).

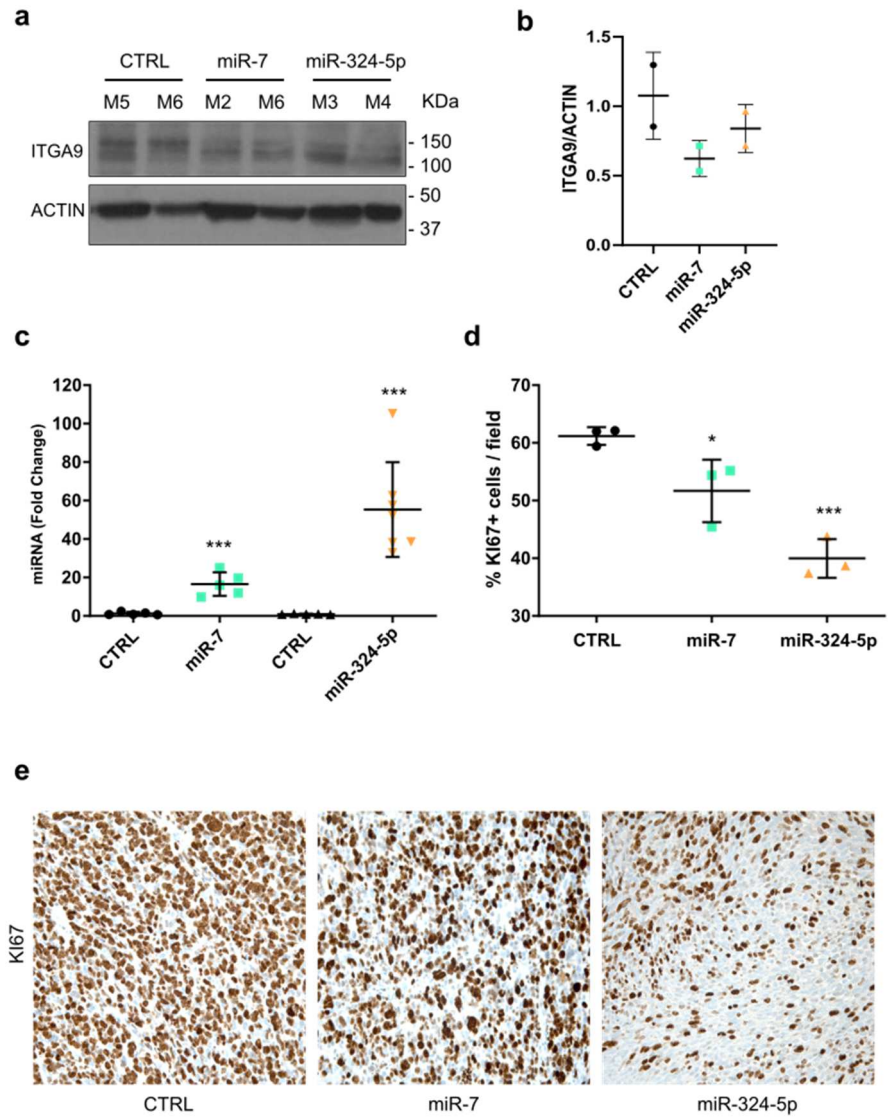

Figure 37. Characterization of *in vivo* primary orthotopic model. a. Western blot showing a reduction in the expression of ITGA9 in tumour samples from miRNA-overexpressing groups at the end point of the study. **b.** Densitometric quantification of Western blot. **c.** Relative miRNA expression in tumour samples at the end of the study. Expression values were referred to those of the control. T-test was used to determine statistical significance. **d.** Quantification of KI67-positive cells in dissected tumours after immunohistochemistry staining. One-way ANOVA was used to determine statistical significance, considering *p<0.05 and ***p<0.001. **e.** Representative slices of tumours showing KI67 immunohistochemical staining.

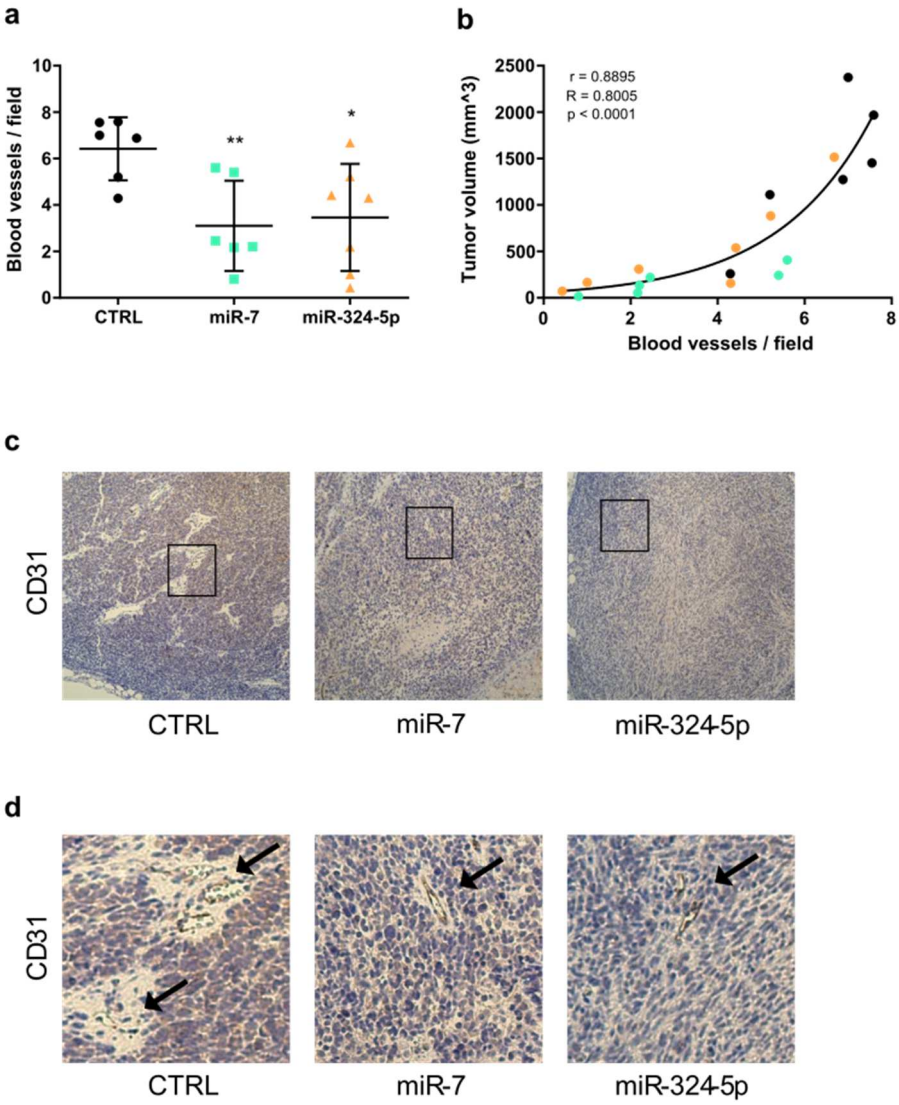

Figure 38. Immunohistochemical staining of CD31 in dissected tumours. a. Quantification of blood vessels in dissected tumours by CD31 immunohistochemical staining. One-way ANOVA was used to determine statistical significance, considering *p<0.05 and **p<0.01. **b.** Correlation between tumour volume and blood vessel density in dissected tumours. The Pearson correlation r, R square and P-values are included in the plot. Non-linear, but exponential curve was used to adjust the correlation. **c.** Representative slices of tumours showing CD31 immunohistochemical staining. **d.** Amplification of areas with CD31-positive staining. Arrows indicate blood vessels.

Finally, slices of dissected tumours were used for immunohistochemical staining of CD31 to evaluate tumour irrigation (Figure 38). CD31, or also called PECAM-1 (from platelet/endothelial cell adhesion molecule 1), is expressed on endothelial cell surface being part of their cellular junctions and it is widely used in experimental studies to quantify tumour neovascularization (254,255). Quantification of tumour vessels revealed a clear reduction in tumours overexpressing both miRNA (Figure 38a) and interestingly, vessel density (expressed as blood vessels per field) was significantly correlated to final tumour volumes (Figure 38b). This suggested a major involvement of angiogenesis in the differences observed among the groups of the study.

1.5 The overexpression of miR-7 lowered the survival of intravenously injected tumour cells *in vivo*

Eventually, effects of miR-7 overexpression on *in vivo* tissue colonization were assessed. In previous experiments, only miR-7 stood out as a modulator of cell invasiveness and only this miRNA was tested in this part of the study.

For this purpose, RD control and miR-7 overexpressing cells, both expressing RFP fluorescent protein, were intravenously injected into severe immunocompromised mice. Cells were pre-treated with doxycycline before being injected, as well as mice during the whole experiment. One week later, mice were euthanized and lungs were isolated and processed for flow cytometry analysis (Figure 28, Materials and methods section).

Detection of RFP-positive cells allowed the quantification of tumour cells that survived in blood after injection and/or extravasate and invade lung tissue parenchyma. The analysis of this specific tissue was based on previous experience of the group which supports that RMS tumour cells preferentially metastasize to lungs *in vivo* (232). With this approach the effects of miR-7 overexpression in important steps for the metastatic cascade (survival in circulation, extravasation and colonization) were considered; however, other important phases remain unaddressed by our experimental design (escape from the primary tumour, intravasation and outgrowth of macrometastases).

Control and miR-7 overexpressing cells in cell culture were previously analysed by flow cytometry to set the specific gates to detect RFP-positive cells (Figure 39 b,c). As a negative control of the experiment, lungs from mice without tumour cell injection were also analysed and no RFP-positive cells were found in the selected gates (Figure 39a). Finally, a mixture of a healthy lung and RFP-positive cells added *ex vivo* was used as a positive control of the experiment (Figure 39d). The gating procedure is detailed in Materials and methods section (Figure 29).

The number of viable RFP-positive cells detected was clearly reduced in mice carrying cells overexpressing miR-7 (Figure 39g), pointing to an impaired survival and/or colonization of lung parenchyma of tumour cells overexpressing miR-7.

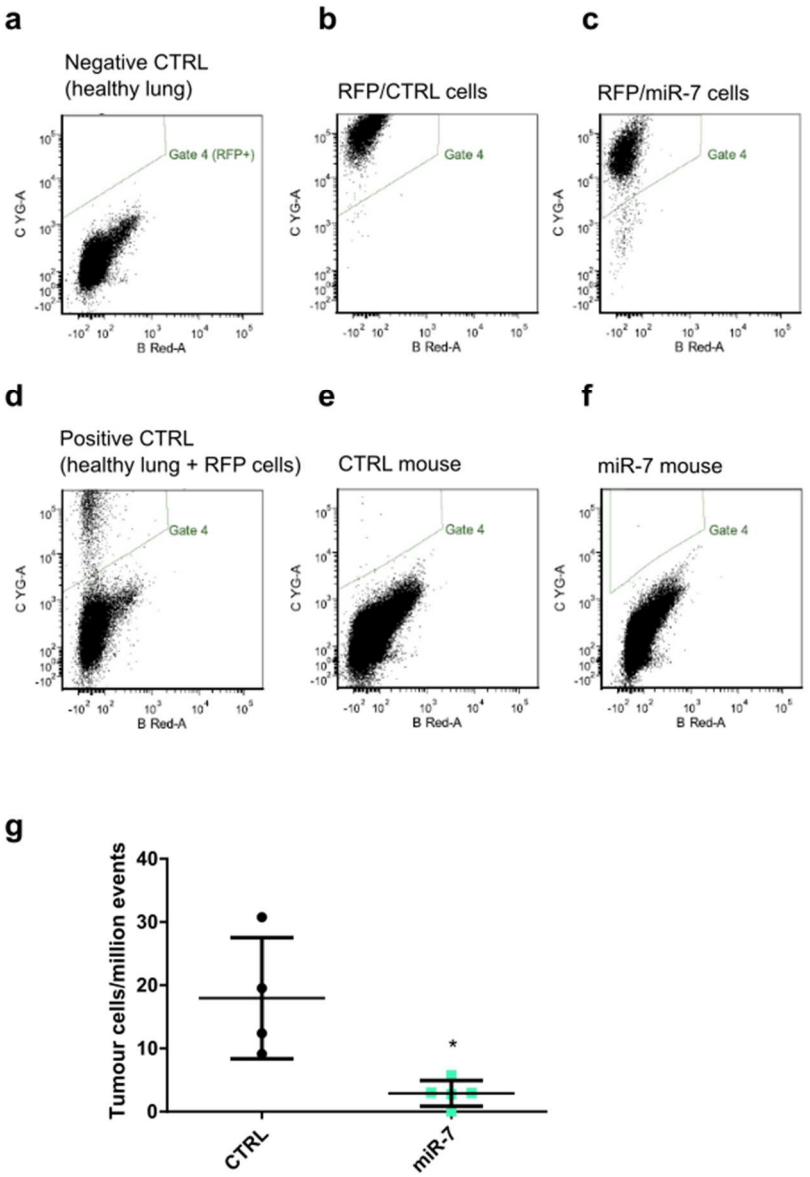

Figure 39. ITGA9 depletion caused by miR-7 reduced survival and/or lung colonization of intravenously injected tumour cells in SCID-beige mice. a. FACS negative control: healthy lung from mice not injected with tumour cells**. b.** RFP-positive control cells analysed by FACS. >95% of cells were found in gate 4. **c.** RFP-positive cells overexpressing miR-7 analysed by FACS. >95% of cells are found in gate 4. **d.** FACS positive control: healthy lung from mice not injected with tumour cells, but RFP-positive cells added *ex vivo* before analysis. **e.** Representative mouse from control group. **f.** Representative mouse from miR-7 group. **g.** Quantification of RFP-positive cells in both groups, expressed as tumour cells per million of events detected by FACS. Statistical significance was determined using t-test, considering *p<0.05.

2. Effects of ITGA9 blockade in NB

2.1 ITGA9 knockdown reduced metastatic dissemination of NB *in vivo*

Previous research of the group revealed a crucial role of ITGA9 in controlling cell invasiveness of NB cell lines *in vitro*. BE(2)C cells were particularly sensitive to ITGA9 downregulation, which produced a clear reduction of invasive capabilities of these cells (232). To demonstrate whether ITGA9 is also involved in the metastatic dissemination of NB cells *in vivo*, a model based on intravenous tumour cell injection was performed.

For this purpose, BE(2)C cells, either control or stably expressing a shRNA against ITGA9 (Figure 40b) were injected through the tail vein of immunocompromised mice and the appearance of metastatic lesions was monitored. shRNA mediated ITGA9 downregulation significantly impaired the capability of cells to engraft and develop metastatic foci in mice. The first metastases were detected by palpation around week 5 in both groups. However, at the end point of the study a reduction of 30% of metastasis formation was observed when ITGA9 was depleted. All mice from the control group developed metastases before day 50, while metastases were only found in 70% of mice from the shITGA9 group. Survivors in the group lacking ITGA9 did not show signs of metastases after allowing them to evolve up to 100 days (Figure 40a).

Body weight was measured throughout the experiment and a trend towards a decrease was observed in mice from control group from day 42 (week 6) onward (Figure 40c), pointing to a worse general state in mice from this group compared to shITGA9 group. In addition, mice from control group

tend to develop more metastatic foci. In fact, 3 or more metastases were found in 80% of mice from the control group, while this happened only in 30% of shITGA9 group (Figure 40d). Finally, metastases found in mice from the control group were significantly bigger than the ones observed in ITGA9-depleted group (Figure 40e).

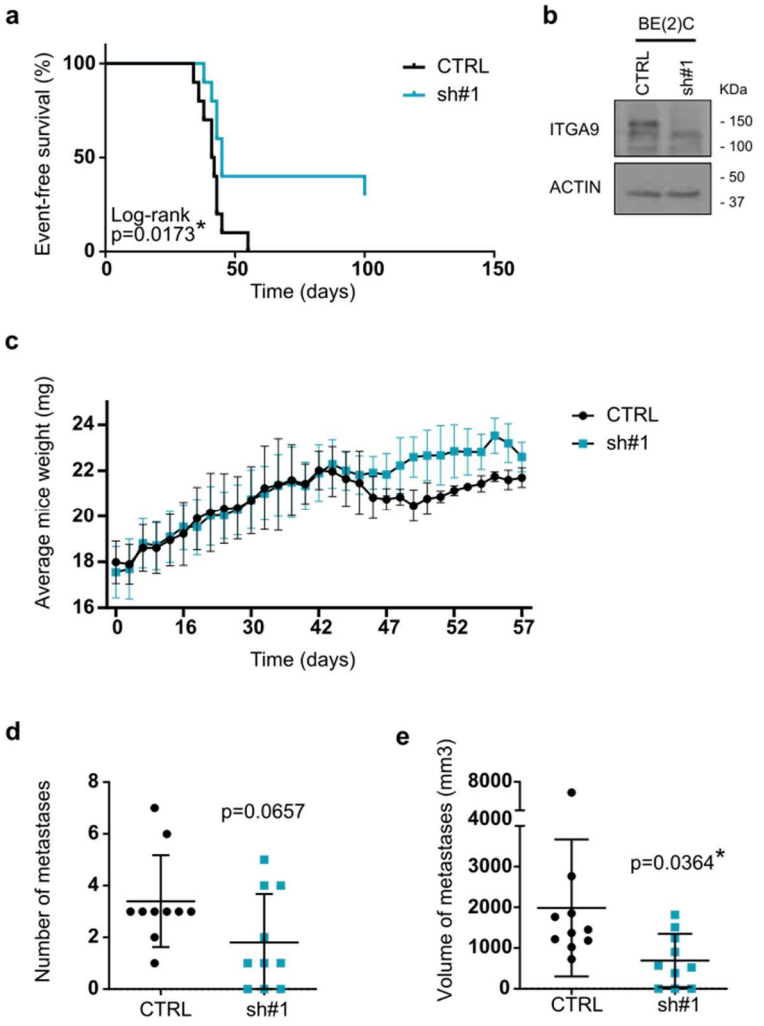

Figure 40. ITGA9 knockdown impaired *in vivo* metastasis formation. a. Event-free survival curves of mice after intravenous injection of BE(2)C cells bearing or not the ITGA9 knockdown. Statistical significance was obtained after Log-rank survival test. **b.** Kinetics of body weight growth during the experiment. **c.** Quantification of metastatic lesions after mice euthanasia. **d.** Tumour volume of metastases measured *ex vivo*. Statistical significance was determined using t-test, considering *p<0.05.

BE(2)C cells had a clear tropism to liver, since most of the observed metastases were hepatic. Only two mice from control group developed non-hepatic metastases, one in the lung and another in the suprarenal gland. In the case of the ITGA9-depleted group, only one animal developed metastasis in the thoracic cavity (Figure 41).

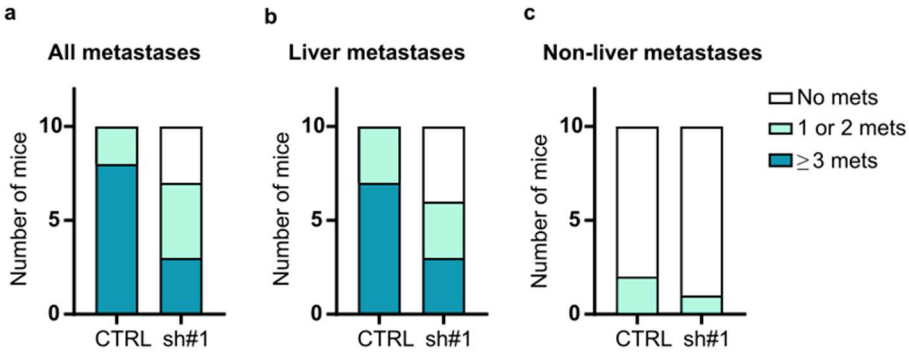

Figure 41. NB cell showed a clear tropism to liver. a. Quantification of mice in each group that developed metastasis. **b.** Quantification of mice in each group that developed liver metastasis. **c.** Quantification of mice in each group that developed non-hepatic metastasis.

2.2 ITGA9 blockade by RA08 reduced metastatic dissemination of NB *in vivo*

No specific inhibitors have been described for ITGA9 so far. Nevertheless, our group in collaboration with the pharmaceutical partner BCN Peptides, has designed a short peptide inspired in the interaction sequence between ITGA9 and ADAM12. This peptide, called RA08, simulates a sequence located in the disintegrin domain of ADAM12 with some modifications including the addition of non-natural amino acids to enhance stability in plasma. Thus, RA08 is a 15 amino acid peptide derived from the disintegrin domain of the native sequence of ADAM12 (sequences in Figure 42). RA08 has been modified at the N-terminus with the inclusion of an unnatural

amino acid (pyroglutamic acid, Pyr), together with other modifications such as the substitution of Cys by Met, the substitution of Phe by 3-mesitylalanine (2,4,6-trimethylphenylalanine, Msa), and the incorporation of two Lys at the N- and C-termini of the sequence. All these modifications aim to increase its stability in plasma and improve its pharmacological properties for inhibiting the ITGA9-ADAM12 interaction. Additionally, the incorporation of two further Lys residues, one at the N-terminus and another at the C-terminus was performed to improve the peptide sequence's solubility when formulated in physiological saline (231) (Figure 42).

ADAM12 SEQUENCE: **Arg-Asp-Ser-Ser-Asn-Ser-Cys-Asp-Leu-Pro-Glu-Phe**

RA08: **Pyr-Lys-Arg-Asp-Ser-Ser-Asn-Ser-Met-Asp-Leu-Pro-Glu-Msa-Lys-NH_2**

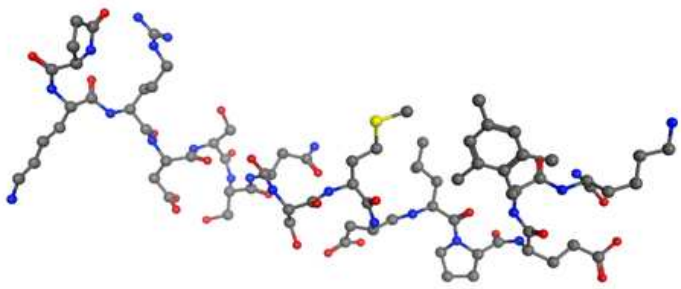

Figure 42. Schematic representation of the structure of the synthetic peptide RA08 and alignment of interaction sequence of ADAM12 and ITGA9 and the RA08 peptide sequence.

Previous studies of the group have demonstrated that RA08 treatment reduced cell invasiveness in NB cell lines and BE(2)C cell line was particularly sensitive to RA08 treatment (232). Cell invasiveness is a process broadly implicated in different phases of the metastatic cascade (local invasion,

intravasation and extravasation, and colonization of distant organs). Thus, in order to test whether RA08 was able to reduce metastasis formation *in vivo*, a model based on intravenous tumour cell injection was performed.

BE(2)C cells were injected through the tail vein of immunocompromised mice, treated during the whole experiment with two different doses of RA08, 1mg/kg and 2mg/kg, and the vehicle (saline solution). Results showed an impaired capability of cells to engraft and develop metastatic foci in mice treated with the higher dose of RA08, while no differences were found for the lower dose. The first metastases were detected around week 5-6 in all groups. However, the 2mg/kg dose provided protection against metastasis in 56% of mice. As a matter of fact, 88% of mice from the control group developed metastasis, 75% of the lower dose and only 44% of the higher dose (Figure 43 a,b).

Body weight was measured throughout the experiment and no significant alterations in mice treated with RA08 were observed, suggesting that the treatment with RA08 did not produce strong toxicity. On the contrary, abrupt changes in body weight were found in the control group, due to the rapid growth of hepatic metastases (Figure 43c). Finally, although no statistically significant differences were observed in terms of number of metastasis and metastasis volume, a trend towards fewer and smaller lesions was observed in the higher dose group (Figure 43 d,e). All metastases were hepatic, except for one ovarian metastasis detected in the lower dose group.

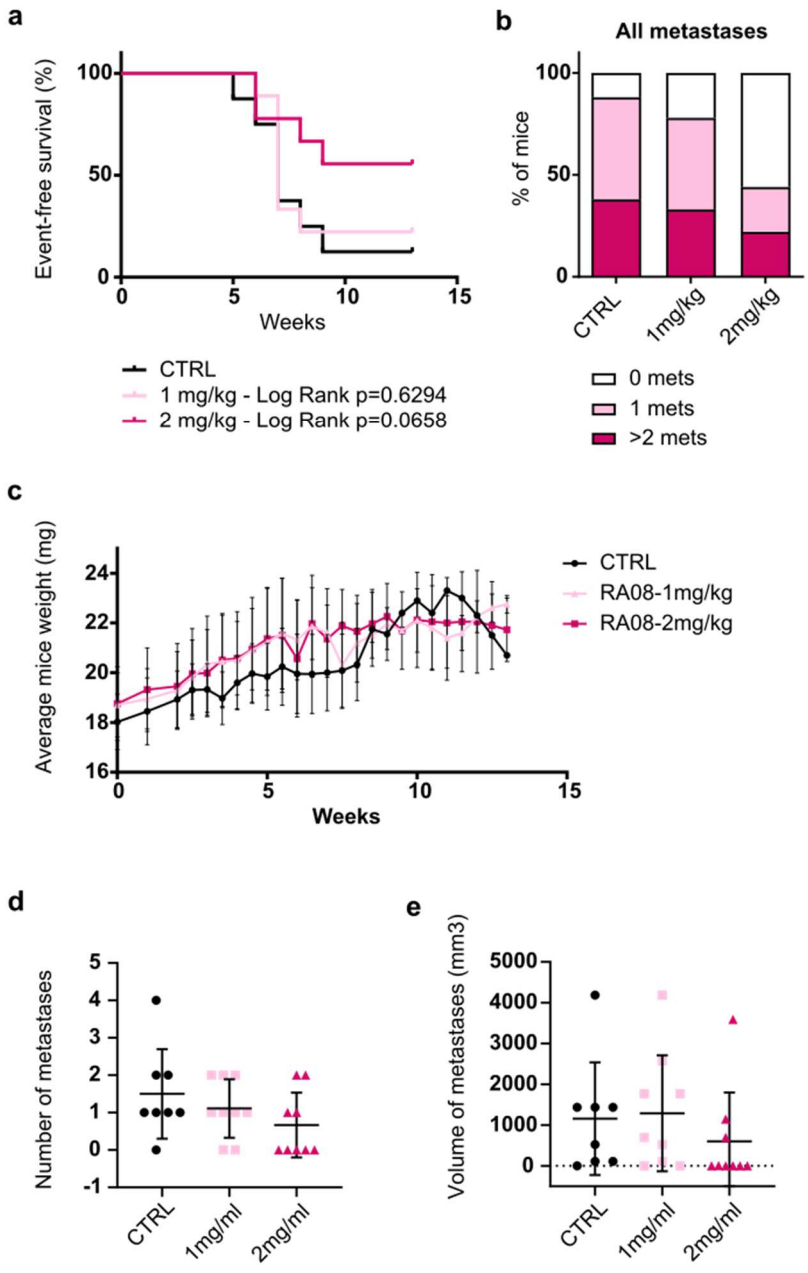

Figure 43. Treatment with RA08 impairs NB *in vivo* metastasis formation. a. Event-free survival curves of mice after intravenous injection of BE(2)C cells and treatment with two different doses of RA08. Log-rank survival test was applied to obtain statistical significance. **b.** Quantification of mice in each group that developed metastasis. **c.** Kinetics of body weight growth during the experiment. **d.** Quantification of metastatic lesions after mice euthanasia. **e.** Tumour volume of metastases measured *ex vivo*. Statistical significance was determined using one-way ANOVA.

3. ITGA9 blockade in BC

With the aim of demonstrating whether ITGA9 blockade could be a good therapeutic option also in BC, experiments after ITGA9 downregulation by shRNA or treatment with RA08 were performed. Expression of ITGA9 was assessed by Western blot in a panel of BC cell lines and MDA-MB-468 and MDA-MB-231 cell lines were selected for further study. MDA-MB-468 was selected as the one with higher ITGA9 protein levels, while MDA-MB-231 had an intermediate expression level (Figure 44). Both cell lines corresponded to basal BC subtypes (256).

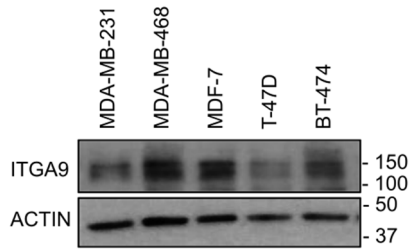

Figure 44. ITGA9 was expressed in BC cell lines.

3.1 ITGA9 knockdown reduced cell invasion in BC *in vitro*

ITGA9 expression was downregulated in MDA-MB-468 and MDA-MB-231 cells stably transduced with two shRNA against ITGA9. Both shRNA were able to decrease ITGA9 protein levels (around 25% in MDA-MB-468 and 55% in MDA-MB-231) compared to control condition. In addition, Western blot was carried out to assess the effects of ITGA9 inhibition on FAK expression and phosphorylation at Tyr397. Results showed a clear reduction of FAK phosphorylation, particularly in MDA-MB-468 cells. Besides, both total and phosphorylated FAK levels where reduced in MDA-MB-231 cells (Figure 45 a,b).

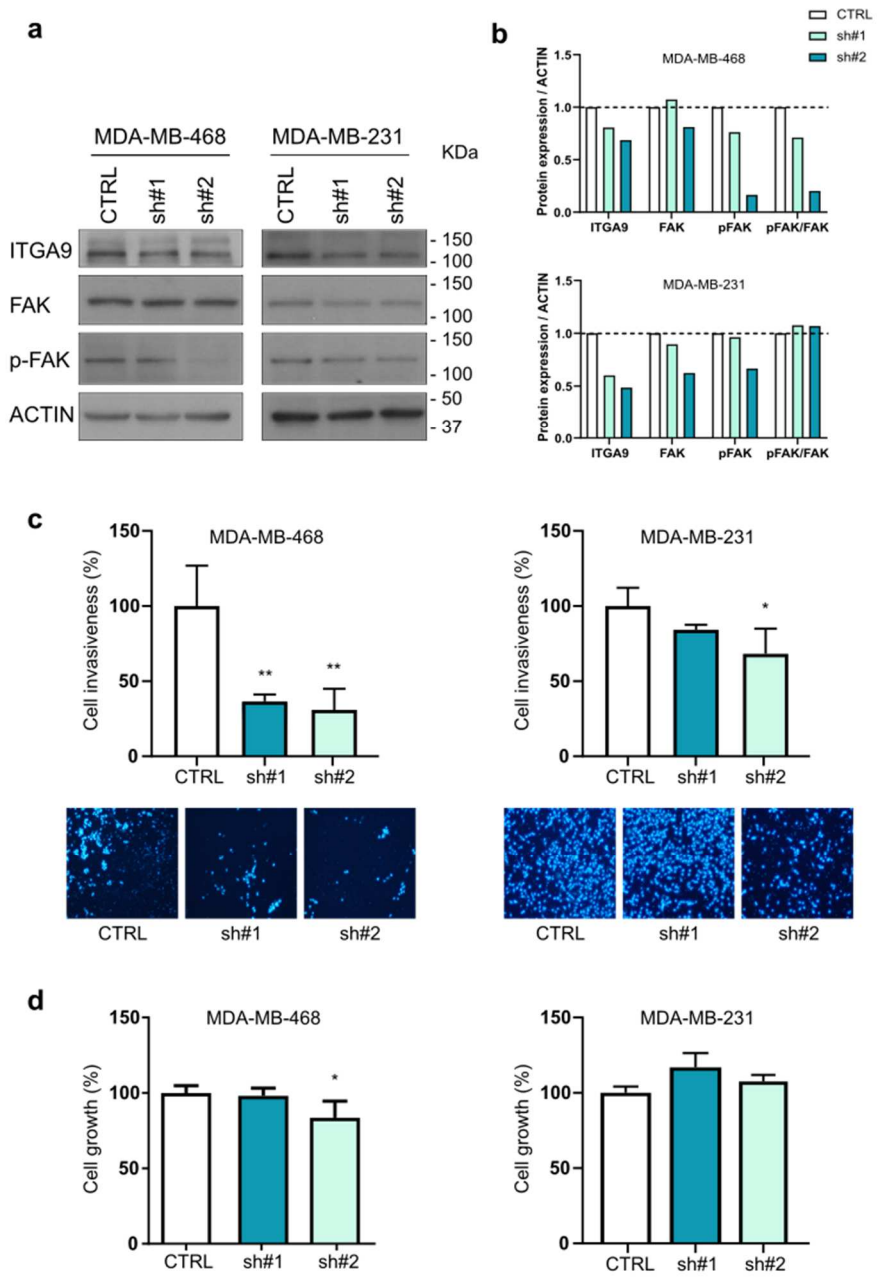

Figure 45. ITGA9 knockdown reduced cell invasion and FAK phosphorylation. a. Representative immunoblot showing ITGA9 knockdown and concomitant reduction in FAK and FAK phosphorylation. **b.** Densitometric quantification of Western blots. **c.** Relative cell invasion after ITGA9 knockdown in MDA-MB-468 and MDA-MB-231 cells and representative images of Transwell invasion assays. **d.** Relative proliferation after ITGA9 knockdown in MDA-MB-468 and MDA-MB-231 cells. Statistical significance was determined by one-way ANOVA, considering *p<0.05 and **p<0.01.

Cell invasiveness was also assessed after ITGA9 knockdown. Results revealed a considerable reduction in MDA-MB-468 cell line with both shRNA (higher than 50%). However, only sh#2 reduced cell invasiveness in MDA-MB-231 cell line (around 30%) (Figure 45c). Finally, the shRNA-mediated ITGA9 silencing showed no significant effects on proliferation, with just a very slight decrease in cell line MDA-MB-468, solely observed with sh#2 (Figure 45d).

3.2 ITGA9 blockade by RA08 reduced cell invasion in BC *in vitro*

In order to describe the effects of ITGA9 blockade by RA08 on cell behaviour, MDA-MB-468 and MDA-MB-231 cells were treated with different concentrations of RA08 (ranging from 100 to 1000nM). Firstly, expression of ITGA9, FAK and FAK phosphorylation (at Tyr397) was assessed by Western blot. Results showed a remarkable reduction in FAK phosphorylation in RA08-treated cells in a dose-dependent manner, whereas total FAK and ITGA9 levels were unaltered. Treatment with RA08 was efficient at 500 and 1000nM in MDA-MB-468, while it was only effective at 1000nM in MDA-MB-231 cell line (Figure 46 a,b).

Treatment with RA08 also produced a significant reduction in cell invasiveness in MDA-MB-468 cells (around 50% reduction at the higher doses), while the MDA-MB-231 cell line showed only a moderate reduction at the highest treatment dose (Figure 46c). On the other hand, the treatment with RA08 did not produce effects on cell growth (Figure 46d).

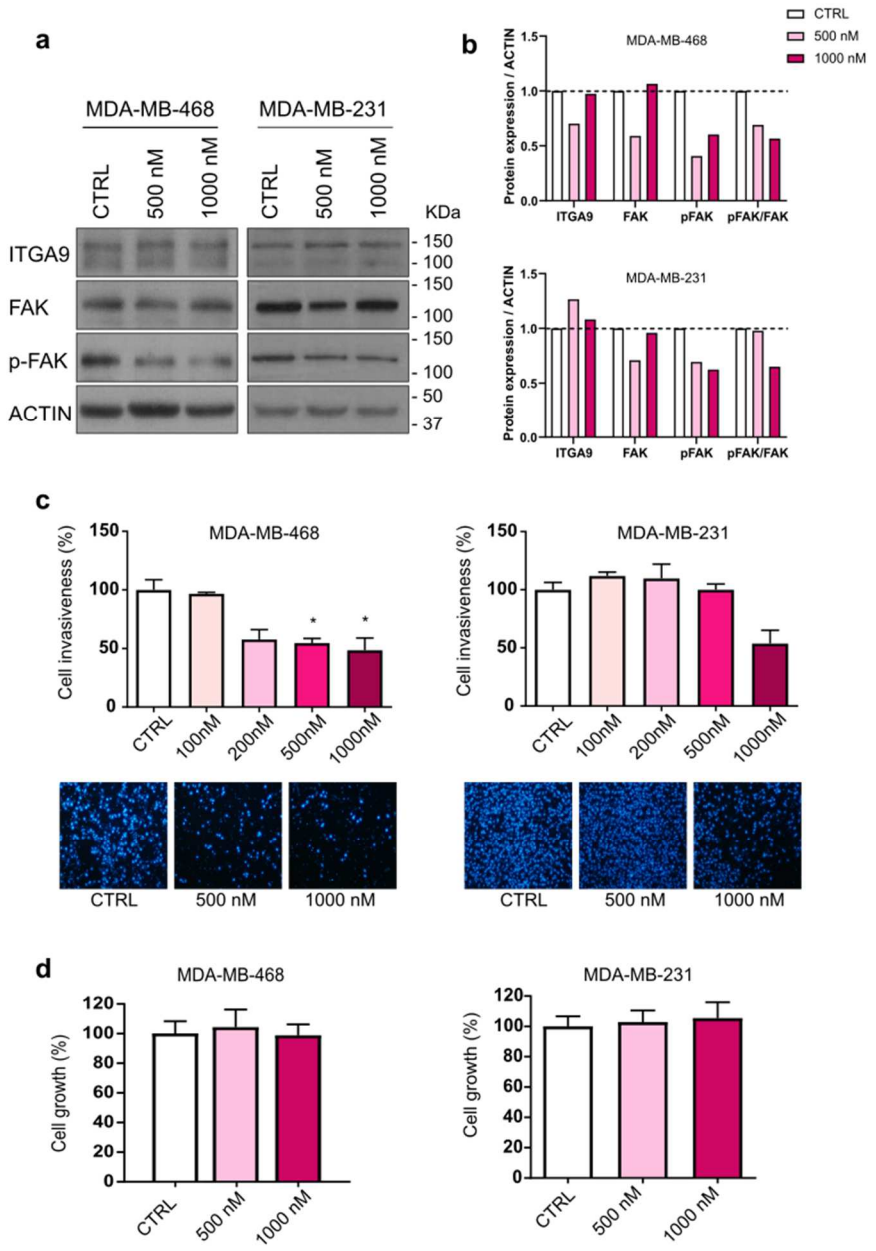

Figure 46. RA08 treatment reduced cell invasion and FAK phosphorylation. a. Representative immunoblot showing ITGA9, FAK and phosphorylated-FAK protein levels. Treatment with RA08 reduced phosphorylated-FAK, while ITGA9 and FAK levels remain unaltered. **b.** Densitometric quantification of Western blots. **c.** Relative cell invasion after treatment with RA08 in MDA-MB-468 and MDA-MB-231 cells and representative images of Transwell invasion assays. **d.** Relative proliferation after RA08 treatment in MDA-MB-468 and MDA-MB-231 cells. Statistical significance was determined by one-way ANOVA, considering *p<0.05.

3.3 ITGA9 blockade by RA08 reduced metastatic dissemination of BC cell *in vivo*

In order to test whether RA08 was able to reduce metastasis formation *in vivo*, a model based on intravenous tumour cell injection was performed. MDA-MB-468 cells, more sensitive to ITGA9 inhibition *in vitro*, were injected through the tail vein of severe immunocompromised mice, treated during the whole experiment with two different doses of RA08, 1mg/kg and 2mg/kg, and the vehicle (saline solution). After 9 weeks of treatment, all mice were euthanized and lungs were isolated. Immunohistochemical staining of GATA3 was done in lung sections to quantify the presence of metastatic cells in this tissue (Figure 47b).

GATA3 is a transcription factor that has been related to the specification and maintenance of luminal cells in adult mammary gland (257). In fact, in gene expression studies, GATA3 has emerged as the most highly enriched transcription factor in the mammary epithelium (258). GATA3 has been often associated to oestrogen receptor expression, although its expression has also been reported in oestrogen-negative BC tumours, such as TNBC (259) and metastatic BC (260). In addition, immunohistochemical profile of pulmonary metastases have revealed that most of the BC metastases are GATA3-positive (261). Based on this, GATA3 immunohistochemical staining was used to quantify the presence of metastatic cells in mouse lungs. Results showed an impaired capability of cells to engraft and develop metastatic foci in mice treated with both concentrations of RA08 (Figure 47a). In addition, body weight was measured throughout the experiment and no significant alterations in mice treated with RA08 were observed, suggesting that the treatment with RA08 did not produce strong toxicity (Figure 47c).

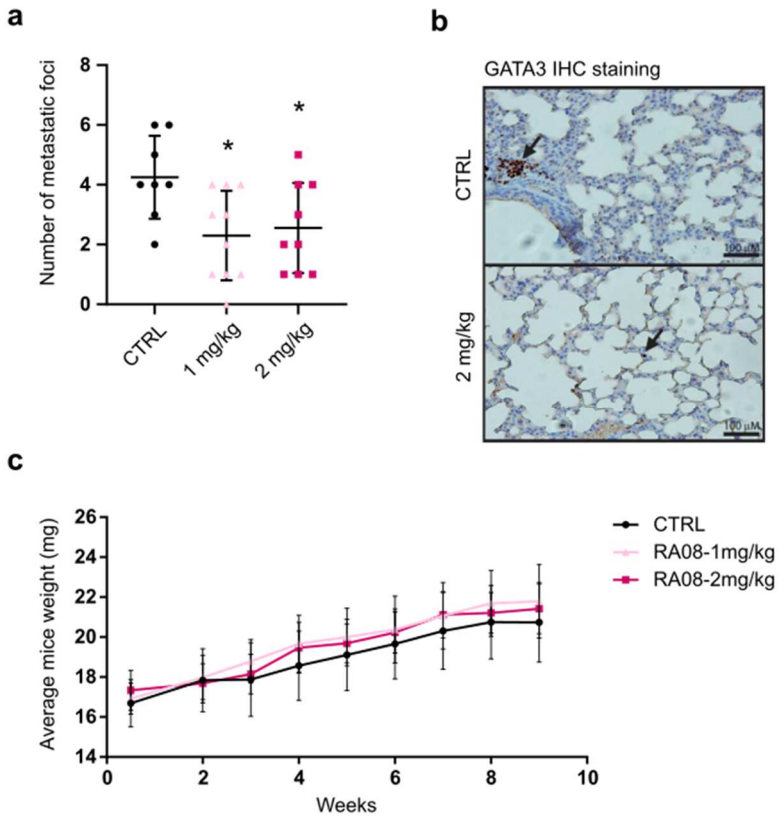

Figure 47. RA08 treatment reduced *in vivo* metastasis of BC cells. a. Quantification of metastatic foci in lung sections after GATA3 immunohistochemical staining. Treatment with both concentrations of RA08 reduced the number of metastatic foci. Statistical significance was determined by one-way ANOVA, considering *p<0.05. **b.** Representative images of GATA3 immunohistochemical staining from lung sections. Arrows indicate GATA3-positive cells. Bar: 100µm. **c.** Kinetics of body weight growth during the experiment.

3.4 ITGA9 blockade by RA08 reduced tumour growth of BC *in vivo*

In order to further characterize the effects of RA08 treatment *in vivo*, a patient derived xenograft (PDX) of BC was used as *in vivo* primary tumour growth model. Tumour fragments from a basal BC PDX were implanted in the breast of mice to generate new orthotopic tumours. Seven days after implantation, mice were randomized and assigned to different groups in

order to receive the vehicle (saline solution) or RA08 treatment at 2mg/kg. Treatment was maintained for 53 days, and then mice were euthanized and all primary tumours were removed.

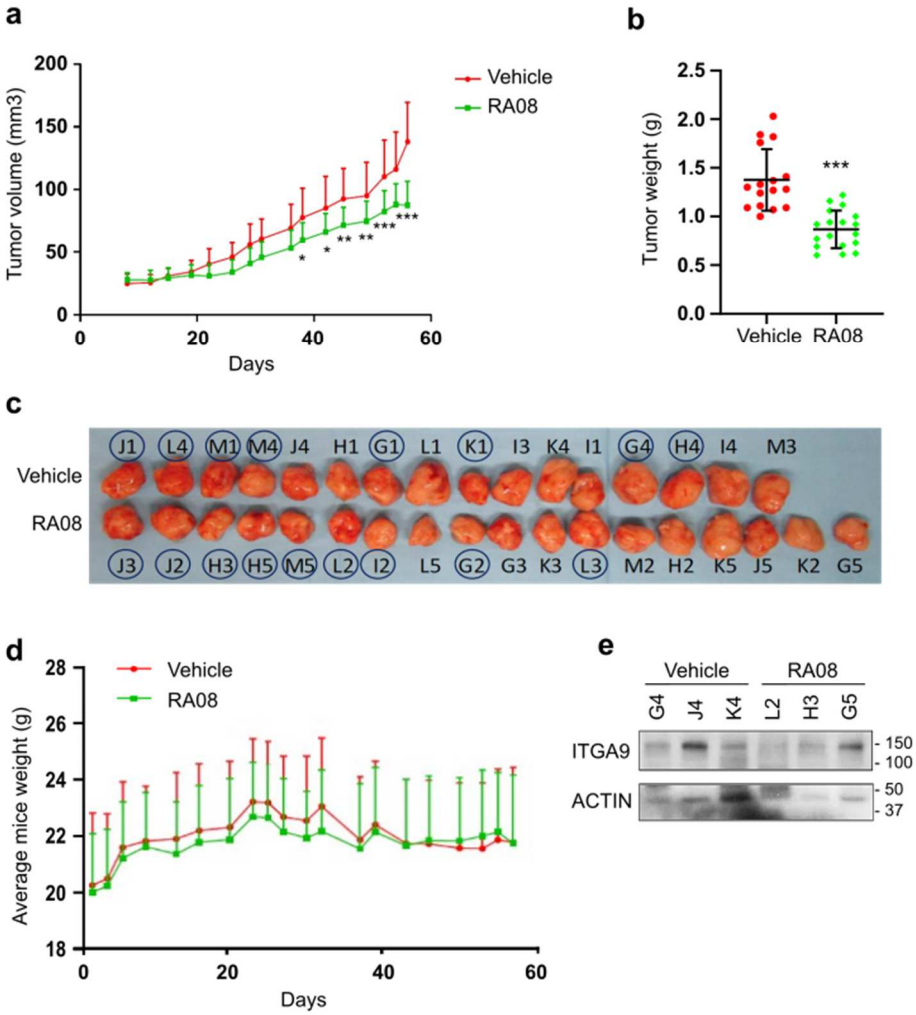

Figure 48. Treatment with RA08 reduced tumour growth *in vivo*. a. Kinetics of tumour growth expressed as mm^3 of tumour volume. Two-way ANOVA was used to determine statistical significance, considering *p<0.05, **p<0.01 and ***p<0.001. **b.** Tumour weight measured *ex vivo* at the end point of the study. Statistical significance was determined by t-Test (p=0.0002). **c.** Photograph of all dissected tumours showing a reduction in tumour size in RA08-treated group. **d**. Kinetics of body weight growth during the experiment. **e.** Western blot showing ITGA9 expression in randomly selected samples of control and treated group. This experiment was performed in collaboration with Dr Villanueva's group and Xenopat.

Tumour volume was measured during all the experimental procedure and differences between the two groups became evident from day 25 onward, although were not statistically significant until day 39. Tumours from the control group grew faster than the ones in the RA08-treated group (Figure 48a). Tumour weight measured at the end point of the experiment also showed differences between groups: tumours from the control group were slightly bigger than the ones in the RA08-treatment group (Figure 48 b,c). Finally, differences in body weight were not detected after treatment with RA08, indicating that RA08 did not produce strong toxicity (Figure 48d).

4. ITGA9 role in non-adherent cell survival

From previous sections it has been concluded that ITGA9 inhibition, either by miRNA, shRNA or treatment with RA08, reduced metastatic colonization *in vivo*. Nevertheless, the mechanisms that drive this effect have not been fully addressed. The involvement of ITGA9 in controlling cell invasiveness has been proven, suggesting ITGA9 could be involved in different steps of the metastatic cascade since cell invasion is necessary for local invasion, intravasation and extravasation, and colonization of distant organs. In this section, the potential role of ITGA9 in non-adherent cell survival, necessary for cell survival in circulation, was also studied.

4.1 ITGA9 silencing did not induce cell cycle arrest or apoptosis, but decreased anchorage-independent growth

For assessing the effects of ITGA9 silencing on apoptosis and cell cycle, RD cell line (from RMS) stably transduced with pGIPZ-empty vector or shRNA-ITGA9 construct was used. ITGA9 knockdown in these cells was very clear

and maintained when cells were grown in adherent and non-adherent conditions (Figure 49 e,f).

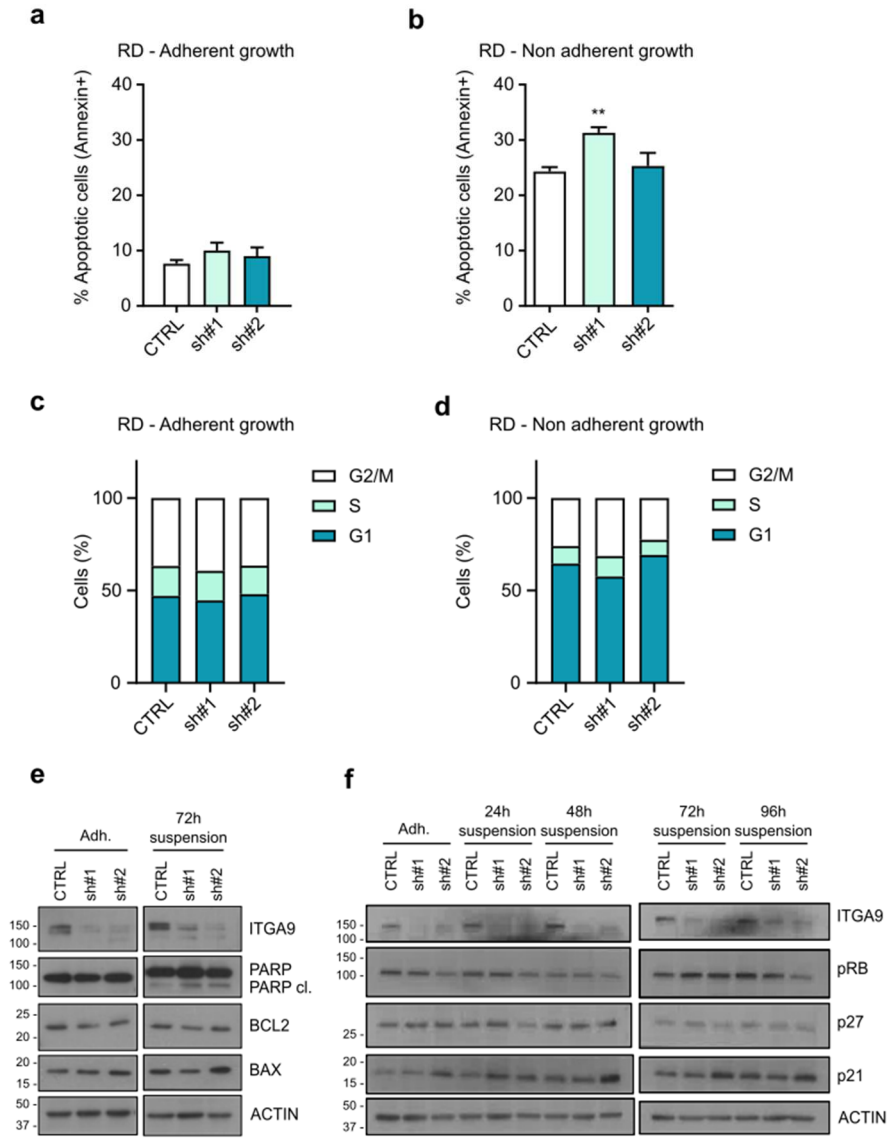

Figure 49. ITGA9 silencing did not induce cell cycle arrest or apoptosis. a,b. Quantification of apoptotic cells by Annexin V in adherent and non-adherent conditions, respectively. **c,d.** Cell cycle distribution of cells grown in adherent and non-adherent conditions, respectively. Statistical significance was determined by one-way ANOVA, considering **p<0.01. **e.** Western blots showing ITGA9 depletion and apoptotic markers. **f.** Western blots showing ITGA9 depletion and protein markers of cell cycle arrest.

Analysis by flow cytometry showed that ITGA9 depletion did not consistently induce apoptosis (Figure 49 a,b) or cell cycle arrest (Figure 49 c,d), neither in adherent nor non-adherent conditions. Only a slight increase (around 5%) in apoptotic cells was observed when cells were grown in non-adherent conditions, but solely with sh#1. In addition, a few protein markers related with apoptosis or cell cycle arrest were assessed by Western blot (Figure 49 e,f). Consistent changes produced by both shRNA were not observed. Only a slight increase in PARP cleavage was observed in ITGA9-depleted cells when they were grown in non-adherent conditions.

Although ITGA9 depletion did not induce apoptosis or cell cycle arrest, a clear reduction in the number of ITGA9-knockdown cells was observed when they were grown in non-adherent conditions (Figure 50 a,b). This confirmed that although cells were not dying or stack into a certain cell cycle phase when ITGA9 was reduced, their growth in suspension was affected. Then, WST-1 assay was used to quantify metabolically active cells in suspension as an indirect measure of cell growth. Results showed that when ITGA9 was knockdown by shRNA or blocked by RA08 treatment the proportion of metabolically active cells significantly decreased. This happened not only in RD cells, from RMS, but also in BE(2)C and MDA-MB-468, from NB and BC respectively (Figure 50 c-i), indicating that ITGA9 blockade reduced anchorage-independent cell growth. Interestingly, cell proliferation in adherent conditions was barely affected by ITGA9 knockdown (Figure 51a) and not affected at all after treatment with RA08 (Figure 51b). This suggested that ITGA9 played a critical role in modulating proliferation in anchorage-independent conditions but not when cells were culture in adherent systems.

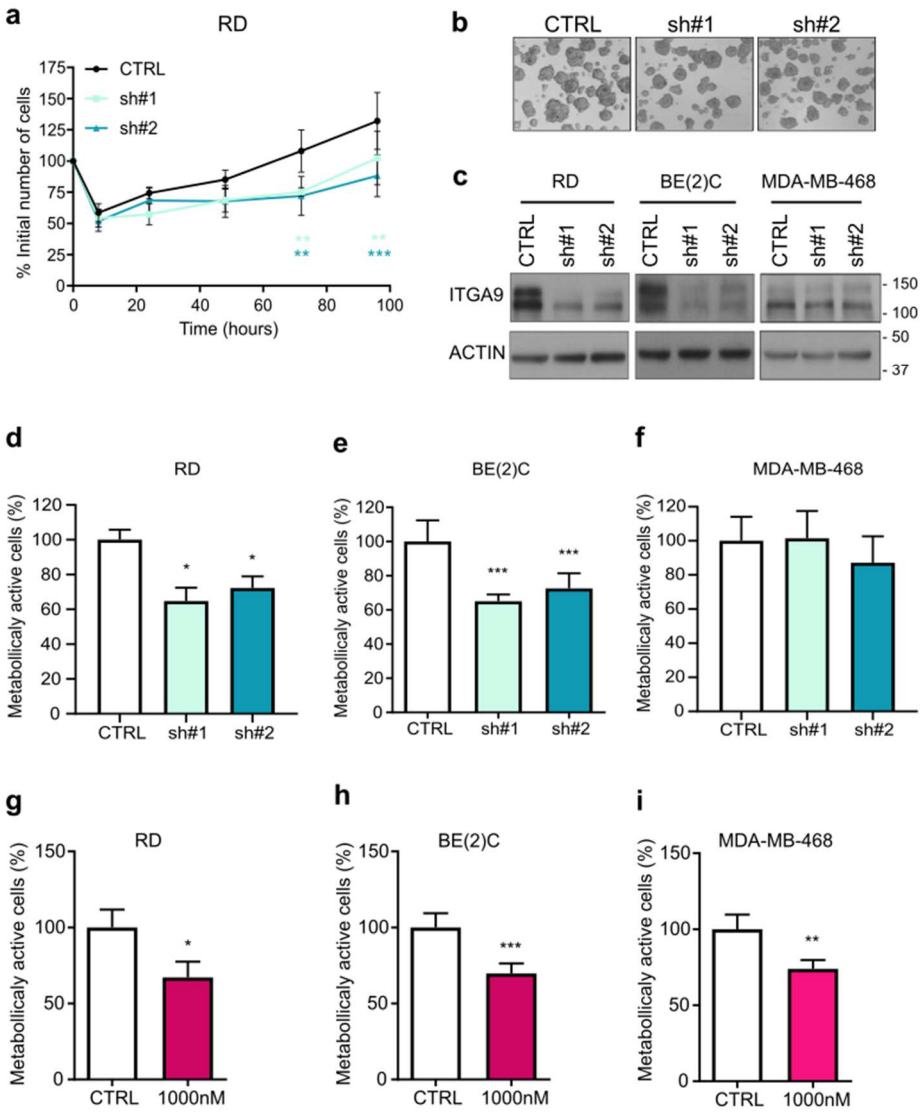

Figure 50. ITGA9 depletion or blockade by RA08 reduced anchorage-independent cell growth. a. Quantification of viable cells in non-adherent conditions after ITGA9 knockdown in RD cells. Values were referred to the initial number of seeded cells. **b.** Representative images of RD cells growing in anchorage-independent conditions**. c.** Western blots showing ITGA9 knockdown in RD, BE(2)C and MDA-MB-468 cell lines**. d-i.** Anchorage-independent cell growth after ITGA9 silencing by shRNA (d-f) or treatment with RA08 (g-i) in RD, BE(2)C and MDA-MB-468, respectively. Each cell line represented a different neoplasia: RD, rhabdomyosarcoma, BE(2)C, neuroblastoma and MDA-MB-468, breast cancer. Statistical significance was determined by one-way ANOVA. Statistical significance was determined by t-Test. *p<0.05, **p<0.01 and ***p<0.0001.

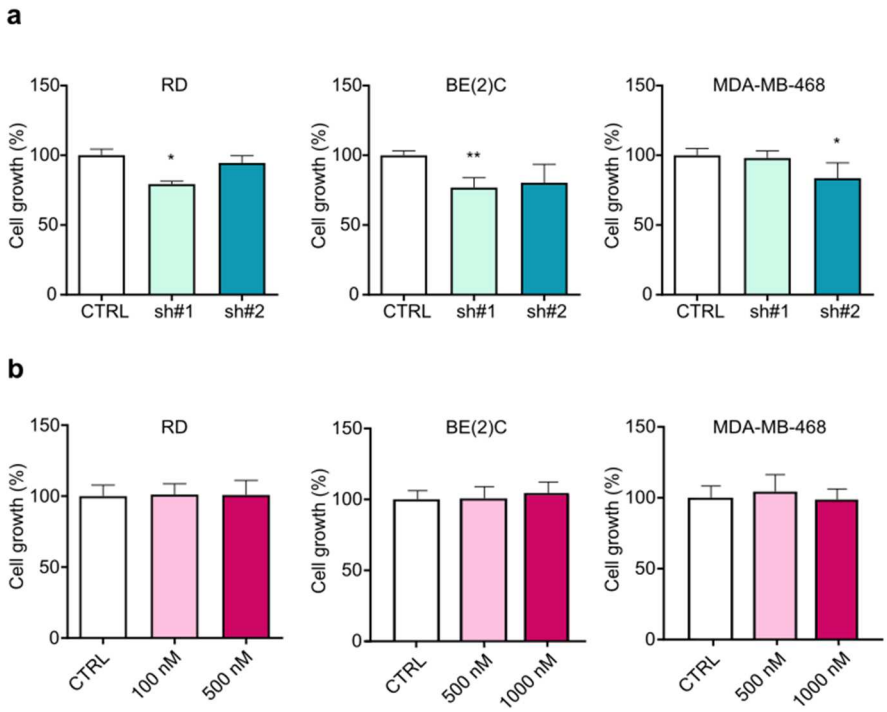

Figure 51. ITGA9 inhibition by shRNA or treatment with RA08 did not affect cell proliferation in adherent conditions. a. Cell growth after ITGA9 silencing by shRNA in RD, BE(2)C and MDA-MB-468 cell lines. **b.** Cell growth after treatment with RA08 in RD, BE(2)C and MDA-MB-468 cell lines. Statistical significance was determined by one-way ANOVA, considering *p<0.05 and **p<0.01.

5. Prognostic value of ITGA9

Analysis of ITGA9 expression in public datasets was done to evaluate the prognostic value of ITGA9 and which patients of RMS, NB or BC could benefit from a putative therapy based on ITGA9 inhibition.

5.1 Prognostic value of ITGA9 in RMS

Analysis of Davicioni et al. dataset (245), available at the R2: Genomic and Visualization Platform (244), comprising 147 patients of RMS, showed that patients from the embryonal (ERMS) subtype tend to have higher ITGA9 expression than patients from the alveolar (ARMS) subtype (Figure 52a). In addition, when ARMS and ERMS patients were analysed separately, differences in ITGA9 expression according to patient outcome were detected. No significant differences in the ARMS subset were observed when patients were divided into their outcomes of alive or dead (Figure 52b), but the analysis of the ERMS subgroup revealed a notable increased expression of ITGA9 in patients that were not cured, compared to alive patients (Figure 52c).

Survival curves of RMS patients were not available, although analysis of ITGA9 effects on patients survival was done following this approach: patients of ARMS or ERMS subtype were divided into high or low ITGA9 expression (Figure 52 d,e). Then, proportion of alive and dead patients was calculated and compared in each group. In the case of ARMS patients, the survival proportion (around 56%) was similar independently of ITGA9 expression (Figure 52 f,g). However, in ERMS patients, survival was clearly lower in the group of high ITGA9 expression (66.67% of survival), compared to the group of low ITGA9 expression (93.33% of survival) (Figure 52 h,i). This suggested a crucial role of ITGA9 in disease progression of ERMS and highlighted the potential prognostic value of ITGA9 in this subset of patients.

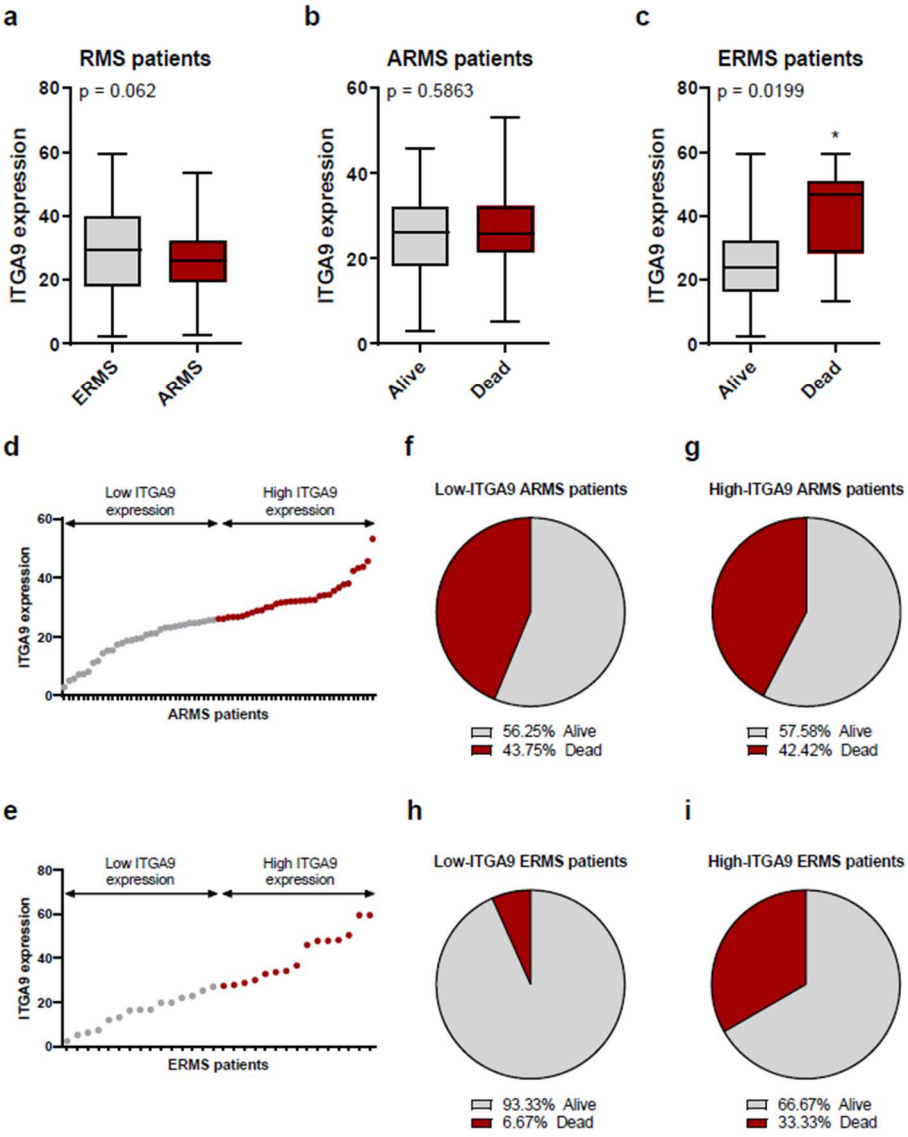

Figure 52. ITGA9 was a bad prognostic marker in ERMS patients. a. ITGA9 expression in a dataset of RMS patients, divided by their histological subtype. **b,c.** ITGA9 expression in ARMS and ERMS patients, segregated according to their clinical outcome. Statistical significance was determined by t-Test, considering *p<0.05. **d,e.** Graph showing ARMS or ERMS patients ordered by ITGA9 expression and segregation of patients into high- and low-ITGA9 expressing groups. **f-i.** Proportion of alive and dead patients in each subgroup.

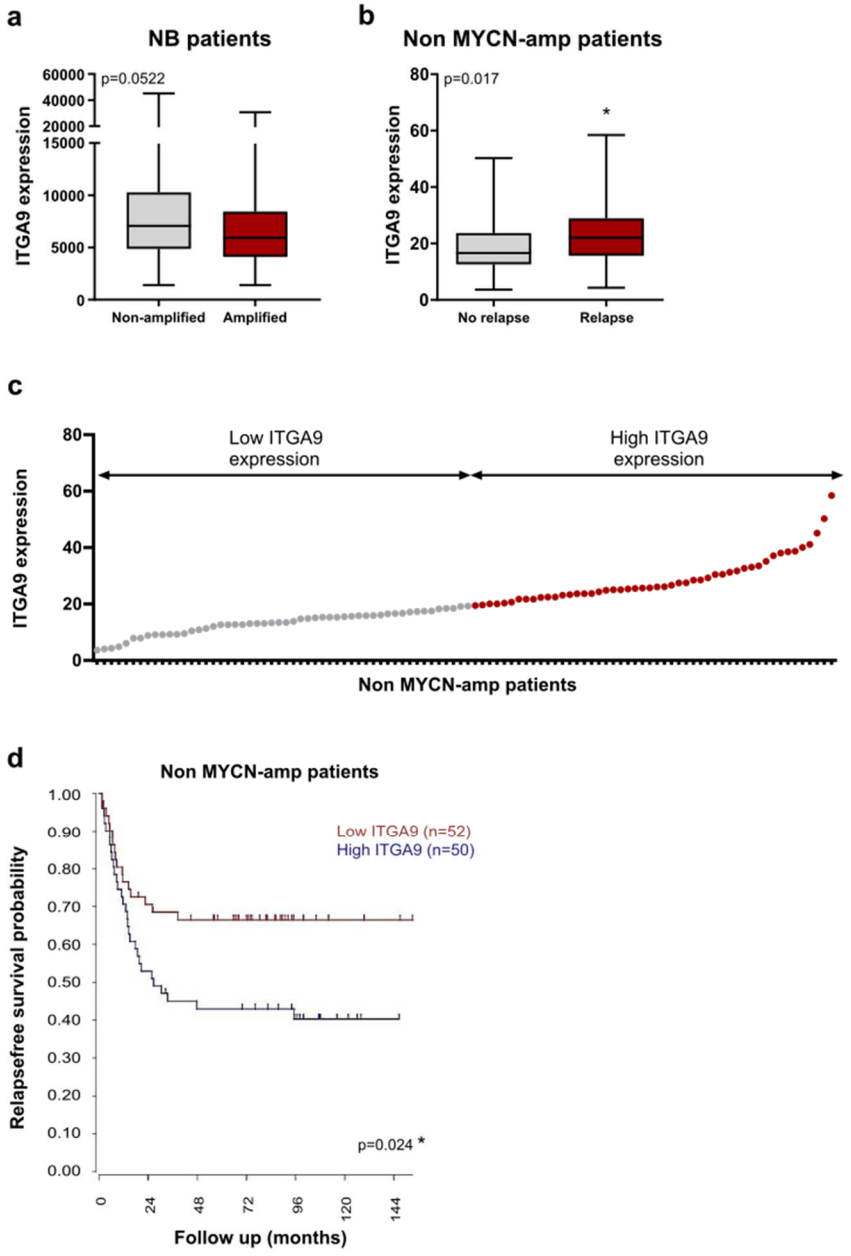

Figure 53. ITGA9 was a bad prognostic factor for MYCN non-amplified NB patients. a. ITGA9 expression in a dataset of NB patients segregated by *MYCN* status. **b.** ITGA9 expression in a dataset of MYCN non-amplified patients, depending on relapse. **c.** Graph showing MYCN non-amplified patients ordered by ITGA9 expression and segregated into high- and low-ITGA9 expressing patients. **d.** Relapse-free survival curve of MYCN non-amplified patients depending on ITGA9 expression.

5.2 Prognostic value of ITGA9 in NB

Analysis of Su et al. dataset (246), available at the R2: Genomic and Visualization Platform (244), that comprised 498 samples of NB patients, showed a trend towards higher ITGA9 expression in MYCN non-amplified patients, one of the most important prognostic factors of NB (Figure 53a).

Using an specific dataset for metastatic MYCN non-amplified patients (247), an increased expression of ITGA9 in patients with relapse was detected (Figure 53b). In addition, when MYCN non-amplified patients were segregated into high and low ITGA9 expression groups (Figure 53c), a significant decreased in relapse-free survival was observed in patients with high expression of ITGA9 (Figure 53d), suggesting ITGA9 has a bad prognostic value for MYCN non-amplified patients.

5.3 Prognostic value of ITGA9 in BC

Analysis of BC patients was done with Kensler K et al. dataset (248), available at the R2: Genomic and Visualization Platform (244), that comprised 1110 patients. Classification of patients by intrinsic subtype showed an increased expression of ITGA9 in samples from basal BC patients, compared to all the other subtypes (HER2, luminal A and luminal B) (Figure 54a).

To further analyse the role of ITGA9 in the survival of this neoplasia, Kaplan-Meier Plotter Platform (249) was used. Results showed a significant reduction in disease-free survival of patients with high-grade tumours (Figure 54b). This difference in terms of survival was clearer in the case of high-grade basal subtype patients (Figure 54c), suggesting that ITGA9 has

an important role in the progression of this subtype of BC and could be a bad prognostic factor for basal subtype patients.

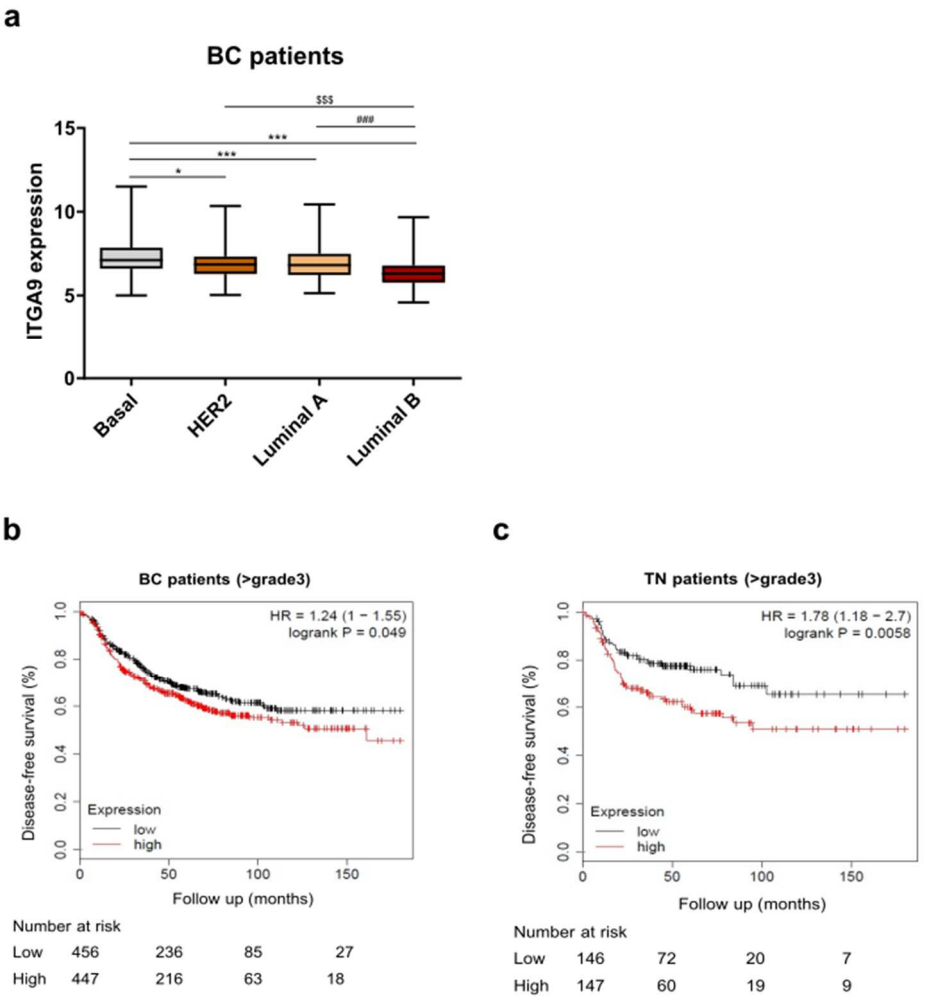

Figure 54. ITGA9 was a bad prognostic marker in patients from the basal subtype. a. ITGA9 expression in BC patients classified according to BC intrinsic subtypes. **b.** Disease-free survival of high-grade BC patients. **c.** Disease-free survival of high-grade basal patients.

V. DISCUSSION

1. Regulation of ITGA9 by miRNA and effects of miR-7 and miR-324-5p overexpression in RMS

In this work the regulation of ITGA9 and consequently, the regulation of α9β1 integrin (since ITGA9 is always a partner of β1 subunit) has been addressed. After screening of miRNAs capable of downregulating ITGA9 expression, miR-7 and miR-324-5p stood out as the best candidates (Figure 31). Overexpression of both miRNAs modulated ITGA9 in two RMS cell lines representing both histological subtypes of this neoplasia and induced a clear reduction of cell proliferation *in vitro* (Figure 34) and tumour growth *in vivo* (Figure 36). However, only overexpression of miR-7 produced a significant drop in cell invasiveness *in vitro* (Figure 34) and survival of intravenously injected tumour cells *in vivo* (Figure 39). Thus, the results herein presented point to the existence of a crucial regulation of ITGA9 by these two miRNAs and a preponderant role in tumour growth and metastasis.

miR-7 is one of the most conserved miRNAs in animals (262). It is encoded by three different genes, *MIR7-1*, *MIR7-2* and *MIR7-3*, that give rise to the same miR-7 mature sequence, being *MIR7-1* (chromosome 9, region 9q21.32) the dominant gene responsible for miR-7 expression. miR-7 has been previously reported to play clear tumour suppressor and anti-metastatic roles by regulating basic cellular processes in several cancers including glioblastoma, lung cancer, melanoma and breast cancer. Usually, a single miRNA can target several genes on its 3'UTR and influence the expression of regulatory clusters according to their biological function (263). In the case of miR-7, there is a long list of regulated genes that includes EGFR, PI3K, PAK1/2, ERK, cdc42, FAK, VE-cadherin, FGFR4, BCL-2, XIAP and Slug, among other. These genes are mostly related to cell

proliferation, apoptosis, differentiation, invasion and EMT (264-273). In fact, miR-7 is considered a network stabilizer, connecting different signalling pathways to ensure cell homeostasis (262). Therefore, it is often downregulated in different cancer cells, for example, in brain, breast, lung, hepatocellular and colon cancer cells (274-280).

Results from this study are in concordance with previous bibliography, since miR-7 exerted anti-oncogenic and anti-metastatic effects on RMS cells. In addition, we added ITGA9 to the list of miR-7 targets, a list that includes other integrin signalling mediators such as FAK and cdc42 (238). Validation of *in vitro* effects by shRNA against ITGA9 (Figure 35) allows us to propose that the observed effects are caused by miR-7 mediated ITGA9 downregulation. However, we could not exclude effects derived from inhibition of other target genes and this reinforces the idea of considering miR-7 as a multi-genic negative regulator of tumour growth and metastasis.

Cells overexpressing miR-7 and injected through the tail vein showed an impaired survival after one-week post-injection. This suggests a crucial role of this miRNA in the early stages of metastasis. However, we cannot ascertain whether the effects on cell survival were observed in cells that remain in circulation (in lung capillaries), were still in process of extravasating or have already reached the lung parenchyma. In addition, with this approach other important phases of the metastatic cascade are not considered (escape from the primary tumour, intravasation and outgrowth of macrometastases). Therefore, further studies will be needed to clarify the specific contribution of miR-7 and ITGA9 downregulation in each step of the metastatic cascade. In addition, considering that the main metastatic sites of RMS are lymph nodes, lungs, bone and bone marrow (134,136), studying the effects of miR-7 on arrival and implantation of

tumour cells in these compartments would be very interesting to develop a possible anti-metastatic therapy based on miR-7 overexpression.

On the other hand, the role of miR-324-5p is not as well established as it is for miR-7. miR-324-5p has been shown to play both oncogenic and tumour suppressor roles in a cancer-specific manner. Most of the available bibliography reported that miR-324-5p has a tumour suppressor role in several cancers (medulloblastoma, multiple myeloma, gastric, colorectal, hepatocellular, breast cancer, etc.) (281-287); however, an oncogenic role of this miRNA has been also described in pancreatic and lung cancer (288,289). In our case, miR-324-5p exerted a clear tumour suppressor function since it reduced cell proliferation and tumour growth.

Several target genes of miR-324-5p have been previously described, although ITGA9 has not been related to this miRNA so far. The list of miR-324-5p target genes includes ETS1, KLF3, ELAVL1, TSPAN8, FBXO11, TGF-β2, SP1, Gli1 and Smo (282-285,288-291). Thus, our results lead us to conclude that miR-324-5p has a tumour suppressor role in RMS and allowed us to include ITGA9 to this list of target genes. However, anti-oncogenic effects of miR-324-5p in RMS resulting from targeting other genes may not be ruled out.

In this case, effects on cell invasiveness were not observed after overexpression of miR-324-5p, as miR-7 overexpression showed. The downregulation of ITGA9 obtained after induction of each miRNA was slightly higher with miR-7 than miR-324-5p, and much higher with shRNA. Besides, miRNA levels assessed by qPCR were substantially higher in the case of miR-7 in both RMS cell lines. This may explain differences observed

in terms of cell invasion. We postulate that miR-324-5p, although downregulated ITGA9, this reduction did not suffice to modulate cell invasiveness. On the contrary, the observed reduction in cell proliferation was higher with miR-7 and miR-324-5p overexpression, than with ITGA9 inhibition by shRNA. This reinforces the idea that these miRNAs act as multi-gene negative regulators of tumour growth and metastasis and their function is not exclusively mediated by inhibition of ITGA9.

The fact that the results in the animal models concur with the conclusions reached *in vitro* is remarkable. Thus, the overexpression of both miRNAs produced a very clear impairment in tumour growth, probably by at least two mechanisms: the first was a reduction in cell proliferation (KI67 index clearly reduced with miRNA overexpression; Figure 37) and the second, but no less important, a significant reduction in tumour vessels which correlated with tumour growth (Figure 38). *In vitro* experiments do not evaluate the interaction between tumour cells and the surrounding environment. Since the main function of ITGA9, one of these miRNA target genes, is to connect the intracellular and extracellular environment, it seems plausible that these interactions could be affected. The interaction between ITGA9 and members of the VEGF family have been previously described not only in tumour cells, but also in endothelial cells where it controls angiogenesis and lymphangiogenesis. And enhanced cell migration has been also observed in endothelial cells mediated by the interaction between ITGA9 and VEGFs (81,85,129,292). In addition, anti-angiogenic effects were previously described after inoculation of miR-7 in glioblastoma and neuroblastoma *in vivo* murine models (293). Therefore, we propose that the inhibition of ITGA9 by miR-7 or miR-324-5p reduced the sprouting of blood vessels in the tumour stroma and this, eventually, reduce cell proliferation and tumour

growth. However, further studies will be needed to characterize affected signalling underneath tumour angiogenesis such as effects on VEGF-mediated signalling.

Results from this part of the project were published (250) and were the first description of the role of miR-7 and miR-324-5p in RMS. Later, another study reached similar conclusions regarding the anti-oncogenic effects of miR-7 in this neoplasia. In this case authors reported induction of cell death and reduced tumour growth *in vivo* after overexpression of miR-7 in RMS cells (294).

The anti-oncogenic effects observed after miR-7 and miR-342-5p overexpression, postulate them as attractive therapeutical options for impeding RMS progression since they would allow the suppression of multiple oncogenes at the same time. Strategies for *in vivo* administration of miR-7 have been already successfully reported in other tumours: intratumor injection of miR-7 and systemic administration by targeted nanoparticles or liposome formulations containing miR-7 reduced tumour growth and metastasis in neuroblastoma, glioma and adrenocortical tumour models (293,295,296). However, delivering of miRNAs to organs other than the liver, remains challenging (297). Therapies based on miRNA replacement are most likely to be given in combination with other therapeutic agents. In fact, studies combining miR-7 with other drugs, such as cisplatin, cetuximab or paclitaxel, suggested that miR-7 may enhance the anti-tumour effects of other agents. Finally, upregulation of miR-7 by small molecules has been also described. Examples of this phenomena are curcumin in pancreatic cancer, antibacterial enoxacin in colorectal and thichostatin A in BC cell lines (298-301).

To sum up, miR-324-5p and, particularly, miR-7 are promising therapeutic options for RMS patients, although still further studies are needed to deeper understand their effects on cell behaviour and how they can be combined with other approaches to maximize their anti-oncogenic effects. In addition, ways of administration to ensure that they selectively arrive to the tumour cells, reducing possible side effects, are still necessary.

2. The role of ITGA9 in NB metastasis

Previous studies of the group had revealed that ITGA9 depletion reduced cell invasiveness in NB cell lines (232). Following this promising result, we decided to validate the role of ITGA9 in murine models of NB metastasis.

Results showed that ITGA9 downregulation by shRNA reduced the capability of cells to engraft and develop metastasis after intravenous injection of tumour cells. Whilst all mice in the control group developed metastasis after 50 days, only 70% of mice in the ITGA9-depleted group developed metastasis, even when they were allowed to evolve until 100 days. In addition, a reduction in the number of metastases per animal and their volume was also observed in the shITGA9 group (Figure 40). Similarly, treatment with RA08 (which was designed to disrupt the interaction between ITGA9 and ADAM12) at 2mg/kg also reduced the formation of metastasis after intravenous injection of NB tumour cells. In this case, while 88% of animals in the control group developed metastasis, only 44% of mice treated with this dose of RA08 developed metastasis. In addition, a trend towards a reduction in number and volume of metastasis was also observed (Figure 43). These results pointed to a preponderant role of ITGA9 in NB colonization and formation of metastasis. The fact that there was a decrease

not only in the number of mice that developed metastasis, but also in the number of metastases per mice and their volume, indicated that probably disrupting ITGA9 function reduced the number of viable cells that arrive to the liver parenchyma and re-enter in the cell cycle in order to form macrometastases, but also it is likely that it affected the proliferation rate of these cells during the outgrowth of the metastatic lesions.

The role of ITGA9 had not been previously addressed in NB, although the role of other integrin heterodimers, including α4β1 integrin, had been previously described (233,234,302). The expression of α4β1 integrin in NB cells turned out to enhance metastasis in a syngeneic tumour model of NB, while antagonism of α4β1 integrin reduced metastasis (233). Considering the high homology between α4 and α9 integrin subunits and their redundancy in ligand interaction (75), this suggested that α9β1 could be also involved in the modulation of metastasis in NB. With these results, we concluded that ITGA9, and consequently α9β1 integrin heterodimer, is a key player in the metastasis of NB cells and its inhibition is a promising strategy for reducing metastasis in these patients.

Our results in murine models are the first evidence reported about the role of ITGA9 in the process of metastasis of NB cells. However, further characterization of ITGA9 involvement in each step of the metastatic cascade is still necessary. Our models were based on intravenous injection of tumour cells and allowed us to detect effects derived from changes in cell survival in circulation, extravasation and colonization of metastatic sites, but other important steps in the metastatic cascade, such escape from the primary tumour and intravasation, remained unexplored with our experimental approach. Thus, studying the effects of ITGA9 inhibition in

models of spontaneous NB metastasis would be of particular interest since they better represent the disease progression that occur in patients. In addition, effects on other type of metastasis should be addressed, since most of the metastases observed in our murine models were hepatic (≈95%). Considering that the most common sites of metastasis in NB patients are regional lymph nodes, bone marrow, bone and liver (164,165,168), this would be essential for developing a potential anti-metastatic therapy.

3. The role of ITGA9 in BC metastasis

In the case of BC, the role of α9β1 had been previously reported and high α9β1 expression had been associated with reduced overall survival and metastasis-free survival of BC patients, especially of those of the basal-like subtype. In concordance with this, α9-blocking antibodies reduced cell invasion, tumour growth and metastasis in BC murine models (118,119). This made this neoplasia specially interesting for testing the effects of the compound RA08 and determine whether blocking ITGA9 could serve as a good anti-metastatic therapy in a wide range of tumour types. In addition, we also decided to validate the effects by shRNA-mediated knockdown of ITGA9.

In both cases, either inhibiting ITGA9 by shRNA (Figure 45) or treatment with RA08 (Figure 46), the effects observed were similar and induced a reduction in cell invasiveness, without affecting cell proliferation. Besides, a concomitant reduction in FAK phosphorylation at Tyr 397 was also observed. Activation of integrins by ligand-binding induces conformational changes, integrin clustering and interaction with intracellular elements that

guide integrin downstream signalling. One of the most important signalling elements involved is the kinase FAK since its recruitment and interaction with integrin cytoplasmic tail induces autophosphorylation at Tyr 397 and subsequent recruitment of other signalling molecules (SFK, MAPK and PI3K for instance) (64,65). Thus, autophosphorylation of FAK is considered one of the main and early events in integrin-mediated signalling and was used in this study as a marker of decreased ITGA9-mediated downstream signalling. This was particularly important since treatment with RA08 did not affect ITGA9 levels, instead of this, it reduced FAK phosphorylation and presumably ITGA9 downstream signalling. In addition, reduction of FAK activation has been directly related to modulation of cell invasion in BC cells since it can regulate several downstream pathways (MAPK and PI3K, for instance) and the formation of focal adhesion complexes that are necessary for cell movement (303,304).

The two BC cell lines used, MDA-MB-468 and MDA-MB-231 were from the basal subtype (256) and expressed ITGA9 in a different extent (Figure 44). In general terms, the MDA-MB-468 cell line was more sensitive to ITGA9 blockade than MDA-MB-231 since it showed a higher reduction in cell invasiveness upon ITGA9 knockdown or treatment with RA08. Relative ITGA9 expression was notably higher in MDA-MB-468 cells, suggesting that the expression level may correlate with cell dependency on this protein. MDA-MB-231 cells, which expressed lower levels of ITGA9, may be more dependent on other integrins for regulating cell invasion capacity. Compensatory effects between integrins have been previously observed in BC and prostate cell lines (305,306). Thus, we cannot exclude that the inhibition of ITGA9 may have not induced changes in the expression of

other integrin heterodimers that could have alleviated effects of ITGA9 silencing in these cells.

MDA-MB-468 cell line was selected for *in vivo* assessment of RA08 effects. Results showed that treatment with RA08 reduced the colonization and outgrowth of BC cancer cells in lungs, after intravenous injection. Both doses of RA08 were effective and reduced the number of metastatic foci to the half (Figure 47). This indicated that probably disrupting ITGA9 function reduced the number of viable cells that arrived at the lung parenchyma and re-entered in the cell cycle to start proliferating. As mentioned above, a reduction in BC metastasis after blockade of ITGA9 has been previously reported (214,215) and the use of FAK inhibitors has been previously tested in pre-clinical models of BC, producing a reduction in metastasis to lungs (307-309). So, our results are in concordance with literature and, although they are not revealing in BC, they allowed us to conclude that RA08 treatment had anti-metastatic effects in a broad spectrum of tumour types (RMS, NB and BC). Therefore, it would be very interesting to test the effects of RA08 in other neoplasia since development of a putative anti-metastatic therapy based on ITGA9 blocking could benefit to numerous cancer patients.

In addition, a PDX model of BC was used to further assess the effects of RA08 treatment on primary tumour growth. *In vitro* experiments did not suggest that RA08 treatment could have effects on tumour growth given cell proliferation was not affected. However, given the strong effects on primary tumour growth observed after ITGA9 inhibition by miRNA, effects on BC tumour growth were plausible. With this approach a 40% reduction in tumour growth was observed after the treatment with RA08 (Figure 48).

Many interactions between cells or with the cell environment are not considered in cellular cultures and may explain the observed effects. Previous studies have shown that ITGA9 plays important roles in normal and tumour angiogenesis and lymphangiogenesis (80,129,130,292) and reduced tumour angiogenesis has been reported after ITGA9 depletion and FAK suppression in BC murine models (119,310,311). This suggests that RA08 effects might be mediated by a reduction of tumour vascularization and would agree with our results obtained after miRNA-mediated ITGA9 inhibition in RMS. Nevertheless, other mechanisms cannot be rule out. As a matter of fact, a reduction in FAK phosphorylation has been related to many signalling pathways that modulate cell proliferation (312-314).

4. The role of α9β1 integrin in non-adherent cell growth in RMS, NB and BC

Cell adhesion to the ECM is essential to maintain tissue homeostasis. A correct interaction between cells and their surrounding is necessary to determine whether a cell is in its correct location and efficiently remove cells that are not, thereby preventing their reattachment and growth in inappropriate places (315). Integrins are the main receptors that mediate cell adhesion to ECM and thus, they can regulate cell viability under these conditions (42,316).

Anoikis is a particular form of cell death induced upon cell detachment from the ECM or due to inappropriate cell adhesion. It could be initiated and mediated by different signalling pathways that eventually trigger the activation of caspases and DNA fragmentation; being considered a type of apoptosis. Because anoikis prevents detached cells from surviving and

colonizing elsewhere, its deregulation is a critical mechanism for metastasis and is emerging as a new hallmark of metastatic malignancies. Tumour cells need to acquire anoikis resistance to survive after detachment from the primary tumour and during their dissemination through the vascular system, to eventually colonize distant organs and generate metastatic lesions (15,41,315-318).

As previously mentioned integrins regulate cell survival depending on their interactions with ECM or surrounding cells by regulating pro-survival pathways and anti-apoptotic proteins. Experimental evidence demonstrated that changes in the integrin repertoire expressed in cancer cells contribute to metastatic dissemination and help cells to overcome anoikis during this process (41,43-45,319-323). Even some authors have proposed the existence of an integrin-mediated death, different from anoikis. According to that, unligated integrins on adherent cells could directly recruit and activate caspase-8 [8], resulting in apoptotic cell death (324,325). Based on this, we decided to study the effects of ITGA9 depletion in non-adherent cell culture conditions. For this purpose, cells were seeded in non-adherent dishes and were allowed to grow forming multicellular tumour spheroids, to mimic circulating tumour cell clusters *in vitro* (326,327). Analysis of apoptosis and cell cycle arrest by flow cytometry or assessment of protein markers by Western blot showed no consistent changes due to ITGA9 depletion (Figure 49). Nonetheless, a reduction in the number of ITGA9-knockdown cells was observed when they were grown in suspension. We noticed that when cells were grown in suspension there was a rapid decrease in the number of viable cells (to the half after 12 hours)

[8] Caspase-8 is one of the initiator caspases that activates caspase-3, which is the most important executor caspase of apoptosis (354).

and then, cells started to proliferate in a very slow rate, that was even more reduced when ITGA9 was knockdown. This allowed us to conclude that although cells were not dying or stack into a certain cell cycle phase, anchorage-independent growth was clearly affected upon ITGA9 depletion. WST-1 assay, which quantifies metabolically active cells as an indirect measure of cell proliferation, was used to quantify anchorage-independent growth and confirmed that there was a reduction after knockdown of ITGA9 or when cells were treated with RA08 in cells from RMS, NB and BC (Figure 50). On the contrary, effects on cell proliferation in adherent systems were not observed (Figure 51).

With these results, we confirmed that ITGA9 inhibition produced an impairment of anchorage-independent cell growth. However, further investigation on the specific molecular pathways that lead to this effect is still necessary. Modulation of non-adherent cell growth by integrins has been previously described (328-332), although this is the first time it is specifically related to ITGA9. This highlights the role of ITGA9 as a potential target to suppress metastatic dissemination in a wide range of cancers since blockade of its function affects not only invasive cell capabilities, but also proliferation rate in suspension. Despite *in vivo* validation of these results is a pending issue, it was suggested that ITGA9 may be important for the maintenance of metastatic cluster cells in circulation.

5. Prognostic value of α9β1 integrin in RMS, NB and BC

The analysis of ITGA9 expression in RMS patients revealed a trend to higher expression in tumours from the embryonal subtype (ERMS), compared to alveolar (ARMS) tumours. Interestingly, analysis of survival in ERMS patients

pointed to an increased expression of ITGA9 in patients that do not survive. In addition, when patients were segregated according to their ITGA9 expression into low- or high-expression groups, survival was clearly reduced in the high-ITGA9 group (form 94% in low-ITGA9 to 67% in high-ITGA9 group). On the contrary, these differences were not found in ARMS subgroup of patients (Figure 52). Altogether, this suggested that ITGA9 could be a bad prognostic factor in ERMS patients. This subgroup of RMS has a good prognosis, with a 5-year survival rate above 70% (333). Unfortunately, despite advances in treatment protocols, there is a proportion of patients that still have disease progression and do not survive. According to these results, ITGA9 could define a subgroup of patients within ERMS, with worse prognosis.

Similarly, using a dataset of NB patients, a trend to higher ITGA9 expression was found in tumours without *MYCN* amplification and ITGA9 expression was higher in patients that relapse within this group. In addition, when MYCN non-amplified patients were divided according to ITGA9 expression, a decrease in relapse-free survival was observed in high-ITGA9 group (from 65% in low-ITGA9, to 40% in high-ITGA9 group) (Figure 53). Thus, our results indicated that within MYCN non-amplified subgroup of patients, the expression of ITGA9 could define another subgroup with worse prognosis. Although MYCN status does not define different NB groups *per se*, it is one of the most important molecular alteration, whose presence confers poor prognosis to NB patients and is associated with advanced-stage, treatment failure and unfavourable histology (171-173).

Expression of any integrin heterodimer had been previously correlated to patient's survival in RMS, so this was the first time that a prognostic value

was given to a member of the integrin family. On the contrary, clinical significance had been given to integrin α4 in NB patients. A previous study pointed that integrin α4 was more frequently expressed in MYCN non-amplified tumors and was associated with poor prognosis in this subset of patients (233). Given the high sequence identity and ligand redundancy between α4 and α9 subunits (75), it seems feasible that prognostic value in NB is shared between these integrins. In any case, this was the first time that ITGA9 was postulated as a prognostic factor in NB.

In addition to the prognostic value, ITGA9 seems to be upregulated in ERMS and MYCN non-amplified tumours, suggesting that MYCN amplification or PAX3/7-FOXO1 fusion genes (present in 80% of ARMS tumours (145,146)) could negatively regulate the expression of this integrin. A study addressing this question in RMS has determined that PAX3-FOXO1, the most frequent fusion gene in ARMS, was not able to regulate ITGA9 expression and vice versa (334). However, regulation of ITGA9 by MYCN has not been addressed in NB.

In both cases, we have observed that higher expression of ITGA9 was associated to poor prognosis in a specific subset of patients that generally are associated to good prognosis, embryonal subtype in RMS and MYCN non-amplified patients in NB. Unresolved questions persist regarding the optimal management for these groups of patients given that some cases still relapse and/or metastasize. The fact that ITGA9 can discriminate a subgroup of patients with worse prognosis should be considered for subsequent studies, as this new set of patients with worst prognosis would be candidates for putative ITGA9-based anti-metastatic therapy or, at least, for an intensification of their treatment.

Finally, analysis of expression in BC dataset of patients showed a higher expression of ITGA9 in patients from the basal subtype, compared to all the other intrinsic subtypes. Besides, an association between more aggressive subtypes and ITGA9 expression was suggested, since the highest ITGA9 expression was observed in patients from the basal subtype, followed by patients from the HER2 subtype, and lower expression was detected in patients from the luminal A and B subtypes. Besides, when patients were segregated into high- or low-ITGA9 expression groups, differences in disease-free survival were observed, particularly when only basal subtype patients were analysed. High expression of ITGA9 was clearly associated to poor prognostic in these patients and reduced disease-free survival (Figure 54). Unlike what was observed in RMS and NB, in this case ITGA9 was associated with worse prognosis of a subset of patients that already have the most aggressive subtype (212). The prognostic value of ITGA9 in BC and particularly in basal subtype has been corroborated by other studies (118,119). This reinforces the idea that BC patients could benefit from a potential anti-metastatic therapy based on the blockade of ITGA9.

In this project, a key role of ITGA9 in metastasis has been described in RMS, NB and BC models, and evidence pointing to ITGA9 expression as a bad prognostic marker in a very specific subset of patients of each of these neoplasia was also presented. Considering that metastasis is the main cause of cancer-associated mortality and is one of the most valuable prognostic factors for cancer patients (10,11), it seems feasible that the prognostic value of ITGA9 is caused by its ability to modulate metastatic behaviour. Thus, a potential anti-metastatic therapy based on ITGA9 blockade could improve patient survival of these subsets of patients. Apart of the potential prognostic value, ITGA9 could be also used as a marker of therapeutic

response. Our results indicated that cell lines with higher levels of ITGA9 were more sensitive to ITGA9 blockade, at least in *in vitro* cell invasion assays. This suggests that tumours with higher ITGA9 expression could be more sensitive to ITGA9 blockade and these patients would be good candidates for a potential anti-metastatic therapy based on ITGA9 inhibition. Further studies with the aim of validating ITGA9 potential as a prognostic factor and/or marker of response are still necessary to develop this targeted therapy, but our results highlighted the therapeutic potential of ITGA9.

6. ITGA9 blockade as a potential treatment for metastasis

The onset of metastasis is one of the most important prognostic factors for cancer patients and very often involves crossing a boundary beyond which the probability of cure becomes clearly lower. As a matter of fact, metastasis is the first cause of cancer-associated deaths (10). Nevertheless, most current treatments are focused on preventing tumour growth and to date, no drugs or other therapeutic approaches have been approved exclusively for preventing metastasis.

Metastasis can be targeted at different time points: the initial phases of invasion, survival of circulating tumour cells, colonization of distant organs and outgrowth of macrometastases, being this last point the most studied at the clinical stage. In clinical trials, anti-metastatic agents with promising results at pre-clinical studies are firstly tested in advanced-disease patients with already metastatic detectable lesions. The use of untried new agents is restricted to these patients until the control of advanced metastatic disease is proven. Then, effective treatments are tested in patients with other

options of standard treatment: early metastatic disease patients first, and then, patients without metastasis in the adjuvant or neoadjuvant setting. All this process makes very hard to test and find effective preventing treatments for metastasis since approaches targeting the first phases of the metastatic cascade would hardly reach early-stage patients (some of whom could develop metastasis) that are the potential beneficiaries of this kind of treatments (335).

Probably, the most advanced studies in metastasis treatment were focused on inhibiting tumour neovasculature (336-338). However, the clinical efficacy of antiangiogenic therapies, most of them targeting VEGF or its receptors, has been disappointing or even pernicious (339-341). These approaches turned out to be good at controlling macrometastases growth in some cases but failed preventing the onset of new metastasis since they do not affect dormant or circulating tumour cells responsible for the metastatic relapse (335). Other therapeutic possibilities against the initial phases of metastasis include the inhibition of matrix metalloproteinases (342) or impairment of tumour cell embolization by reducing clumping with platelets (343). Unfortunately, none of these have successfully reached the clinical setting. Therefore, the development of treatments aimed at blocking metastatization is a pending clinical need.

Results from this project indicated that ITGA9 inhibition (by different strategies including miRNA, shRNA and treatment with RA08) could be viewed as a sequential interference of the different steps in the metastatic cascade, rather than a complete blockade of a single phase (Figure 55). Thus, blockade of ITGA9 expression or function reduced cell invasiveness, anchorage-independent growth and metastasis appearance.

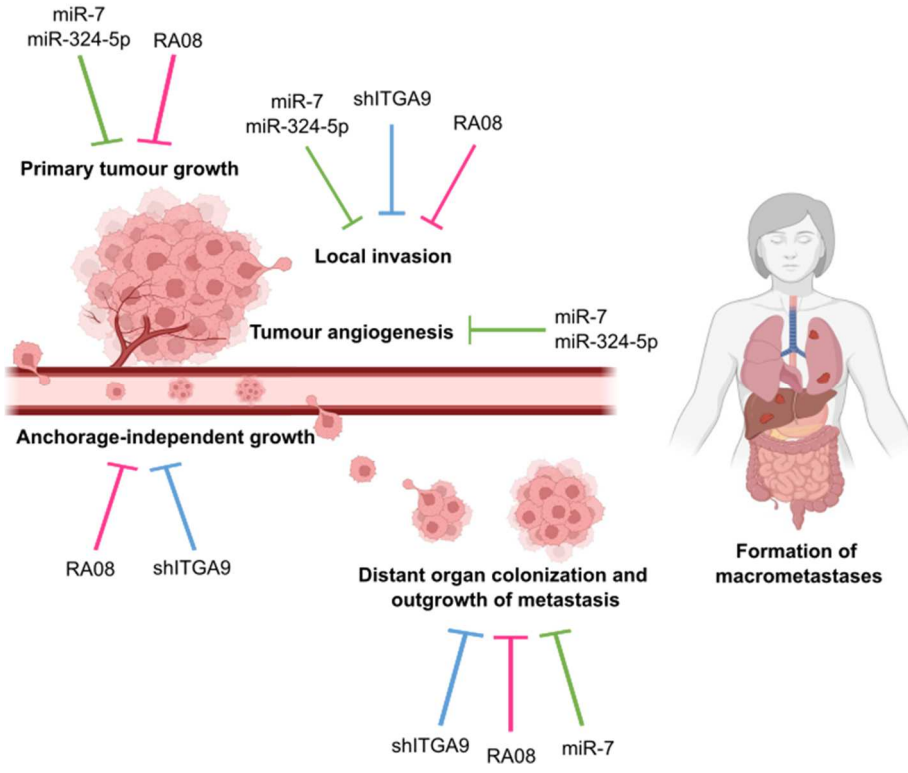

Figure 55. ITGA9 blockade, either by genetic tools (miRNA and shITGA9) or RA08 pharmacologic inhibition, hinders different steps in the metastatic cascade and eventually, reduces the formation of macrometastases.

The most promising advance presented in this project is the characterization of the anti-metastatic effects of RA08 treatment in different neoplasia. The design of RA08 was inspired in the sequence of interaction between ADAM12 and ITGA9, and it acts as a peptidomimetic able to hinder ligand binding to ITGA9. Its anti-metastatic effects were previously described in RMS, and now they were validated in other neoplasia such as NB and BC. Using murine models based on tumour cell intravenous injection, it was demonstrated that treatment with RA08 reduced the appearance of metastasis, without producing any apparent toxicity. Beyond the effects of RA08 on metastasis, the low toxicity of the compound makes

it particularly interesting, since a putative therapy for metastasis prevention is expected to be long-term, probably spanning several months and absence of associated non-desirable side-effects would enormously facilitate its possible implantation in treatment regimens.

In some cases, by the time of diagnosis, metastasis has already occurred (344) and this could be a limitation for a potential RA08-based anti-metastatic therapy. However, there are other clinical situations in which it could be applied. There is a great variability in the temporal course of metastasis, which strongly depends on cancer type. For instance, in small cell lung cancer and pancreatic cancer, metastatic disease often appears at the time of (or shortly after) the initial diagnosis, whereas many patients with breast and prostate cancers, among many others, tend to show metastasis after a prolonged period (345). These clinical differences have raised an important question of whether this period of dormancy offers a therapeutic opportunity to control metastatic disease (346). Moreover, circulating tumour cells in paediatric solid tumours, such as RMS and NB, are quite common in compartments such as peripheral blood or bone marrow, and are thought to contain cells that may originate metastases, often a long time after diagnosis. In addition, detection of circulating tumour cells has been found to be associated with a higher probability to develop metastases (162,347). In these circumstances, we propose that RA08 could be a potential anti-metastatic treatment and could prevent the onset of new metastases, consequently increasing disease-free survival of cancer patients.

Finally, a potential treatment with RA08 is most likely to be given in combination with other therapeutic agents during adjuvant and

maintenance regimens. Therefore, possible synergic, additive or antagonistic effects with other chemotherapeutics should be addressed in future studies. So far, we have shown that treatment with RA08 reduced also primary tumour growth (Figure 48). This makes RA08 treatment an interesting peptide to test in combination with other chemotherapeutic agents. In addition, combination with other targeted-therapies in current development, such as other integrin inhibitors (305) or FAK/Src inhibitors (312,348,349), could be also considered to improve the anti-metastatic effects as previous studies suggest.

Deeper understanding of the molecular mechanisms that drive metastasis and further characterization of RA08 effects is still essential for developing a future therapy. However, although there is still a long way to reach the clinics, results here presented are very promising and suggest that ITGA9 blockade by RA08 could be a potential anti-metastatic agent able to reduce metastasis onset and growth in a wide range of tumour types.

VI. CONCLUSIONS

First. miR-7 and miR-324-5p downregulate ITGA9 expression in rhabdomyosarcoma cell lines of both histological subtypes, embryonal and alveolar rhabdomyosarcoma.

Second. Overexpression of miR-7 and miR-324-5p reduced cell proliferation *in vitro* and tumour growth *in vivo* in rhabdomyosarcoma cell lines. Effects on tumour growth were produced by two mechanisms: reduction in cell proliferation and reduction of tumour angiogenesis.

Third. Overexpression of miR-7 reduced cell invasiveness *in vitro* and survival of tumour injected cells *in vivo* in rhabdomyosarcoma murine models.

Fourth. Inhibition of ITGA9 by shRNA or treatment with RA08 reduced metastasis formation in neuroblastoma murine models.

Fifth. Inhibition of ITGA9 by shRNA or treatment with RA08 reduced FAK activation and invasiveness of breast cancer cells *in vitro*.

Sixth. Treatment with RA08 reduced *in vivo* lung colonization and tumour growth in breast cancer murine models.

Seventh. Inhibition of ITGA9 by shRNA or treatment with RA08 did not reduce cell proliferation in adherent conditions, but reduced anchorage-independent cell growth in rhabdomyosarcoma, neuroblastoma and breast cancer cell lines.

Eight. ITGA9 was a bad prognostic marker of patients with embryonal rhabdomyosarcoma, MYCN non-amplified neuroblastoma and basal-subtype breast cancer since high ITGA9 tumour expression reduced survival in these subsets of patients.

Ninth. ITGA9 blockade, either by genetic tools or treatment with RA08, had anti-metastatic effects in rhabdomyosarcoma, neuroblastoma and breast cancer.

Tenth. A therapy based on the inhibition of ITGA9 is proposed as an interesting therapeutic alternative for patients of a broad spectrum of tumour types. This inhibition would reduce the metastatic capacity of cancer cells, preventing metastatic spreading and improving patient's survival.

VII. REFERENCES

1. Bray, F. *et al.* Global cancer statistics 2018: GLOBOCAN estimates of incidence and mortality worldwide for 36 cancers in 185 countries. *CA. Cancer J. Clin.* **68**, 394–424 (2018).

2. Organization, W. H. *International statistical classification of diseases and related health problems: tenth revision.* (2019). Available from: https://apps.who.int/iris/handle/10665/42980

3. Sung, H. *et al.* Global Cancer Statistics 2020: GLOBOCAN Estimates of Incidence and Mortality Worldwide for 36 Cancers in 185 Countries. *CA. Cancer J. Clin.* **71**, 209–249 (2021).

4. Bhakta, N. *et al.* Childhood cancer burden: a review of global estimates. *Lancet Oncol.* **20**, e42–e53 (2019).

5. Saletta, F., Seng, M. S. & Lau, L. M. S. Advances in paediatric cancer treatment. *Transl. Pediatr.* **3**, 156–182 (2014).

6. Peris Bonet, R., Pardo Romaguera, E., Muñoz López, A., Sayas Sánchez, N. & Valero Poveda, S. *Registro Español de Tumores Infantiles (RETI-SEHOP 1980-2016)*. (2017).

7. Steliarova-Foucher, E., Stiller, C., Lacour, B. & Kaatsch, P. International Classification of Childhood Cancer, Third Edition. *Cancer* **103**, 1457–1467 (2005).

8. Spector, L. G., Pankratz, N. & Marcotte, E. L. Genetic and Nongenetic Risk Factors for Childhood Cancer. *Pediatr. Clin. North Am.* **62**, 11–25 (2015).

9. Gatta, G. *et al.* Childhood cancer survival in Europe 1999-2007: results of EUROCARE-5-a population-based study. *Lancet Oncol.* **15**, 35–47 (2014).

10. Dillekås, H., Rogers, M. S. & Straume, O. Are 90% of deaths from cancer caused by metastases? *Cancer Med.* **8**, 5574–5576 (2019).

11. Fares, J., Fares, M. Y., Khachfe, H. H., Salhab, H. A. & Fares, Y. Molecular principles of metastasis: a hallmark of cancer revisited. *Signal Transduct. Target. Ther.* **5**, 1–16 (2020).

12. Hanahan, D. & Weinberg, R. A. Hallmarks of Cancer: The Next Generation. *Cell* **144**, 646–674 (2011).

13. Massagué, J. & Obenauf, A. C. Metastatic colonization by circulating tumour cells. *Nature* **529**, 298–306 (2016).

14. Seguin, L., Desgrosellier, J. S., Weis, S. M. & Cheresh, D. A. Integrins and cancer: regulators of cancer stemness, metastasis, and drug resistance. *Trends Cell Biol.* **25**, 234–240 (2015).

15. Valastyan, S. & Weinberg, R. A. Tumor Metastasis: Molecular Insights and Evolving Paradigms. *Cell* **147**, 275–292 (2011).

16. Majidpoor, J. & Mortezaee, K. Steps in metastasis: an updated review. *Med. Oncol.* **38**, 1–17 (2021).

17. Lamouille, S., Xu, J. & Derynck, R. Molecular mechanisms of epithelial-mesenchymal transition. *Nat. Rev. Mol. Cell Biol.* **15**, 178–196 (2014).

18. Lu, W. & Kang, Y. Epithelial-Mesenchymal Plasticity in Cancer Progression and Metastasis. *Dev. Cell* **49**, 361–374 (2019).

19. Dongre, A. & Weinberg, R. A. New insights into the mechanisms of epithelial–mesenchymal transition and implications for cancer. *Nat. Rev. Mol. Cell Biol.* **20**, 69–84 (2019).

20. Karamanou, K., Franchi, M., Vynios, D. & Brézillon, S. Epithelial-to-Mesenchymal Transition and invadopodia markers in breast cancer: Lumican a key regulator. *Semin. Cancer Biol.* **62**, 125–133 (2020).

21. Al-Khadairi, G. *et al.* PRAME promotes epithelial-to-mesenchymal transition in triple negative breast cancer. *J. Transl. Med.* **17**, 1–14 (2019).

22. Yu, Y. *et al.* miR-190 suppresses breast cancer metastasis by regulation of TGF-β-induced epithelial-mesenchymal transition. *Mol. Cancer* **17**, 1–12 (2018).

23. Sannino, G., Marchetto, A., Kirchner, T. & Grünewald, T. G. Epithelial-to-Mesenchymal and Mesenchymal-to- Epithelial Transition in Mesenchymal Tumors : A Paradox in Sarcomas? *Cancer Res.* **17**, 4556–4562 (2017).

24. Ehnman, M., Chaabane, W., Haglund, F. & Tsagkozis, P. The Tumor Microenvironment of Pediatric Sarcoma: Mesenchymal Mechanisms Regulating Cell Migration and Metastasis. *Curr. Oncol. Rep.* **21**, 1–11 (2019).

25. Feng, Z. M. & Guo, S. M. Tim-3 facilitates osteosarcoma proliferation and metastasis through the NF-κB pathway and epithelial-mesenchymal transition. *Genet. Mol. Res.* **15**, 1–9 (2016).

26. Preussner, J. *et al.* Oncogenic Amplification of Zygotic Dux Factors in Regenerating p53-Deficient Muscle Stem Cells Defines a Molecular Cancer Subtype. *Cell Stem Cell* **23**, 794–805 (2018).

27. Liu, C. *et al.* Epigenetically upregulated GEFT-derived invasion and metastasis of rhabdomyosarcoma via epithelial mesenchymal transition promoted by the Rac1/Cdc42-PAK signalling pathway. *EBioMedicine* **50**, 122–134 (2019).

28. Hoshino, A. *et al.* Tumour exosome integrins determine organotropic metastasis. *Nature* **527**, 329–335 (2015).

29. Zhang, L. *et al.* MicroRNA-410-3p upregulation suppresses proliferation, invasion and migration, and promotes apoptosis in rhabdomyosarcoma cells. *Oncol. Lett.* **18**, 936–943 (2019).

30. Masià, A. *et al.* Notch-mediated induction of N-cadherin and α9-integrin confers higher invasive phenotype on rhabdomyosarcoma cells. *Br. J. Cancer* **107**, 1374–1383 (2012).

31. Ye, M. *et al.* Downregulation of MEG3 promotes neuroblastoma development through FOXO1-mediated autophagy and mTOR-mediated epithelial-mesenchymal transition. *Int. J. Biol. Sci.* **16**, 3050–3061 (2020).

32. Tian, X. *et al.* Polo-like kinase 4 mediates epithelial-mesenchymal transition in neuroblastoma via PI3K/Akt signaling pathway article. *Cell Death Dis.* **9**, 1–14 (2018).

33. Reymond, N., D'Água, B. B. & Ridley, A. J. Crossing the endothelial barrier during metastasis. *Nat. Rev. Cancer* **13**, 858–870 (2013).

34. Reymond, N. *et al.* Cdc42 promotes transendothelial migration of cancer cells through β1 integrin. *J. Cell Biol.* **199**, 653–668 (2012).

35. Fröhlich, C. *et al.* ADAM12 is expressed in the tumour vasculature and mediates ectodomain shedding of several membrane-anchored endothelial proteins. *Biochem. J.* **452**, 97–109 (2013).

36. Anderberg, C. *et al.* Deficiency for endoglin in tumor vasculature weakens the endothelial barrier to metastatic dissemination. *J. Exp. Med.* **210**, 563–579 (2013).

37. Tremblay, P. L., Huot, J. & Auger, F. A. Mechanisms by which E-Selectin Regulates Diapedesis of Colon Cancer Cells under Flow Conditions. *Cancer Res.* **68**, 5167–5176 (2008).

38. Khuon, S. *et al.* Myosin light chain kinase mediates transcellular intravasation of breast cancer cells through the underlying endothelial cells: a three-dimensional FRET study. *J. Cell Sci.* **123**, 431–440 (2010).

39. Carman, C. V. Mechanisms for transcellular diapedesis: probing and pathfinding by 'invadosome-like protrusions'. *J. Cell Sci.* **122**, 3025–3035 (2009).

40. Azzi, S., Hebda, J. K. & Gavard, J. Vascular permeability and drug delivery in cancers. *Front. Oncol.* **3**, 1–14 (2013).

41. Paoli, P., Giannoni, E. & Chiarugi, P. Anoikis molecular pathways and its role in cancer progression. *Biochim. Biophys. Acta - Mol. Cell Res.* **1833**, 3481–3498 (2013).

42. Hamidi, H. & Ivaska, J. Every step of the way: integrins in cancer progression and metastasis. *Nat. Rev. Cancer* **19**, 533–548 (2018).

43. Alanko, J. *et al.* Integrin endosomal signalling suppresses anoikis. *Nat. Cell Biol.* **17**, 1412–1421 (2015).

44. Guha, D. *et al.* Integrin-EGFR interaction regulates anoikis resistance in colon cancer cells. *Apoptosis* **24**, 958–971 (2019).

45. Dolinschek, R. *et al.* Constitutive activation of integrin αvβ3 contributes to anoikis resistance of ovarian cancer cells. *Mol. Oncol.* **15**, 503–522 (2021).

46. Wang, W. C. *et al.* Survival Mechanisms and Influence Factors of Circulating Tumor Cells. *Biomed Res. Int.* **2018**, 1–9 (2018).

47. Kanwar, N. *et al.* Identification of genomic signatures in circulating tumor cells from breast cancer. *Int. J. Cancer* **137**, 332–344 (2015).

48. Steinert, G. *et al.* Immune Escape and Survival Mechanisms in Circulating Tumor Cells of Colorectal Cancer. *Cancer Res.* **74**, 1694–1704 (2014).

49. Lo, H. C. *et al.* Resistance to natural killer cell immunosurveillance confers a selective advantage to polyclonal metastasis. *Nat. Cancer* **1**, 709–722 (2020).

50. Auguste, P. *et al.* The host inflammatory response promotes liver metastasis by increasing tumor cell arrest and extravasation. *Am. J. Pathol.* **170**, 1781–1792 (2007).

51. Eichbaum, C. *et al.* Breast Cancer Cell-derived Cytokines, Macrophages and Cell Adhesion: Implications for Metastasis. *Anticancer Res.* **31**, 3219–3228 (2011).

52. Hiratsuka, S. *et al.* Endothelial focal adhesion kinase mediates cancer cell homing to discrete regions of the lungs via E-selectin up-regulation. *Proc. Natl. Acad. Sci. U. S. A.* **108**, 3725–3730 (2011).

53. Osmani, N. *et al.* Metastatic Tumor Cells Exploit Their Adhesion Repertoire to Counteract Shear Forces during Intravascular Arrest. *Cell Rep.* **28**, 2491–2500 (2019).

54. Sökeland, G. & Schumacher, U. The functional role of integrins during intra- and extravasation within the metastatic cascade. *Mol. Cancer* **18**, 1–19 (2019).

55. Shibue, T. & Weinberg, R. A. Integrin B1-focal adhesion kinase signaling directs the proliferation of metastatic cancer cells disseminated in the lungs. *Proc. Natl. Acad. Sci. U. S. A.* **23**, 10290–10295 (2009).

56. Ghajar, C. M. *et al.* The perivascular niche regulates breast tumour dormancy. *Nat. Cell Biol.* **15**, 807–817 (2013).

57. Summers, M. A., McDonald, M. M. & Croucher, P. I. Cancer cell dormancy in metastasis. *Cold Spring Harb. Perspect. Med.* **10**, 1–9 (2020).

58. Talukdar, S. *et al. Dormancy and cancer stem cells: An enigma for cancer therapeutic targeting*. *Advances in Cancer Research* vol. 141 (Elsevier Inc., 2019). Available from: http://dx.doi.org/10.1016/bs.acr.2018.12.002

59. Yang, X., Liang, X., Zheng, M. & Tang, Y. Cellular Phenotype Plasticity in Cancer Dormancy and Metastasis. *Front. Oncol.* **8**, 1–12 (2018).

60. Recasens, A. & Munoz, L. Targeting Cancer Cell Dormancy. *Trends Pharmacol. Sci.* **40**, 128–141 (2019).

61. Tamkun, J. W. *et al.* Structure of Integrin, a Glycoprotein Involved in the Transmembrane Linkage between Fibronectin and Actin. *Cell* **46**, 271–282 (1986).

62. Kechagia, J. Z., Ivaska, J. & Roca-Cusachs, P. Integrins as biomechanical sensors of the microenvironment. *Nat. Rev. Mol. Cell Biol.* **20**, 457–473 (2019).

63. Barczyk, M., Carracedo, S. & Gullberg, D. Integrins. *Cell Tissue Res.* **339**, 269–280 (2010).

64. Takada, Y., Ye, X. & Simon, S. The integrins. *Genome Biol.* **8**, 1–9 (2007).

65. Campbell, I. D. & Humphries, M. J. Integrin Structure, Activation, and Interactions. *Cold Spring Harb. Perspetives Biol.* **3**, 1–15 (2011).

66. Bachmann, M., Kukkurainen, S., Hytönen, V. P. & Wehrle-Haller, B. Cell adhesion by integrins. *Physiol. Rev.* **99**, 1655–1699 (2019).

67. Shattil, S. J., Kim, C. & Ginsberg, M. H. The final steps of integrin activation: the end game. *Nat. Rev. Mol. Cell Biol.* **11**, 288–300 (2010).

68. Seguin, L., Desgrosellier, J. S., Weis, S. M. & Cheresh, D. A. Integrins and cancer: regulators of cancer stemness, metastasis, and drug resistance. *Trends Cell Biol.* **1113**, 1–7 (2014).

69. Takagi, J. Structural basis for ligand recognition by integrins. *Curr. Opin. Cell Biol.* **19**, 557–564 (2007).

70. Plow, E. F., Haas, T. A., Zhang, L., Loftus, J. & Smith, J. W. Ligand Binding to Integrins. *J. Biol. Chem.* **275**, 21785–21788 (2000).

71. Legate, K. R. & Fässler, R. Mechanisms that regulate adaptor binding to β-integrin cytoplasmic tails. *J. Cell Sci.* **122**, 187–198 (2009).

72. Liu, S., Slepak, M. & Ginsberg, M. H. Binding of Paxillin to the α9 Integrin Cytoplasmic Domain Inhibits Cell Spreading. *J. Biol. Chem.* **276**, 37086–37092 (2001).

73. Cooper, J. & Giancotti, F. G. Integrin signaling in cancer: mechanotransduction, stemness, epithelial plasticity, and therapeutic resistance. *Cancer Cell* **35**, 347–367 (2019).

74. Liu, W. *et al.* The molecular effect of metastasis suppressors on Src signaling and tumorigenesis: new therapeutic targets. *Oncotarget* **6**, 35522–35541 (2015).

75. Palmer, E., Rüegg, C., Ferrando, R., Pytela, R. & Sheppard, D. Sequence and tissue distribution of the integrin α9 subunit, a novel partner of β1 that is widely distributed in epithelia and muscle. *J. Cell Biol.* **123**, 1289–1297 (1993).

76. Roy, S. *et al.* The role of α9β1 integrin in modulating epithelial cell behaviour. *J. Oral Pathol. Med.* **40**, 755–761 (2011).

77. Rao, H. *et al.* α9β1: A Novel Osteoclast Integrin That Regulates Osteoclast Formation and Function. *J. Bone Miner. Res.* **21**, 1657–1665 (2006).

78. Kon, S., Atakilit, A. & Sheppard, D. Short form of α9 promotes α9β1 integrin-dependent cell adhesion by modulating the function of the full-length α9 subunit. *Exp. Cell Res.* **317**, 1774–1784 (2011).

79. Yang, J. T., Rayburn, H. & Hynes, R. O. Cell adhesion events mediated by α4 integrins are essential in placental and cardiac development. *Development* **121**, 549–560 (1995).

80. Huang, X. Z. *et al.* Fatal bilateral chylothorax in mice lacking the integrin α9β1. *Mol. Cell. Biol.* **20**, 5208–5215 (2000).

81. Høye, A. M., Couchman, J. R., Wewer, U. M., Fukami, K. & Yoneda, A. The newcomer in the integrin family: Integrin α9 in biology and cancer. *Adv. Biol. Regul.* **52**, 326–339 (2012).

82. Xu, S. *et al.* Integrin-α9β1 as a Novel Therapeutic Target for Refractory Diseases: Recent Progress and Insights. *Front. Immunol.* **12**, 1–17 (2021).

83. Hight-Warburton, W. & Parsons, M. Regulation of cell migration by α4 and α9 integrins. *Biochem. J.* **476**, 705–718 (2019).

84. Duval, C., Zaniolo, K., Leclerc, S., Salesse, C. & Guérin, S. L. Characterization of the human α9 integrin subunit gene: Promoter analysis and transcriptional regulation in ocular cells. *Exp. Eye Res.* **135**, 1–8 (2015).

85. Mishima, K. *et al.* Prox1 Induces Lymphatic Endothelial Differenteiation via Integrin a9 and Other Singaling Cascades. *Mol. Biol. Cell* **18**, 1421–1429 (2007).

86. Xu, Y., Zhang, J., Zhang, Q., Xu, H. & Liu, L. Long non-coding RNA hoxa11-as modulates proliferation, apoptosis, metastasis and EMT in cutaneous melanoma cells partly via MIR-152-3p/ ITGA9 Axis. *Cancer Manag. Res.* **13**, 925–939 (2021).

87. Fan, J. *et al.* Long Noncoding RNA CCAT1 Functions as a Competing Endogenous RNA to Upregulate ITGA9 by Sponging MiR-296-3p in Melanoma. *Cancer Manag. Res.* **12**, 4699–4714 (2020).

88. Arribas, J., Bech-Serra, J. J. & Santiago-Josefat, B. ADAMs, cell migration and cancer. *Cancer Metastasis Rev.* **25**, 57–68 (2006).

89. Murphy, G. The ADAMs: signalling scissors in the tumour microenvironment. *Nat. Rev. Cancer* **8**, 929–941 (2008).

90. Nyren-Erickson, E. K., Jones, J. M., Srivastava, D. K. & Mallik, S. A disintegrin and metalloproteinase-12 (ADAM12): Function, roles in disease progression, and clinical implications. *Biochim. Biophys. Acta* **1830**, 4445–4455 (2013).

91. Gilpin, B. J. *et al.* A Novel, Secreted Form of Human ADAM 12 (Meltrin α) Provokes Myogenesis in Vivo. *J. Biol. Chem.* **273**, 157–166 (1998).

92. Powell, R. M., Wicks, J., Holloway, J. W., Holgate, S. T. & Davies, D. E. The Splicing and Fate of ADAM33 Transcripts in Primary Human Airways Fibroblasts. *Am. J. Respir. Cell Mol. Biol.* **31**, 13–21 (2004).

93. Giebeler, N. & Zigrino, P. A Disintegrin and Metalloprotease (ADAM): Historical Overview of Their Functions. *Toxins (Basel).* **8**, 1–14 (2016).

94. Eto, K. *et al.* Functional Classification of ADAMs Based on a Conserved Motif for Binding to Integrin α9β1. Implications for Sperm-egg Binding and Other Cell Interactions. *J. Biol. Chem.* **277**, 17804–17810 (2002).

95. Bridges, L. & Bowditch, R. ADAM-Integrin Interactions: Potential Integrin Regulated Ectodomain Shedding Activity. *Curr. Pharm. Des.* **11**, 837–847 (2005).

96. Eto, K. *et al.* RGD-independent Binding of Integrin α9β1 to the ADAM-12 and -15 Disintegrin Domains Mediates Cell-Cell interaction. *J. Biol. Chem.* **275**, 34922–34930 (2000).

97. Lafuste, P. *et al.* ADAM12 and α9β1 Integrin Are Instrumental in Human Myogenic Cell Differentiation. *Mol. Biol. Cell* **16**, 861–870 (2005).

98. Thodeti, C. K. *et al.* Hierarchy of ADAM12 binding to integrins in tumor cells. *Exp. Cell Res.* **309**, 438–450 (2005).

99. Thodeti, C. K. *et al.* ADAM12-mediated focal adhesion formation is differently regulated by β1 and β3 integrins. *FEBS Lett.* **579**, 5589–5595 (2005).

100. Zhao, Z. *et al.* Interaction of the disintegrin and cysteine-rich domains of ADAM12 with integrin α7β1. *Exp. Cell Res.* **298**, 28–37 (2004).

101. Lydolph, M. C. *et al.* α9β1 Integrin in melanoma cells can signal different adhesion states for migration and anchorage. *Exp. Cell Res.* **315**, 3312–3324 (2009).

102. Thodeti, C. K. *et al.* ADAM12/Syndecan-4 Signaling Promotes β1 Integrin-Dependent Cell Spreading Through Protein Kinase Cα and RhoA. *J. Biol. Chem.* **278**, 9576–9584 (2003).

103. Luo, M. L. *et al.* An ADAM12 and FAK positive feedback loop amplifies the interaction signal of tumor cells with extracellular matrix to promote esophageal cancer metastasis. *Cancer Lett.* **422**, 118–128 (2018).

104. Jacobsen, J. & Wewer, U. Targeting ADAM12 in Human Disease: Head, Body or Tail? *Curr. Pharm. Des.* **15**, 2300–2310 (2009).

105. Shinde, A. V. *et al.* Identification of the Peptide Sequences within the EIIIA (EDA) Segment of Fibronectin That Mediate Integrin α9β1-dependent Cellular Activities. *J. Biol. Chem.* **283**, 2858–2870 (2008).

106. Sun, X. *et al.* The EDA-containing cellular fibronectin induces epithelial-mesenchymal transition in lung cancer cells through integrin α9β1-mediated activation of PI3-K/AKT and Erk1/2. *Carcinogenesis* **35**, 184–191 (2014).

107. Gupta, S. K. & Vlahakis, N. E. Integrin α9β1: Unique signaling pathways reveal diverse biological roles. *Cell Adhes. Migr.* **4**, 194–198 (2010).

108. Maldonado, M. & Dharmawardhane, S. Targeting Rac and Cdc42 GTPases in Cancer. *Cancer Res.* **78**, 3101–3111 (2018).

109. Gupta, S. K. & Vlahakis, N. E. Integrin α9β1 mediates enhanced cell migration through nitric oxide synthase activity regulated by Src tyrosine kinase. *J. Cell Sci.* **122**, 2043–2054 (2009).

110. Chen, C., Young, B. A., Coleman, C. S., Pegg, A. E. & Sheppard, D. Spermidine/spermine N1-acetyltransferase specifically binds to the integrin α9 subunit cytoplasmic domain and enhances cell migration. *J. Cell Biol.* **167**, 161–170 (2004).

111. DeHart, G. W., Jin, T., McCloskey, D. E., Pegg, A. E. & Sheppard, D. The α9β1 integrin enhances cell migration by polyamine-mediated modulation of an inward-rectifier potassium channel. *Proc. Natl. Acad. Sci. U. S. A.* **105**, 7188–7193 (2008).

112. Hibi, K. *et al.* Aberrant upregulation of a novel integrin alpha subunit gene at 3p21.3 in small cell lung cancer. *Oncogene* **9**, 611–619 (1994).

113. Fiorilli, P. *et al.* Integrins mediate adhesion of medulloblastoma cells to tenascin and activate pathways associated with survival and proliferation. *Lab. Investig.* **88**, 1143–1156 (2008).

114. Brown, M. C. *et al.* Regulatory effect of nerve growth factor in α9β1 integrin–dependent progression of glioblastoma. *Neuro. Oncol.* **10**, 968–980 (2008).

115. Basora, N. *et al.* Expression of the α9β1 integrin in human colonic epithelial cells: resurgence of the fetal phenotype in a subset of colon cancers and adenocarcinoma cell lines. *Int. J. Cancer* **75**, 738–743 (1998).

116. Peng, Y. *et al.* Identification of key biomarkers associated with cell adhesion in multiple myeloma by integrated bioinformatics analysis. *Cancer Cell Int.* **20**, 1–16 (2020).

117. Zhang, Y. L. *et al.* Integrin α9 suppresses hepatocellular carcinoma metastasis by Rho GTPase signaling. *J. Immunol. Res.* **2018**, 1–11 (2018).

118. Allen, M. D. *et al.* Clinical and functional significance of α9β1 integrin expression in breast cancer: a novel cell-surface marker of the basal phenotype that promotes tumour cell invasion. *J. Pathol.* **223**, 646–658 (2011).

119. Wang, Z. *et al.* Integrin α9 depletion promotes β-catenin degradation to suppress triple-negative breast cancer tumor growth and metastasis. *Int. J. Cancer* **145**, 2767–2780 (2019).

120. Mostovich, L. A. *et al.* Integrin alpha9 (ITGA9) expression and epigenetic silencing in human breast tumors. *Cell Adhes. Migr.* **5**, 395–401 (2011).

121. Strelnikov, V. V. *et al.* Abnormal promoter DNA hypermethylation of the integrin, nidogen, and dystroglycan genes in breast cancer. *Sci. Rep.* **11**, 2264–2278 (2021).

122. Ghosh, A. *et al.* Frequent alterations of the candidate genes hMLH1, ITGA9 and RBSP3 in early dysplastic lesions of head and neck: Clinical and prognostic significance. *Cancer Sci.* **101**, 1511–1520 (2010).

123. Senchenko, V. N. *et al.* Discovery of frequent homozygous deletions in chromosome 3p21.3 LUCA and AP20 regions in renal, lung and breast carcinomas. *Oncogene* **23**, 5719–5728 (2004).

124. Mitra, S. *et al.* RBSP3 is frequently altered in premalignant cervical lesions: clinical and prognostic significance. *Genes Dev.* **49**, 155–170 (2010).

125. Xu, T. J. *et al.* MiR-148a inhibits the proliferation and migration of glioblastoma by targeting ITGA9. *Hum. Cell* **32**, 548–556 (2019).

126. Gupta, S. K., Oommen, S., Aubry, M. C., Williams, B. P. & Vlahakis, N. E. Integrin α9β1 promotes malignant tumor growth and metastasis by potentiating epithelial-mesenchymal transition. *Oncogene* **32**, 141–150 (2013).

127. Zhang, J. *et al.* MicroRNA-125b suppresses the epithelial–mesenchymal transition and cell invasion by targeting ITGA9 in melanoma. *Tumor Biol.* **37**, 5941–5949 (2016).

128. Ou, J. *et al.* Endothelial cell-derived-fibronectin extra domain A promotes colorectal cancer metastasis via inducing epithelial-mesenchymal transition. *Carcinogenesis* **35**, 1661–1670 (2014).

129. Vlahakis, N. E. *et al.* Integrin α9β1 directly binds to vascular endothelial growth factor (VEGF)-A and contributes to VEGF-A-induced angiogenesis. *J. Biol. Chem.* **282**, 15187–15196 (2007).

130. Ou, J. *et al.* Endostatin suppresses colorectal tumor-induced lymphangiogenesis by inhibiting expression of fibronectin extra domain A and integrin α9. *J. Cell. Biochem.* **112**, 2106–2114 (2011).

131. Oommen, S., Gupta, S. K. & Vlahakis, N. E. Vascular endothelial growth gactor A (VEGF-A) induces endothelial and cancer cell migration through direct binding to integrin α9β1: Identification of a specific α9β1 binding site. *J. Biol. Chem.* **286**, 1083–1092 (2011).

132. Ou, J. J., Wu, F. & Liang, H. J. Colorectal tumor derived fibronectin alternatively spliced EDA domain exserts lymphangiogenic effect on human lymphatic endothelial cells. *Cancer Biol. Ther.* **9**, 186–191 (2010).

133. Ward, E., DeSantis, C., Robbins, A., Kohler, B. & Jemal, A. Childhood and adolescent cancer statistics, 2014. *CA. Cancer J. Clin.* **64**, 83–103 (2014).

134. Skapek, S. X. *et al.* Rhabdomyosarcoma. *Nat. Rev. Dis. Prim.* **5**, 1–19 (2019).

135. Perkins, S. M., Shinohara, E. T., DeWees, T. & Frangoul, H. Outcome for children with metastatic solid tumors over the last four decades. *PLoS One* **9**, 8–13 (2014).

136. Wasti, A. T., Mandeville, H., Gatz, S. & Chisholm, J. C. Rhabdomyosarcoma. *Paediatr. Child Health (Oxford).* **28**, 157–163 (2018).

137. Institute, B. (MD): N. C. (US). Childhood Rhabdomyosarcoma Treadment (PDQ): Health Professional Version. PDQ Pediatric Treatment Editorial Board. *PDQ Cancer Information Summaries*. Available from: https://www.ncbi.nlm.nih.gov/books/NBK65802/ (2020).

138. Rudzinski, E. *et al.* The World Health Organization Classification of Skeletal Muscle Tumors in Pediatric Rhabdomyosarcoma: A Report From the Children's Oncology Group. *Arch. Pathol. Lab. Med.* **139**, 1281–1287 (2015).

139. Fletcher, C. D. ., Bridje, J. ., Hogendoorn, P. & Mertens, F. WHO Classification of Tumours of Soft Tissue and Bone. in *World Health Organization Classification of Tumours* Vol. 5 (International Agency for Research on Cancer, 2013).

140. Kashi, V. P., Hatley, M. E. & Galindo, R. L. Probing for a deeper understanding of rhabdomyosarcoma: Insights from complementary model systems. *Nat. Rev. Cancer* **15**, 426–439 (2015).

141. Loh, W. E. *et al.* Human chromosome 11 contains two different growth suppressor genes for embryonal rhabdomyosarcoma. *Proc. Natl. Acad. Sci. U. S. A.* **89**, 1755–1759 (1992).

142. Bridge, J. A. *et al.* Novel Genomic Imbalances in Embryonal Rhabdomyosarcoma Revealed by Comparative Genomic Hybridization and Fluorescence In Situ Hybridization: An Intergroup Rhabdomyosarcoma Study. *Genes Chromosom. Cancer* **27**, 337–344 (2000).

143. Shern, J. F. *et al.* Comprehensive Genomic Analysis of Rhabdomyosarcoma Reveals a Landscape of Alterations Affecting a Common Genetic Axis in Fusion-Positive and Fusion-Negative Tumors. *Cancer Discov.* **4**, 216–231 (2014).

144. Seki, M. *et al.* Integrated genetic and epigenetic analysis defines novel molecular subgroups in rhabdomyosarcoma. *Nat. Commun.* **6**, 1–8 (2015).

145. Barr, F. *et al.* Rearrangement of the PAX3 paired box gene in the paediatric solid tumour alveolar rhabdomyosarcoma. *Nat. Genet.* **3**, 113–117 (1993).

146. Davis, R., D'Cruz, C., Lovell, M., Biegel, J. & Barr, F. Fusion of PAX7 to FKHR by the Variant t(1;13)(p36;q14) Translocation in Alveolar Rhabdomyosarcoma. *Adv. Br.* **54**, 2869–2872 (1994).

147. Wachtel, M. & Schäfer, B. W. PAX3-FOXO1: Zooming in on an "undruggable" target. *Semin. Cancer Biol.* **50**, 115–123 (2018).

148. Lisboa, S. *et al.* Genetic diagnosis of alveolar rhabdomyosarcoma in the bone marrow of a patient without evidence of primary tumor. *Pediatr. Blood Cancer* **51**, 554–557 (2008).

149. Shinkoda, Y., Nagatoshi, Y., Fukano, R., Nishiyama, K. & Okamura, J. Rhabdomyosarcoma Masquerading as Acute Leukemia. *Pediatr. Blood Cancer* **52**, 286–287 (2009).

150. López-Andrade, B. *et al.* Rhabdomyosarcoma debut masquerading as acute lymphoblastic leukemia: A case report and review of the literature. *Clin. Case Reports* **7**, 1545–1548 (2019).

151. Hettmer, S. & Wagers, A. J. Uncovering the origins of rhabdomyosarcoma. *Nat. Med.* **16**, 171–173 (2010).

152. Charytonowicz, E., Cordon-Cardo, C., Matushansky, I. & Ziman, M. Alveolar rhabdomyosarcoma: Is the cell of origin a mesenchymal stem cell? *Cancer Lett.* **279**, 126–136 (2009).

153. Wagers, A. J. & Conboy, I. M. Cellular and oMlecular Signatures of Muscle Regeneration: Current Concepts and Controversies in Adult Myogenesis. *Cell* **122**, 659–667 (2005).

154. Langenau, D. M. *et al.* Effects of RAS on the genesis of embryonal rhabdomyosarcoma. *Genes Dev.* **21**, 1382–1395 (2007).

155. Tiffin, N., Williams, R. D., Shipley, J. & Pritchard-Jones, K. PAX7 expression in embryonal rhabdomyosarcoma suggests an origin in muscle satellite cells. *Br. J. Cancer* **89**, 327–332 (2003).

156. Ren, Y. X. *et al.* Mouse Mesenchymal Stem Cells Expressing PAX-FKHR Form Alveolar Rhabdomyosarcomas by Cooperating with Secondary Mutations. *Cancer Res.* **68**, 6587–6597 (2008).

157. Keller, C. *et al.* Alveolar rhabdomyosarcomas in conditional Pax3:Fkhr mice: cooperativity of Ink4a/ARF and Trp53 loss of function. *Genes Dev.* **18**, 2614–2626 (2004).

158. Drummond, C. J. *et al.* Hedgehog Pathway Drives Fusion-Negative Rhabdomyosarcoma Initiated From Non-myogenic Endothelial Progenitors. *Cancer Cell* **33**, 108–124 (2018).

159. Mauer, H. *et al.* The Intergroup Rhabdomyosarcoma Study-I. A final report. *Cancer* **61**, 209–220 (1988).

160. Crist, W. M. *et al.* Intergroup Rhabdomyosarcoma Study-IV: Results for Patients With Nonmetastatic Disease. *J. Clin. Oncol.* **19**, 3091–3102 (2001).

161. EpSSG RMS 2005. A protocol for non-metasttic rhabdomyosarcoma (2008). Available from: https://www.skion.nl/workspace/uploads/Protocol-EpSSG-RMS-2005-1-3-May-2012_1.pdf

162. Gallego, S. *et al.* Detection of bone marrow micrometastasis and microcirculating disease in rhabdomyosarcoma by a real-time RT-PCR assay. *J. Cancer Res. Clin. Oncol.* **132**, 356–362 (2006).

163. Wishart, D. S. *et al.* DrugBank 5.0: A major update to the DrugBank database for 2018. *Nucleic Acids Res.* **46**, D1074–D1082 (2018).

164. Matthay, K. K. *et al.* Neuroblastoma. *Nat. Rev. Dis. Prim.* **2**, 1–21 (2016).

165. Swift, C. C., Eklund, M. J., Kraveka, J. M. & Alazraki, A. L. Updates in Diagnosis, Management, and Treatment of Neuroblastoma. *Radiogr. Pediatr. imaging* **38**, 566–580 (2018).

166. Heck, J. E., Ritz, B., Hung, R. J., Hashibe, M. & Boffetta, P. The epidemiology of neuroblastoma: a review. *Paediatr. Perinat. Epidemiol.* **23**, 125–143 (2009).

167. Bethesda, N. C. I. Neuroblastoma Treatment (PDQ): Health Professional Version. PDQ Pediatric Treatment Editorial Board. *PDQ Cancer Information Summaries.* Available from: https://www.ncbi.nlm.nih.gov/books/NBK65747/ (2021).

168. Maris, J. M., Hogarty, M. D., Bagatell, R. & Cohn, S. L. Neuroblastoma. *Lancet* **369**, 2106–2120 (2007).

169. Blaes, F. & Dharmalingam, B. Childhood opsoclonus-myoclonus syndrome: diagnosis and treatment. *Expert Rev. Neurother.* **16**, 641–648 (2016).

170. Taggart, D., Dubois, S. & Matthay, K. Radiolabeled metaiodobenzylguanidine for imaging and therapy of neuroblastoma. *Q. J. Nucl. Med. Mol. IMAGING* **52**, 403–418 (2008).

171. Thorner, P. S. The molecular genetic profile of neuroblastoma. *Diagnostic Histopathol.* **20**, 76–83 (2014).

172. Ahmed, A. A., Zhang, L., Reddivalla, N. & Hetherington, M. Neuroblastoma in children: Update on clinicopathologic and genetic prognostic factors. *Pediatr. Hematol. Oncol.* **34**, 165–185 (2017).

173. Campbell, K. *et al.* Association of heterogeneous MYCN amplification with clinical features, biological characteristics and outcomes in neuroblastoma: A report from the Children's Oncology Group. *Eur. J. Cancer* **133**, 112–119 (2020).

174. Huang, M. & Weiss, W. A. Neuroblastoma and MYCN. *Cold Spring Harb. Perspect. Med.* **3**, 1–22 (2013).

175. Okawa, E. R. *et al.* Expression and sequence analysis of candidates for the 1p36.31 tumor suppressor gene deleted in neuroblastomas. *Oncogene* **27**, 803–810 (2008).

176. Fujita, T. *et al.* CHD5, a Tumor Suppressor Gene Deleted From 1p36.31 in Neuroblastomas. *J. Natl. Cancer Inst.* **100**, 940–949 (2008).

177. Henrich, K. O., Schwab, M. & Westermann, F. 1p36 Tumor Suppression - A Matter of Dosage? *Cancer Res.* **72**, 6079–6088 (2012).

178. Mlakar, V. *et al.* 11q deletion in neuroblastoma: A review of biological and clinical implications. *Mol. Cancer* **16**, 1–12 (2017).

179. Mossé, Y. P. *et al.* Identification of ALK as a major familial neuroblastoma predisposition gene. *Nature* **455**, 930–935 (2008).

180. Janoueix-Lerosey, I. *et al.* Somatic and germline activating mutations of the ALK kinase receptor in neuroblastoma. *Nature* **455**, 967–970 (2008).

181. Zeineldin, M. *et al.* MYCN amplification and ATRX mutations are incompatible in neuroblastoma. *Nat. Commun.* **11**, 1–20 (2020).

182. Cheung, N. K. V. *et al.* Association of Age at Diagnosis and Genetic Mutations in Patients With Neuroblastoma. *JAMA - J. Am. Med. Assoc.* **307**, 1062–1071 (2012).

183. Sausen, M. *et al.* Integrated genomic analyses identify ARID1A and ARID1B alterations in the childhood cancer neuroblastoma. *Nat. Genet.* **45**, 12–17 (2013).

184. Slack, A. *et al.* p53 is a direct transcriptional target of MYCN in neuroblastoma. *Cancer Res.* **70**, 1377–1388 (2010).

185. Tsubota, S. & Kadomatsu, K. Origin and initiation mechanisms of neuroblastoma. *Cell Tissue Res.* **372**, 211–221 (2018).

186. Kholodenko, I. V., Kalinovsky, D. V., Doronin, I. I., Deyev, S. M. & Kholodenko, R. V. Neuroblastoma Origin and Therapeutic Targets for Immunotherapy. *J. Immunol. Res.* **2018**, 1–25 (2018).

187. Simões-Costa, M. & Bronner, M. E. Insights into neural crest development and evolution from genomic analysis. *Genome Res.* **23**, 1069–1080 (2013).

188. Bronner, M. E. & Simões-costa, M. The neural crest migrating into the 21st century. *Curr Top Dev Biol* **116**, 115–134 (2016).

189. Zage, P. E., Whittle, S. B. & Shohet, J. M. CD114: A New Member of the Neural Crest-Derived Cancer Stem Cell Marker Family. *J. Cell. Biochem.* **118**, 221–231 (2017).

190. Weiss, W. A., Aldape, K., Mohapatra, G., Feuerstein, B. G. & Bishop, J. M. Targeted expression of MYCN causes neuroblastoma in transgenic mice. *EMBO J.* **16**, 2985–2995 (1997).

191. Zhu, S. *et al.* Activated ALK Collaborates with MYCN in Neuroblastoma Pathogenesis. *Cancer Cell* **21**, 362–373 (2012).

192. Marshall, G. M. *et al.* The prenatal origins of cancer. *Nat. Rev. Cancer* **14**, 277–289 (2014).

193. Alam, G. *et al.* MYCN Promotes the Expansion of Phox2B-Positive Neuronal Progenitors to Drive Neuroblastoma Development. *Am. J. Pathol.* **175**, 856–866 (2009).

194. Heukamp, L. C. *et al.* Targeted Expression of Mutated ALK Induces Neuroblastoma in Transgenic Mice. *Sci. Transl. Med.* **4**, 1–9 (2012).

195. Cohn, S. L. *et al.* The International Neuroblastoma Risk Group (INRG) Classification System: An INRG Task Force Report. *J. Clin. Oncol.* **27**, 289–297 (2009).

196. Monclair, T. *et al.* The International Neuroblastoma Risk Group (INRG) Staging System: An INRG Task Force Report. *J. Clin. Oncol.* **27**, 298–303 (2009).

197. Tolbert, V. P. & Matthay, K. K. Neuroblastoma: clinical and biological approach to risk stratification and treatment. *Cell Tissue Res.* **372**, 195–209 (2018).

198. Park, J. R., Bagatell, R. & Hogarty, M. Children's Oncology Group's 2013 Blueprint for Research: Neuroblastoma. *Pediatr. Blood Cancer* **60**, 985–993 (2013).

199. Pearson, A. D. *et al.* High-dose rapid and standard induction chemotherapy for patients aged over 1 year with stage 4 neuroblastoma: a randomised trial. *Lancet Oncol.* **9**, 247–256 (2008).

200. Whittle, S. B. *et al.* Overview and recent advances in the treatment of neuroblastoma. *Expert Rev. Anticancer Ther.* **17**, 369–386 (2017).

201. Amoroso, L. *et al.* Topotecan-Vincristine-Doxorubicin in Stage 4 High-Risk Neuroblastoma Patients Failing to Achieve a Complete Metastatic Response to Rapid COJEC: A SIOPEN Study. *Cancer Res. Treat.* **50**, 148–155 (2018).

202. Ladenstein, R. *et al.* Busulfan and melphalan versus carboplatin, etoposide, and melphalan as high-dose chemotherapy for high-risk neuroblastoma (HR-NBL1/SIOPEN): an international, randomised, multi-arm, open-label, phase 3 trial. *Lancet Oncol.* **18**, 500–514 (2017).

203. Sait, S. & Modak, S. I. Anti-GD2 immunotherapy for neuroblastomas. *Expert Rev. Anticancer Ther.* **17**, 889–904 (2017).

204. Harbeck, N. *et al.* Breast cancer. *Nat. Rev. Dis. Prim.* **5**, 1–31 (2019).

205. Paul, A. & Paul, S. The breast cancer susceptibility genes (BRCA) in breast and ovarian cancers. *Front. Biosci. - Landmark* **19**, 605–618 (2014).

206. DeSantis, C., Siegel, R. L., Bandi, P. & Jemal, A. Breast cancer statistics, 2011. *CA. Cancer J. Clin.* **61**, 409–418 (2011).

207. DeSantis, C. E. *et al.* Breast cancer statistics, 2015: convergence of incidence rates between black and white women. *CA. Cancer J. Clin.* **66**, 31–42 (2016).

208. Skibinski, A. & Kuperwasser, C. The origin of breast tumor heterogeneity. *Oncogene* **34**, 5309–5316 (2015).

209. Koo, M. M. *et al.* Typical and atypical presenting symptoms of breast cancer and their associations with diagnostic intervals: Evidence from a national audit of cancer diagnosis. *Cancer Epidemiol.* **48**, 140–146 (2017).

210. McDonald, E. S., Clark, A. S., Tchou, J., Zhang, P. & Freedman, G. M. Clinical diagnosis and management of breast cancer. *J. Nucl. Med.* **57**, 9S-16S (2016).

211. Jafari, S. H. *et al.* Breast cancer diagnosis: Imaging techniques and biochemical markers. *J. Cell. Physiol.* **233**, 5200–5213 (2018).

212. Tsang, J. Y. S. & Tse, G. M. Molecular Classification of Breast Cancer. *Adv. Anat. Pathol.* **27**, 27–35 (2020).

213. Li, J., Chen, Z., Su, K. & Zeng, J. Clinicopathological classification and traditional prognostic indicators of breast cancer. *Int. J. Clin. Exp. Pathol.* **8**, 8500–8505 (2015).

214. Perou, C. M. *et al.* Molecular portraits of human breast tumours. *Nature* **406**, 747–752 (2000).

215. Parker, J. S. *et al.* Supervised risk predictor of breast cancer based on intrinsic subtypes. *J. Clin. Oncol.* **27**, 1160–1167 (2009).

216. Nik-Zainal, S. *et al.* Landscape of somatic mutations in 560 breast cancer whole-genome sequences. *Nature* **534**, 47–54 (2016).

217. Gröbner, S. N. *et al.* The landscape of genomic alterations across childhood cancers. *Nature* **555**, 321–327 (2018).

218. O'Meara, T. A. & Tolaney, S. M. Tumor mutational burden as a predictor of immunotherapy response in breast cancer. *Oncotarget* **12**, 394–400 (2021).

219. Feng, Y. *et al.* Breast cancer development and progression: Risk factors, cancer stem cells, signaling pathways, genomics, and molecular pathogenesis. *Genes Dis.* **5**, 77–106 (2018).

220. Zhang, M., Lee, A. V. & Rosen, J. M. The cellular origin and evolution of breast cancer. *Cold Spring Harb. Perspect. Med.* **7**, 1–14 (2017).

221. Zhou, J. *et al.* Stem cells and cellular origins of breast cancer: Updates in the rationale, controversies, and therapeutic implications. *Front. Oncol.* **9**, 1–12 (2019).

222. Sims, A. H., Howell, A., Howell, S. J. & Clarke, R. B. Origins of breast cancer subtypes and therapeutic implications. *Nat. Clin. Pract. Oncol.* **4**, 516–525 (2007).

223. Meyer, D. S. *et al.* Luminal expression of PIK3CA mutant H1047R in the mammary gland induces heterogeneous tumors. *Cancer Res.* **71**, 4344–4351 (2011).

224. Van Keymeulen, A. *et al.* Reactivation of multipotency by oncogenic PIK3CA induces breast tumour heterogeneity. *Nature* **525**, 119–123 (2015).

225. Liu, X. *et al.* Somatic loss of BRCA1 and p53 in mice induces mammary tumors with features of human BRCA1-mutated basal-like breast cancer. *Proc. Natl. Acad. Sci. U. S. A.* **104**, 12111–12116 (2007).

226. Giuliano, A. E. *et al.* Breast Cancer-Major changes in the American Joint Committee on Cancer eighth edition cancer staging manual. *CA. Cancer J. Clin.* **67**, 290–303 (2017).

227. Koh, J. & Kim, M. J. Introduction of a new staging system of breast cancer for radiologists: An emphasis on the prognostic stage. *Korean J. Radiol.* **20**, 69–82 (2019).

228. Hortobagyi, G. N. *et al.* American Joint Committee on Cancer - Breast chapter 8th edition. in *American Joint Committee on Cancer* 589–636 (2017).

229. Matsumoto, N. *et al.* A Novel α9 Integrin Ligand, XCL1/Lymphotactin, Is Involved in the Development of Murine Models of Autoimmune Diseases. *J. Immunol.* **199**, 82–90 (2017).

230. Sato-Nishiuchi, R. *et al.* Polydom/SVEP1 is a ligand for integrin α9β1. *J. Biol. Chem.* **287**, 25615–25630 (2012).

231. Fernández-Carneado, J. *et al.* Peptides for the treatment of cancer and/or metastasis. EP19383084.1 (2019).

232. Molist, C. La integrina α9β1 com a diana terapèutica en el càncer pediàtric. (2019).

233. Young, S. A. *et al.* Integrin α4 enhances metastasis and may be associated with poor prognosis in MYCN-low neuroblastoma. *PLoS One* **10**, 1–17 (2015).

234. Meyer, A., Van Golen, C. M., Kim, B., Van Golent, K. L. & Feldman, E. L. Integrin expression regulates neuroblastoma attachment and migration. *Neoplasia* **6**, 332–342 (2004).

235. Li, M., Wang, Y., Li, M. & Wu, X. Integrins as attractive targets for cancer therapeutics. *Acta Pharm. Sin. B* **In press**, (2021).

236. Horizon Discovery, L. GIPZ lentiviral shRNA. https://horizondiscovery.com (2021).

237. Horizon Discovery, L. TRIPZ inducible lentiviral shRNA. https://horizondiscovery.com (2021).

238. Korać, P., Antica, M. & Matulić, M. Mir-7 in cancer development. *Biomedicines* **9**, 1–20 (2021).

239. Livak, K. J. & Schmittgen, T. D. Analysis of Relative Gene Expression Data Using Real-Time Quantitative PCR and the 2−ΔΔCT Method. *Methods* **25**, 402–408 (2001).

240. Chen, H.-C. Boyden Chamber Assay. in *Cell Migration. Developmental Methods and Protocols* 15–22 (2005).

241. Van Engeland, M., Nieland, L. J. W., Ramaekers, F. C. S., Schutte, B. & Reutelingsperger, C. P. M. Annexin V-Affinity Assay: A Review on an Apoptosis Detection System Based on Phosphatidylserine Exposure. *Cytometry* **31**, 1–9 (1998).

242. Demchenko, A. P. Beyond annexin V: fluorescence response of cellular membranes to apoptosis. *Cytotechnology* **65**, 157–172 (2013).

243. Darzynkiewicz, Z., Bedner, E. & Smolewski, P. Flow cytometry in analysis of cell cycle and apoptosis. *Semin. Hematol.* **38**, 179–193 (2001).

244. Koster, J. R2: Genomics Analysis and Visualization Platform. *http://r2.amc.nl* (2021).

245. Davicioni, E. *et al.* Identification of a PAX-FKHR gene expression signature that defines molecular classes and determines the prognosis of alveolar rhabdomyosarcomas. *Cancer Res.* **66**, 6936–6946 (2006).

246. Su, Z. *et al.* An investigation of biomarkers derived from legacy microarray data for their utility in the RNA-seq era. *Genome Biol.* **15**, 523–548 (2014).

247. Asgharzadeh, S. *et al.* Prognostic significance of gene expression profiles of metastatic neuroblastomas lacking MYCN gene amplification. *J. Natl. Cancer Inst.* **98**, 1193–1203 (2006).

248. Kensler, K. H. *et al.* PAM50 Molecular Intrinsic Subtypes in the Nurses' Health Study Cohorts. *Cancer, Epidemiol. Biomarkers Prev.* **6**, 798–807 (2019).

249. Győrffy, B. Survival analysis across the entire transcriptome identifies biomarkers with the highest prognostic power in breast cancer. *Comput. Struct. Biotechnol. J.* **19**, 4101–4109 (2021).

250. Molist, C. *et al.* miRNA-7 and miRNA-324-5p regulate alpha9-integrin expression and exert anti-oncogenic effects in rhabdomyosarcoma. *Cancer Lett.* **477**, 49–59 (2020).

251. Hinson, A. *et al.* Human rhabdomyosarcoma cell lines for rhabdomyosarcoma research: utility and pitfalls. *Front. Oncol.* **3**, 1–12 (2013).

252. Jackson, D. Production of a mouse monoclonal. *World Pumps* **20**, 22–24 (2002).

253. Sun, X. & Kaufman, P. D. Ki-67: more than a proliferation marker. *Chromosoma* **127**, 175–186 (2018).

254. Wang, D. *et al.* Immunohistochemistry in the evaluation of neovascularization in tumor xenografts. *Biotech. Histochem.* **83**, 179–189 (2008).

255. Lertkiatmongkol, P., Liao, D., Mei, H., Hu, Y. & Newman, P. Endothelial functions of PECAM-1 (CD31). *Curr. Opin. Hematol.* **23**, 253–259 (2016).

256. Mota, A. D. E. L. *et al.* Molecular characterization of breast cancer cell lines by clinical immunohistochemical markers. *Oncol. Lett.* **13**, 4708–4712 (2017).

257. Asselin-Labat, M. L. *et al.* Gata-3 is an essential regulator of mammary-gland morphogenesis and luminal-cell differentiation. *Nat. Cell Biol.* **9**, 201–209 (2007).

258. Kouros-Mehr, H., Slorach, E. M., Sternlicht, M. D. & Werb, Z. GATA-3 Maintains the Differentiation of the Luminal Cell Fate in the Mammary Gland. *Cell* **127**, 1041–1055 (2006).

259. Krings, G., Nystrom, M., Mehdi, I., Vohra, P. & Chen, Y. Y. Diagnostic utility and sensitivities of GATA3 antibodies in triple-negative breast cancer. *Hum. Pathol.* **45**, 2225–2232 (2014).

260. Tozbikian, G. H. & Zynger, D. L. A combination of GATA3 and SOX10 is useful for the diagnosis of metastatic triple-negative breast cancer. *Hum. Pathol.* **85**, 221–227 (2019).

261. Vidarsdottir, H. *et al.* Immunohistochemical profiles in primary lung cancers and epithelial pulmonary metastases. *Hum. Pathol.* **84**, 221–230 (2019).

262. Li, X., Cassidy, J. J., Reinke, C. A., Fischboeck, S. & Carthew, R. W. A MicroRNA Imparts Robustness against Environmental Fluctuation during Development. *Cell* **137**, 273–282 (2009).

263. Oliveira, A. C. *et al.* Understanding the Modus Operandi of MicroRNA Regulatory Clusters. *Cells* **8**, 1–18 (2019).

264. Tian, S. *et al.* miR-7-5p Promotes Hepatic Stellate Cell Activation by Targeting Fibroblast Growth Factor Receptor 4. *Gastroenterol. Res. Pract.* **2020**, 1–9 (2020).

265. Zhou, N. *et al.* MiR-7 inhibited peripheral nerve injury repair by affecting neural stem cells migration and proliferation through cdc42. *Mol. Pain* **14**, 1–11 (2018).

266. Xiong, S. *et al.* MicroRNA-7 Inhibits the Growth of Human Non-Small Cell Lung Cancer A549 Cells through Targeting BCL-2. *Int. J. Biol. Sci.* **7**, 805–814 (2011).

267. Cao, Q. *et al.* MicroRNA-7 inhibits cell proliferation , migration and invasion in human non-small cell lung cancer cells by targeting FAK through ERK / MAPK signaling pathway. *Oncotarget* **7**, 77468–77481 (2016).

268. Zeng, C. Y. A. N., Zhan, Y. I. S., Huang, J. U. N. & Chen, Y. O. U. X. MicroRNA-7 suppresses human colon cancer invasion and proliferation by targeting the expression of focal adhesion kinase. *Mol. Med. Rep.* **13**, 1297–1303 (2016).

269. Kong, X. *et al.* MicroRNA-7 Inhibits Epithelial-to-Mesenchymal Transition and Metastasis of Breast Cancer Cells via Targeting FAK Expression. *PLoS One* **7**, 1–12 (2012).

270. Liu, S. *et al.* MicroRNA-7 downregulates XIAP expression to suppress cell growth and promote apoptosis in cervical cancer cells. *FEBS Lett.* **587**, 2247–2253 (2013).

271. Fang, Y., Xue, J., Shen, Q., Chen, J. & Tian, L. MicroRNA-7 Inhibits Tumor Growth and Metastasis by Targeting the Phosphoinositide 3-Kinase/Akt Pathway in Hepatocellular Carcinoma. *Hepatology.* **2010,** 1852–1862 (2011).

272. Sun, X. *et al.* miR-7 reverses the resistance to BRAFi in melanoma by targeting EGFR/IGF-1R/CRAF and inhibiting the MAPK and PI3K/AKT signaling pathways. *Oncol. Rep.* **7**, 53558–53570 (2016).

273. Webster, R. J. *et al.* Regulation of Epidermal Growth Factor Receptor Signaling in Human Cancer Cells by MicroRNA-7. *J. Biol. Chem.* **284**, 5731–5741 (2009).

274. Saydam, O. *et al.* miRNA-7 attenuation in schwannoma tumors stimulates growth by upregulating three oncogenic signaling pathways. *Cancer Res.* **71**, 852–861 (2011).

275. Kefas, B. *et al.* microRNA-7 inhibits the Epidermal Growth Factor Receptor and the Akt pathway and is down-regulated in glioblastoma. *Cancer Res.* **68**, 3566–3572 (2008).

276. ZHAO, J. *et al.* Promoter mutation of tumor suppressor microRNA-7 is associated with poor prognosis of lung cancer. *Mol. Clin. Oncol.* **3**, 1329–1336 (2015).

277. Zhang, N. *et al.* MicroRNA-7 is a novel inhibitor of YY1 contributing to colorectal tumorigenesis. *Oncogene* **32**, 5078–5088 (2013).

278. Li, M. *et al.* MiR-7 reduces the BCSC subset by inhibiting XIST to modulate the miR-92b/Slug/ESA axis and inhibit tumor growth. *Breast Cancer Res.* **22**, 1–14 (2020).

279. Yu, S. *et al.* SP1-induced lncRNA TINCR overexpression contributes to colorectal cancer progression by sponging miR-7-5p. *Aging (Albany. NY).* **11**, 1389–1403 (2019).

280. Gajda, E., Grzanka, M., Godlewska, M. & Gawel, D. The role of miRNA-7 in the biology of cancer and modulation of drug resistance. *Pharmaceuticals* **14**, 1–23 (2021).

281. Ferretti, E. *et al.* Concerted microRNA control of Hedgehog signalling in cerebellar neuronal progenitor and tumour cells. *EMBO J.* **27**, 2616–2627 (2008).

282. Tang, B. *et al.* MicroRNA-324-5p regulates stemness, pathogenesis and sensitivity to bortezomib in multiple myeloma cells by targeting hedgehog signaling. *Int. J. Cancer* **142**, 109–120 (2018).

283. Cao, L. *et al.* MIR-324-5p suppresses hepatocellular carcinoma cell invasion by counteracting ECM degradation through post-transcriptionally downregulating ETS1 and SP1. *PLoS One* **10**, 1–16 (2015).

284. Gu, C., Zhang, M., Sun, W. & Dong, C. Upregulation of miR-324-5p inhibits proliferation and invasion of colorectal cancer cells by targeting ELAVL1. *Oncol. Res.* **27**, 515–524 (2019).

285. Lin, H., Zhou, A. J., Zhang, J. Y., Liu, S. F. & Gu, J. X. MiR-324-5p reduces viability and induces apoptosis in gastric cancer cells through modulating TSPAN8. *J. Pharm. Pharmacol.* **70**, 1513–1520 (2018).

286. Zheng, Z., Li, J., An, J., Feng, Y. & Wang, L. High miR-324-5p expression predicts unfavorable prognosis of gastric cancer and facilitates tumor progression in tumor cells. *Diagn. Pathol.* **16**, 1–9 (2021).

287. Song, L. *et al.* Sinomenine inhibits breast cancer cell invasion and migration by suppressing NF-κB activation mediated by IL-4/miR-324-5p/CUEDC2 axis. *Biochem. Biophys. Res. Commun.* **464**, 705–710 (2015).

288. Wan, Y. *et al.* miR-324-5p Contributes to Cell Proliferation and Apoptosis in Pancreatic Cancer by Targeting KLF3. *Mol. Ther. - Oncolytics* **18**, 432–442 (2020).

289. Ba, Z., Zhou, Y., Yang, Z., Xu, J. & Zhang, X. miR-324-5p upregulation potentiates resistance to cisplatin by targeting FBXO11 signalling in non-small cell lung cancer cells. *J. Biochem.* **166**, 517–527 (2019).

290. Zhang, X., Zhang, L., Chen, M. & Liu, D. miR-324-5p inhibits gallbladder carcinoma cell metastatic behaviours by downregulation of transforming growth factor beta 2 expression. *Artif. Cells, Nanomedicine Biotechnol.* **48**, 315–324 (2020).

291. Tomar, S. *et al.* ETS1 induction by the microenvironment promotes ovarian cancer metastasis through focal adhesion kinase. *Cancer Lett.* **414**, 190–204 (2018).

292. Vlahakis, N. E., Young, B. A., Atakilit, A. & Sheppard, D. The lymphangiogenic vascular endothelial growth factors VEGF-C and -D are ligands for the integrin α9β1. *J. Biol. Chem.* **280**, 4544–4552 (2005).

293. Babae, N. *et al.* Systemic miRNA-7 delivery inhibits tumor angiogenesis and growth in murine xenograft glioblastoma. *Oncotarget* **5**, 6687–6700 (2014).

294. Yang, L. *et al.* MiR-7 mediates mitochondrial impairment to trigger apoptosis and necroptosis in Rhabdomyosarcoma. *Biochim. Biophys. Acta - Mol. Cell Res.* **1867**, 118826–118838 (2020).

295. Wang, W. *et al.* Regulation of epidermal growth factor receptor signaling by plasmid-based MicroRNA-7 inhibits human malignant gliomas growth and metastasi in vivo. *Neoplasma* **60**, 274–283 (2013).

296. Glover, A. R. *et al.* microRNA-7 as a tumor suppressor and novel therapeutic for adrenocortical carcinoma. *Oncotarget* **6**, 36675–36688 (2015).

297. Brown, R. A. M. *et al.* Evaluation of microRNA delivery in vivo. *Methods Mol. Biol.* **1699**, 155–178 (2018).

298. Ma, J. *et al.* Curcumin inhibits cell growth and invasion through up-regulation of miR-7 in pancreatic cancer cells. *Toxicol. Lett.* **231**, 82–91 (2014).

299. Melo, S. *et al.* Small molecule enoxacin is a cancer-specific growth inhibitor that acts by enhancing TAR RNA-binding protein 2-mediated microRNA processing. *Proc. Natl. Acad. Sci. U. S. A.* **108**, 4394–4399 (2011).

300. Tu, C. Y. *et al.* Trichostatin A suppresses EGFR expression through induction of microRNA-7 in an HDAC-independent manner in lapatinib-treated cells. *Biomed Res. Int.* **2014**, 1–11 (2014).

301. Horsham, J. L. *et al.* Clinical potential of microRNA-7 in cancer. *J. Clin. Med.* **4**, 1668–1687 (2015).

302. Wu, L. *et al.* Distinct FAK-Src activation events promote α5β1 and α4β1 integrin-stimulated neuroblastoma cell motility. *Oncogene* **27**, 1439–1448 (2008).

303. Fu, X. D. *et al.* Progesterone receptor enhances breast cancer cell motility and invasion via extranuclear activation of focal adhesion kinase. *Endocr. Relat. Cancer* **17**, 431–443 (2010).

304. Kurio, N. *et al.* Anti-tumor effect in human breast cancer by TAE226, a dual inhibitor for FAK and IGF-IR in vitro and in vivo. *Exp. Cell Res.* **317**, 1134–1146 (2011).

305. Parvani, J. G., Galliher-Beckley, A. J., Schiemann, B. J. & Schiemann, W. P. Targeted inactivation of β1 integrin induces β3 integrin switching, which drives breast cancer metastasis by TGF-β. *Mol. Biol. Cell* **24**, 3449–3459 (2013).

306. Knyazev, E. N., Nyushko, K. M., Alekseev, B. Y., Samatov, T. R. & Shkurnikov, M. Y. Suppression of ITGB4 Gene Expression in PC-3 Cells with Short Interfering RNA Induces Changes in the Expression of β-Integrins Associated with RGD-Receptors. *Cell Technol. Biol. Med.* **159**, 541–545 (2015).

307. Walsh, C. *et al.* Oral delivery of PND-1186 FAK inhibitor decreases tumor growth and spontaneous breast to lung metastasis in pre-clinical models. *Cancer Biol. Ther.* **9**, 778–790 (2010).

308. Woo, J. K. *et al.* Daurinol blocks breast and lung cancer metastasis and development by inhibition of focal adhesion kinase (FAK). *Oncotarget* **8**, 57058–57071 (2017).

309. Xu, Q. *et al.* The extracellular-regulated protein kinase 5 (ERK5) enhances metastatic burden in triple-negative breast cancer through focal adhesion protein kinase (FAK)-mediated regulation of cell adhesion. *Oncogene* **40**, 3929–3941 (2021).

310. Sinha, S. *et al.* Cucurbitacin B inhibits breast cancer metastasis and angiogenesis through VEGF-mediated suppression of FAK/MMP-9 signaling axis. *Int. J. Biochem. Cell Biol.* **77**, 41–56 (2016).

311. Nipin, S. *et al.* Nobiletin inhibits angiogenesis by regulating Src/FAK/STAT3-mediated signaling through PXN In ER+ breast cancer cells. *Int. J. Mol. Sci.* **18**, 1–13 (2017).

312. Shen, M. *et al.* Tinagl1 Suppresses Triple-Negative Breast Cancer Progression and Metastasis by Simultaneously Inhibiting Integrin/FAK and EGFR Signaling. *Cancer Cell* **35**, 64–80 (2019).

313. Kim, H., Son, S., Ko, Y. & Shin, I. CTGF regulates cell proliferation, migration, and glucose metabolism through activation of FAK signaling in triple-negative breast cancer. *Oncogene* **40**, 2667–2681 (2021).

314. Paul, R. *et al.* FAK activates AKT-mTOR signaling to promote the growth and progression of MMTV-Wnt1 driven basal-like mammary tumors. *Breast Cancer Res.* **22**, 1–15 (2020).

315. Nguyen, D. X., Bos, P. D. & Massagué, J. Metastasis: From dissemination to organ-specific colonization. *Nat. Rev. Cancer* **9**, 274–284 (2009).

316. Hamidi, H., Pietilä, M. & Ivaska, J. The complexity of integrins in cancer and new scopes for therapeutic targeting. *Br. J. Cancer* **115**, 1–7 (2016).

317. Taddei, M. L., Giannoni, E., Fiaschi, T. & Chiarugi, P. Anoikis: An emerging hallmark in health and diseases. *J. Pathol.* **226**, 380–393 (2012).

318. Cao, Z., Livas, T. & Kyprianou, N. Anoikis and EMT: Lethal 'Liaisons' during Cancer Progression. *Crit. Rev. Oncog.* **21**, 155–168 (2016).

319. Fujita, M. *et al.* Anoikis resistance conferred by tenascin-C-derived peptide TNIIIA2 and its disruption by integrin inactivation. *Biochem. Biophys. Res. Commun.* **536**, 14–19 (2021).

320. Zhang, K. *et al.* Oncogenic K-Ras upregulates ITGA6 expression via FOSL1 to induce anoikis resistance and synergizes with αV-Class integrins to promote EMT. *Oncogene* **36**, 5681–5694 (2017).

321. Pan, Y., Zhu, X., Wang, K. & Chen, Y. MicroRNA-363-3p suppresses anoikis resistance in human papillary thyroid carcinoma via targeting integrin alpha 6. *Acta Biochim. Biophys. Sin. (Shanghai).* **51**, 807–813 (2019).

322. Ivanova, I. A. *et al.* FER kinase promotes breast cancer metastasis by regulating α6- and β1-integrin-dependent cell adhesion and anoikis resistance. *Oncogene* **32**, 5582–5592 (2013).

323. Chen, I. H. *et al.* HPW-RX40 restores anoikis sensitivity of human breast cancer cells by inhibiting integrin/FAK signaling. *Toxicol. Appl. Pharmacol.* **289**, 330–340 (2015).

324. Desgrosellier, J. S. & Cheresh, D. A. Integrins in cancer: biological implications and therapeutic opportunities. *Nat. Rev. Cancer* **10**, 9–22 (2010).

325. Bozzo, C. *et al.* Activation of caspase-8 triggers anoikis in human neuroblastoma cells. *Neurosci. Res.* **56**, 145–153 (2006).

326. Nath, S. & Devi, G. R. Three-Dimensional Culture Systems in Cancer Research: Focus on Tumor Spheroid Model. *Pharmacol. Ther.* **163**, 94–108 (2016).

327. Weiswald, L. B., Bellet, D. & Dangles-Marie, V. Spherical Cancer Models in Tumor Biology. *Neoplasia (United States)* **17**, 1–15 (2015).

328. Schooley, A. M., Andrews, N. M., Zhao, H. & Addison, C. L. β1 Integrin Is Required for Anchorage-Independent Growth and Invasion of Tumor Cells in a Context Dependent Manner. *Cancer Lett.* **316**, 157–167 (2012).

329. Tancioni, I. *et al.* FAK inhibition disrupts a β5 integrin signaling axis controlling anchorage-independent ovarian carcinoma growth. *Mol. Cancer Ther.* **13**, 2050–2061 (2014).

330. DeRita, R. M. *et al.* Tumor-Derived Extracellular Vesicles Require β1 Integrins to Promote Anchorage-Independent Growth. *iScience* **14**, 199–209 (2019).

331. Bertotti, A., Comoglio, P. M. & Trusolino, L. β4 integrin activates a Shp2-Src signaling pathway that sustains HGF-induced anchorage-independent growth. *J. Cell Biol.* **175**, 993–1003 (2006).

332. Desgrosellier, J. S. *et al.* An integrin αvβ3-c-Src oncogenic unit promotes anchorage-independence and tumor progression. *Nat. Med.* **15**, 1163–1169 (2009).

333. Amer, K. M. *et al.* Epidemiology, Incidence, and Survival of Rhabdomyosarcoma Subtypes: SEER and ICES Database Analysis. *J. Orthop. Res.* **37**, 2226–2230 (2019).

334. Lacey, A. *et al.* Nuclear receptor 4A1 (NR4A1) as a drug target for treating rhabdomyosarcoma (RMS). *Oncotarget* **7**, 31257–31269 (2016).

335. Ganesh, K. & Massagué, J. Targeting metastatic cancer. *Nat. Med.* **27**, 34–44 (2021).

336. Sitohy, B., Nagy, J. A. & Dvorak, H. F. Anti-VEGF/VEGFR therapy for cancer: Reassessing the target. *Cancer Res.* **72**, 1909–1914 (2012).

337. Jayson, G. C., Hicklin, D. J. & Ellis, L. M. Antiangiogenic therapy-evolving view based on clinical trial results. *Nat. Rev. Clin. Oncol.* **9**, 297–303 (2012).

338. Bridges, E. & Harris, A. L. Vascular-Promoting therapy reduced tumor growth and progression by improving chemotherapy efficacy. *Cancer Cell* **27**, 7–9 (2015).

339. Haibe, Y. *et al.* Resistance Mechanisms to Anti-angiogenic Therapies in Cancer. *Front. Oncol.* **10**, 1–23 (2020).

340. Montemagno, C. & Pagès, G. Resistance to Anti-angiogenic Therapies: A Mechanism Depending on the Time of Exposure to the Drugs. *Front. Cell Dev. Biol.* **8**, 1–21 (2020).

341. Ebos, J. M. L. *et al.* Accelerated Metastasis after Short-Term Treatment with a Potent Inhibitor of Tumor Angiogenesis. *Cancer Cell* **15**, 232–239 (2009).

342. Coussens, L. M., Fingleton, B. & Matrisian, L. M. Matrix metalloproteinase inhibitors and cancer: Trials and tribulations. *Science (80-.).* **295**, 2387–2392 (2002).

343. Bambace, N. M. & Holmes, C. E. The platelet contribution to cancer progression. *J. Thromb. Haemost.* **9**, 237–249 (2011).

344. Fidler, I. J. & Kripke, M. L. The challenge of targeting metastasis. *Cancer Metastasis Rev.* **34**, 635–641 (2015).

345. Aguirre-Ghiso, J. A. Models, mechanisms and clinical evidence for cancer dormancy. *Nat. Rev. Cancer* **7**, 834–846 (2007).

346. Wan, L., Pantel, K. & Kang, Y. Tumor metastasis: Moving new biological insights into the clinic. *Nat. Med.* **19**, 1450–1464 (2013).

347. Parareda, A. *et al.* Prognostic impact of the detection of microcirculating tumor cells by a real-time RT-PCR assay of tyrosine hydroxylase in patients with advanced neuroblastoma. *Oncol. Rep.* **14**, 1021–1027 (2005).

348. Lv, P., Chen, K. & Zhu, H.-L. Recent advances of small molecule focal adhesion kinase (FAK) inhibitors as promising anticancer therapeutics. *Curr. Med. Chem.* (2021).

349. Jia, J. *et al.* Dual inhibition of αV integrins and Src kinase activity as a combination therapy strategy for colorectal cancer. *Anticancer. Drugs* **24**, 237–250 (2013).

350. Hoang, N. T., Acevedo, L. A., Mann, M. J. & Tolani, B. A review of soft-tissue sarcomas: translation of biological advances into treatment measures. *Cancer Manag. Res.* **10**, 1089–1114 (2018).

351. Shimada, H. *et al.* Histopathologic Prognostic Factors in Neuroblastic Tumors: Definition of Subtypes of Ganglioneuroblastoma and an Age-Linked Classification of Neuroblastomas. *J. Natl. Cancer Inst.* **73**, 405–416 (1984).

352. Zamzami, N. & Kroemer, G. Condensed matter in cell death. *Nature* **401**, 127–128 (1999).

353. Zarzosa, P. *et al*. Patient-derived xenografts for childhood solid tumors: a valuable tool to test new drugs and personalize treatments. *Clin Transl Oncol.* **19**, 44-50 (2017).

353. Elmore, S. Apoptosis: A Review of Programmed Cell Death. *Toxicol. Pathol.* **35**, 495–516 (2007).

VIII. ANNEX: Publications and patents

Accepted publications:

1. Giralt I, Gallo-Oller G, **Navarro N**, Zarzosa P, Pons G, Magdaleno A, Segura MF, Sánchez de Toledo J, Moreno L, Gallego S and Roma J. Dickkopf proteins and their role in cancer: a family of wnt antagonists with a dual role. Pharmaceuticals (2021). DOI: 10.3390/ph14080810

2. Molist C*, **Navarro N***, Giralt I, Zarzosa P, Gallo-Oller G, Pons G, Magdaleno A, Moreno L, Guillén G, Hladun R, Garrido M, Soriano A, Segura MF, Sánchez de Toledo J, Gallego S and Roma J. miRNA-mediated regulation of alpha9-Integrin in rhabdomyosarcoma: tumor-suppressor roles for miRNA-7 and miRNA-324-5p. Cancer Letters, pp. 49-59 (2020). DOI: 10.1016/j.canlet.2020.02.035 *Contributed equally.

3. Almazán-Moga A, Zarzosa P, Vidal I, Molist C, Giralt I, **Navarro N**, Soriano A, Segura MF, Alfranca A, Garcia-Castro J, Sánchez de Toledo J, Roma J and Gallego S. Hedgehog pathway inhibition hampers sphere and holoclone formation in Rhabdomyosarcoma. Stem Cells International, pp. 1-14 (2017). DOI: 10.1155/2017/7507380

4. Almazán-Moga A, Zarzosa P, Molist C, Velasco P, Pyszek J, Simon-Keller K, Giralt I, Vidal I, **Navarro N**, Segura MF, Soriano A, Navarro S, Tirado OM, Ferreres JC, Santamaria A, Rota R, Hahn H, Sánchez de Toledo J, Roma J and Gallego S. Ligand-dependent Hedgehog pathway activation in Rhabdomyosarcoma: the oncogenic role of the ligands. British Journal of Cancer, pp. 1-12 (2017). DOI: 10.1038/bjc.2017.305

5. Zarzosa P, **Navarro N**, Giralt I, Molist C, Almazán-Moga A, Vidal I, Soriano A, Segura MF, Hladun R, Villanueva A, Gallego S and Roma J. Patient-derived xenografts for childhood solid tumors: a valuable tool to test new drugs and personalize treatments. Clinical and Translational Oncology, pp. 44-50 (2016). DOI: 10.1007/s12094-016-1557-2

Patents:

Jimena Fernandez, Berta Ponsati, Antonio Parente, Mariona Vallès-Miret, Josep Farrera-Sinfreu, Anna Almazán-Moga, Josep Roma, Soledad Gallego, José Sánchez de Toledo, Lucas Moreno, **Natalia Navarro**, Carla Molist. Peptides for the treatment of cancer and/or metastasis (EP19383084.1). 05/12/2019. BCN Peptides SA.